Durability of Selected Membrane Materials when Exposed to Chlorine Gas

Doctoral Thesis

by

Marianne Sørflaten Eikeland

Telemark University College (HIT), Department of Technology
Institute of Process Technology

and

Norwegian University of Science and Technology (NTNU)

Porsgrunn, Norway
March 2001

To Kjersti
For the love and inspiration
you bring into my life.

Acknowledgment

Abstract

This thesis is focusing on the durability of selected membrane materials when exposed to chlorine gas in the temperature range 30-100°C. Studies of the changes of membrane separation properties and the mechanisms promoting these changes have been studied.

The selected membrane materials were poly(dimethylsiloxane) (PDMS), Fluorel®[1], fluorosilicone, and blends of PDMS and Fluorel.

The thesis is organised in seven chapters. The first chapter gives an introduction to the background of the work. The second chapter presents the theory for gas separation using dense rubbery membranes. The properties of the selected membrane materials are presented in chapter three. The fourth chapter describes degradation mechanisms for polymeric materials in general and for the selected membrane materials in particular. Presentation of the experimental work is given in chapter five, while the results with discussions are presented in chapter six. The conclusions and recommendations for further studies are given in chapter seven.

Five appendixes are attached: Appendix A describes the calculations of permeability and solubility coefficients and the accuracy of the experimental measurements. Appendix B summarises the measured values in tables and Appendix C describes the analytical methods. Appendix D gives the properties of the gases used in the experiments. Appendix E is the article "Durability of Poly(dimethylsiloxane) when Exposed to Chlorine Gas", submitted to the Journal of Applied Polymer Science.

Highly crosslinked PDMS was found to have an initial high permeability for chlorine gas and a high Cl_2/O_2 selectivity. However when exposed to chlorine gas the permeability decreased significantly. Crosslinking of the PDMS polymer chain and chlorination of the polymer gave a denser polymer structure and thus lower permeability.

Fluorel showed very low permeabilities and selectivities for the gases in question and was thus not interesting for this membrane separation. It was however found that permeability decreased upon exposure to chlorine gas followed by an increased selectivity for Cl_2/O_2 in this material. This may be a result of chlorination or crosslinking. Also the degree of crystallinity will influence the transport through the membrane. The FT-IR analysis showed no significant changes in the structure of Fluorel.

Different blends of poly(dimethylsiloxane) and Fluorel were tested. These materials had initially high permeabilities and high selectivities. The permeability however decreased significantly upon exposure to Cl_2 and the membrane was ruined after few days. Chlorination of the methyl group in PDMS, (C-Cl bond), and formation of cyclic compounds or crosslinking were observed also in the blends.

Fluorosilicone showed initially high permeabilities and good selectivities but degraded quickly upon exposure to chlorine gas. This fact ruled out this material.

---

[1] Fluorel is the trademark of 3M for the copolymer of vinylidenefluoride and hexafluoropropylene.

Table of contents

Symbol list

A	surface area	$[m^2]$
b	affinity constant of Langmuir isotherm	$[Pa^{-1}]$
c	concentration	$[kg/m^3]$
c'_h	saturation capacity of Langimuir isotherm	$[m^3(STP)/m^3]$
c_i	concentration	$[kg/m^3]$
D_{AB}	mutual diffusion coefficient	$[m^2/s]$
D_i	diffusion coefficient	$[m^2/s]$
D_0	temperature independent constant	[-]
dc_i/dx	concentration gradient	[-]
E_d	activation energy for diffusion through the membrane	[J/mole]
E_p	activation energy for permeability through the membrane	J/mole]
G_M	Gibbs free energy of mixing	[J/mole]
H_M	enthalpy of mixing	[J/mole]
H_s	enthalpy of sorption	[J/mole]
J_i	flux	$[m^3(STP)/(m^2 \, s)]$
k	Boltzman constant	[J/K]
k_d	Henry's law constant	$[m^3(STP)/(m^3 \, Pa)]$
l	thickness	[m]
M_w	molecular weight	[kg/kmole]
n	number of moles	[-]
P_i	permeability coefficient	$[m^3(STP) \, m/m^2 \, Pa \, h]$
P_0	temperature independent constant	[-]
p_h	pressure at high pressure side	[Pa]
p_l	pressure at low pressure side	[Pa]
p_{vap}	vapour pressure	[Pa]
R	gas constant	[8.314 J/mole K])
S_i	solubility coefficient	$[m^3(STP)/m^3 \, Pa]$
S_0	temperature independent constant	[-]
S_M	entropy of mixing	[J/(mole K)]
T	temperature	[K]
T_c	crystallisation temperature	[K]
T_{crit}	critical temperature	[K]
T_g	glass transition temperature	[K]
T_m	melting temperature	[K]
V	volume	$[m^3]$
V_f	fractional free volume	[-]

Greek symbols

α	constant	[-]
α^*	separation factor	[-]
$\Delta\alpha$	difference of thermal expansion	$[K^{-1}]$
β	constant	[-]
χ	Flory-Huggins interaction parameter	[-]
ε	potential energy	$[kg \, m^2/s^2]$
ε/k	Lennard Jones potential	[K])
ρ	density	$[kg/m^3]$
σ	surface tension	[N/m]
υ	volume fraction	[-]
ω	weight fraction	[-]

x

Chapter 1: Introduction

Summary

This chapter gives a brief introduction to the background of the work. A short presentation of membrane separation of aggressive gases is given in section 1.1, together with a brief presentation of published literature on separation of Cl_2 gas. Section 1.2 presents the background for the intended industrial application. The selected materials are described briefly in section 1.3, while section 1.4 summarises the results.

1.1 Introduction

Sour gases such as SO_2, CO_2, H_2S and Cl_2 are all unwanted effluents to the atmosphere and purification of the gas streams is needed to remove or recycle these components. Different technologies are used for gas purification, and membrane technology is a relatively new approach. Membrane technology has the benefits of having low energy consumption and combines easily with other separation processes. The separation can be carried out continuously and the modules are small and compact and easy to upscale. The lifetime of the membrane may however be crucial for gas separation [1].

Materials used to compose a membrane can vary significantly both in structure and functionality depending on the separation problem. For gas separation membrane materials are mostly polymers, but ceramics, carbon membranes and glass membranes are materials under development. In this work the focus has been on polymeric membranes.

An understanding of the transport properties for the gases in the membrane is necessary in order to find an optimal material for the specific separation process. Solution-diffusion mechanism is the most usual physical model to describe the gas transport through dense (nonporous) membranes. Differences in solubility and diffusivity of the gas molecules in the polymer are the driving force for the separation. Polarity, kinetic diameter and critical temperature of the gases are all characteristics influencing the transport rate of the gas molecules through the particular membrane. The membrane should preferably have both high permeability and selectivity for a given gas pair, and be mechanically strong. The membrane should have a high performance over an extended period of time to meet the economical requirements for the process.

The lifetime or durability of the membrane is crucial when it is exposed to aggressive gases. Even though the polymer is said to be chemically stable, the polymer and the aggressive gas may interact in such a way that the polymer structure changes, and with this the membrane properties, especially the separation properties.

Membrane separation for chlorine purification is a new approach. Separation of chlorine gas with membranes is very challenging because very few materials will be chemically stable towards this gas and at the same time exhibit satisfactory separation properties.

Lokhandwala et.al. [2] have published a study on recovery of chlorine from tail gas. The tail gas consists of 20% chlorine in 50-70% air, the balance being hydrogen and carbon dioxide. They found that silicone rubber was stable in the presence of chlorine gas provided that the membranes were completely crosslinked and had no residual functional groups. Their tests were performed at low temperatures (-40°C to 25°C).

Hägg [3] has studied purification of aggressive chlorine gas with different membrane materials since 1994. This has been part of a big project for magnesium industry. The aim was to remove O_2 from a process gas stream consisting of more than 90% Cl_2 gas. The Cl_2 would be used in the process for the magnesium production. Different materials were considered for the separation process: silicone rubber, perfluorinated polymers, carbon membranes and glass membranes.

The current thesis has with background in Hägg's work, focused on the durability of different polymeric materials when exposed to dry, highly concentrated chlorine gas at temperatures in the range 30-100°C. The materials analysed in this work have been poly(dimethylsiloxane) (PDMS), Fluorel, blends of the PDMS and Fluorel, and fluorosilicone. The focus has been changes in separation properties and chemical structure of the material upon Cl_2 exposure at different temperatures over several weeks.

1.2   The industrial application

Norsk Hydro is the world largest producer of magnesium, and one of their plants are located in Porsgrunn, Norway. Traditional magnesium production is very energy demanding as it usually involves electrolysis (of $MgCl_2$) with additional complicated unit operations for the handling of the produced chlorine gas from the electrolysis and the hydrochloric acid further down the production line. The process stream coming from the electrolysis contains mainly Cl_2 (90-95 %), the rest being air leaking into the system. The amount of O_2 must be reduced to less than 0.2 wt% before H_2 is reacted with Cl_2 further down the line in order to avoid the formation of water [3].

The Cl_2 gas is reacted with H_2 to produce HCl for conversion of magnetite (MgO) to magnesium chloride; se Figure 1.1, which is then going to the electrolysis where Mg and Cl_2 are produced. The gas coming from the electrolysis is dry and at app. 80°C and slightly above atmospheric pressure as it reaches a membrane unit, which is planned integrated in the process line. Figure 1.1 is indicating where the membrane unit will be placed.

A membrane process for the purification of concentrated chlorine gas must be carefully designed if it is to replace current technology. Due to the given process conditions, such a process will need other considerations than the removal of chlorine as minor impurity from a waste gas stream. This implies that the process should preferably be run at moderate pressures (1-2 bar absolute), and at a temperature above 65°C. A chlorine gas stream coming from electrolysis will always contain compounds like chlorinated hydrocarbons (CHC) in minor concentrations. These compounds are very toxic and only slowly degrade in nature. This aspect must also be addressed in a total process solution for the purification of Cl_2 gas. Another key issue is keeping the system completely dry in order to avoid any formation of the corrosive gas HCl. These process conditions have been used to set the experimental conditions of the membrane separation experiments that have been carried out.
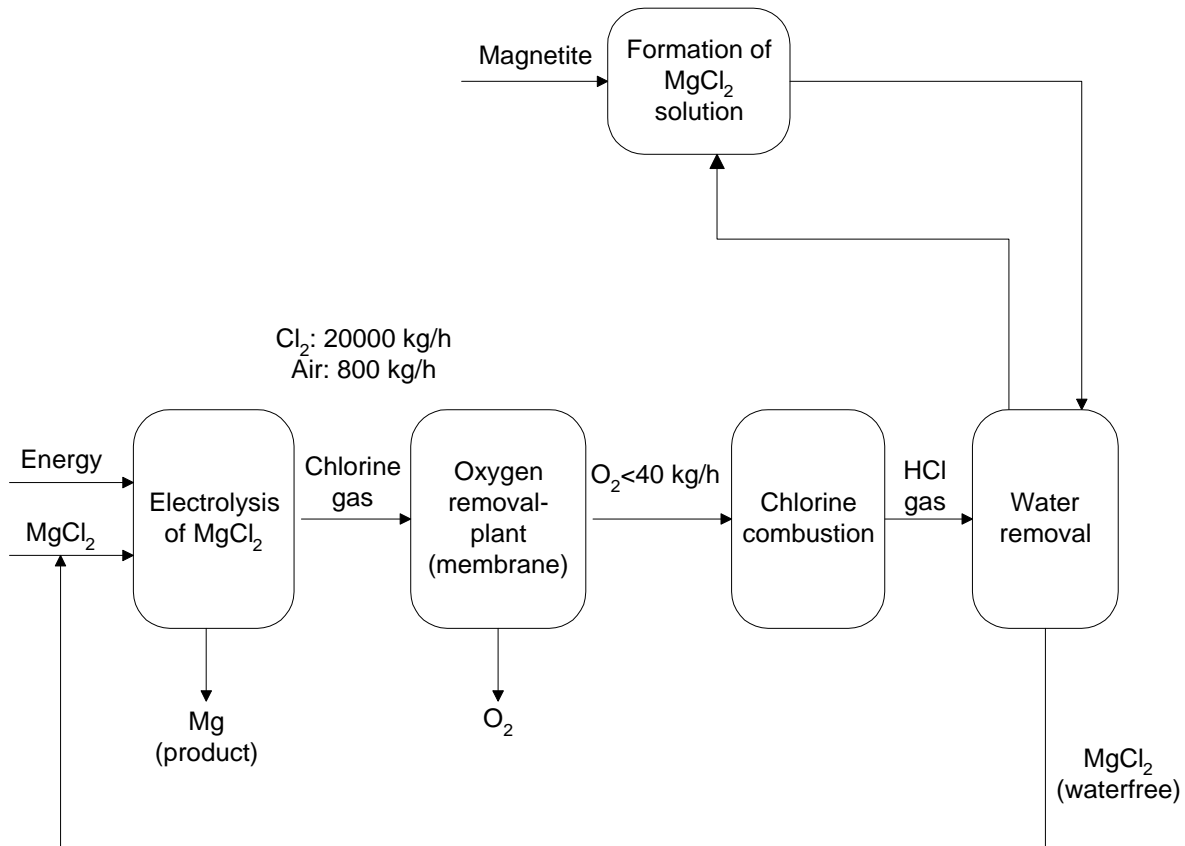
Figure 1.1: Simplified flow diagram for the production of magnesium. The place for integration of a membrane process is shown [3].

1.3   Scope of work

Documentation of the membrane durability and degradation mechanisms as a function of time is very important to estimate membrane lifetime. For integration of membrane modules in industrial processes the lifetime of the membrane material is crucial. The process stream will often transport large volumes of gas and liquids at pressures and temperatures where the durability of common membrane materials is yet not fully understood. If the membranes must be replaced too often, the solution may become too expensive, or if the membrane is damaged dangerous situations may occur.

This thesis is focused on the durability of selected membrane materials over time when exposed to chlorine gas in temperature range 30-100°C. Studies of changes in the membrane separation properties and the mechanisms that promoted these changes have been in focus.

The objectives of the present work have thus been:
1. Document the durability of selected membrane materials over time when exposed to pure chlorine gas in the temperature range 30-100°C.
2. Study the mechanisms that promote changes in the materials when exposed to chlorine gas.
3. Study changes in the separation properties of the membrane.

The materials studied are poly(dimethylsiloxane) (PDMS), Fluorel®[2], fluorosilicone, and blends of PDMS and Fluorel. It was also necessary to evaluate the stability of the support materials when exposed to chlorine gas at high temperatures.

PDMS is a membrane in its rubbery state with low glass transition temperature (Tg = -123°C). PDMS has high gas permeability for organic vapours and gases with high critical temperatures. PDMS is also known to exhibit properties like being chemically and thermally stable [4]. The PDMS was chosen because of its high permeability for chlorine gas, and high Cl_2/O_2 selectivities.

Fluorel is a copolymer of vinylidenefluoride (VDF) and hexafluoropropylene (HFP), and has been studied for the purpose to blend it with PDMS to achieve a better stability of the membrane and increase the permeability of the chlorine gas. Fluorel is a fluoroelastomer, which generally possess a number of outstanding properties. Fluoroelastomers offer exceptional resistance to chemicals, oils and solvents, and they can withstand high temperatures [5].

Fluorosilicone has been studied as an alternative membrane material. The wide temperature range of fluorosilicone rubber (-75°C to 170°C), and in particular its resistance to oil and aggressive solvents is of interest to the industry. The material has excellent dielectric properties in addition to resistance to aggressive media [6]. Like PDMS, fluorosilicone exhibits high permeability for chlorine gas, and high Cl_2/O_2 selectivity. The polymer structure is more open and should maintain a high permeability upon chlorine exposure.

Poly(vinylidenefluoride) (PVDF) and poly(tetrafluoroethylene)(PTFE) exhibit both chemical and thermal stability to the process conditions, and are therefore used as support layer for the membrane.

1.4   Summary of results

The permeabilities and selectivities were measured for N_2, O_2 and Cl_2 in the different polymeric membranes over the temperature range 30-100°C. The membranes have, between the permeability measurements, been exposed to chlorine gas to study changes in separation properties due to the exposure.

The sorption of N_2, O_2, Cl_2, in the selected membrane materials was measured as a function of temperature.

All polymers were exposed to chlorine gas at the temperatures 30 and 60°C for 4 weeks in a glass chamber (i.e. statically exposure) and studied by FT-IR for possible degradation.

The PDMS was also analysed with ^{1}H-NMR and SEM (Scanning Electron Microscope). Differential Scanning Calorimetry (DSC) has also been used for the documentation.

---

[2] Fluorel is the trademark of 3M for the copolymer of vinylidenefluoride and hexafluoropropylene), and is similar to Viton the trademark of DuPont

Highly crosslinked PDMS was found to have high permeability for chlorine gas and a high Cl_2/O_2 selectivity. However upon chlorine exposure the permeability of the gases decreased significantly. This was due to further crosslinking of the PDMS polymer chain, and to chlorination of the polymer. Both factors imply a denser polymer structure and thus a lower permeability. The reaction rate of the chlorination increased with temperature. The sorption curve for Cl_2 documented that chlorine will go into the membrane after sorption equilibrium has been reached; and that a chlorination reaction was taking place. Analysis with FT-IR and ^{1}H NMR showed that hydrogen in the methyl group in PDMS was substituted by chlorine.

Fluorel showed very low permeabilities and selectivities for the gases in question and was thus not interesting for the membrane process. It was however found that permeability decreased upon exposure to chlorine gas followed by an increased selectivity for Cl_2/O_2 in this material. This could be a result of chlorination or crosslinking. Increased temperatures gave increased permeability, which may be due to changes in the degree of crystallinity. The sorption curve for Cl_2 in Fluorel documented that additional chlorine would go into the membrane after sorption equilibrium had been reached; and that a chlorination reaction was taking place. The FT-IR analysis showed no significant changes in the polymer structure.

Different blends of poly(dimethylsiloxane) and Fluorel were tested. These materials had initially high permeabilities and high selectivities. The permeability however decreased significantly upon exposure to Cl_2 and the membrane was ruined after few days. Chlorination of the methyl group in PDMS, (C-Cl bond), and formation of cyclic compounds or crosslinking were observed also in the blends.

Fluorosilicone showed initially high permeabilities and good selectivities but degraded quickly upon exposure to chlorine gas. This fact ruled out this material. Also for Fluorosilicone the sorption curve for Cl_2 documented that additional chlorine would go into the membrane after sorption equilibrium had been reached; and that chlorination reactions were taking place. The FT-IR spectra show a narrower peak for the Si-O-Si bond indicating formation of cyclic compounds or crosslinks.

FT-IR analysis of poly(vinylidenefluoride) (PVDF) and poly(tetrafluoroethylene)(PTFE) after exposure to chlorine gas at 60°C for 4 weeks did not show any chemical changes and these materials were therefore judged as suitable support materials.

The results obtained for the PDMS will be published in an article: "Durability of Poly(dimethylsiloxane) When Exposed to Chlorine Gas", submitted to Journal of Applied Polymer Science. "The durability of selected composite membranes" was presented as a poster at the Third International Symposium of Euromembrane in 1997 [7].

References to Chapter 1

1. M. Mulder; Basic Principles of Membrane Technology, 2nd Ed., Kluwer Academic Publishers, The Netherlands 1996.
2. K. A. Lokhandwala, S. Segelke, P. Nguyen, R. W Baker, T. T. Su, I. Pinnau; A Membrane Process To Recover Chlorine from Chloralkali Plant Tail Gas, Ind. Eng. Chem. Res., vol. 38, p. 3606-3613, 1999.
3. M-B Hägg; Membrane purification of chlorine gas: Contributions towards an integrated process solution in Magnesium production, Dissertation Dr.Tech, The Norwegian University of Science and Technology, Trondheim, Norway 2000.
4. S. J. Clarson, J. A. Semlyen; Siloxane Polymers, Ellis Horwood - PTR Prentice Hall, USA 1993.
5. J. M. Charrier; Polymeric Materials and Processing, Hanser Publisher, Germany 1991.
6. D. Klages, U. Raupbach; Fluorosilicone Rubber - a modern material, Gummi Fasern Kunststoffe, International Polymer Sci.and Tech., vol. 22, No. 5 p T/11-T/13, 1995.
7. M. Sørflaten; Purification of Chlorine Gas with Polymeric Membranes- a study of durability of selected composite membranes, Third International Symposium of Euromembrane, University of Twente, The Netherlands 1997.

Chapter 2: Gas Separation using Dense Rubbery Polymers

Summary

Polymeric membranes have been successfully used in many gas separation applications. The success is largely based on their mechanical and thermal stability, along with good gas separation properties. Understanding the nature of transport phenomena involved during gas permeation through polymeric membranes is thus of fundamental and practical interest. The membrane material and its properties determine these transport mechanisms.

This chapter will give a brief presentation of the principles of gas separation through dense rubbery polymers.

2.1   Gas separation

A membrane can be considered as a permselective barrier or interface between two phases. The word selective indicates that the barrier is not equally permeable for different components. This difference in permeability can be used to separate liquids or gases. In a membrane process the feed is separated into two streams: the stream that flows through the membrane (permeate), and the retained stream from the feed stream (retentate). Figure 2.1 gives a schematic representation of a membrane separation process.
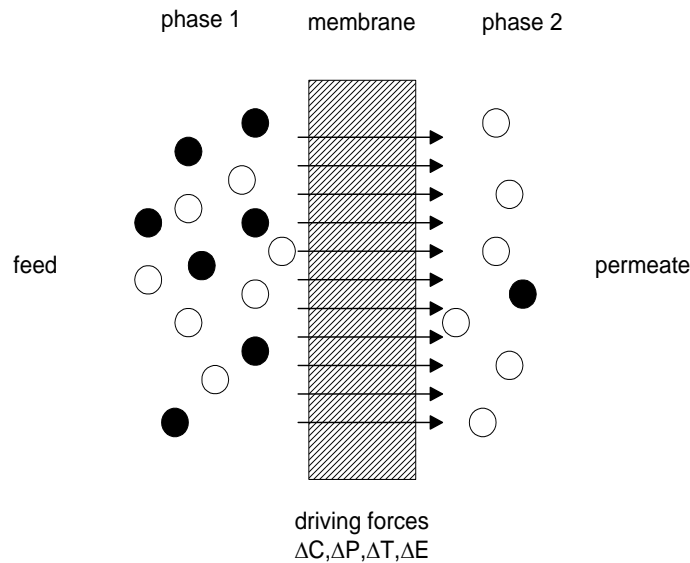
Figure 2.1: Schematic representation of a two-phase system separated by a membrane, where ΔC, ΔP, ΔT, ΔE is the driving force across the membrane representing differences in concentration, pressure, temperature or electrochemical potential respectively [1].

Gases can be separated in microporous as well as in nonporous membranes. The selectivity of microporous membranes is generally rather low because of the Knudsen diffusion transport mechanism. For binary mixtures the maximum separation factor can, generally, be estimated from the square root of the ratio of the molecular weights of the different components. Significantly high selectivities can be obtained in nonporous (dense) membranes where transport is based on the solution-diffusion mechanism, (this will be discussed further in section 2.1.2) [1, 2].

2.1.1   Preparation of asymmetric membranes for gas separation

Dense homogenous polymer films can separate various gaseous or liquid mixtures very efficiently. However, normal thickness (20-200 µm) leads to very low permeation rates. Membranes must be very thin (of the order 0.1 to 2 µm) to give an acceptable permeability flux. The mechanical strength of such membranes is very poor and support is needed.

An asymmetric membrane consists of a very thin selective skin layer (0.1-2 µm) on a porous substructure (thickness 100-200 µm). Two techniques are used to prepare asymmetric membranes: The first utilises the phase inversion process and leads to an integral symmetric membrane in which the skin and substructure consist of the same polymer. In the second

technique an extremely thin polymer film is deposited on a preformed microporous substructure leading to a composite membrane (Figure 2.2).

In a composite membrane, different polymers may be used. Polymers that show the desired selectivity for a certain separation problem, but have a poor mechanical strength or film forming properties, are unsuited for use as integral asymmetric membranes. However, they may be utilised as the selective barrier in composite membranes.
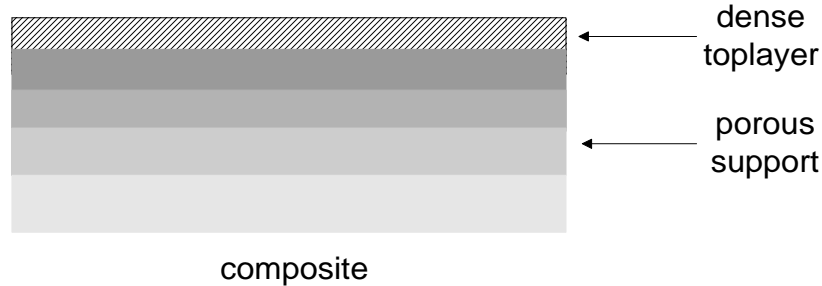
composite

Figure 2.2: Schematic representation of a composite membrane.

Asymmetric membranes are used primarily in pressure-driven processes such as reverse osmosis, ultra filtration or gas separation, where their unique properties (high mass transfer rate and good mechanical stability) can be utilised. Asymmetric membranes have high degree of filtration and are very resistant to fouling. Conventional symmetric structures act as depth filters and retains particles within their initial structure. These trapped particles plug the membrane and thus the flux declines during use. Asymmetric membranes are surface filters and retain all reject materials at the surface, where they can be removed when the feed solution moves parallel to the membrane surface [1].

2.1.2   Solution - diffusion transport mechanism in dense membranes

The solution-diffusion mechanism is the most commonly used physical model to describe the gas transport in dense membranes. Several processes are involved when a gas or vapour permeates trough a polymer membrane:

1. Adsorption and solution of the gas at the interface of the membrane, a sorption process;
2. Random movement of the dissolved gas in and through the membrane, a diffusion process;
3. Release of the gas at the opposite interface, a desorption process.

The term permeation is used to describe the overall mass transport of the penetrant gas across the membrane, whereas the term diffusion refers only to the movement of the gas inside the polymer. The sorption and desorption are fast, and gas solution equilibrium is established at the membrane interfaces when constant gas pressures are maintained. In contrast the diffusion step is very slow, and hence is the rate-determining step in the permeation process [3].

Gas separation through nonporous membranes depends on differences in the permeabilities of various gases through the given membrane. The permeability will depend on the nature of the polymer and the penetrant gas, and generally on the penetrant pressure (concentration) and

temperature. Figure 2.3 gives a schematic drawing of a nonporous membrane separating two gas phases (for units see symbol list page *ix*).
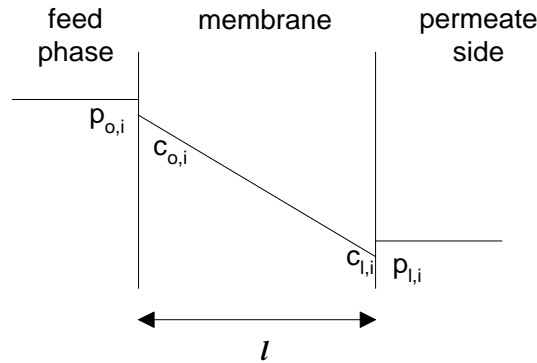
Figure 2.3: Nonporous membrane separating two gas phases, where l is the membrane thickness [1].

In gas separation, a gas at a pressure, $p_{o,i}$, is applied to the feed side of the membrane, while the permeate gas at a lower pressure, $p_{l,i}$, is removed from the downstream side of the membrane. Fick's law is the simplest description of gas diffusion through a nonporous structure i.e.:

$$J_i = -D_i \frac{dc_i}{dx}$$

(2.1)

where J_i is the flow rate through the membrane, D_i is the diffusion coefficient, and the driving force dc_i/dx is the concentration gradient across the membrane. Under steady state conditions this equation can be integrated across the membrane:

$$J_i = -\frac{D_i \left(c_{o,i} - c_{l,i}\right)}{l}$$

(2.2)

where $c_{o,i}$ and $c_{l,i}$ are the concentrations in the membrane on the upstream and the downstream side respectively, whereas *l* is the thickness of the membrane.

For ideal systems, the concentrations are related to the partial pressures by Henry's law, which states that a linear relationship exists between the concentration inside the membrane (c_i) and the partial pressure of gas outside the membrane (p_i), i.e.:

$$c_i = S_i \, p_i$$

(2.3)

where S_i is the solubility coefficient of component *i* in the membrane.

Combining Eq. (2.2) with Eq. (2.3) gives equation (2.4), which is usually used for the gas permeability flux through nonporous membranes.

$$J_i = -\frac{D_i S_i \left(p_{o,i} - p_{l,i}\right)}{l}$$

(2.4)

The product of the diffusion coefficient D_i (a kinetic factor) and the solubility coefficient S_i (a thermodynamic factor) is called permeability coefficient P_i, i.e.:

$$P_i = D_i\, S_i \qquad\qquad (2.5)$$

This leads to the familiar expression:

$$J_i = -\frac{P_i\left(p_{o,i} - p_{l,i}\right)}{l} \qquad\qquad (2.6)$$

Eq. (2.6) shows that the flow rate across the membrane is proportional to the difference in partial pressure and inversely proportional to the membrane thickness.

The pressure dependence of P is determined by the pressure dependences of D and S, as seen from Eqs. (2.7) and (2.8):

$$\overline{D}\left(c_i\right) = \frac{\displaystyle\int_{cl,i}^{co,i} D(c_i)\,dc}{\left(c_{l,i} - c_{o,i}\right)} \qquad\qquad (2.7)$$

$$\overline{S}\left(c_i\right) = \frac{c_{o,i} - c_{l,i}}{p_{o,i} - p_{i,l}} \qquad\qquad (2.8)$$

where $\overline{D}(c_i)$ and $\overline{S}(c_i)$ are the mean diffusion and solubility coefficients, respectively.

To understand and discuss the gas transport or its mechanism in a polymer membrane it is necessary to investigate the diffusion and solubility coefficients, as well as the permeability coefficient, and their pressure (concentration) dependences (discussed in section 2.2).

The overall selectivity of a polymer membrane towards two different penetrant gases A and B is commonly expressed in terms of an "ideal" separation factor, $\alpha^*(A/B)$, which is defined by the relation, cf Eq. (2.9):

$$\alpha^*(A/B) = \frac{P_A}{P_B} = \frac{D_A}{D_B}\frac{S_A}{S_B} \qquad\qquad (2.9)$$

where the ratios D_A/D_B and S_A/S_B are known as the "diffusivity (or mobility) selectivity" and the "solubility selectivity", respectively. These ratios represent contributions to the overall selectivity due to the differences in the diffusivities and solubilities of gases A and B in a polymer [1, 3, 4].

2.1.3 Material properties

To describe the fundamentals of gas separation, factors relating to the nature of the polymer (i.e. chemical structure) need to be considered. Two parameters are very important in the context of the current study: the glass transition temperature (T_g) and the degree of crystallinity. These parameters are determined by structural factors such as chain flexibility, chain interaction and molecular weight.

The glass transition temperature determines whether a polymer is in the glassy or in the rubbery state, i.e. at temperatures above or below the glass transition temperature, T_g, of the polymers, respectively. Segmental motion is limited for a polymer in the glassy state, whereas in the rubbery state enough thermal energy is available to allow rotation in the main chain. The glass transition temperature is mainly determined by chain flexibility, i.e. the character of the backbone chain and the presence and nature of the side chains or side groups. Rotation around the bond in the backbone chain makes the polymer rather flexible like the (-C-C-) bond. However when the backbone chain is completely unsaturated (-C=C-) the rotation is impossible and a very rigid chain is obtained. Introduction of heterocyclic and aromatic groups leads to substantial decrease in flexibility. A further class of polymer does not contain carbon atoms in the backbone chain; such polymers are called inorganic polymers. Silicone rubber is an example of inorganic polymer, which consists of the (-Si-O-) backbone. This chain is very flexible. (-P≡N-) is another example of inorganic polymer, where the chain is quite rigid. The character of the side groups also determines the chain flexibility, which determine to some extent whether rotation around the main chain can take place readily or whether steric hindrance occurs. In addition, the character of the side group has strong effect on interchain interaction. Interaction between the chains is increased when polar side groups are introduced and as the polarity of side groups are increased the T_g value increase [1].

The gas transport occurs by markedly different mechanisms in rubbery and glassy polymers. In the glassy state, the selectivity of the membrane is relatively high and the permeability through the membrane relatively low. Above T_g the polymer membrane is in this rubbery state, the permeability is increased, the selectivity decreased. Depending on the application, a polymer membrane can be used in the glassy state, to take the benefit of the relatively higher selectivities, or relatively higher permeabilities in the rubbery state.

The chain length is an important parameter in determining the properties of a polymer. Polymers generally consist of a large number of chains and these do not necessarily have the same chain length. The consequence of the existence of different chain lengths in polymers is that a uniform molecular weight (MW) does not exist but rather a molecular weight average. The MW distribution is an important property relative to membrane preparation and characterisation. Higher polymer MW leads to higher gas permeability for both thermodynamic and kinetic reasons: (1) polymer solubility decreases with increasing MW with the result that a higher MW polymer will gel at an earlier stage during desolvation and entrap more free volume (discussed in section 2.1.5); (2) viscosity and chain entanglement increases with MW, both of which results in earlier gelation and a higher level of free volume; (3) higher MW polymers are stiffer and exhibit higher T_g values [1, 2].

Chain interactions in linear and branched polymers only secondary interaction forces act between the different chains, whereas in network polymers the various chains are bound to each other covalently. Secondary intermolecular forces are considerably weaker than primary covalent bonds. Nevertheless they have a strong effect on the physical properties of the polymer and consequently on its permeability because of the larger number of interactions possible. Three different types of secondary force can be considered:

- -dipole forces (Debye forces)
- -dispersion forces (or London forces)
- -hydrogen bonding forces

Table 2.1: Average values of strength of primary and secondary forces [1].

type of force	kJ/mole
covalent	≈ 400
ionic	≈ 400
hydrogen bonding	≈ 40
dipole	≈ 20
dispersion	≈ 2

Some polymers contain groups or atoms in which the charge is not distributed homogenously. The effect of the charge distribution (dipole) is only apparent at short distances. Such dipoles exert a strong attraction to other permanent dipoles and dipole-dipole interaction takes place. Examples of some groups with permanent dipoles are hydroxyl (-OH), carbonyl (-C=O) or halides (-I, -Br, -Cl, or -F). Although many polymers do not contain groups or atoms with a permanent dipole, interaction forces known as dispersion forces, can still exist between the chains. Dispersion forces are the weakest, but also the most common, forces capable of inducing chain interaction.

The strongest secondary forces are hydrogen bonds. These appear when a hydrogen atom is attached to an electronegative atom such as oxygen (hydroxyl) is attracted by an electronegative group in another chain. The forces in these cases can be so strong that the polymer can hardly be dissolved, as demonstrated by polyamides and cellulose [1].

2.1.4   Amorphous and crystalline polymers

Polymers can in principle exist in two states; amorphous or crystalline. The expression "amorphous" generally indicates the absence of shape or implies the absence of the characteristic regular arrangement. Some polymers are highly crystalline primarily because their structure is conducive to packing, while others are crystalline primarily because of strong secondary forces, for still other polymers both factors may be favourable for crystallisation. Some polymers are not completely crystalline, the degree of crystallinity being far less than 100%. These polymers are called semi-crystalline and consist of an amorphous and a crystalline fraction as illustrated in Figure 2.4 [1].
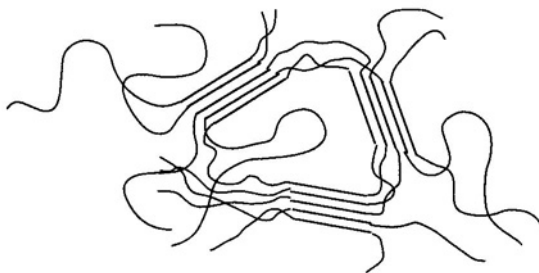
Figure 2.4: Morphology of a semi-crystalline polymer [1].

It should be mentioned that a regular structure does not automatically lead to crystallinity. A polymer melt, with regular structure, may upon rapid cooling solidify in a metastable amorphous state. Crystallinity can frequently be induced, however, by heating slowly to temperatures near the melting temperature to impart to the polymer molecules sufficient motion to allow them to line up in an orderly array [5].

Crystallites have a large influence not only on the mechanical properties but also on transport properties of a polymer. Since transport proceeds mainly via the amorphous regions, it is very important to know the degree of crystallinity in the polymer. Hence the characterisation of crystalline data gives information that may be related directly to the permeability. The amount of crystallinity directly influences the diffusion rate and hence the permeability flux if the diffusion primarily takes place in the amorphous region, and if the crystallites are considered to be impermeable [1].

The influence of crystallinity on the tensile modulus E^3 is depicted in Figure 2.5. In the glassy state the mechanical properties are little influenced by the presence of crystallites. On passing through the glass transition temperature, T_g, the amorphous glassy state is transformed into the rubbery state (curve a). The crystalline phase remains, however, unchanged, i.e. the chains remain in the crystal lattice, which maintain its rigidity until the melting temperature (T_m). Hence for a perfect crystalline polymer (100% crystallinity) changes in the modulus are most likely at the melting temperature, rather than the glass transition temperature. In semi-crystalline polymers the glassy phase exhibits the same mechanical properties as for a completely amorphous polymer. However, in the rubbery state the mechanical properties will depend on the crystalline content of the polymer. Generally the tensile modulus of a semi-crystalline polymer decreases as a function of temperature (curve b). This figure also depicts the tensile modulus of a completely crystalline polymer (curve a) indicating that no rubbery state is observed in this case and that the modulus only decreases drastically at the melting point [1, 6].

Mass transfer is generally greater in amorphous polymers than in highly crystalline or cross-linked polymers. Thus crystallisation and orientation are to be avoided when high permeabilities and transmembrane fluxes are desired. However, the physical properties of the polymer, particularly mechanical strength, and its selectivity may then be adversely affected. The final product is a compromise between required strength, selectivity and mass transfer rate. The principle aim is to create a membrane as thin as possible, consistent with the required strength and absence of pinholes and defects.

---

[3] A modulus is the ratio between the applied stress and the corresponding deformation. The reciprocals of the moduli are called compliances.
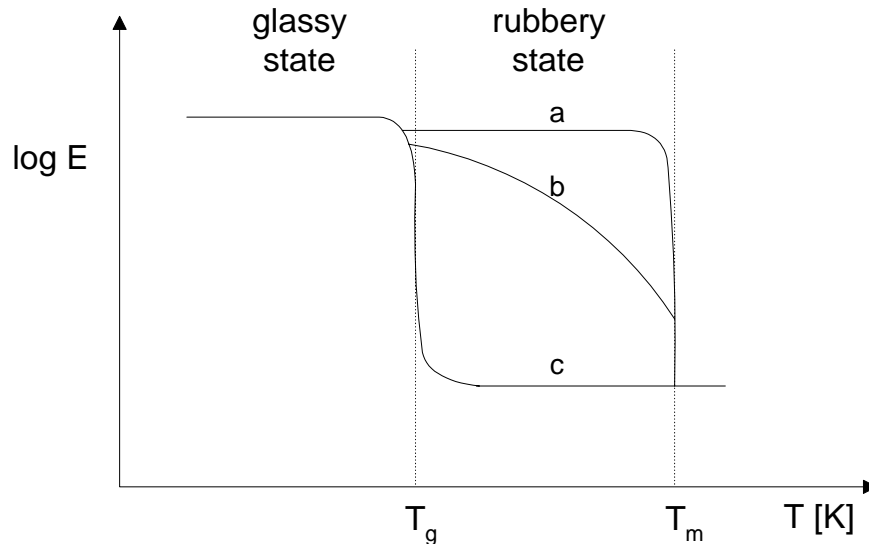
Figure 2.5: Tensile modulus of a semi-crystalline polymer as a function of the temperature. a) completely crystalline polymer; b) semi crystalline polymer; c) amorphous polymer [1].

2.1.5 Free volume

Depending on whether a polymer is in its glassy or rubbery state, it will often have large differences in the permeability. In the glassy state, the mobility of the chain segments are very limited and the thermal energy too small to allow rotation around the main chain. Only a few segments have sufficient energy for mobility although some mobility may occur in side groups. Above the glass transition temperatures, i.e. rubbery state, the mobility of the chain segments is increased and "frozen" microvoids no longer exist. The change in physical behaviour from the glassy to the rubbery state is discontinuous. In addition to the modulus, all kinds of physical properties change at the glass transition temperature such as specific volume, specific heat, refractive index and permeability. Figure 2.6 represents the specific volume and the free volume of a polymer as a function of temperature.

The free volume V_f may be defined as the volume unoccupied by the macromolecules. In glassy state ($T<T_g$) the free volume fraction V_f is virtually constant. However above the glass transition temperature the free volume increases linearly according to:

$$V_f = V_{f,T_g} + \Delta\alpha\left(T - T_g\right)$$

(2.10)

where $\Delta\alpha$ is the difference between the value of the thermal expansion coefficient above and below T_g. The concept of free volume is very important in the transport of non-interacting penetrants, such as nitrogen, helium and oxygen. For interacting penetrants, such as organic vapours and liquids, segmental motions are a function of penetrant concentration [1].
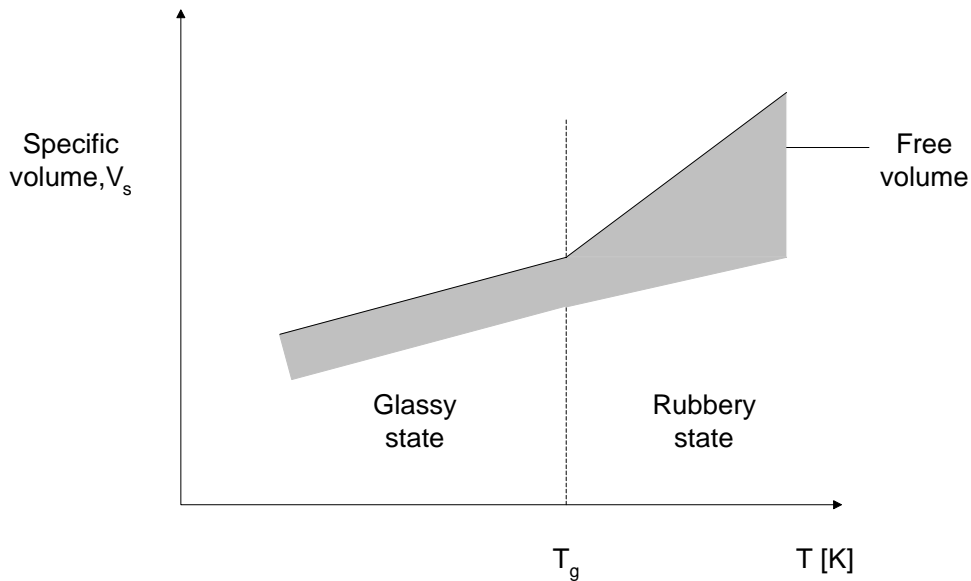
Figure 2.6: Specific volume of an amorphous polymer as a function of the temperature [1].

2.2   Transport in rubbery polymers

Rubbers are essentially high molecular weight liquids with the ability to adjust their segmental configurations rapidly over significant distances (>0.5-1 nm), and local volumes. Nevertheless, the rotational and translation motions of sorbed penetrants are rapid compared to the motions of the polymer. The limiting step in diffusion of small molecules (ex. CO_2, SO_2, propane) through the rubber involves the generation of a sufficiently large gap for the penetrants to move into, with subsequent collapse of the sorbed cage that previously housed the penetrants (Figure 2.7). This description emphasises the mutual nature of the diffusion process, since both the penetrants and the surrounding polymer segments tend to undergo an immediately translation in their positions as a result of the event. Given the overall mass of the polymer and the small fraction of the total chain involved in a diffusion jump by a small penetrant, this change is minimal, even for the polymer [7].
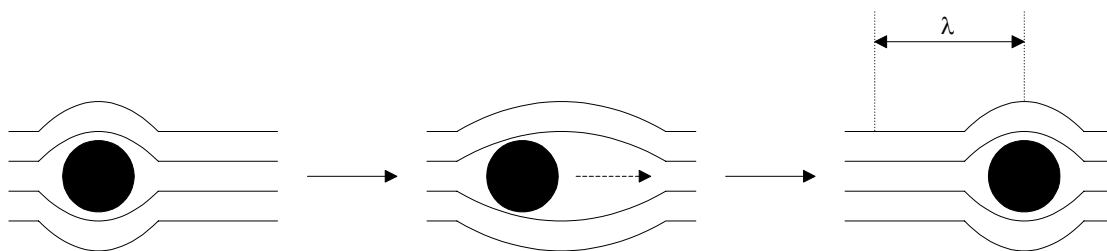
Figure 2.7: Generation of a gap for the penetrants with subsequent collapse of the volume that previously housed the penetrants [7].

Regions of crystallinity or points of chemical crosslinking affect the transport properties of a rubber causing restriction of swelling and suppression of long-range chain segmental motion. Semi-crystalline polymers, however, are more complex due to tortuosity caused by presence of typically impermeable crystalline regions.

Crystalline domains in rubbery is impermeable for even tiny gas molecules. This is confirmed by studies of gas sorption and transport. The solubility coefficient $(\bar{S_i})$ of both gases and low

activity vapours are essentially proportional to the volume fraction of amorphous material (Φ_a), and solubility coefficient for the totally amorphous material (S_a). The effects of crystallinity on the diffusion coefficient can be more complex than this simple volumetric exclusion, since crystallites may act not only as tortuous barriers, but also as effective restrictors of chain motion analogous to chemical crosslinking [7].

2.2.1 Sorption

Figure 2.8 schematically illustrates typical sorption isotherms plots of concentration versus pressure for polymer-gas systems. The solubility, S, in glassy polymers will usually show non ideal behaviour with sorption isotherms like the ones shown schematically in Figure 2.8b. The non-ideal behaviour describes a system where both solubility and diffusivity is concentration dependent, and the dual-sorption model may describe the sorption. In the dual-sorption model the concentration of the gas, Figure 2.8c, may be expressed by a combination of Henry's law and Langmuir absorption.

$$c = c_d + c_h \qquad\qquad (2.11)$$

$$c = k_d\, p + \frac{c'_h\, bp}{1 + bp} \qquad\qquad (2.12)$$

where p is the pressure, b is the affinity constant, k_d is the Henry's law constant c'_h is the saturation constant [1]. Rubbery polymers, crystalline and non-crystalline, are in focus in this work. Glassy polymers are thus not part of this study and the dual sorption model will therefore not be discussed any further.
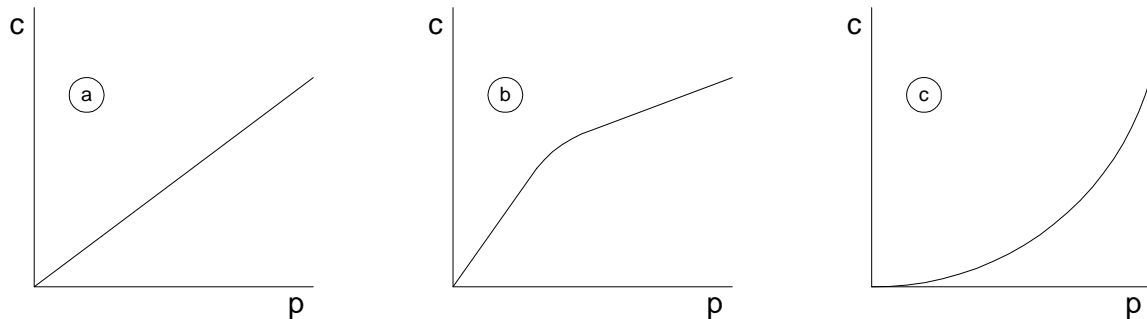
Figure 2.8: Sorption isotherms through a dense membrane a) ideal sorption according to Henry's law, b) dual sorption, c) non-ideal sorption [1].

The physical properties of the gas have great influence on permeation in such a way that large and easily condensable molecules will have high solubility coefficients and will permeate faster than small ones, and the selectivity for a gas pair may, in a rubbery polymer be the inverse to that of a glassy polymer.

The sorption of gases in rubbery polymers will be a linear function of solubility coefficient, S_i, and partial pressure p_i, according to Henry's law, see Figure 2.8a (for example, the sorption of N_2 and O_2 in PDMS will typically follow Henry's law). When strong interactions occur between a gas vapour or liquid and the polymer, the sorption isotherm is highly non-linear also in rubbery polymers. Free volume models and Flory-Huggins thermodynamics describes the transport through the polymer (see Figure 2.8c). This is relevant for the transport of Cl_2 through the polymers tested, and will be elaborated on in Chapter 6.

Linear sorption isotherms are obtained when the penetrant solution obeys Henry's law, that is:

$$S(c_i) = S(0) \quad \text{(constant)} \tag{2.13}$$

where S(0) is the solubility coefficient at the limit zero pressure. This is usually the case when the temperature is higher than the critical temperature of the gas T_{crit} ($T > T_{crit}$). On the other hand, isotherms that are convex to the pressure axis are observed with gases that exhibit high solubility in the polymer and plasticise the polymer at higher pressures. This is the case when T is close to T_{crit} or lower ($T < T_{crit}$) and the sorption isotherms is described by the Flory-Huggins equation

$$\ln(p / p_{vap}) = \ln(\upsilon) + \ln(1 - \upsilon) + \chi(1 - \upsilon)^2 \tag{2.14}$$

where p is the pressure of the gas, p_{vap} is the vapour pressure at the temperature, v is the volume fraction of the dissolved gas, and χ is the Flory-Huggins parameter. This equation reduces to the exceptional form when the penetrants concentration is low [3].

$$c / p = \left[S(0) \exp(\alpha c) \right] \tag{2.15}$$

where α is a constant that characterise the concentration dependency.

The temperature dependence of the solubility coefficient over small ranges of temperature can be represented by the van't Hoff-type relation:

$$S = S_0 \exp(-\Delta H_s / RT) \tag{2.16}$$

where S_0 is a constant and ΔH_s is the enthalpy of solution (the heat of solution). (The S_0 given here should not be confused with S(0) in equation 2.13 which represents the solubility coefficient at zero pressure (eq. 2.13)). The solubility of the penetrant gases in polymers commonly decreases with increasing temperature; that is the solution process is exothermic; hence, ΔH_s is generally negative. However, ΔH_s also depend on the nature of the polymer, and the sign for smaller gases, such as H_2, He and Ne, is often positive. The solubility of different gases are determined largely by their critical temperatures or other related measures of tendency to exist in a condensed phase such as boiling points or Lennard -Jones potential, ε/k (where ε is potential energy constant and k is Boltzman constant) (Figure 2.9). The Lennard-Jones potential increases with increasing T_{crit}, and T_{crit} can be a scaling factor for the solubility. When the solubility coefficient is pressure dependent, S(0) expressed in eqs. 2.14 or 2.15 are usually used for S in eq. 2.16 [1, 3].
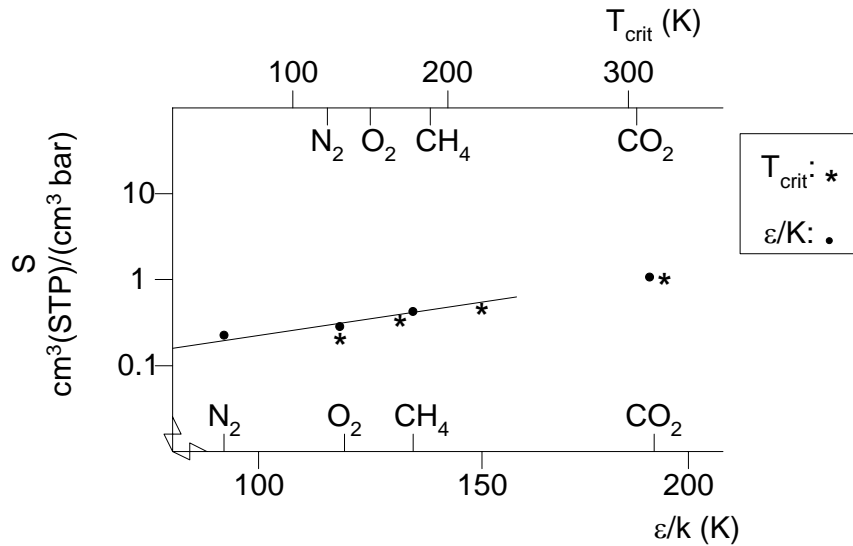
Figure 2.9: Solubility of various inert gases in silicone rubber (PDMS) as function of critical temperature (T_{crit}) and Lennard-Jones potential (ε/k) [8].

2.2.2 Diffusion

The other factor affecting the permeability is the diffusivity. The diffusion coefficient depends mainly on two factors: the molecular size of the gaseous penetrant and the choice of the polymer. The size of the gas molecule is reflected in the diffusion coefficient, i.e. the smaller the size the higher the diffusion coefficient. Diffusion coefficients of penetrants can usually be determined from both permeability measurements and independent sorption measurements, from absorption and desorption kinetics.

In rubbery polymers, diffusion coefficients of small and less soluble penetrant gases with low T_{crit}, such as He, H_2 and Ne, are essentially independent of pressure (concentration) at ambient temperature:

$$D(c) = D(0) \quad \text{(constant)} \tag{2.17}$$

The low solubility of such gases is due to their weak interactions with the polymer. On the other hand, diffusion coefficients of penetrant gases of higher T_{crit}, such as organic vapours, are strongly dependent on concentration and can be linear or exponential functions of penetrant concentration, as shown in Figure 2.10 (a) and (b) respectively, or may be a more complex function of concentration.

$$D(c) = D(0) \exp(\alpha c) \tag{2.18}$$

$$D(c) = D(0)\,(1 + \beta c) \tag{2.19}$$

where D(0) is the diffusion coefficient in the zero-concentration limit and α and β are constants characterising the concentration dependence.
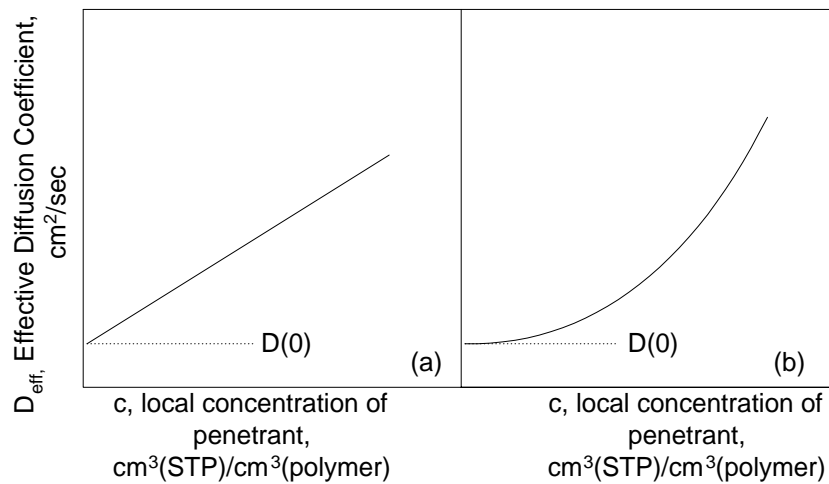
Figure 2.10: Schematic representation of typical concentration dependent forms for diffusion coefficients. Typical for (a) gas-rubbery polymer systems, (b) vapor-rubbery polymer systems [3].
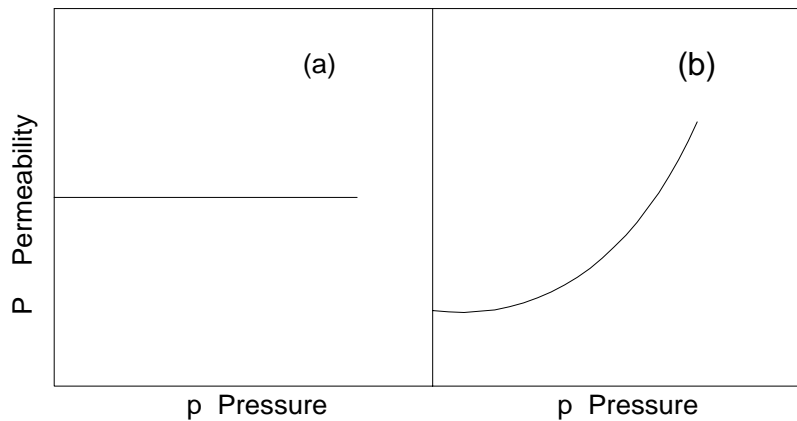
Figure 2.11: Schematic representation of some pressure-dependent forms of permeability coefficients. a) Typical for gas-rubbery polymer systems, b) vapor-rubbery polymer systems [3].

The product of gas diffusivity D(c) (described by eqs. (2.17)-(2.19)) and solubility S(c), (described by eqs. (2.13)-(2.15)) expresses the pressure dependences present in Figure 2.11(a) and (b). The relations are commonly observed for gas permeability in rubbery polymers.

The mutual diffusion coefficient of many penetrant gases in rubbery polymers exhibits exponential temperature dependence over a limited range of temperatures

$$D = D_0 \ \exp(-E_d / RT)$$

(2.20)

where D_0 is a pre-exponential factor and E_d is the apparent activation energy for diffusion. For highly soluble penetrant gases, such as organic vapours, the effective diffusion coefficient is strongly concentration dependent, and may increase or show a more complex form with increasing concentration.

2.2.3 Permeability

Permeability is dependent both on solubility and diffusivity (eq. 2.5). The temperature effect of the permeability coefficients for small non- interactive gases is mainly determined by diffusion since the solubility does not change so much with temperature. In this case the temperature dependency of permeability and diffusivity are about the same. For the larger molecules the situation is more complex since diffusion and solubility is opposing. Furthermore, both parameters are concentration dependent and should be considered from component to component [1].

$$P = D_0 S_0 e^{\frac{-(\Delta H_s + E_d)}{RT}} = P_0 e^{\frac{-E_p}{RT}} \qquad (\,2.21\,)$$

Some aspects of permeability dependency are given below

1. As the gas permeability of a polymer decreases, its selectivity to different gas pairs generally increases. This is the well-known "inverse" permeability /selectivity behaviour which is often mentioned in the membrane literature.

2. With exception (for example poly(trimethylsilylpropyne), the polymers that exhibit a high permeability and a low selectivity are in the "rubbery" state at ambient temperature, i.e., their glass-transition temperature, T_g, is lower than the ambient temperature. By contrast, the polymers with a low permeability but a high selectivity are in the "glassy state", i.e., their T_g is above ambient temperature.

3. Small molecular size and high critical temperatures of permeating gases tend to give high permeabilities. Small molecular size yields high diffusion coefficients, while high critical temperatures promote higher solubility in the membranes [4].

2.3 Special considerations for gas transport through polymeric membranes

2.3.1 Plasticisation and hydrostatic effects

At high partial pressures plasticisation may occur when a permeating gas exhibits a high chemical affinity for the polymer.

Plasticisation is typically an unfavourable phenomenon in the separation applications because permselectivity is reduced as the diffusivity of a slower penetrant is increased. In the case of gases, plasticisation phenomenon is suppressed due to hydrostatic compression in some polymers despite rather high sorption levels. Analysis in terms of the free-volume approach requires consideration of the compressibility of the rubbery matrix. In fact, exposure to hydrostatic pressure of low solubility gases such as helium or nitrogen may actually compress out free volume thereby reduce the ability of polymer segments to open gaps for movement of other segments or sorbed penetrants [7].

The critical temperature (T_{crit}) is a measure of the ease of condensation. Below a certain temperature (the critical temperature T_{crit}) the gas can be liquefied, simply by increasing the pressure. Under theses circumstances the volume is reduced and the molecules are compressed so close together that condensation occurs. Both the critical temperature and the solubility of gas in polymer increase as the molecular dimensions increase. Gases with low

critical temperatures (He, N_2) show a decrease in permeability with increasing pressures, while the permeability is increasing with increasing pressure for gases with high critical temperatures (CO_2, C_2H_4) in a rubber polymer. For methane with an intermediate critical temperature, the permeability shows negligible pressure dependence [7]. Two competing effects can explain these results. For nitrogen a decrease in the diffusion with increasing pressure indicate that the free volume of the polymer is reduced due to nitrogen's hydrostatic pressure. At higher nitrogen pressures the solubility is sufficient to oppose the compressive effect and cause the diffusivity to start increase with pressure as free volume is added by the penetrant. For methane and carbon dioxide a slight decrease in diffusivity with increasing pressure is observed, but both gases regain their original diffusivity at higher pressures due to their high solubilities. Ethylene exhibits an immediate increase in the diffusivity with pressure that is not surprising given its significant solubility and the large dilation in volume with increasing ethylene pressure. The two competing factors that determines the volume dilation of the polymer are (1) the sorption of gas into the polymer that results in an increase in free volume; and (2) the hydrostatic pressure on the film that reduces the free volume The second effect is usually small and is overcome for gases that have significant sorption levels. The net result of these two opposing effects determines whether the permeability (and diffusivity) will increase or decrease with increasing pressure [7, 9].

Transport plasticisation is defined as significant increase in the diffusivity of a penetrant due to facilitation of local polymer segmental motion caused by another penetrant molecule in its neighbourhood. This definition applies both to the increase in the diffusivity of a penetrant caused by the presence of its own kind and that due to increases caused by a different component. Even for pure component penetrants, a detailed fundamental analysis of this phenomenon on a molecular basis has not been achieved; however various free-volume analyses are available [7].

2.3.2   Crosslinking

To avoid swelling, crosslinking is of vital importance. Crosslinking occurs via chemical reaction, the chains being connected together by covalent bonding and joined together to form a three-dimensional network. One characteristic is that the polymer then becomes insoluble. Crosslinking has large effect on physical, mechanical and thermal properties of the resulting polymers. Improvements are most significant above the glass transition temperature. Creep compression and relaxation are generally improved on crosslinking. Among other properties thermal expansion and heat capacity are lowered, and heat distortion temperature, tensile strength, and refractive index are raised. Glass transition temperature increases with increasing crosslinking density.

The poly(dimethylsiloxane) (PDMS) studied in this work is crosslinked to different degrees to see if it changes in the membrane properties.

A simple crosslinking reaction is exemplified in Figure 2.12 by polymer chains with several functional groups designated A that are capable of reacting among themselves to form chemical bonds A-A. If these polymer chains are exposed to conditions such that the functional group react, then all the chains in the reaction vessel will tie each other through A-A bonds. In principles the polymer molecules in the reaction vessel will have formed one giant molecule [10].

In the example above the macromolecules were self-reacting, but this is not necessary for network formation. Crosslinking can be brought about by (1) vulcanisation, using peroxides, sulphur, or sulphur-containing compounds; (2) free radical reactions caused by ionising radiation; (3) photolysis involving photosensitive functional groups; (4) chemical reactions of labile functional groups; or (5) columbic interactions of ionic species [5].

linear polymer

crosslinked polymer
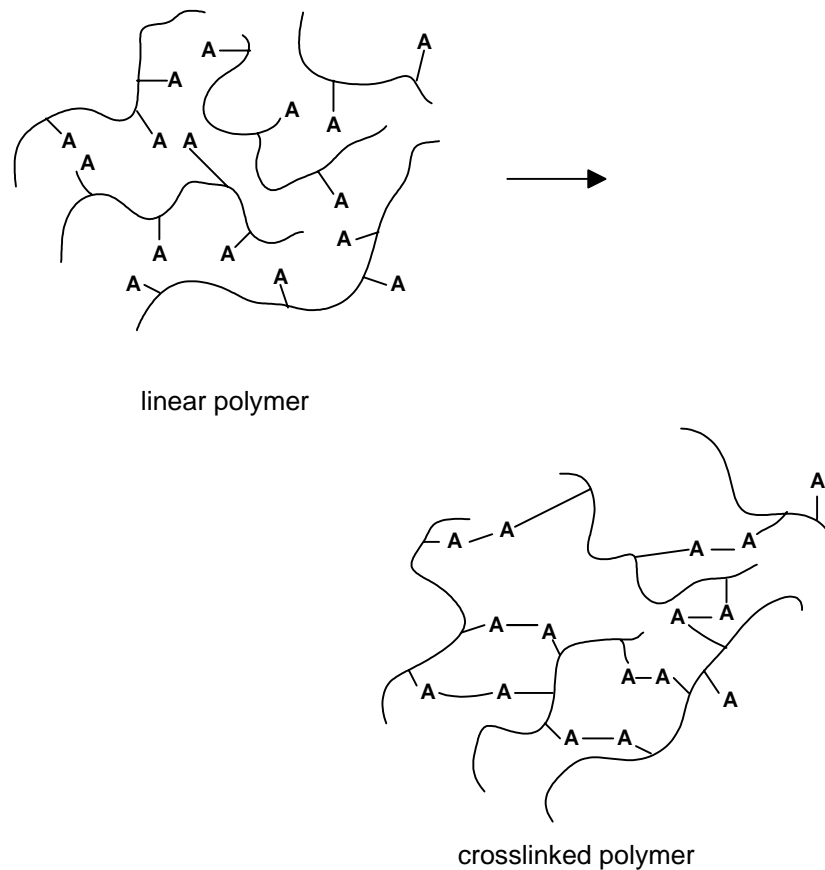
Figure 2.12: Illustrating crosslinking between the functional groups A between linear polymers [10].

In silicone rubber technology, high-temperature peroxide crosslinking, platinum-catalysed hydrosilylation, and moisture-sensitive hydrolysis curing are well known techniques for vulcanisation [11].

The crosslinking density in polymer networks is usually estimated throughout solvent absorbency (swelling) measurements. An alternative method for estimating the crosslinking density is based on the change in the heat capacity of the polymer by crosslinking [12].

References to Chapter 2

1. M. Mulder; Basic Principles of Membrane Technology, 2nd Ed., Kluwer Academic Publishers, The Netherlands 1996.
2. R. E. Kesting, A. K. Fritzsche; Polymeric Gas Separation Membranes, John Wiley & Sons Inc., USA 1993.
3. N. Toshima; Polymers for Gas Separation, VCH Publishers (UK) Ltd., USA 1992.
4. S. A. Stern; Review Polymers for gas separation: the next decade, J. Membr. Sci., vol 94 p. 1-65, 1994.

5.   M. P. Stevens; Polymer Chemistry: an introduction, 3rd Ed., Oxford University Press Inc., USA 1999.

6.   J. M. Charrier; Polymeric Materials and Processing, Hanser Publisher, Germany 1991.

7.   Mark, Bikales, Overberger and Menges; Transport Properties in Encyclopaedia of Polymer Science and Engineering, Suppl. vol., 2nd Ed., John Wiley & Sons Inc., p. 724 - 799, USA 1989.

8.   P. J. Flory; Principles of Polymer Chemistry, Cornell Univ. Press, Ithaca, Chapters 12 and 13, New York, 1953.

9.   S. M. Jordan; The Effects of CO_2 exposure on permeation behaviour in Si-Rubber and glassy polycarbonates, Ph.D. dissertation, University of Texas 1988.

10.   S. S. Labana; Crosslinking in Encyclopaedia of Polymer Science and Engineering, Suppl. vol., 2nd Ed., p. 213-216, John Wiley & Sons Inc., USA 1989.

11.   H. Inoue, K. Matsukawa; Thermal Cross-linking of Chlorinated Polydimethylsiloxane-Poly (vinyl chloride) blends, J. Appl. Polym. Sci., vol. 46, Nr. 2, p. 363-368, 1992.

12.   R. Vera-Graziano, F. Hernandez, J. V. Cauich-Rodriguez; Study of Crosslinking, Density in Polydimethylsiloxane Networks by DSC, J. Appl. Polym. Sci., vol. 55, p.1317-1327, 1995.

Chapter 3: The Selected Membrane Materials

Summary

For the separation of chlorine/oxygen several polymeric materials were considered. Criteria for the material selection were that the membrane should have a reasonably high permeability for either chlorine or oxygen, and a high selectivity for this gas pair. The membrane should be chemical resistant to chlorine and be thermally and mechanically stable. The gases should preferably not plasticise the material.

In previous studies poly(dimethylsiloxane) (PDMS) was found to show nice initial separation properties for chlorine/oxygen [1]. Based on these findings the durability of this membrane with respect to chlorine exposure and temperature was studied.

Other polymeric materials have also been evaluated for the separation of chlorine/oxygen. These materials were Fluorel (copolymer of vinylidenefluoride and hexafluoropropylene), Fluorosilicone, and blends of PDMS and Fluorel.

In this chapter the selected polymer materials are presented. Also the support material is presented, since the durability of the support may influence the total durability of the membrane.

3.1   Poly(dimethylsiloxane) (PDMS)

Silicones consist of a silicon-oxygen backbone with organic groups (R) attached to the silicon atoms by silicon-carbon bonds. In commercial silicones most R groups are methyl; longer alkyl chains, fluoroalkyl, phenyl, vinyl or a few other groups are substituted for specific purpose. Silicones have an unusual list of properties. Primary among these are thermal and oxidative stability and physical properties little affected by temperature. Other characteristics of silicones include high degree of chemical stability, high gas permeability, and low surface tension. As the general formula implies, the molecular structure can vary considerably to include linear, branched, and crosslinked structures. These structural forms and the R groups provide many combinations of useful properties that lead to a wide range of commercially important applications [2]. In this section only poly(dimethylsiloxane) (PDMS) will be discussed.

3.1.1   Properties

Poly (dimethylsiloxane) with structural formula as given in Figure 3.1 is a polymer in its rubbery state with low glass transition temperature (T_g = -123°C) and low crystallisation temperatures (T_c = -40°C). The basic properties for PDMS, as stated by Clarson and Semlyen [3], include thermal stability and high permeability to small molecules, organic vapours and gases with high critical temperatures. PDMS also exhibits properties like low surface tension and a low solubility parameter. These unusual combinations of properties made PDMS a natural first choice for the separation of Cl_2/O_2, where Cl_2 would be the fastest permeating component. Some of the key properties of PDMS are summarised in Table 3.1.
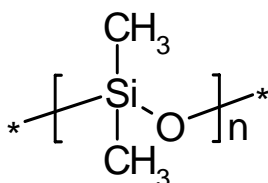
Figure 3.1: Structural formula for PDMS.

The origin of many of the properties listed below for PDMS lies in the strength and flexibility of the silicone bond, its partial ionic character and the low interactive forces between the methyl groups [3]. The siloxane chain is very flexible and bending and torsional movement around the Si-O axis is fairly free, especially with small substituents, e.g., methyl, on the silicon atoms. Rotation is also free about the Si-C axis in methylsilicone compounds. As a result of the freedom of motion, the intermolecular distances between methyl-siloxane chains are greater than between structurally related hydrocarbons, and intermolecular forces are smaller. The small rotational barriers contribute to properties such as low modulus[4], low glass transition temperature, and high permeability [2].

Siloxane bond (Si-O) energy (445 kJ/mole) is higher than both the carbon-carbon bond (346 kJ/mole) and the carbon-oxygen bond (358 kJ/mole). The extra energy required to dissociate a siloxane bond has thus much to do with the thermal stability of silicones. The carbon-silicon

---

[4] Modulus is the ratio between the applied stress and the corresponding deformation.

bond of 306 kJ/mole is thus less than the above values. Practical experiments shows a methyl group on silicon in PDMS is more thermally and oxidatively stable than a methyl group that is part of a hydrocarbon chain. This is attributed to the polarity or degree of ionic character of the siloxane chain. Silicon-oxygen interatomic distance is considerably smaller than the sum of the atomic radii and this is attributed to a resonance type structure having both polar and covalent bond character. This is an expected consequence of the unsymmetrical bond with relatively large differences in electro negativities of silicon and oxygen. The electro negativity difference of 1.7, results in a polar or ionic bond contribution of 41%. The silicon being the positive member, acts as an electron drain somewhat polarising the methyl group and rendering it less susceptible to attack than its bond energy would suggest [3].

The surface tension of PDMS (σ = 20 mN/m at 20°C) is at least 10 mN/m lower than most common organic polymers [3].

The wide range of commercial applications for linear PDMS result from its special properties. These include high chemical and thermal stability and low toxicity. Some examples of the commercial applications of linear PDMS are as follows: rubbers, resins, water repellents, release agents, dielectric fluids, antifoams, polishes, lubricants, and medical and pharmaceutical uses [3].

Table 3.1: Properties of poly(dimethylsiloxane) [2, 3, 4].

Crystallisation temperature	-40/-50°C
Glass Transition Temperature	-123°C
Density (25°C)	0.977 kg/m^3
Refractive Index (25°C)	1.40
Surface Tension (25°C)	21 mN/m
Dielectric constant (100Hz)	2.86
Tensile strength, (25°C)	2.4 MPa
Elongation, (25°C)	400 %
Si-C Bond Energy	282 kJ/mol
Si-C Bond Length	190 pm
Si-O Bond Energy	447 kJ/mol
Si-O Bond Length	164 pm
Si-O-Si Angle	120-145°C

3.2   Fluorel; a Fluoroelastomer

If linear perfluorocarbon[5] macromolecules are crosslinked, they do not exhibit elastomeric properties at ambient or lower temperatures because of severely restricted rotation about the carbon-carbon bonds and the consequent lack of alternative conformations. Thus, a tetrafluoroethylene (TFE) homopolymer cannot be an elastomer even if it has no crystallinity in the temperature range mentioned [5]. Elastomers require low levels of crystallinity. Polymers prepared from, for instance, vinylidenefluoride (VDF) have low glass transition temperatures but are crystalline. Amorphous elastomers are obtained by copolymerising with monomers possessing a bulky side group attached to the vinyl group [6].

Alternating difluoromethyl and methyl groups are the principal structural feature of vinylidenefluoride (VDF). This polymer has a sufficiently low T_g (-40°C) for elastomeric

---

[5] Full fluorinated polymer chains are called perfluorinated polymers.

properties, but very strong intermolecular forces causes crystallisation and, thus, restricted conformational freedom. Because of these properties of the homopolymers, most fluorocarbon elastomers are based on structures that interrupt this crystallinity and yet benefit from the low T_g of short VDF sequences. For example copolymerisation of VDF and hexafluoropropylene in the molar ratio of 3.5:1 respectively produces a fluoroelastomer with no crystallinity and a T_g of about -20°C. This structure is shown in Figure 3.2 (60 wt% VDF is the basis of the fluorocarbon elastomer industry) [5].

$$-\!\!-\![(CF_2CH_2)_m(CF_2CF)_n]\!-\!\!-$$
$$|$$
$$CF_3$$
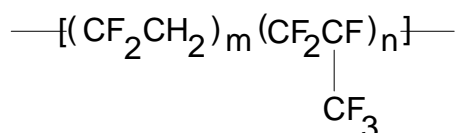
Figure 3.2: Structural formula of the copolymer vinylidenefluoride-hexafluoropropylene. Trademarks Fluorel™ is from 3M and Viton™ from DuPont.

3.2.1   Properties

Fluorine containing elastomers are designed to maintain rubber-like elasticity in extremely severe environments at high temperature and in contact with various chemicals.

At service temperatures above 0°C, non-crosslinked elastomers are highly viscous, incompressible liquids. To prevent permanent flow deformation under an imposed force and to develop reversible elastic properties, these flexible macromolecules must be crosslinked. In general crosslinking is performed chemically by vulcanisation to produce thermo set elastomers networks. However, physical crosslinking by crystallisation of hard segments in segmented or grafted copolymers can also provide a network structure in so-called thermoplastic elastomers [6].

Increased fluorine levels, as expressed with a higher glass transition temperature are affecting low temperature performance. Fluoroelastomers withstand higher temperatures better than all other elastomers with exception of perfluoroelastomers [6].

Vinylidenefluoride based polymers are the largest group of fluoroelastomers in terms of production volume and variety. Their properties serve as a standard for comparing other fluoroelastomers (fluorosilicones) that may be superior in certain respects such as low temperature flexibility, but are less satisfactory at high temperatures and in destructive fluids. Physical properties of fluoroelastomers are given in Table 3.2.

A standard VDF/HFP dipolymer when exposed to ASTM oil no. 3 for 168 hours at 150°C swells only 1.7 vol% compared to up to 20 vol% for HNBR (hydrogenated nitrile rubber) elastomers and up to 30 vol% for fluorosilicone. They also show extremely low permeability to a broad range of substances, and is thus suited as seals. They have excellent resistance to atmospheric oxidation and sunlight. They are also more resistant to burning than hydrocarbon rubbers. However solvents like esters and ketones may dissolve the polymer.

VDF/HFP elastomers contain about 60 wt% VDF (roughly 3.5 moles of VDF for each mole of HFP). Such polymers are commercially produced over a wide range of molecular weight. They can be cured with polyamines and polyols, yielding products with good resistance to chemicals at high temperatures. They are used in compression, transfer and injection molding

for the production of O-rings, valve stem seals and shaft seals, in extrusion for fuel hose and tubing, and in solution coatings for fabrics, tanks and chemical containers [6].

Table 3.2: Physical properties of VDF/HFP fluoroelastomer [4, 6, 7, 8].

Crystallisation temperature	not given
Glass Transition Temperature	app. -20°C
Density (25°C)	1.77-1.91 kg/m^3
Refractive Index (25°C)	not given
Surface Tension PVDF	25 mN/m
Surface Tension PHFP	16 mN/m
Dielectric constant (100Hz)	5.56
Tensile strength	16 MPa*
Elongation	197 %*
C-C Bond Energy	360 kJ/mol
C-C Bond Length	153 pm
C-F Bond Energy	447-485 kJ/mol
C-F Bond Length	136 pm
C-H Bond Energy	413 kJ/mole
C-H Bond Length	110 pm
C-C-C Angle	109.5°

* Given for VITON® A-500

3.3   Blends of PDMS and Fluorel

In search for new polymeric materials, mixing of two or more polymers has attracted much interest as a means of arriving at new property combinations without having synthesised novel structures. A major feature encountered when two polymers are mixed is that in the majority of combinations the components tend to phase separate to form heterogeneous mixtures that do not exhibit enhanced properties. Only in a limited number of cases do amorphous polymers blend to form one-phase mixtures.

The miscibility of a mixture is determined by the Gibbs free energy of mixing ΔG_M that is related to the entropic ΔS_M and enthalpic ΔH_M components through the relation:

$$\Delta G_M = \Delta H_M - T\Delta S_M \qquad\qquad (3.1)$$

If the system is to be miscible then ΔG_M should be negative [9].

3.3.1   Properties

Yoshida have compared properties of silicone rubber and fluoroelastomer with the ones obtained for silicone rubber/ fluoroelastomer composite. These properties are given in Table 3.3. Fluoroelastomers have excellent heat and oil resistance. Unfortunately, they have poor flexibility at low temperatures. The silicones have good low temperature resistance. Making a composite of these two materials can enhance properties of each polymer. The resulting silicone/fluoroelastomer composite demonstrates better low temperature flexibility than do to fluoroelastomers on their own, as well as superior oil-resisting properties to silicone rubbers [10].

Table 3.3:Comparisons of mechanical properties of silicone rubber, fluoroelastomer, silicone rubber/ fluoroelastomer composite and fluorosilicone [10].

	Silicone rubber	Fluoro-elastomer	Silicone/ Fluoroelastomer	Fluoro-silicone
Brittleness temperature (°C)	<-60	-15	<-60	<-60
Low temperature flexibility (°C) (Gehman torsion T10)	-51	-14	-19	-63
Tensile strength (MPa)	8,8	12,6	8,9	8,0
Elongation (%)	160	230	380	270
Hardness	77	69	70	66

3.3.2   Miscibility of fluoropolymer/silicone rubber blend

Silicone polymers usually have poor miscibility with other polymers. Therefore, phase separation readily occurs, and the silicone polymers are mainly accumulated on surfaces because of their low surface energy. In order to avoid surface migration of the silicone components due to phase separation, introduction of chemical bonds between two or more polymers is preferable to fix their dispersion states just after dynamic mixing. Crosslinking is a useful method to chemically fix two or more polymers [11].

All known fluoroelastomer/silicone blends are facing two main problems
1. Principal because the rubbers are totally immiscible.
2. The polymers show different crosslinking behaviour and crosslinking takes place preferably within their pure phases. Co-vulcanisation occurs just in secondary degree.

The aim is to produce chemical bonds to connect fluoropolymer and polydiorganosiloxane to form a homogenous polymer phase with a uniform glass transition temperature, placed between the glass transition temperatures of the individual polymers.

Fluoropolymer with olefin double bond side groups, as given in the following equation, can be mixed with polyorganosiloxane:

$$F\text{-}Polymer\text{-}X\text{-}CH=CH_2$$
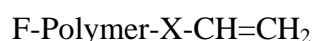
The Si-H addition of unsaturated carbon-carbon bond is carried out by thermal, radical and/or noble metal complex catalysis in solution or substance. The Si-H addition is given in the following schema:

$$P\text{-}X\text{-}CH=CH_2 + \text{-}Si\text{-}H \rightarrow P\text{-}X\text{-}CH_2\text{-}CH_2\text{-}Si\text{-}$$

Vulcanisation occurs either in one step, in which the Si-H addition itself is used to build up the network (crosslinks), or in connection to the Si-H, addition gives fluoropolymers grafted with silicone. This gives a fluoropolymer blend with special characteristics. Suitable fluoropolymers have side groups with double-bonds which are obtained through copolymerisation of fluoromonomere with small quantity of the suitable monomer with at least two vinyl groups, like alkenylisocyanurate. These monomers must be able to flow and not be in a crosslinked state, and thus not be withheld in the polymer network.

A suitable catalyst for the addition of Si-H to the double bonded carbon-carbon bond is platinum complex catalyst [12].

Silicone/fluoroelastomer composites can be adopted into general use for various automotive applications, namely oil seals, O-rings, gaskets and various hoses [10].

3.4   Fluorosilicone

The loose term fluorosilicone means polymer containing C-F bonds rather than Si-F bonds. This latter functionality is however too reactive and has utility only in intermediates. Fluorinated carbon groups directly attached to silicone atoms are likewise insufficiently hydrolytically and thermally stable so no commercially promising fluorosilicone material can be totally fluorinated, there must be a hydrocarbon bridging group or spacer between the two entities. Thus the repeating structure of interest here is: $[R_fX(CH_2)_n]_y(CH_3)_x(SiO)_z$. The X group is a consequence of the chemistry chosen to link the R_f fluorocarbon group to hydrocarbon spacer. It can be oxygen or sulphur, for example, but is not present in commercial materials. The R_f group could be linear or branched, aliphatic or aromatic, but in practice has been limited to the CF_3 group until recently when longer aliphatic groups such as $CF_3(CF_2)_3$ have been introduced. The length of the hydrocarbon spacer, n, is optimally two. Any longer and the fluorocarbon benefits are diluted. If the spacer is shorter (n=1) similar hydrolytic and thermal deficiencies arises as when n is zero. When z is two and x and y are unity, linear polymers that are usually fluids [6]. The structural formal of the fluorosilicone used in this thesis is given in Figure 3.3:
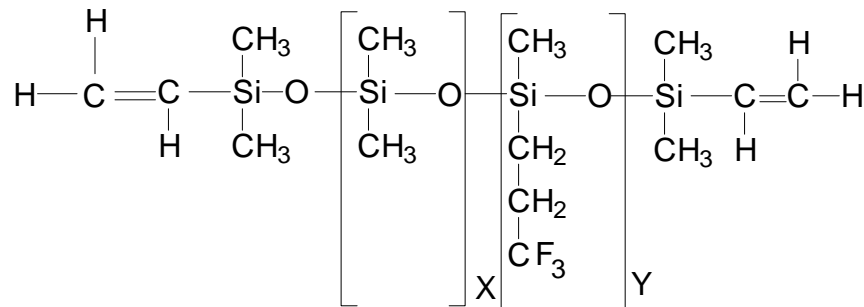
Figure 3.3: Structural formula of fluorosilicone.

3.4.1   Properties

The most important properties of fluorosilicone rubbers from a technical point of view are [13]:

- a wide thermal range of applications from -60 to +230°C
- resistance to weathering and ozone
- little change to the physical constants in relation to temperature
- high elasticity
- good dielectric properties
- hydrophobic behaviour (water-repellent- but not as pronounced as with silicone rubbers)
- easy to separate (adhesion to sticky surfaces slight or non-existent)
- excellent resistance to mineral oils, fuels and solvent

The wide temperature range of fluorosilicone rubber makes it interesting for many commercial applications. In particular its resistance to oil and aggressive solvents is of

interest to the oil refining industry, plastics and chemical industries. Because of its excellent dielectric properties in conjunction with its resistance to aggressive media, the electrical engineering industry places great value on fluorosilicone rubber [13].

Table 3.4: Properties of Fluorosilicone [3 , 4, 6].

Crystallisation Melting Point	not found
Glass Transition Temperature	- 75°C
Density (25°C)	1.35-1.65 kg/m^3
Refractive Index (25°C)	not found
Liquid Surface Tension (25°C)	24.4 mN/m
Dielectric constant (100 Hz)	6.85
Tensile strength	8.0 MPa
Elongation	480 %

3.5   Comparing three materials

The most attractive characteristics of silicone elastomers are (a) the retention of many desirable properties over a wide range of temperatures, (b) their good resistance to thermal oxidation and (c) their flexibility at very low temperatures. The mechanical strength of silicone elastomers, however, even when reinforced by inorganic fillers, is generally low and they exhibit also a rather low resistance to both polar and non-polar solvents [14].

In contrast to silicones and fluorosilicones, fluorocarbon elastomers display a better oil and solvent resistance and mechanical strength, but exhibit a much higher T_g and, consequently, they display inferior low temperature elastomeric properties. Furthermore the lack of crystallinity in fluorocarbon elastomers, usually copolymers and terpolymers of vinylidenefluoride with hexafluoropropylene and/or tetrafluoro-ethylene, can only provide a limited resistance to polar solvents [14].

Fluorine in fluoropolymers is almost always present in partial or complete replacement of hydrogen in hydrocarbon groups. Substitution of the larger, more electronegative fluorine atom for hydrogen generally decreases solubility and surface energy increases thermal stability and resistance to chemical attack. It is the strong C-F bonds and the inaccessible of the carbon chain to potential reactants, which produces the thermal and chemical resistance of fluorocarbon polymers. However, silicone materials already have these advantages by virtue of their inorganic siloxane backbone so major enhancement of such properties on fluorine incorporation is not expected [6].

Table 3.5: The glass transition temperatures of discussed materials [3, 6, 15]

	Glass Transition Temperature, T_g, [°C]
Poly(dimethylsiloxane), PDMS	-123
Poly(vinylidenefluoride), PVDF	-35
Poly(hexafluoropropylene), PHFP	11
Poly(tetrafluoroethylene), PTFE	-130
Fluorel	-20
Fluorosilicone	-75

3.6   The support material

The membranes are delivered or made as a composite, and the durability of the support and substructure are of major importance when the membranes are exposed to aggressive media. Several materials were tested for this purpose in the author's master thesis [16]. Both poly(tetrafluoroethylene) (PTFE) and poly(vinylidenefluoride) (PVDF) is chemical and thermal stable and are mechanical strong. Microporous PVDF and PTFE were found to be suitable as substrate/support in a composite membrane where PDMS or other suitable selective polymers will be applied as a thin layer (2-10 μm).

3.6.1   Poly(tetrafluoroethylene) (PTFE)

The perfluorinated polymers are polyolefines that have been fully fluorinated. The strong carbon-fluorine (C-F) bonds, the crystalline structure and the relatively weak interaction between chain segments in the crystals, contribute to properties such as excellent chemical and thermal resistance. Fully fluorinated polymers exhibit unique properties for use in aggressive environments. PTFE is a straight-chain polymer of tetrafluoroethylene (TFE) of the general formula given in Figure 3.4.

$$-\!\!\left(CF_2CF_2\right)_{\!n}\!\!-$$
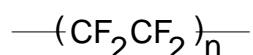
Figure 3.4: Structural formula of poly(tetrafluoroethylene)

The perfluorinated polymers are in general highly crystalline. This will greatly influence the transport of gases through the materials as increased crystallinity means a reduced effective permeation area, since the gases are basically permeating through the amorphous phase. A closely packed crystalline structure will correspond to unusually high material density [6,17].

Physical properties: The structure of PTFE chains are unusual because they are completely linear. The branching that occurs during free radical polymerisation of polyethylene cannot take place during the polymerisation of TFE. Furthermore, PTFE chains are stiffer than polyethylene chains because their fluorine atoms are larger than hydrogen atoms. Steric hindrance prevents a PTFE chain from assuming a planar zigzag structure; instead it is forced to adopt a zigzag structure with a helical twist along the chain axis. Crystals of PTFE are made up of chains with an 180^0 twist every 13 to 15 carbon atoms depending on the temperatures. The high melting point of PTFE (327^0C) is due to the small entropy change produced during melting, which in turn results from the stiffness of the chains [5].

The chemical bonding forces within the chains, and the polymer surface are unusual:

$$\begin{array}{cccccc}
F & F & F & F & F & F \\
| & | & | & | & | & | \\
-C-C-C-C-C-C- \\
| & | & | & | & | & | \\
F & F & F & F & F & F
\end{array}$$

⟵ C—F bond energy =481.3 kJ/mole

⟵ interchain energy =3.2 kJ/mole

$$\begin{array}{cccccc}
F & F & F & F & F & F \\
| & | & | & | & | & | \\
-C-C-C-C-C-C- \\
| & | & | & | & | & | \\
F & F & F & F & F & F
\end{array}$$

⟵ surface energy =18.6 mN/m
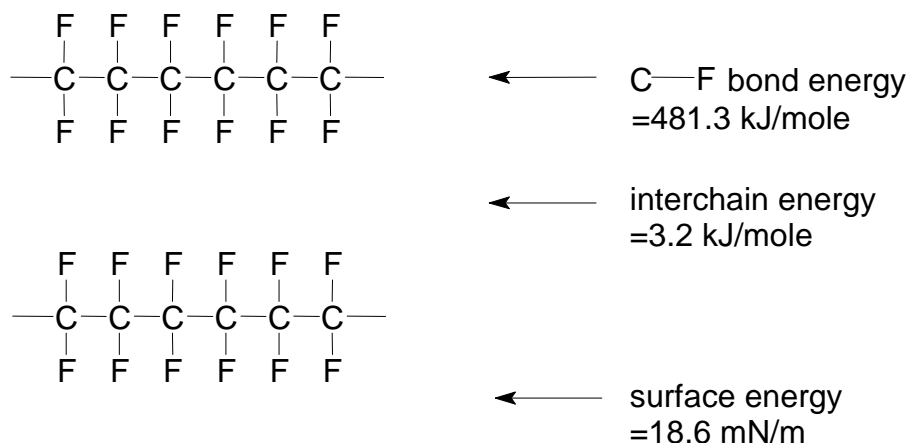
Figure 3.5: Illustration of the intra- and inter chain energy in PTFE [5]

The C-F bond energy is among the highest known. However, the interchain energy is very low. This combination of unusually strong and weak forces results in many unique properties.

Chemical Resistance*:* Poly(tetrafluoroethylene) is resistant to attack by most chemicals, including aqua regia, hot fuming nitric acid, hot caustic, gaseous chlorine, chlorosulfic acid, organic esters, ketones, and alcohols. The only materials known to attack PTFE are molten alkali metals, chlorine trifluoride and gaseous fluorine at elevated temperature and pressure.

Thermal stability*:* In both air and nitrogen PTFE has an extremely high thermal stability. Rate of decomposition are not measurable below ca. 440°C, decomposition rates are high at 540°C [5].

3.6.2   Poly(vinylidenefluoride) (PVDF)

Poly (vinylidenefluoride) (PVDF) is produced by the addition polymerisation of 1,1-difluoroethene ($CH_2=CF_2$). The homopolymer is characterised by alternating carbon-hydrogen bonds with carbon-fluorine bonds:

$$-(CH_2CF_2)_n-$$
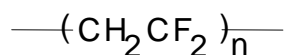
Figure 3.6: Structural formula of poly(vinylidenefluoride)

The structure of PVDF homopolymer is typically regular; however, some variability related to chain branching, head to head molecular formation and tail-to-tail molecular formation will exist depending on polymerisation method and reactant product [6].

Poly(vinylidenefluoride) (PVDF) is a linear, high molecular mass, semi-crystalline polymer that can exist in three distinct crystalline forms denoted as β(I) orthorhombic, α(II) pseudo-orthorombic) and γ(III) monoclinic [5].

The high crystallinity and surface tension properties of PVDF give the polymer very low permeation values. In inert gas testing directly comparing fluoropolymers, PVDF is generally

either the least permeable, or very close to the performance of the least permeable polymer. Degree of permeation has been linked to the polarity of the permeate and the substrate

Physical properties: Poly(vinylidenefluoride) has a highly regular structure; with most VDF units joined head to tail and with ca. 5% of the monomer joined head to head. Crystallinity is between 40 to 60%; three different crystalline forms exist. Because of its polymorphism, the melting point of PVDF is not precisely defined (154-184°C). The melting point of the more common phase II form is ca. 170°C; a glass transition temperature is observed at -40°C [5].

Chemical resistance*:* PVDF is resistant to a wide group of chemicals at high temperatures. Most acids and acid mixtures, weak bases, halogens, halogenated solvents, hydrocarbons, alcohols, salts, and oxidants pose little problem for PVDF up to and above 90°C for long-term use [6]. It is however, soluble in polar solvents such as acetone and ethyl, butyl, and amyl acetate [5].

Thermal stability*:* The thermal stability of PVDF is inferior to PTFE. PVDF has been found to undergo sensitised thermal decomposition by certain additives such as silica, titanium dioxide and antimony oxide. These inorganic compounds catalyse thermal decomposition of the polymer at temperatures above 375°C [6].

References to Chapter 3

1. M-B. Hägg; Membrane Purification of Cl_2 gas, I: Permabilities as function of temperature for Cl_2, O_2, N_2, H_2 in two different types of PDMS membranes, J. Membr. Sci., vol 170, p. 173-190, 2000.
2. B. Hardman, A. Torkelson; Silicones in Encyclopaedia of Polymer Science and Engineering, Suppl. vol., 2nd Ed., p. 1048-1055, John Wiley & Sons Inc., USA 1989.
3. S. J. Clarson, J. A. Semlyen; Siloxane Polymers, Ellis Horwood-PTR Prentice Hall, New Jersey 1993.
4. C. C. Ku, R. Liepins; Electrical Properties of Polymers-Chemical Principles, Hanser Publishers, Munich, Germany 1987.
5. J. Scheirs (Editor); Modern Fluoropolymers: high performance polymer for diverse applications, John Wiley & Sons Inc., Great Britain 1997.
6. D. P. Clarson, W. Schmiegel; Organic Fluoropolymers in Ullmann's Encyclopaedia of Industrial Chemistry, vol. A11, p.393-429, VCH Publishers, Germany 1994.
7. R. C. Weast (Editor); Handbook of Chemistry and Physics, 66th Edition, CRC Press Inc., USA 1986.
8. D. W. van Krevelen; Properties of Polymers, 3rd Ed., Elsevier Science Publishers B. V., The Netherlands 1990.
9. J M. G. Cowie; Miscibility in Encyclopaedia of Polymer Science and Engineering, Suppl. vol., 2nd Ed., p. 629-632, John Wiley & Sons Inc., USA 1989.
10. H. Yoshida; American Chemical Society Rubber Division, Article no. 22, 1989.
11. H. Inoue, K. Matsukawa; Thermal Cross-linking of chlorinated Polydimethylsiloxane-Poly (vinyl chloride) blends, J. Appl. Polym. Sci., vol 46, p. 363-368, 1992.
12. G. Langstein, R. Krüger, H. Alberts, H. H.Moretto; EP 0 582 841 B1, BAYER AG, Leverkusen, Germany 1994.
13. D. Klages, U. Raupbach; Fluorosilicone Rubber - a modern material, Gummi Fasern Kunststoffe, International Polymer Sci.and Tech., vol 22, No.5, p. T/11-T/13,1995.

14. L. Mascia, S. H. Pak, G. Caporiccio; Properties Enhancement of Fluorosilicone Elastomers with Compatibilised Crystalline Vinylidene Fluoride Polymers, Eur. Polym. J., vol. 31, No. 5, p. 459-565, 1995.
15. J. M. Charrier; Polymeric Materials and Processing, Hanser Publisher, Germany 1991.
16. M. Sørflaten; The Study of PDMS membrane with regards to material properties and degradation (in Norwegian), M. Sci. Thesis, Telemark University College, Porsgrunn, Norway 1996.
17. W. R. Vieth; Diffusion In and Through Polymers- Principles and Applications, Hanser Publishers, Munich, Germany 1991.

Chapter 4: Overview of Degradation and Stabilisation Mechanisms in General

Summary

This chapter presents an overview of degradation and stabilisation mechanisms of polymeric materials in general. Each material is presented with a description of its stability and possible routs of degradation focusing on the objectives for the work (presented in chapter 1.3).

4.1   General degradation mechanisms

The importance of degradation is largely determined by where the material is used. For polymers, degradation is frequently associated with chain cleavage and a decrease in molecular weight. However, in some cases, crosslinking can render a polymer brittle, whereas in other cases colour change is often objectionable but need not necessarily be accompanied by backbone scission. In broad terms, degradation usually involves a chemical modification of the polymer caused by its environment; a modification that often is (but not always) detrimental to the performance of the polymeric materials.

From the extensive study of degradation of many polymeric materials, a limited range of key degradative processes have been identified. From these reactions, it is possible to anticipate processes likely to be important in the deterioration of any new polymer system.

A meaningful comparison of the intrinsic resistance of polymers from different generic classes to a particular degradative process is difficult because of the wide range of test conditions, the sensitivity of polymers to trace impurities and additives, and the diverse physical forms of the polymers, i.e., thickness, shape, morphology, orientation etc. In addition, deterorientation may result from exposure to two or more combined processes. For example, photo deterioration is nearly always a combination of light attack and thermal oxidation. Resistance to thermal oxidation is particularly difficult parameter to determine because of the key role of impurities in trigging the deterioration [1].

4.1.1   Primary bond - scission reactions

All degradation processes originate from an initial bond-breaking reaction. This may represent the total extent of degradation, or it may be the prelude to a series of secondary chemical reactions leading to further bond scission, recombination, or substitution reactions [1].

Bond cleavage to give a free radical pair
Chemical bonds may be broken by energy input in the form of heat, radiation, mechanical action etc. (Figure 4.1). The near UV component of sunlight, i.e., ca. 280-390 nm, is energetic enough to cleave bonds with energies ≤ 400-300 kJ/mol, i.e., most single C-C links and many heteroatom links. Bond cleavage occurs provided that the light of the appropriate wavelength is absorbed [1].
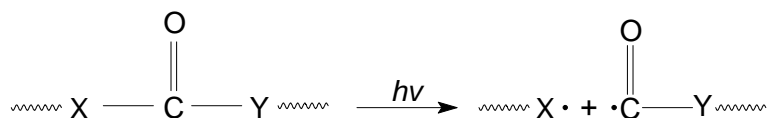
Figure 4.1: Bond cleavage to give a free radical pair [1].

Bond rearrangement to give molecular products
These may involve the heat- or light-induced cleavage of a backbone or side chain or rearrangement [1].

Figure 4.2 Bond rearrangement to give molecular product [1].

Ionic cleavage reactions

Many polymers containing heteroatoms in the backbone undergo ionic cleavage reactions. For example, amide, imides, urethane, urea, carbonate, and ester groups undergo a base, i.e. B^-, catalysed hydrolysis

Figure 4.3: Base catalysed hydrolysis [1].

Acid catalysed hydrolysis follows the general pattern:

Figure 4.4: Acid catalysed hydrolysis [1].

This reaction occurs for urethanes, amides, imides (X is N; Y is C=O), carbonates (X is O-C=O; Y is O), siloxanes (X is O; Y is Si), and acetals (X is O; Y is C) [1].

4.1.2   Secondary chemical reactions

Radicals from the primary process may take part in further reactions:

Self-reactions
Macroalkyl radicals may combine to give a crosslink, branch, or linear product or disproportionate.

Additional reactions
Radical chain ends may add to unsaturated groups present in the backbone and terminate the reaction.

Depolymerisation
Once a C-H bond is broken and a backbone radical is formed, scission of C-C links in the backbone adjacent to the radical site becomes much more favourable because of the 63-170 kJ/mol drop in C-C bond energy in the radical, as compared with the saturated backbone. A radical site on the chain end of an addition polymer may lead to a progressive depolymerisation, i.e., unzipping, with the generation of monomer (Y is H or other small group) [1].

Figure 4.5: A radical site leading to depolymerisation (Y is H or other small group) [1].

Chain reactions involving oxygen

At ambient temperatures the chemical structures of most polymers are quite stable against the attack of molecular oxygen (O_2). That oxidative degradation is a quite common phenomenon; notwithstanding is due to ease with which various initiating reactions occur. The most prominent modes of initiation refer to the generation of free radicals capable of reacting rapidly with O_2. The thermal decomposition of hydroperoxides is considered to be of outmost importance. Many hydroperoxides decompose at relatively low temperatures according to the following reaction [2]:

$$ROOH \rightarrow RO\cdot \; + \; \cdot OH \qquad\qquad (4.1)$$

·OH radicals are very reactive. They react with many organic substances with encounter controlled rate constants. Commonly they either abstract hydrogen atoms or undergo addition reactions. Regarding polymer degradation, H atom abstraction processes proceeding according to reaction (4.2) are most important:

$$RH \; + \; \cdot OH \rightarrow R\cdot + H_2O \qquad\qquad (4.2)$$

At sufficiently high oxygen concentrations, reaction will be followed by

$$R\cdot \; + \; O_2 \rightarrow ROO\cdot \qquad\qquad (4.3)$$

and

$$ROO\cdot \; + \; RH \rightarrow ROOH \; + \; R\cdot \qquad\qquad (4.4)$$

The two latter reactions correspond to the propagation steps of autooxidation processes [2].

4.1.3   Metal-catalysed degradation processes

Many commercial polymers contain metallic compounds as impurities or deliberately incorporated additives. The bulk of the latter types are pigments, whereas the former include polymerisation catalyst residues or debris from processing equipment [1].

Several investigators have demonstrated, for example, that residual polymerisation catalysts lower the thermal stability [3].

4.1.4   Thermal oxidation

Metal impurities arise through contamination from reaction or storage vessels and in certain cases they are remainders of polymerisation catalysts. Metal catalysts can affect the autooxidation process according to various mechanisms depending on experimental conditions, such as medium, type of metal salts, metal ion concentration, etc.

The main function of metal ions consists in including the decomposition of hydroperoxides by redox reactions, thus generating free radicals [2]:

$$M^{n+} + ROOH \rightarrow RO\cdot + OH^- + M^{(n+1)+} \qquad\qquad (4.5)$$

$$M^{(n+1)+} + ROOH \rightarrow RO_2\cdot + H^+ + M^{n+} \qquad\qquad (4.6)$$

4.1.5 Photo degradation

Organic polymers undergo chemical reactions upon irradiation with ultraviolet (UV) light, because they posses chromophoric groups capable of absorbing UV light. This fact is important because the spectrum of sunlight penetrating the earth's atmosphere contains a portion of UV light. Photoreactions are usually induced when organic polymers are subjected to outdoor exposures. In general, photoreactions in commercial polymers are harmful: they cause brittleness and colour changes. Photolytical reactions of special importance are UV light initiated oxidative chain reactions, i.e. autooxidative processes. It does not make any difference whether the initiation occurs via thermolysis, mechanical stress, chemical attack, or via photolysis with regard to the end products formed. An interesting phenomenon in photolytic oxidation of polymers is that additional chromophores are created during chain propagation. These chromophores can give rise to the initiation of new chain reactions upon prolonged irradiation and thus to rapid deterioration of the polymer [2].

At wavelengths below 300 nm hydroperoxides are photolytically decomposed:

$$ROOH + h\nu \rightarrow RO\cdot + \cdot OH \qquad\qquad (4.7)$$

The latter reaction is considered to be very important in the photo-initiated oxidation of many commercial polymers [2].

4.1.6 Polymer crosslinking and branching

Crosslinking and branching processes may be beneficial or destructive, depending on the end use envisaged. They are advantageous if heat deflection, creep and softening temperatures are to be raised, shrinkage memory is required, or molecular weights must be adjusted; but detrimental if flexibility and elongation are reduced [1].

4.1.7 Mechanical degradation

Electron-spin resonance spectroscopy has graphically demonstrated that stretching, milling, and any type of polymer shearing process produce free radicals as a result of main chain fracture. Mechanical work, thus, generates primary radicals, and oxidation follows to form the usual oxidation products [1].

4.1.8 Degradation by ionising radiation

The effects of ionising radiation are apparent in the deterioration of nuclear-power station components, sterilisation of medical supplies, controlled crosslinking, and radiation-initiated

graft polymerisation. The interaction of high-energy radiation with polymers leads to a cascade of very fast physical and physiochemical processes that culminate in the generation of free radicals and produce the detected products. Polymer sensitivity to radiation varies; for example, aromatic polymers are relatively resistant to γ-irradiation. Aliphatic polymers are damaged largely as a result of the postirradiation thermal oxidation.

Because radiation effects occur at random throughout a polymer, radicals are formed in crystalline phases as well as in the O_2-accessible amorphous regions.

Ionising radiation leads to crosslinking and branching of many polymers, although, it is complicated by the interfering effects of oxygen [1].

4.1.9 Molecular weight

Polymers tend to have a higher stability with increasing molecular weight although it is not immediately obvious whether this is due to more difficult diffusion of products from more viscous materials or a genuine indication of the involvement of chain ends [3].

4.1.10 Discolouration

The formation of discoloured material is difficult to explain. No investigations concerning the mechanism have been published. In thermo-oxidative degradation, discoloration increases with time, temperature, and oxygen content in the same general way as crosslinking and formation of volatiles.

The temperature at which the thermo-oxidative degradation is carried out plays an important role when structural changes and colour formation are concerned [4].

4.1.11 Evaluation of deterorientation

Spectroscopic methods are most informative for characterising the chemistry of degradation and have added advantage of being non-destructive.

IR and NMR spectroscopy are the most definitive techniques for the identification of degradation products. IR has a higher sensitivity than NMR, but less resolution. FT-IR offers the power of computer manipulation of spectra and enhanced signal to noise ratios that allow detection of low concentrations of products. The NMR technique has superb discrimination of differing functional groups, but is limited by low sensitivity

Gas chromatography and mass spectrometry have often been applied to the identification of volatiles from thermal and photo degradation. They can be particularly valuable in enhancing the quality of thermal analysis information.
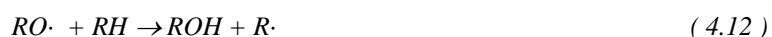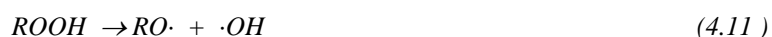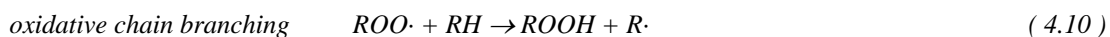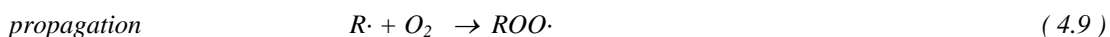
Thermal analysis techniques DTA, TGA, DSC, have been used to study polymer thermal decomposition.

Gel estimation and gel permeation chromatography give a direct estimation of crosslinking, branching, and chain scission processes [1].

4.2   Inhibition of degradation mechanisms

For many applications, stabilisers must be used to inhibit degradation to assure the required life expectancy. There are two general approaches to the stabilisation of polymers: structural modification and the use of additives. In the first case, the chemical structure of the polymer is modified to eliminate or reduce trace impurities or weak links. The second general approach to stabilisation involves additives blended into the polymer mass. A variety of additives have been developed to stabilise polymers against the several modes of degradation. Thus, for example, there are additives to protect against thermal oxidation, ultraviolet degradation, burning and the attack of ozone.

The mechanism responsible for the thermal oxidation of hydrocarbon polymers has been established. A series of publications lead to acceptance of the following scheme for oxidative degradation of hydrocarbon polymers [5]:

initiation	$RH \rightarrow R\cdot$	(4.8)
propagation	$R\cdot + O_2 \rightarrow ROO\cdot$	(4.9)
oxidative chain branching	$ROO\cdot + RH \rightarrow ROOH + R\cdot$	(4.10)
	$ROOH \rightarrow RO\cdot + \cdot OH$	(4.11)
	$RO\cdot + RH \rightarrow ROH + R\cdot$	(4.12)
	$HO\cdot + RH \rightarrow HOH + R\cdot$	(4.13)

It is evident from the reaction scheme for oxidation that a chain reaction is involved in the propagation stage. Oxidative chains in polymer oxidation may consist of hundreds of individual steps. Thus a single initiation reaction could be responsible for degradative reactions in many other molecules or sites within the same molecule. When this chain reaction is coupled with the generation of additional oxidative chains in the branching step, it is easy to understand why hydrocarbon polymers are so susceptible to oxidative degradation, and why the oxidation becomes autocatalytic.

The reaction scheme in Figure 4.6 also suggests steps in the mechanism where stabilisation should occur. Additives capable of competing with the polymer for reaction with propagating radicals ($ROO\cdot$) could interrupt or break the chain and, thus stabilises against oxidation

The stabiliser represented as AH in Figure 4.6 is a labile hydrogen donor and the radical by-products will not continue to propagate the reaction, or at least will be considerably less reactive than a polymer radical ($R\cdot$). Oxidative degradation cannot be stopped, but it can be inhibited to extend the useful life of polymers. Further opportunity for stabilisation is suggested by the reaction scheme at initiation step. This might be accomplished by reducing those impurities or imperfections in the polymer structure that are responsible for generation of the first free radicals.
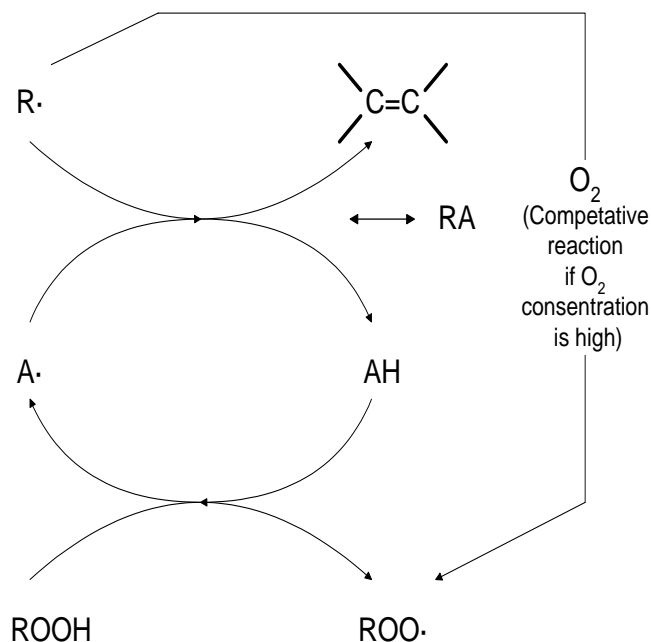
Figure 4.6: Stabilisation with additives, where AH is a labile hydrogen donor [5].

Stabilisers have been developed to protect the polymer under the extreme conditions encountered during processing. To be effective, these short-term stabilisers must be sufficiently mobile within the molten polymer to reach sites of incipient degradation before extensive reaction can occur. Therefore, the short-term stabilisers are low molecular weight compounds that are usually lost through evaporation or extraction during long-term exposure under normal use conditions. Long-term stabilisers must be incorporated into the polymer to protect it from degradation during extended exposure. These stabilisers are of higher molecular weight so that they are not as readily lost by evaporation or extraction [5].

4.3   Degradation mechanisms of Siloxane

The siloxane bond energy (Si-O) is larger than that of carbon-carbon and carbon-oxygen bonds. Clearly the extra energy required to dissociate a siloxane bond has much to do with the substantial thermal stability of silicones.

Experience shows that a methyl group on silicon in PDMS is more thermally and oxidatively stable than a methyl group that is part of a hydrocarbon chain.

The partially ionic siloxane backbone has a weakness shared by other semi-inorganic polymers with alternating backbone atoms, a tendency to nucleophilic or electrophilic attack resulting in a susceptibility to hydrolysis by water, particularly at extremes of pH.

Thermal and hydrolytic degradation of organosiloxane polymers are remarkably dependent on impurity levels, residual traces of acidic and basic catalysts, and filler types of treatment. Intermolecular forces between pendant groups and the unique flexibility of siloxane backbone are of central importance in the structure/property/use relationship of organosiloxane polymers. The combined effect of these two properties is responsible for the physical attributes of siloxane [6].

4.3.1   Thermal degradation of Siloxanes

Detailed information on the thermal degradation of linear poly(dimethylsiloxane) has been obtained during fifty years of studying the products resulting from exposing the polymers to a variety of conditions that lead to depolymerisation. The purely thermal degradation of linear PDMS under vacuum results in depolymerisation yielding cyclic oligomers as illustrated in Figure 4.7. The cyclic trimer has been reported to be the most abundant product, with decreasing amounts of tetramer, pentamer, hexamer and higher cyclic oligomers [6]. Under purely thermal conditions polysiloxanes degrade by the following depolymerisation reaction to form these mixtures of cyclic siloxanes, as represent by the following equation [7]:
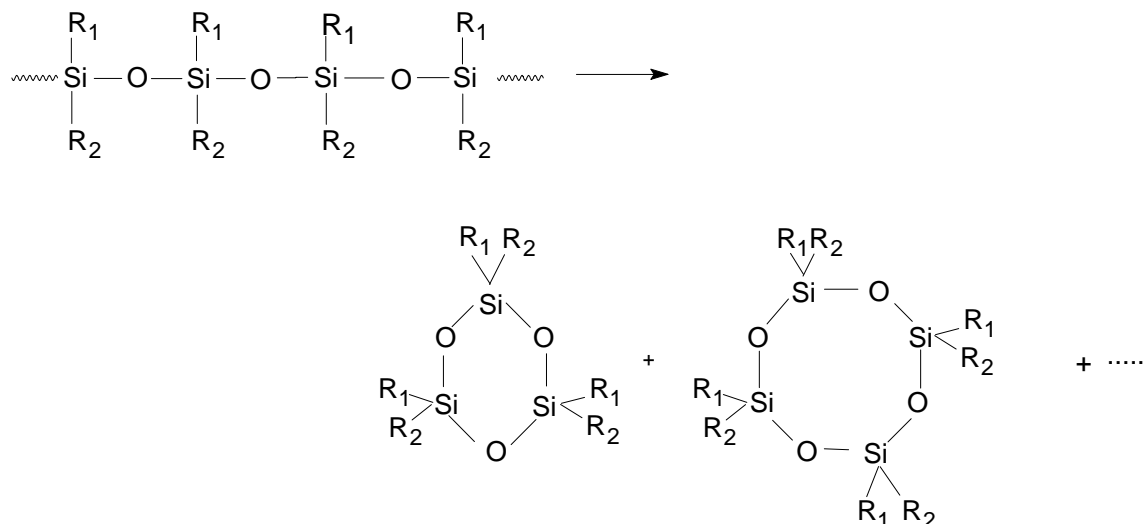
Figure 4.7: Thermal degradation of siloxane [7].

Rigorously purified polysiloxanes are stable under high vacuum or in an inert atmosphere to at least 350-400°C due to the strength of the Si-O bond (447 kJ/mole).

At elevated temperatures (350-400°C) in an inert atmosphere linear polysiloxanes degrade by a process that yields a mixture of volatile, low molecular weight products, which are of the same chemical composition as the original polymer. For PDMS, for example, the analyses of both the original polymer and the degradation products corresponds to structures with the general formula $[(CH_3)_2SiO]_n$. In addition, the absence of char or infusible residue after thermal degradation of the PDMS suggests that the degradation mechanism does not involve splitting of the Si-C or C-H, but that these bonds remain stable at degradation temperatures. Thus, in absence of oxygen, degradation of polysiloxanes occurs primarily through hetrolytical cleavage of the Si-O main chain bonds by a depolymerisation reaction rather than a random homolytic thermal dissociation. Three mechanisms are proposed for thermal degradation of PDMS [7]:

1. the unzipping mechanism of the silanol terminated polymer
2. the random chain scission mechanism of the trimethylsilyl end-terminated polymer
3. the externally catalysed mechanisms for the polymer contained ionic impurities

All these mechanisms involve siloxane rearrangement reactions, but they differ fundamentally in the location of site in the polymer chain at which the degradation process begins.

The unzipping mechanisms are based on the reactions of polymer end-group as the reactive group responsible for the start of the degradation process. Polysiloxanes which are terminated by silanol end-groups can "back-bite" to undergo a siloxane exchange and rearrangement reaction, which leads to the formation of low molecular cyclic compounds as shown in Figure 4.8 [7]:
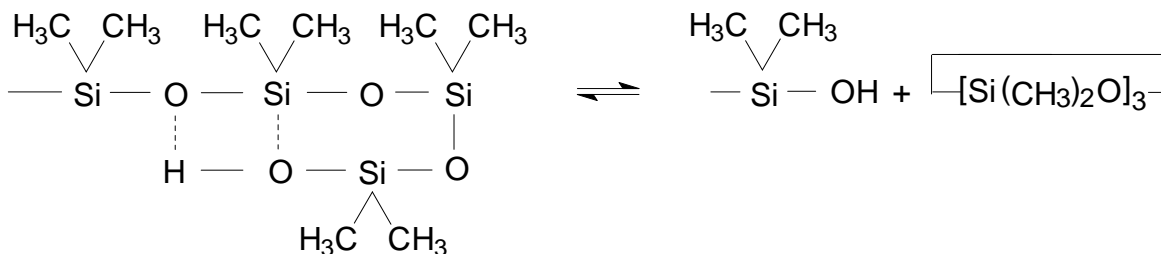

Figure 4.8: Polysiloxanes terminated by silanol end-groups leading to the formation of low molecular cyclic compounds [7].

The six and eight membered cyclic compounds would be expected to be the most prominent components because of their higher rate of formation. They also have the highest thermodynamic stability. By this reaction, degradation can lead to complete polymer depolymerisation and annihilation without change in composition of the products.

The random scission mechanism, which involves initiation of polysiloxane depolymerisation by a random attack on the siloxane units along the main chain followed by unzipping of the reactive fragments, was proposed for thermal degradation of trimethyl end-terminated polymers. An investigation of the degradation of the trimethylsilyl end-terminated PDMS by TGA revealed that this process started in argon at 390-410°C with an activation energy of 159±12.5 kJ/mol. Considering that the value obtained corresponds to less than one half of the siloxane bond dissociation energy of 494 kJ/mol, it was concluded that depolymerisation of the polysiloxanes was governed mainly by molecular structural and kinetic factors rather than by bond energies. To account for the surprisingly low activation energy for the polysiloxane depolymerisation reaction a mechanism was proposed by which siloxane bond rearrangement occurs through the formation of an intramolecular, cyclic, four-centred transition state, which is involved in the rate determining step of the polysiloxane degradation process, as shown in Figure 2.9 [7].
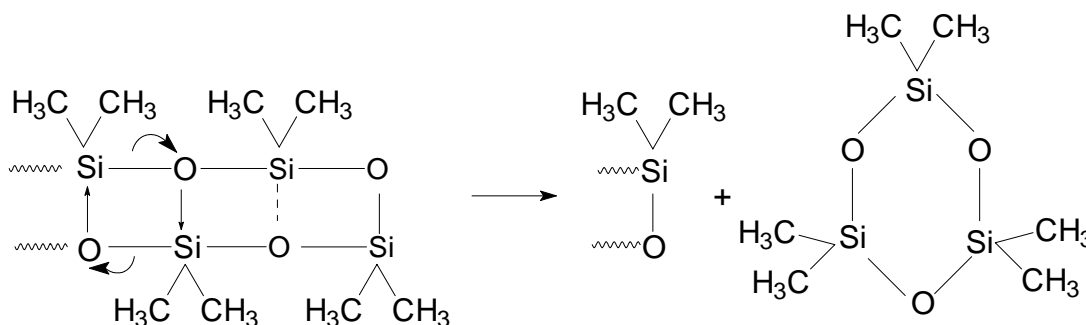

Figure 4.9: Siloxane bond rearrangement through the formation of an intramolecular, cyclic compound [7].

The important features of this mechanism are that the reaction may occur at any point along the polymer chain by formation of a loop within the chain backbone, and initiation of such degradation reaction does not require either reactive end groups or nucleophilic impurities.

The likelihood of a random scission process is supported by the observation that a marked decrease in polymer molecular weight occurred during degradation.

The third mechanism for polysiloxane thermal depolymerisation considers initiation by an external catalyst. This scheme assumes that the presence of ionic impurities is responsible for the onset of a stepwise reaction in which the Si-C bond scission also occurs as indicated by the observed formation of methane. The presence of residual polymerisation catalyst dramatically decreases the thermal stability of PDMS. The mechanism of such a process would likely involve an ionic cleavage of the siloxy bonds induced by the presence of the active chain ends, but an alternative has also been suggested according to which each step of this reaction must be separately catalysed by hydroxide ion, as shown in Figure 4.10 [7]:
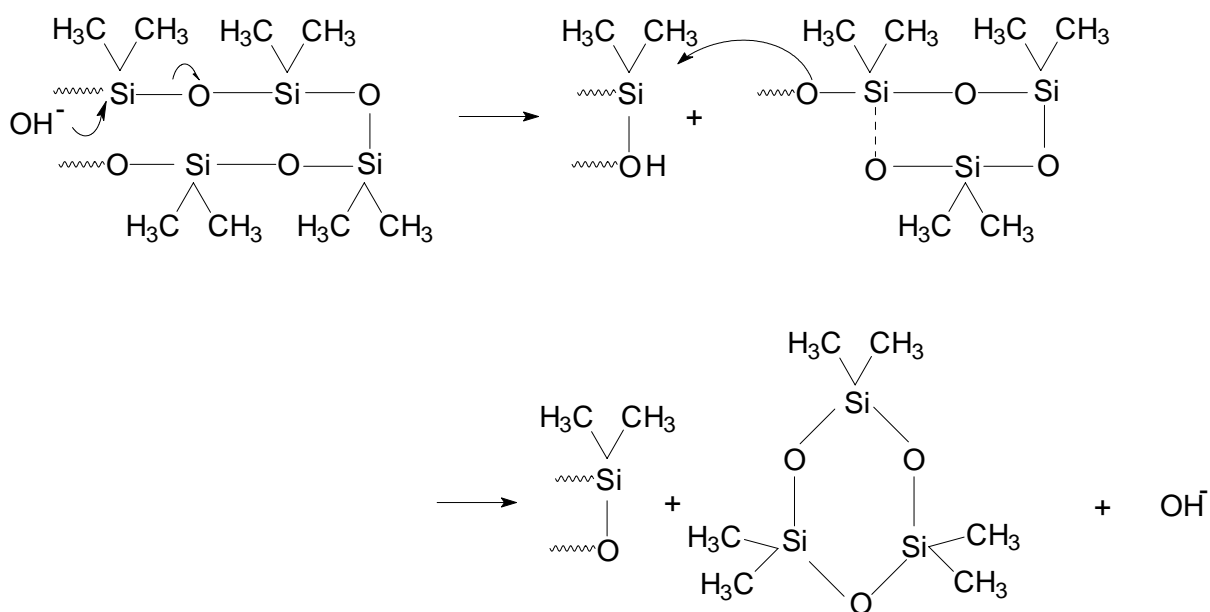
Figure 4.10: Siloxane degradation catalysed by hydroxide ion [7].

The activation energy for such a reaction pathway should be considerably lower than that required for an non-catalysed degradation reaction [7].

It has also been demonstrated that hydroxyl terminated PDMS is less thermally stable than PDMS end-blocked with trimethylsilyl $(CH_3)_3Si$- groups, where the former depolymerise by a mechanism proceeding via the terminal hydroxyl groups as shown above. It should be noted however that the volatile products - the cyclic oligomers - were found to be the same for the two types of PDMS. In both systems neither methane nor hydrogen were found and no C-H or Si-O bond cleavages were detected in the absence of catalytic species [6].

The major reason of thermal decomposition of polysiloxanes at degradation temperature is not the insufficient stability of the Si-O main chain bonds, but rather the higher thermodynamic stability of low molecular weight cyclosiloxane degradation products relative to their open-ended high molecular weight linear counterparts. In other words, at degradation conditions polysiloxanes reach their ceiling temperatures at which depolymerisation mechanisms onset through the so-called siloxane redistribution reactions. Thus improvements in their high temperature stability may be achieved by preventing, or at least grately restricting, the cyclisation reactions, which can be accomplished for example by introducing into the -Si-O-main-chain backbones some bulky and thermally stable building blocks that would impose by

steric hindrance to the closure of cyclosiloxane degradation products. However, if retention of elastomeric properties of the parent polysiloxanes is also desirable, the selected building blocks should not disrupt their low temperature flexibility, i.e. they should not increase considerably the T_g values of the resulting polymers [8].

Thermal stability of the crosslinked PDMS determined with TGA, is much higher than that of the non-crosslinked polymer. The non-crosslinked liquid polymer loses weight above 100°C, suggesting the presence of low molecular weight siloxane; while for the crosslinked PDMS it initiates above 425°C. It can also be observed that thermal stability increases with the crosslinking level [9].

4.3.2   Thermo oxidative stability and degradation

Dynamic thermal gravimetric analysis has revealed that the degradation of poly(dimethylsiloxane) in air involves an extra weight loss step, which does not occur when the same polymer is degraded in an inert atmosphere. The steps start at about 350°C and are characterised by activation energy of about 92-126 kJ/mol. A similar behaviour was observed for fluorosilicone polymers for which the activation energy is about 121-142 kJ/mol. It have been reported [10] that after a five hour exposure at 300°C, the number of CH_3 groups in poly(dimethylsiloxane) appreciably decrease in the ratio of carbon/silicon from 2.0 to 1.74. At 350°C this decrease is more prominent and the C/Si ratio drops to the value of 0.32. It is well know that during thermo oxidative degradation the polymer becomes insoluble and the structure of the residue changes over the course of the reaction, apparently because of crosslinking through formation of Si-O-Si bridges. The volatile products of thermo oxidative degradation of PDMS consist mainly of carbon monoxide (25%) and water (17%) but they also include smaller amounts of carbon dioxide (2%), formaldehyde, methanol and traces of formic acid. Based on these results, the following free radical mechanisms have been proposed for the thermo oxidative degradation process in which the initial step consists of the reaction of oxygen with pendant organic groups to form a polymeric hydroperoxide (Figure 4.11) [7].
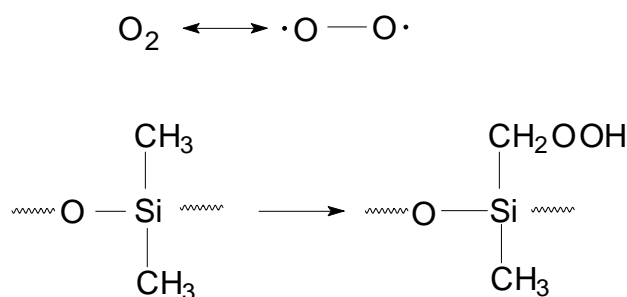

Figure 4.11: Free radical mechanisms have been proposed for the thermo oxidative degradation process in which the initial step consists of the reaction of oxygen with pendant organic groups to form a polymeric hydroperoxide [7].

The hydroperoxide decomposes to form the corresponding hydroxyl and silyl radicals and formaldehyde, which is one of the main degradation products (Figure 4.12):
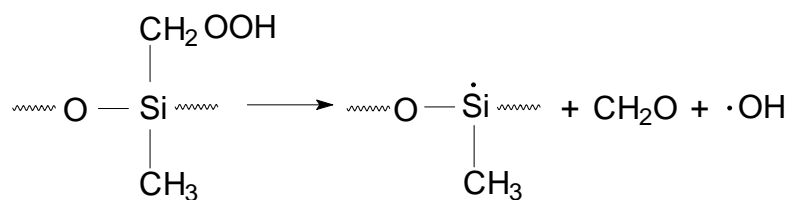
Figure 4.12: Decomposition of hydroperoxide of PDMS [7].

The two different radicals then recombine to form the silanol group as shown in Figure 4.13:
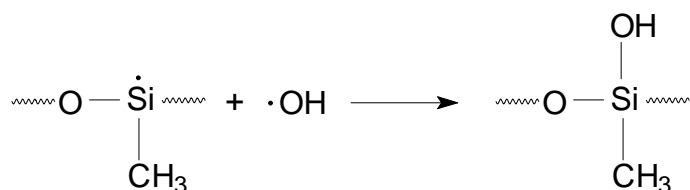
Figure 4.13: Recombination to form a silanol group [7].

which, in turn, can undergo a silanol condensation reaction to form the crosslinks proposed and to yield water as by product shown in Figure 4.14:
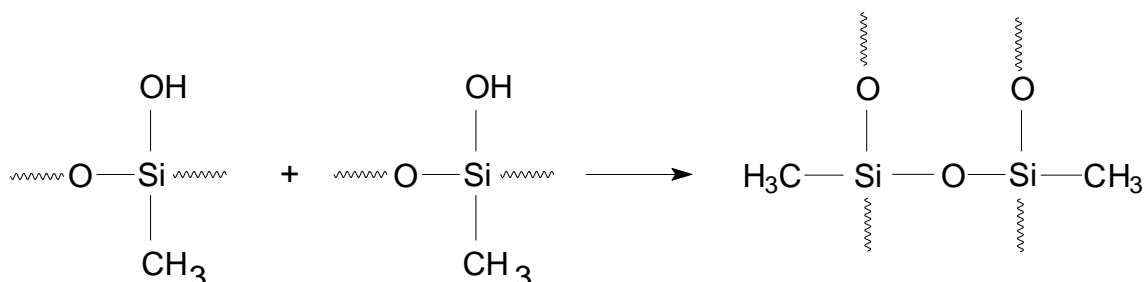
Figure 4.14: Condensation reaction of silanol to form crosslinks [7].

At higher degradation temperatures, thermal decomposition of formaldehyde yields carbon monoxide and hydrogen. Carbon monoxide becomes the principle degradation product, although minor quantities of formic acid and carbon dioxide can also be accounted for by the oxidation reactions of formaldehyde.

These mechanisms of polysiloxane thermo oxidative degradation may be predominant only at relatively low temperatures, up to about 300-350°, because above this temperature range main siloxy bonds can rupture, and the degradation process can become much more complicated.

Because of the crosslinking reactions, which occur during thermo oxidative degradation, polysiloxanes do not loose molecular weight in the early stages of degradation, and they can retain their elasticity even for thousands of hours at temperatures up to 200°C or for several hundred hours at about 220°C [7].

4.3.3   Chemical resistance of PDMS

Study of the mechanism of decomposition of siloxanes in acidic or basic media is of great importance for the interpretation of data on the chemical degradation of polyorganosiloxanes, and also on the polycondensation and catalytic regrouping of these compounds.

There are at present a number of points of view as to mechanism of acid decomposition of organosiloxanes. It has been suggested that the scission of organosiloxanes is effected according to the S_N-1 mechanism (Figure 4.15), according to which there is fast and equilibrium protonation of the oxygen of the siloxane group with subsequent slow decomposition of the protonated form into a silanol and a silyl cation, the latter reacting rapidly with a nucleophilic reagent, e.g., an alcohol [11]:

(fast)

(slow)

(fast)
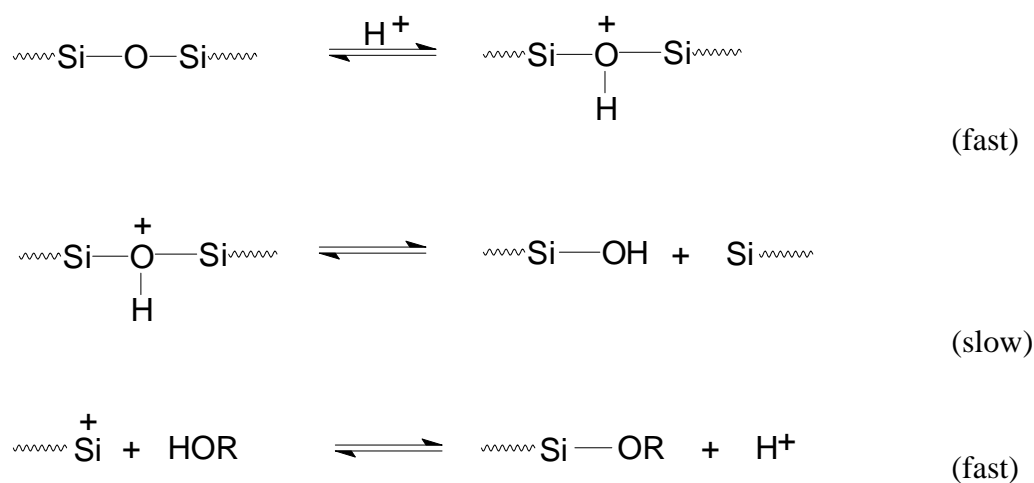
Figure 4.15: Acid decomposition of organosiloxanes after the S_N-1 mechanism [11].

There had also been suggested a bimolecular mechanism, S_N-2 (Figure 4.16), according to which the limiting stage is interaction of a nucleophilic reagent with the protonated form of the organosiloxane:

(fast)

(slow)

(fast)
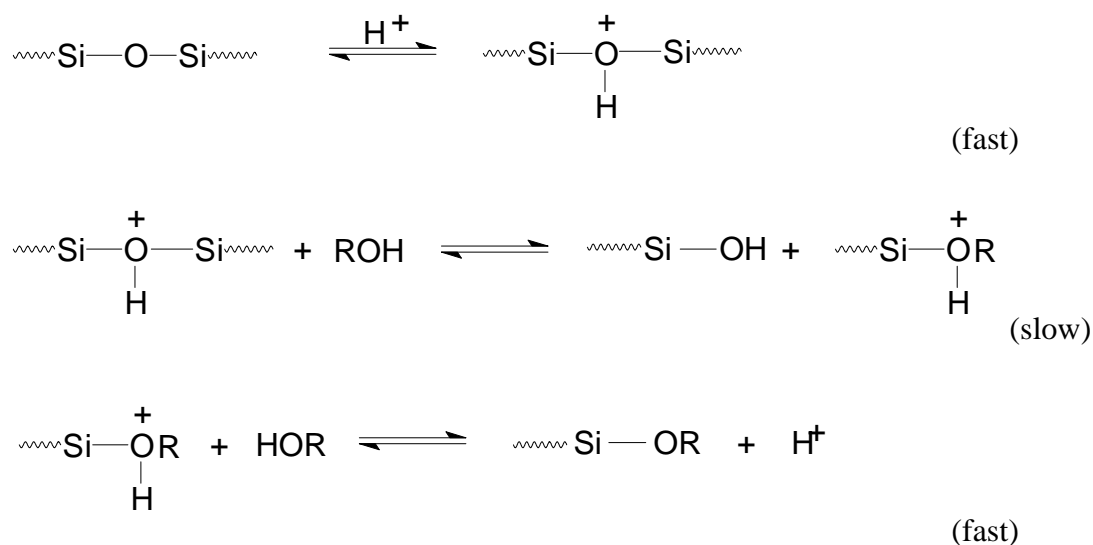
Figure 4.16: Acid decomposition of organosiloxanes after the S_N-2 mechanism [11].

Water has no appreciable effect on silicone rubbers. Alkalies may have some deleterious effect, though resistance is nevertheless generally classed as good. Resistance to organic solvents is less good and some swelling of the membrane may be observed [12].

4.3.4 Chemical resistance of PDMS to chlorine

This project is trying to establish the factors that affect the rate of degradation of silicones when exposed to Cl_2. It is conceivable that HCl is produced in these reactions. Under such circumstances the reactions predicted to arise include acid catalysed chain scission (Figure 4.17A, loss of crosslinking - increases swelling), depolymerisation (Figure 4.17B, dry weight loss) and acid catalysed crosslinking (Figure 4.18, decreased swell) [13].
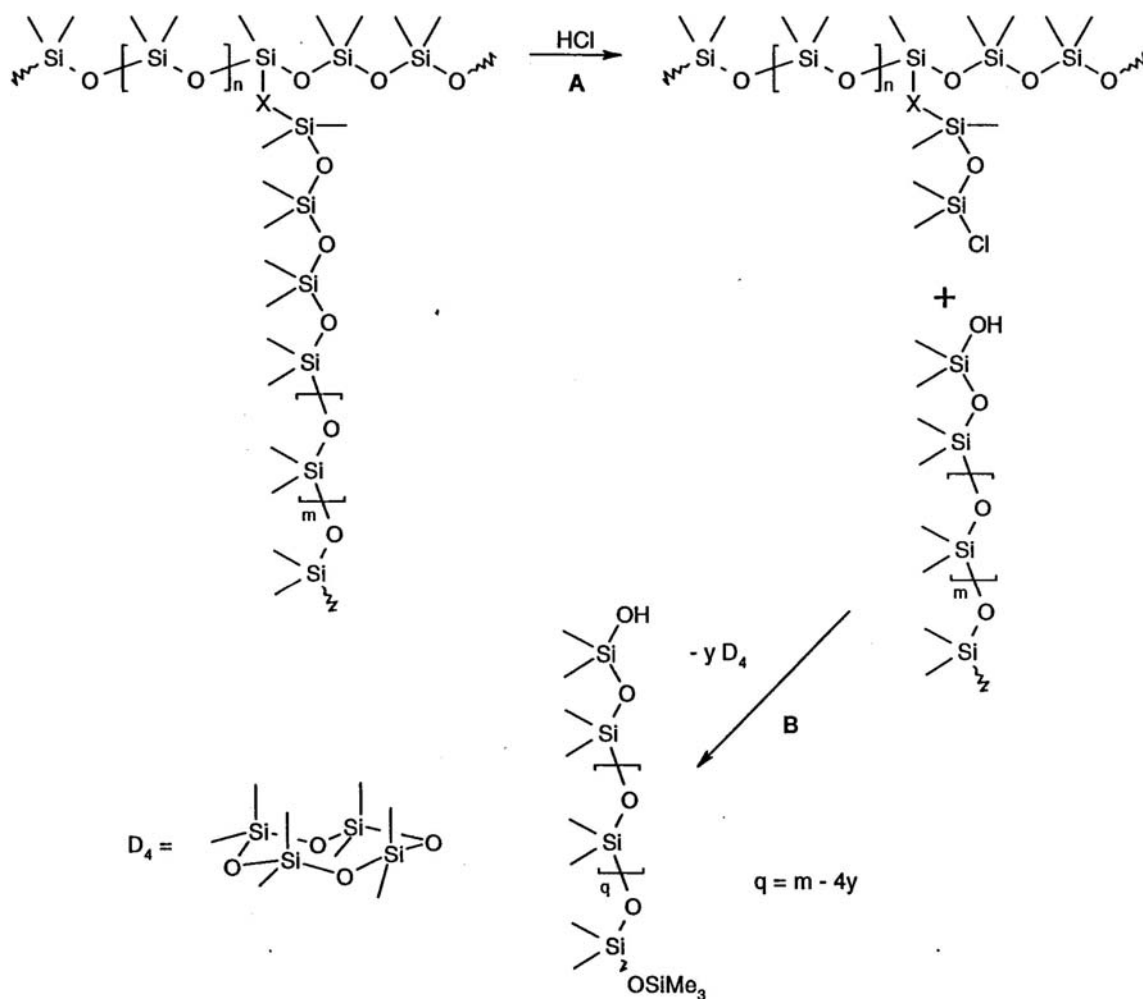
Figure 4.17: (A) Acid catalysed chain scission with the result of loss of crosslinking and (B) depolymerisation with dry weight loss [13].
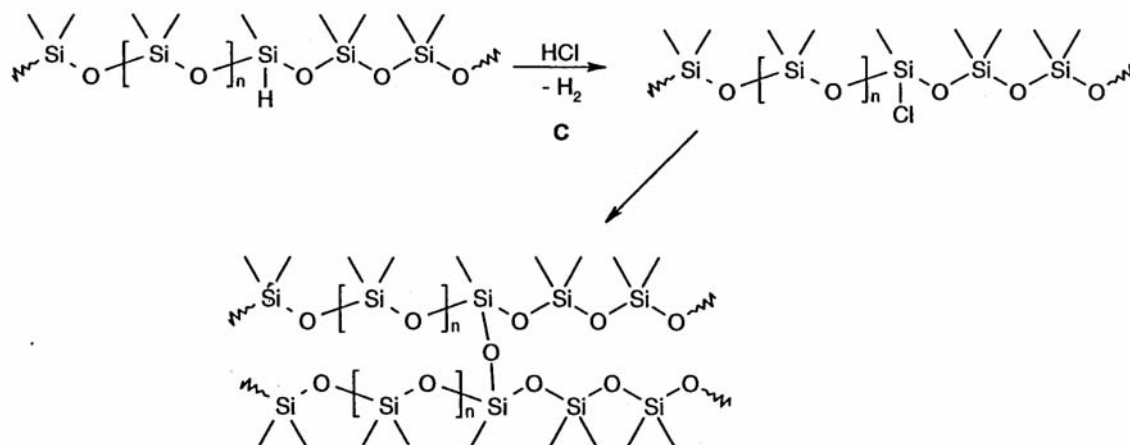
Figure 4.18: Acid catalysed crosslinking [13].

The reaction with chlorine is more complex. Based on the known degradation pathways of silicones by oxidation, it is likely that the chlorine will initiate reaction by hydrogen abstraction. This can lead to new crosslinking by one or two ways. The first is through carbon radical generation and crosslinking (Figure 4.19A). Similar processes are used in the peroxide cure of silicone rubbers. Alternatively, the radical can be further oxidised and under hydrolysis, crosslink through oxygen (Figure 4.19B). This is a similar process to that shown in Figure 4.18.
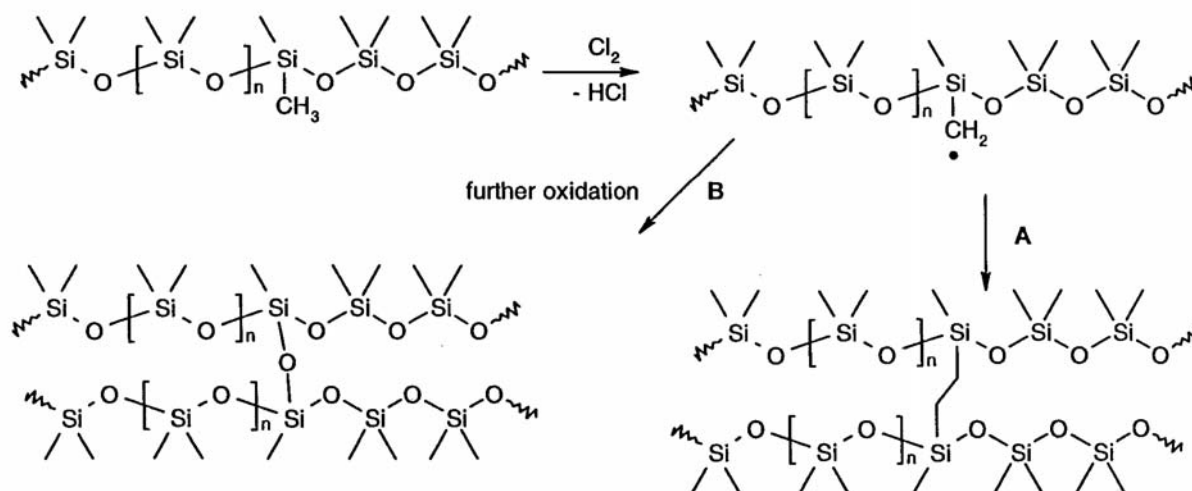
Figure 4.19: (A). Carbon radical generation and crosslinking and (B) radical oxidised and under hydrolysis, crosslink through oxygen [13].

4.4   Degradation mechanisms of Fluoroelastomer

The chemical and thermal stability of fluoroelastomers is a function of its fluorine content. For example, as the fluorine content of fluoroelastomers is increased from 66 to 70% the volume swell in certain media drops from 96 to only 10 %. However, as the fluorine content of the polymer is increased so is cost as well, due to the preparation and refinement of the expensive perfluorinated monomers [14].

The high thermal and chemical stability of fluoroelastomers can be mostly related to the high bond energy of C-F. High bond energy of the C-C and C-H links is also observed in the presence of fluorine. Copolymers of vinylidenefluoride (VDF) and hexafluoropropylene (HFP) have excellent resistance to oils, fuels and lubricants as well as to aliphatic and aromatic hydrocarbons. However, due to the polar character of the main VDF monomer, they are highly swelled when in contact with polar solvents such as low molecular weight esters, ethers, ketones and amines. Improvements can be obtained by reducing the amount of the polymer, obtaining polymers with higher total fluorine content. However lower VDF monomer gives higher chain stiffness, so inferior low temperature flexibility results.

4.4.1 Thermal degradation of Fluoroelastomers

Fluoroelastomers present one of the most thermally stable elastomer systems currently available. However because of their chemical structure there is a possibility of elimination of hydrogen fluoride (HF) from the fluoroelastomer main chain at elevated temperatures (Figure 4.20). This is an analogue to the splitting out of hydrogen chloride (HCl) from PVC.
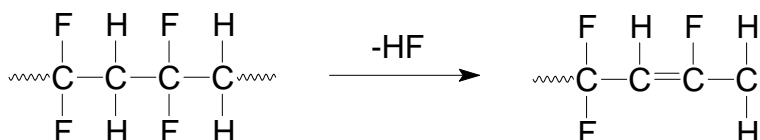
Figure 4.20: Elimination of hydrogen fluoride (HF) from fluoroelastomer [14].

Hexafluoropropylene (HFP) and vinylidenefluoride (VDF) undergo crosslinking when exposed to low-level gamma radiation. Crosslinking in PVDF is usually accompanied by increase in tensile strength and a decrease in both the degree of crystallinity and melting point. The overall resistance of PVDF to nuclear radiation is very good. However, HFP-VDF exposed to radiation resulted in weight loss. Linear relationship exists between the dose and the loss of weight [14].
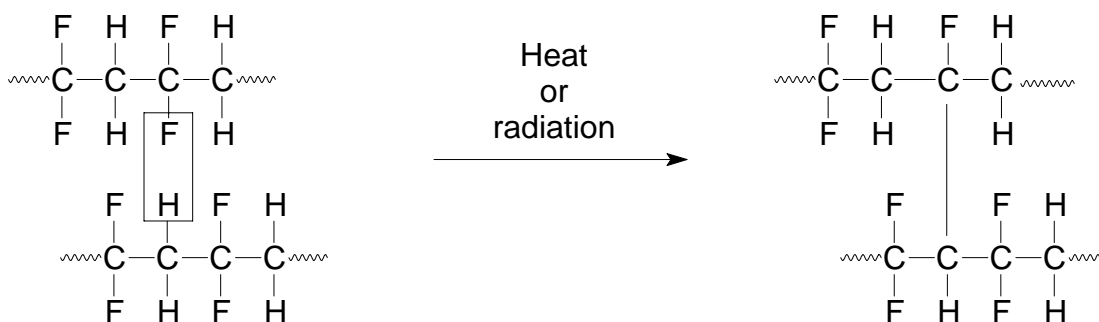
Figure 4.21: HFP-VDF exposed to radiation results in weight loss [14].

4.4.2 Chemical resistance of Fluoroelastomers

VDF based fluoroelastomers generally have good resistance to strong acids. For example Viton®-type fluoroelastomers remain tough and elastic even after prolonged exposure at 150°C in anhydrous hydrofluoric acid or chlorosulfonic acids. However, problems can occur when elastomers are formulated with acid acceptors based on oxides or hydroxides of alkali

metals. In this case, acids can react directly with these additives and cause surface cracks and failure.

One of the main failure modes of fluoroelastomeric components is swell, since a relatively small degree of swelling can lead to dramatic reduction in physical properties. Both methanol and carbon dioxide, because of its high polarity, can swell fluoroelastomers while amines initially harden the rubber by excessive crosslinking and ultimately can dissolve the fluoroelastomers. It is necessary to select a VDF based polymer with fluorine content exceeding 69.5 % if swelling problems are to avoid.

Exposure of Viton® gaskets to ozone leads to a 20 % reduction in the elongation, while chlorine exposure cause a 6 % reduction in the tensile strength [14].

4.4.3   Chemical resistance of Fluoroelastomers to chlorine

Fluoroelastomers might be chlorine substituted as shown in Figure 4.22. This will give increased chain stiffness and decrease in low temperature flexibility:
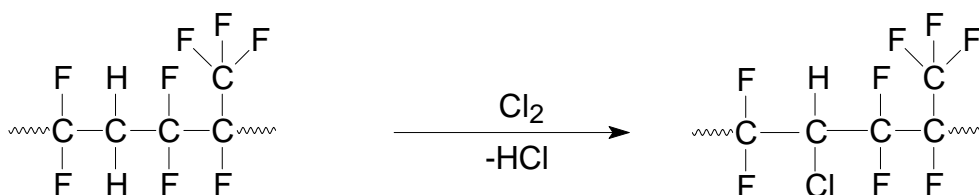
Figure 4.22: Chlorine substituted Fluoroelastomers

4.5   Degradation mechanisms of Fluorosilicone

Poly(methyl-3,3,3 trifluoropropylene-siloxane) has a T_g of -75°C. Unlike PDMS it does not exhibit a low crystallisation temperature, due to the inability of the polymer chains to pack into a crystalline lattice. Because of the low T_g, and absence of a low temperature crystallisation, the fluorosilicone remains quite flexible at very low temperatures [14].

The role of fluorine and carbon-fluorine bond in achieving a high degree of solvent resistance and stability is well known in organic polymer systems. The two properties were combined in silicone polymers by incorporation of fluorine into polyalkylsiloxane systems. Incorporation of the carbon-fluorine bond rather than the silicone-fluorine bond is a principal factor influencing the choice of structure for polyalkylsiloxane systems. The latter, although of high thermal stability, is subject to hydrolysis and therefore, is less useful than the former. The second structural consideration is the location of fluorine relative to silicone in the alkyl substituent. Because of the great electronegativity and strong inductive effect of fluorine, the position alpha to silicone, e.g., $CF_3SiRR'R''$, suffers a major disadvantage: hydrolytic cleavage of the silicon-carbon bond. In addition, thermal rearrangement is possible with the formation of silicon-fluorine bonds as shown in Figure 4.23 [15]:

$$CF_3 \overset{\overset{R}{|}}{\underset{\underset{R''}{|}}{Si}} — R' \xrightarrow{\triangle} [CF_2\!:\,] + F\overset{\overset{R}{|}}{\underset{\underset{R''}{|}}{Si}} — R'$$
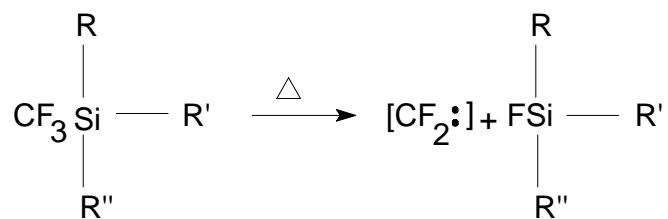
Figure 4.23: Thermal rearrangement with formation of silicone fluorine bonds [15].

This rearrangement appears to be similar to the alpha elimination mechanism proposed for one mode of carbon formation. The position beta to silicon, $CF_3CH_2SiRR'R''$, also suffers the same disadvantage, hydrolytic instability and thermal rearrangement. In the latter, the side chain is eliminated as an olefin (Figure 4.24) [15]:

$$CF_3CH_2\overset{\overset{R}{|}}{\underset{\underset{R''}{|}}{Si}} — R' \xrightarrow{\triangle} CF_2\!=\!CH_2 + F\overset{\overset{R}{|}}{\underset{\underset{R''}{|}}{Si}} — R'$$
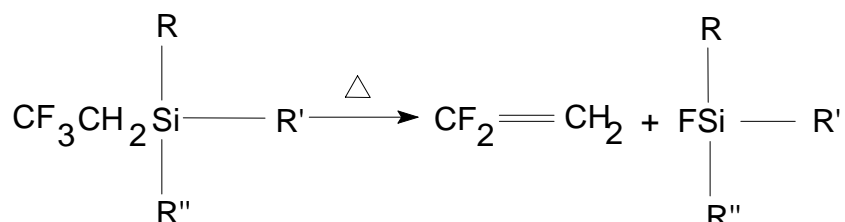
Figure 4.24: Hydrolytic instability and thermal rearrangement of silicon in beta position [15].

Therefore, the gamma position, $CF_3CH_2CH_2SiRR'R''$, is the obvious choice for maximum stability and ease of preparation. Positions beyond gamma are also suitable, but their usefulness is limited by the oxidation of the CH bonds in the alkyl group [15].

4.5.1   Thermal degradation of Fluorosilicone

Fluorosilicones are in an interesting thermodynamics state where they are actually in equilibrium with their cyclic trimer and tetramers (Figure 4.25).

$$\left[\begin{array}{c} \gamma\;\; CF_3 \\ | \\ \beta\;\; CH_2 \\ | \\ \alpha\;\; CH_2 \\ | \\ Si — O \\ | \\ CH_3 \end{array} \right]_n \;\;\rightleftharpoons\;\; \text{cyclic oligomers}$$
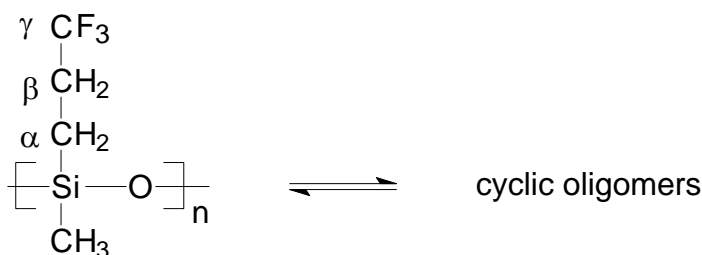
Figure 4.25:Equilibrium between linear and cyclic oligomers Fluorosilicone [14].

However, it is the oligomers, not the polymer, which is thermodynamically favoured. Thermal degradation of fluorosilicones can occur by a reversion mechanism where heat shifts the equilibrium towards the tetramers. Thus, the polymer breaks down to form the cyclic tetramers (a thermodynamically stable compound). Basic compounds such as KOH accelerate this reaction. This degradation pathway is more dominant in the absence of oxygen since oxidative crosslinking becomes competitive in oxygen containing atmosphere.

The hydrocarbon spacer provided by two methyl groups gives optimum thermal stability and copolymerising with 3,3,3-trifluoropropylene provides the γ fluorosubstituent.

Silicones in general are known for their excellent retention of properties at elevated temperatures. Fluorosilicone elastomers are no exception although they have slightly reduced high temperature stability compared PDMS [14].

4.5.2   Chemical resistance of Fluorosilicone

Fluorosilicone resists deterioration by solvents, acids, chlorides and other severe chemicals as well as low-pressure steam and condensate [16]. Fluorosilicone also perform well with low volume swells in alcohol/fuel blends, once the solvent is removed the physical properties return nearly to the original non-swollen state. Coupled with its resistance to mineral oils, fuels and solvents, fluorosilicone rubbers most striking properties are its heat resistance. It is more resistant than most plastics and rubbers with purely organic bases. Generally, it may be assumed to be able to withstand long-term exposure to temperatures of 210 to 230°C.

One striking property of fluorosilicone rubber is its flexibility at very low temperatures (down to about -60°C) [17].

Fluorosilicone elastomers are especially suited for applications involving exposure to fuels, oils, hydraulic fluids and various other chemicals. Fluid resistance is excellent to almost all solvents with a few exceptions, e.g., some esters and ketones due to higher swells. Even dilute caustic solutions, nitric acid, hydrochloric acid, and sulphuric acid have little effect on fluorosilicone rubbers [15].

4.5.3   Chemical resistance of Fluorosilicone to chlorine

A study of the given polymer structure given for the Fluorosilicone (from the supplier Silicone Specialty Fabricators, USA) the polymer chain is vinyl terminated with C-C double bounds (Figure 4.26). Double bonds are reactive towards various chemicals. In chlorine environment the addition of chlorine atoms would take place to saturate the double bonds (Figure 4.26). This will lead "new" polymer after the chlorination reaction, which might be stable against further chlorination.
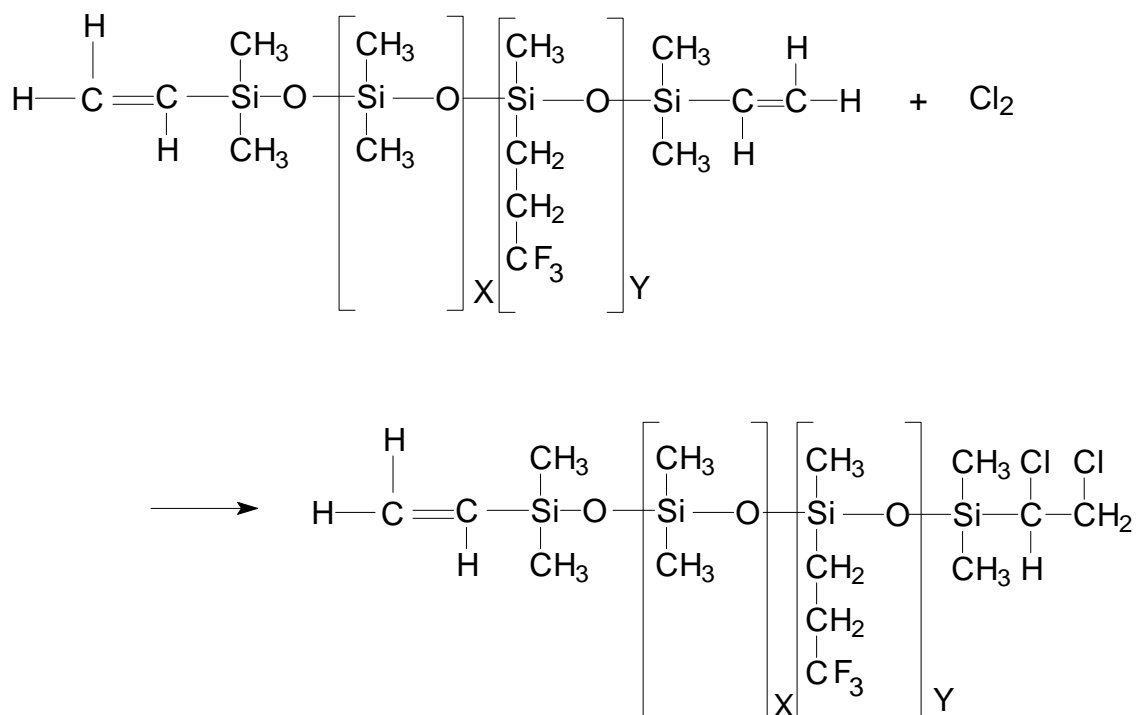
Figure 4.26: Cl₂ addition of vinyl terminated Fluorosilicone

References to Chapter 4

1.   D. J. Carlsson, D. W. Wiles; Degradation in Encyclopaedia of Polymer Science and Engineering, vol. 4, p. 630-696, John Wiley & Sons Inc., USA 1986.
2.   W. Scnable; Polymer Degradation - Principles and Practical Applications, Hanser Publishers, Germany 1992.
3.   N. Grassie and I. G. Macfarlane; The Thermal Degradation of Polysiloxanes-I Polydimethylsiloxane, Eur. Polym. J., vol. 14, p. 875-884, 1978.
4.   A. Holmström, E. M. Sörvik; Thermal Degradation of Polyethylene in a Nitrogen Atmosphere of Low Oxygen Content. III. Structural Changes Occurring in Low-Density Polyethylene at Oxygen Content Below 1.2%, J. Appl. Polym. Sci., vol 18, p. 3153-3178, 1974.
5.   W. L. Hawkins; Stabilisation in Encyclopaedia of Polymer Science and Engineering, vol. 4, p. 630-696, 1996.
6.   S. J. Clarson, J. A. Semlyen; Siloxane Polymers, Ellis Horwood-PTR Prentice Hall, USA 1993.
7.   P. R. Dvornic, R.W. Lenz; High temperature Siloxane Elastomer, Hüthig & Wepf Verlag, Germany 1990.
8.   P. R. Dvornic; Some Recent Advances in the Silicone Containing Polymers, Materials of Sci. Forum, vol. 214, p. 131-138, Transtec Publications, Switzerland 1996.
9.   R. Vera-Graziano, F. Hernandez, J. V. Cauich-Rodriguez; Study of Crosslinking, Density in Polydimethylsiloxane Networks by DSC, J. Appl.Polym. Sci., vol. 55, p.1317-1327, 1995.
10. K.A. Andrianov; Metalorganic Polymers, Interscience, p.50, New York 1965.
11. Yu. V. Moiseev and G.E. Zaikov; Chemical Resistance of polymers in aggressive media, Consultants Bureau, New York 1987.

12. M.E.Hodgson; Silicone Rubber Membranes, Filter Media-Development and Innovation Filtration Society Symposium, p. 418-419, Manchester, October 3rd 1972.

13. M. A. Brook, S. Balduzzi, M. Mohamed, R. Stan; Report 2 to Norsk Hydro-Tel-Tek, Acid Lability of Silicone Membranes (confidential), Chemistry Department McMaster University, Canada, Feb.1999.

14. J. Scheirs (Editor), M.T. Maxson, A.W. Norris, M. J. Owen; Modern Fluoropolymers: high performance polymer for diverse applications, Chapter 20, John Wiley & Sons, Great Britain 1997.

15. Y. K. Kim; Poly(fluorosilicones) in Kirk-Othmer Encyclopaedia of Chemical Technology, 3rd Ed., vol.11, p. 74-81, USA 1978.

16. K. Parker; Harsh chemicals can't beat fluorosilicone lubricant, Eng. & Maintenance, October 1991.

17. D. Klages, U. Raupbach; Fluorosilicone Rubber - a modern material, Gummi Fasern Kunststoffe, International Polymer Sci.and Tech., vol 22, No.5, p. T/11-T/13,1995.

Chapter 5: Experimental and Methods

Summary

In this chapter the experimental work and analytical methods are presented. Section 5.1 describes the membrane preparation techniques. The poly(dimethylsiloxane) polymers were synthesised at the McMaster University in Canada, the composite membranes were prepared and produced at the GKSS Research Centre in Germany. The Fluorel membranes were prepared at Telemark University College, Norway, while the fluorosilicone membranes were delivered from McMaster University and Specialty Silicone Fabricators, USA.

The experimental equipment and procedures are described in section 5.2. Permeability measurements, absorption measurements, durability tests and swelling tests (only for PDMS) are all described in this section.

Different analytic methods have been used for the documentation of the materials. These techniques have been: Fourier Transform Infrared spectroscopy (FT-IR), Scanning Electron Microscopy (SEM), Nuclear Magnetic Resonance (NMR) and Differential Scanning Calorimetry (DSC).

5.1 Preparation of the membrane samples

The development of a membrane with certain properties demands detailed knowledge about the material properties. Material properties can be changed by different ways of curing, substitution of groups, blending or copolymerisation and changes in production variables such as temperature and pressure. The membrane separation properties can thus be varied, but there is a long way by trial and error to develop an optimal membrane for a given separation process.

5.1.1 Poly(dimethylsiloxane)

For the poly (dimethylsiloxane) (PDMS) membranes it was first of all focused on the polymer production process itself in order to understand the influence of the curing, and degree of crosslinking for the most suitable PDMS polymer.

The silicone materials were synthesised and cured at McMaster University, Canada, and the composite membranes were produced at GKSS, Germany.

The PDMS membranes were cured in three different ways [1]:
1) Free Radical Curing, with three different degrees of crosslinking.
2) Room Temperature Vulcanisation (RTV), with three different degrees of crosslinking:
   a) with tin catalysed RTV cure
   b) with metal free RTV cure
3) Hydrosilylation with Pt-catalyst, with three different degrees of crosslinking:
   a) hydrosilylation cure with poly(methylsilicone)
   b) hydrosilylation cure with poly(dimethyl)- and (diphenylsilicone)

The composite membranes with *Free Radical Curing* could not be prepared on the support material (in this case support of polypropylene (PP) was used) since it melted at the curing temperatures (above 100°C). Only films without support were therefore prepared. At 110°C some crosslinking took place, but very slowly. The concentration of peroxides used in the curing process had to be increased, and also the temperature had to be increased. This resulted in good crosslinking, but too thick films and even brittle films. At this point the membrane was ruled out as an alternative and no samples was available for chlorine exposure [2].

The *RTV cured* membranes, with and without a tin catalyst, were of poor quality. The polymerisation and curing process could explain this fact: it was easy to prepare the silicones, but it turned out to be difficult to prepare nice membranes since the time limit before it was all polymerised was very short and difficult to control. It quickly became very viscous, and the way used to spread out the silicones on the support resulted in an uneven surface and also holes. The polymerisation process was not suitable for membrane scale up. The RTV membranes for the chlorine project were therefore rejected from further investigations [2].

The hydrosilylation membranes were prepared with a Pt-catalyst. These membranes were prepared in two series: one "ordinary" PDMS, and one with diphenyl groups. Both the films and the membranes were fairly easy to prepare.

Hydrosilylation is a widely used process for preparation of silicone elastomers. The crosslinking takes place between two different, complementary polymers: one containing Si-H groups, the other Si-CH=CH$_2$ groups. The reaction occurs rapidly and under very mild conditions (Figure 5.1). Differences in the nature of the catalyst and addition of specific inhibitors can affect the temperature for hydrosilylation (ambient $\rightarrow$ 100°C). There are no by-products produced in the process although residual platinum that remains trapped in the gel can turn the elastomer somewhat yellow [3].
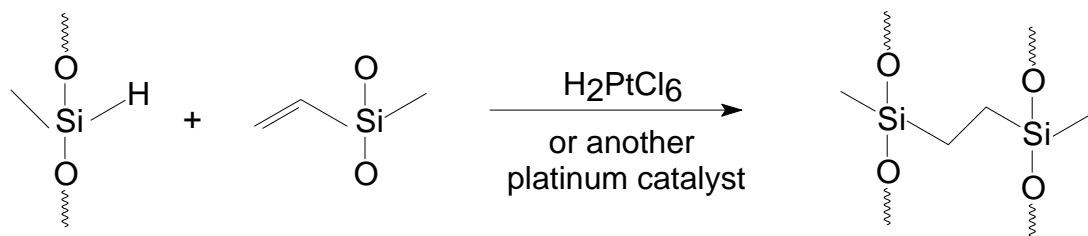

Figure 5.1: Hydrosilylation.

The membranes cured by hydrosilylation consist of following starting materials: vinyl-dimethyl-terminated poly(dimethylsiloxane)(PDMS) (-(CH$_3$)$_2$SiO-)$_n$; vinyldimethylterminated poly(diphenylsiloxane), poly(dimethylsiloxane) copolymer, poly(hydrogenmethylsiloxane) (PHMS) (-H(CH$_3$) SiO-)$_n$; platinium-divinyltetramethyldisiloxane; hexanes reagent grade [1].

The poly(dimethylsiloxane) and poly(hydrogenmethylsiloxane) were weighed in a beaker and diluted with hexanes (10 ml hexane/gram total polymer mixture for aluminium dish and 80 ml/gram total polymer mixture for the metal mould). The polymeric solution was then poured into an aluminium dish or metal mould followed by the addition of 6 drops of a solution of platinum catalyst (1 drop of catalyst in 10 ml of hexanes = 0.001 g/ml). The dish or mould was covered with a watch glass while evaporation of solvent at room temperature was carried out over 8 hours. Curing was then carried out at 80°C for 2 days [1].

The PDMS membrane produced with 85 wt% poly(dimethylsiloxane) and 15 wt% poly(hydrogenmethylsiloxane) had the highest degree of crosslinking. Reducing the amount of poly(hydrogenmethyl)siloxane gave a decrease in the degree of crosslinking [1].

5.1.2   Fluorel

The starting materials was Fluorel - the copolymer of vinylidenefluoride and hexafluoropropylene (-(CF$_2$CH$_2$)$_m$(CF$_2$CFCF$_3$)-)$_n$; ethyl-methyl ketone and methanol. The Fluorel was weighted (e.g. 3 wt%) and dissolved in a mixture of 90 vol% ethyl-methyl ketone and 10 vol % methanol (MeOH).

The membranes were prepared as composite membranes on a PVDF support. This was done in two different ways: either by casting directly on the support material, or by dip-coating. Casting the membranes was done by pouring the polymer solution directly on the support material (figure 5.1), and drying in a heating oven. The thickness could then be determined by the volume and concentration of the polymer solution. The selective layer may become uneven, especially if the drying process is to fast. Dip-coating is a simple technique for preparing composite membranes with a thin dense top layer. The support material is then

dipped in the polymer solution, and a thin layer of solution adheres to it. This film is dried in an oven where the solvent evaporates and where crosslinking also occurs.

The heating procedure was to increase the temperature to 80°C after the dipped or casted membrane were placed in the oven and kept at this temperature over night, at least 18 hours to ensure total evaporation of the solvent. The oven was cooled slowly to room temperature before the membrane was taken out.
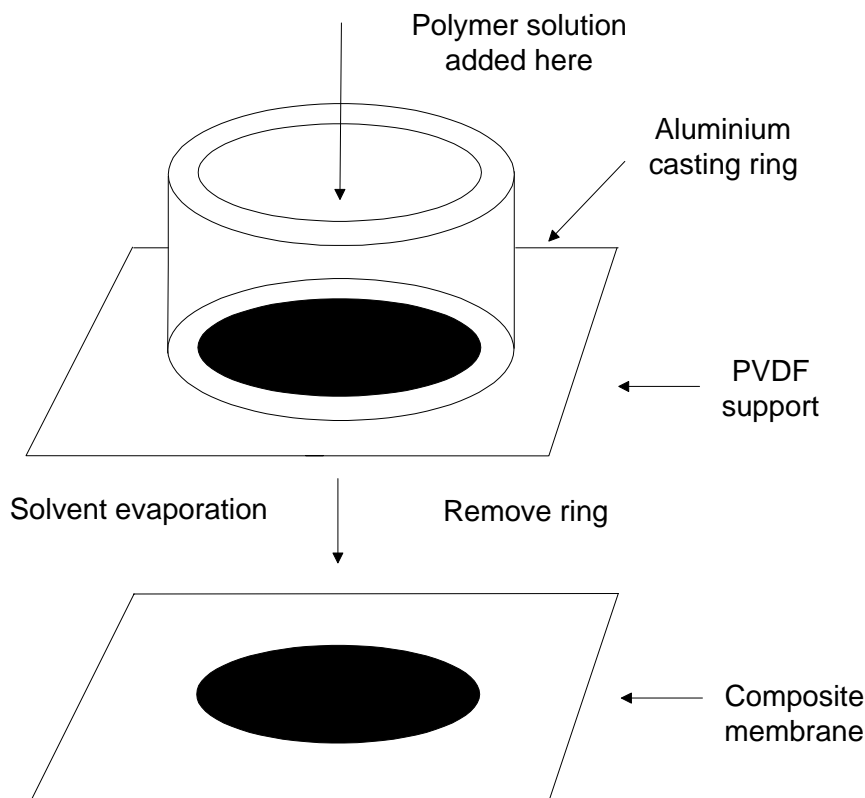
Figure 5.2: Casting of thin membrane films on a PVDF support material [1].

5.1.3   Blends of PDMS and Fluorel

To examine the possibility of blending PDMS and Fluorel for increased membrane stability and permeability, the following starting materials were used: poly(dimethylsiloxane) PDMS Dehensive®942 (two-component system in petrolether fluid); catalyst OL (1.1.3.3-tetramethyl-1.3-divinyldisiloxane-platinum) and isooctane, Fluorel, methanol and ethyl-methyl ketone.

PDMS Deh.® 942 was mixed carefully with isooctane. Then the mixture of isooctane and the catalyst were mingled in the first solution and stirred for ½ hour. Fluorel was prepared as described above.

Blends of 3 wt% PDMS and 3 wt% Fluorel were blended in different ratio so 1:1, 1:2, 2:1, and 2.5:1 parts PDMS and Fluorel respectively. The mixtures were dipcoated on a support material, consisting of a microporous poly(vinylidenefluoride) (PVDF) substrate on a woven poly(tetrafluoroethylene) (PTFE) support, and dried at 90°C for 18 hours.

5.1.4 Fluorosilicone

Three different types of fluorosilicone were available. Two membranes were prepared and delivered from the McMaster University. This polymer is (dimethyl-trifluoropropylenemethyl siloxane). The fluorosilicone were black, cured by Pt-catalysed addition cure. One sample was directly coated on PVDF support, spread (not evenly) by a pasteur pipette. The film was viscous and difficult to control in terms of thickness. The membrane was dried for 3 hour at room temperature and 15 minutes at 120°C. The other sample was coated from THF (tetrahydrofuran)- dried for 3 hour at room temperature and 15 minutes at 120°C.

The third fluorosilicone membrane was supplied from Specialty Silicone Fabricators, USA This polymer was poly(methyl- (3,3,3- trifluoropropylene)siloxane) which had vinyl terminated end groups. The membrane was transparent.

5.2 Methods to examine the durability of membranes - equipment and procedures

To examine the separation properties and the durability of polymer materials: both static exposure in a glass chamber and dynamic exposure in a membrane permeation cell have been used. Permeability measurements give the permeability flux of gases through the membrane, and the ideal selectivity is obtained. Changes in the permeability flux may occur during exposure to chlorine gas, and thus also changes in the selectivity. Absorption measurements give the sorption of gases in the material, which together with the permeability give an indication of the diffusivity. If the sorption does not reach equilibrium (at given pressure and temperature) this may be an indication of degradation taking place.

Long-term exposure of aggressive gases to the polymeric material gives an indication of the lifetime of the material. Changes in the material can also be analysed by FT-IR, SEM, NMR and DSC. These methods are described in section 5.3.

5.2.1 Permeability measurements

Permeation apparatus
Figure 5.3 shows the flow sheet of the system used for permeability measurements. This system was fully automatised with valve actuators and pressure controllers, and the process was operated from a computer. The system was mounted in a temperature-regulated cabinet. There was a high-pressure tank on the feed side and a low-pressure tank on the permeate side; each tank has a volume of 1 dm^3.

The permeability flux through the membrane $[m^3(STP)/(m^2\,Pa\,h)]$ was recorded as an increase in pressure (mbar) on permeate (vacuum) side as a function of time, using MKS Instruments pressure transducer. The data were logged directly into a computer using LabView. Next the data were converted by MatLab, given the temperature and membrane area, to flux J =P/l $[m^3$ (STP)/m^2 bar h]. The calculations performed are given in appendix A.1.
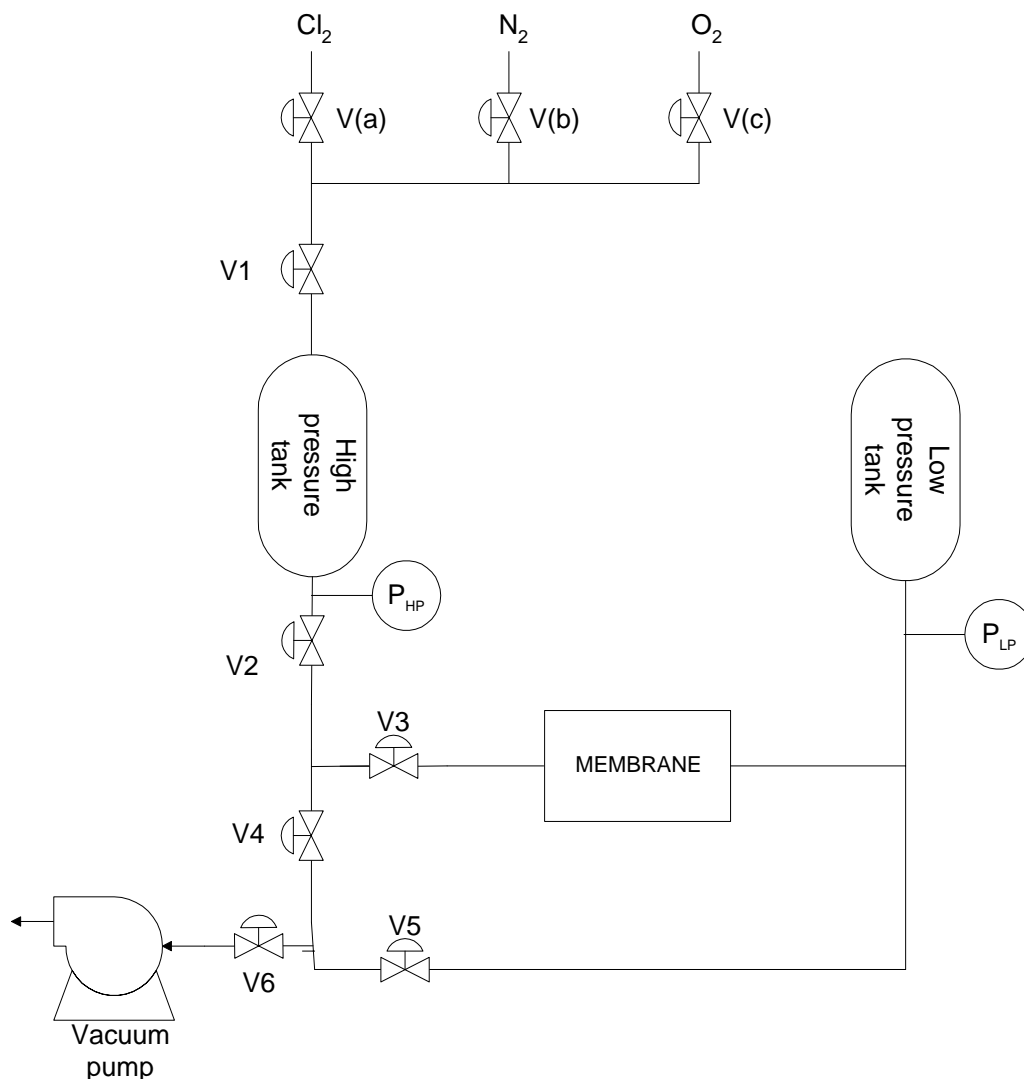
Figure 5.3: Flow sheet of the permeation apparatus.

Procedure
Before each permeability measurement, the system was evacuated until the pressure was less than 1 mbar. The system was evacuated over night when starting up the experiment, and between each exposure the evacuation time was at least 1 hour.

The high-pressure tank was then filled with the gas (N_2, O_2 or Cl_2) at a given pressure (e.g. 2 bara). Valves V2 and V3 were then opened and the pressure increase downstream was registered, and permeability calculated.

The permeabilities of N_2, O_2, and Cl_2 were measured at different temperatures: 30-100°C. The membrane was exposed to Cl_2 by filling the membrane cell with gas between the permeability measurements. The total time of exposure was from a few days to several weeks, with regular measurements of gas permeability during the exposure time.

Accuracy of the permeability measurements is discussed in appendix A.1.

Membrane cell
Small defect free pieces (diam. 2.4 cm) were cut out of the membranes and mounted in small membrane cells (Figure 5.4) for permeability measurements. It is crucial that the membrane is

without pinholes and cracks. The membrane cell could easily be disconnected from the apparatus for cleaning or change of membrane. The cross-section of the membrane cell used for the measurements is shown in Figure 5.5. It has a membrane diameter of 1.9 cm (Area = 2.8 cm^2). Previous experiments had shown that the membrane would degrade faster in direct contact with the stainless steel sinter, so this was changed to a Teflon sinter.

Figure 5.4: Membrane cell for permeability measurements with a gas tank of a volume 0.05 dm^3 (upstream side).
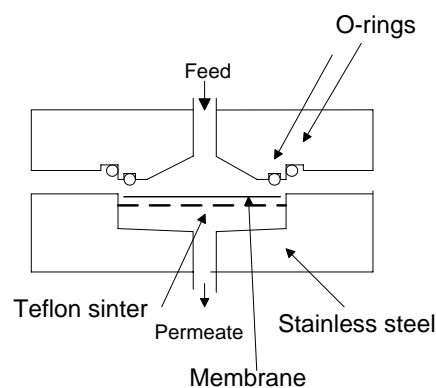
Figure 5.5: Cross-section of the membrane cell with a Teflon sinter.

5.2.2 Absorption measurements

Absorption apparatus

A weighted sample of the polymer was placed in the sample cell. The sample cell was mounted in an insulated temperature controlled cabinet equipped with MKS Instruments pressure transducer, Figure 5.6. The volume of the sample cell and connected tubing had been carefully calibrated. The exact weight and density of the polymer sample were measured before it was placed in the sorption chamber. The system was evacuated before the absorption measurements could start. The time of the evacuation may differ from polymer to polymer, depending on whether it is in its glassy or rubbery state and the production method of the membrane (solvent left in the polymer matrix). The evacuation time was recommend to be at least two times the sorption time.
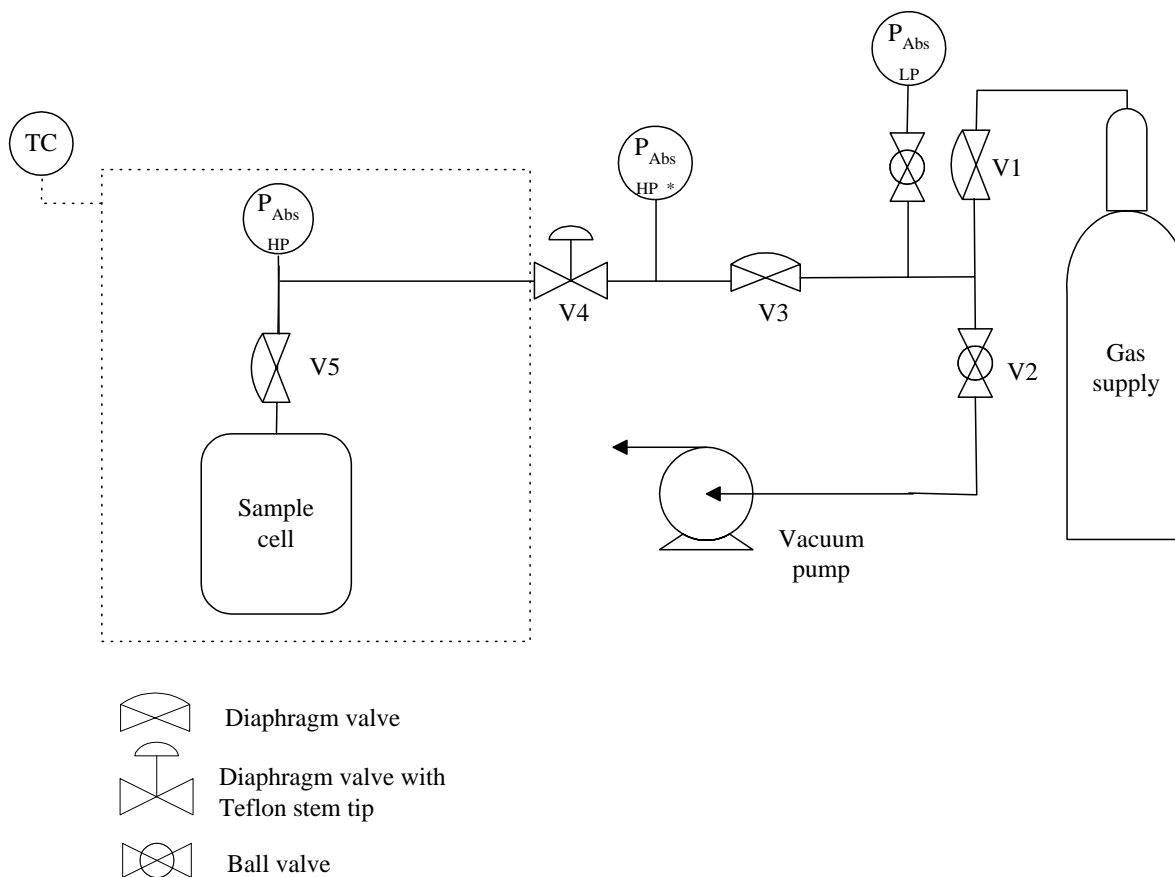
Figure 5.6: The flow sheet of the absorption system. The dotted line indicates the temperature-regulated cabinet.

Procedure

After evacuation valve V5 was closed. The system was filled with gas and all valves were closed. The pressure in the reference volume (volume between V4 and V5) had to be high enough to obtain wanted pressure in the sample cell when opening V5 (e.g. 1.66 bar in the reference volume will give 1 bar in the absorption cell when opening V5 for PDMS). The pressure was logged in LabView before and after V5 was opened. The measurement was running until the pressure gradient in the sorption cell was zero ($dp/dt = 0$). The absorption equilibrium was reached for gas saturation in the polymer sample. The sorbed volume of gas in the sample could be calculated from the reduction in pressure (mbar), either as solubility coefficient, S [$cm^3(STP)/(cm^3 \cdot bar)$] or as sorption level, C [(g gas)/(100 g sample)], in the polymer at a given pressure and temperature. The analysis of the data (logged by LabView) was performed with a MatLab program. The pressures at the start and the end of the measurements were noted and the sorption was calculated. New polymer samples were used for each temperature. The absorption was measured in the sequence N_2, O_2 and Cl_2. Figure 5.7 shows a typical sorption curve for O_2 in Fluorosilicone.

Calculation of the solubility coefficients and accuracy of the absorption measurements is given in appendix A.2.
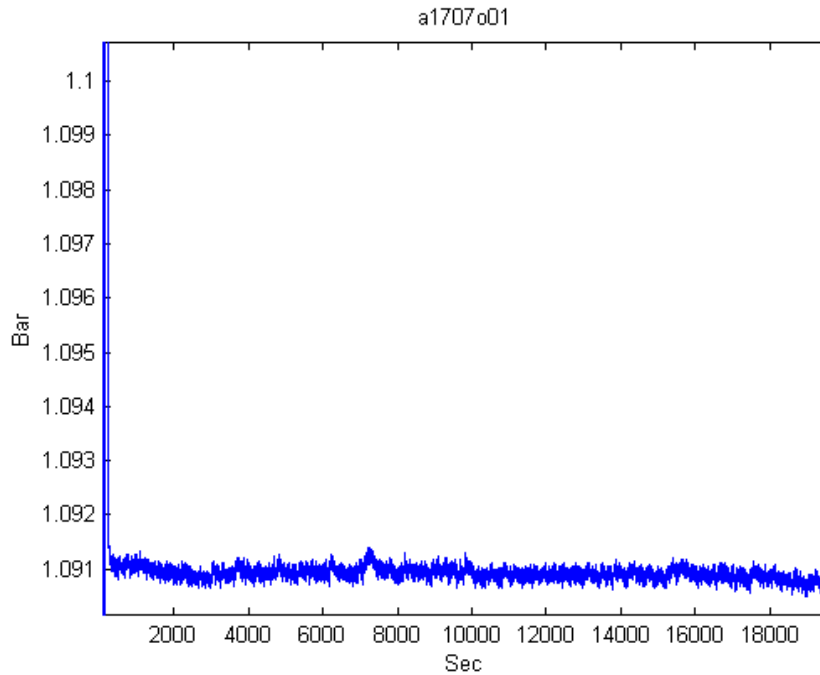
Figure 5.7: Typical sorption curve for O_2 in Fluorosilicone.

Absorption cell

When the absorption of corrosive gases like chlorine was measured, it was necessary to protect the polymer against direct contact with the iron/steel in the absorption cell (Figure 5.8). This is because the possibility of iron chloride formation, which catalyses degradation of the polymer. A glass container was placed inside the sample cell. The glass container had a cover with a small hole so the gas can easily flow through and into the polymer (left in Figure 5.8).

The density of the glass container was measured, and the volume of the container was corrected for before calculating the absorption.

Figure 5.8: The absorption cell with the glass container.

5.2.3   Durability tests in glass chamber

To examine the durability of polymers exposed to chlorine gas over longer time, a glass chamber was used. The glass chamber is needed to avoid the formation of iron chloride, which can have a catalytic effect on the degradation mechanism. The chamber is formed as shown in Figure 5.9.

Procedure
The samples to be exposed for chlorine gas were placed on glass racks inside the chamber. The chamber was evacuated, and filled with chlorine gas at approximately 1-1.5 bara. The chamber was placed in a temperature-regulated oven, at 30°C or 60°C, for a given exposure time (e.g. 4 weeks). The chamber was carefully evacuated after the exposure, letting the chlorine gas dissolve in an alkaline liquid (NaOH). The chamber was swept with nitrogen gas before opened.

The samples exposed at these conditions were: Poly(dimethylsiloxane), Fluorel, PDMS blended with Fluorel in the ratio 2:1 and 2.5:1, Fluorosilicone and the substructure PVDF/PTFE. The samples were weighted before and after exposure, and analysed by FT-IR.

Figure 5.9: Glass chamber used for durability tests of polymer samples.

5.2.4   Swelling tests

By introducing various degrees of crosslinking in a rubbery polymer, the swelling will be restricted and segmental motion of the polymer chains suppressed. The permselectivity may then be maintained, but the permeability will decrease. To examine the degree of swelling the changes in crosslinking density is found.

The following protocol was thus adapted for swelling tests [4]:
1. Weigh the membrane
2. Swell the membrane (subjected to soxhlet extraction using cyclohexane for 12 hours, weigh swollen)
3. Dry the membrane at 70°C for 12 hours (weigh dry, difference in weight 1-3 reflects loss of starting materials)

5.3 Description of analytical methods

Different analysis methods have been used to examine the changes in the polymer after exposure to chlorine gas. All samples have been examined with FT-IR. The poly(dimethylsiloxane) have also been examined with NMR. Other analysis techniques have been used in some extent to examine surfaces, densities and thermal changes. A brief summary of each method is given in appendix C. This section just gives a short presentation of the instruments used.

5.3.1 FT-IR

Measurements of infrared absorption with Fourier Transformation have many applications both in qualitative and quantitative analysis. The most important one is to identify organic components. Absorption of infrared radiation is based on small differences in energy that exists between different vibration- and rotation conditions for the atoms in the molecule. Vibrations given for one particular bond linkage will not necessary give the same wavelength in different components, because the bond linkage has different chemical environment. This makes it relatively easy to identify the chemical structure of a molecule [5]. A spectrum of a polymer is easily obtained, and changes, like for instants degradation, in the polymer can be detected very fast. This is why FT-IR is a good technique to analyse, among other factors, degradation of polymer materials.

The FT-IR analysis for the composite membranes PDMS, Fluorel and Fluorosilicone was performed with a Horizontal Attenuated Total Reflectance (HATR), an internal reflection assocery, with a ZnSe crystal. Background spectrum was detected of the crystal. To make a spectrum, the sample was pressed onto the crystal and analysed. The HATR can simplify the FT-IR analysis of polymer films, pastas, gels, semi-solids and powders.

Instrument information / settings:

Instrument:	Perkin-Elmer System 1600
Detector:	DTGS
Resolution:	4 cm^{-1}
Scans:	16

Internal reflectance spectra are similar but not identical to ordinary absorption spectra. In general, while the same peaks are observed, their relative intensities differ. The absorbance, although dependent on the angel of incidence, are independent of sample thickness, because the radiation penetrates only a few micrometers into the sample [5]. With this technique the intensity of the bond will increase when the wavenumber is decreased. The sensitivity is larger in the range 2000-700 cm^{-1}, than in the range 4000-2000 cm^{-1}. The ZnSe crystal has a transmission range between 17000-650 cm^{-1}.

5.3.2 Nuclear Magnetic Resonance (NMR)

NMR provides much valuable information to the polymer chemist. Structural units of polymers are identified from a combination of chemical shift data and spin-spin splitting. With the very high resolution afforded by modern NMR instruments one may gain insight into polymer stereochemistry and monomer sequencing

The NMR technique utilises the property of spin (angular momentum and its associated magnetic moment) possessed by nuclei whose atomic number and mass number are not both even. Such nuclei are ^{1}H and ^{13}C, ^{15}N, ^{17}O, and ^{19}F. Application of a strong magnetic field to materials containing such nuclei splits the energy level into two, representing states with spin parallel and antiparallel to the field. Transition between the states lead to absorption or emission of energy [6].

The analyses were carried out in a BRUKER DCX-300 digital NMR with a proton resonance frequency of 300.13 MHz. The samples were prepared in 5 mm of diameter sample tubes in $CDCl_3$ without any internal standard.

5.3.3 Scanning Electron Microscope (SEM)

To obtain an electron microscopic image the surface of a solid sample is swept with a raster pattern with a finely focused beam of electrons. A raster is a scanning pattern similar to that used in a cathode-ray tube, in which an electron beam is (1) swept across a surface in a straight line, (2) returned to its starting position, and (3) shifted downward by a standard increment. This process is repeated until a desired area of the surface has been scanned. Several signals are produced from a surface when it is scanned with an energetic beam of electrons. These signals include backscattered, secondary, and Auger electrons; X-ray fluorescence; and other photons of various energies. All of these signals have been used for surface studies, but the two most common are backscattered and secondary electrons, which serve as a basis of scanning electron microscopy. Scanning Electron microscope provides morphologic and topographic information about the surfaces of solids that is usually necessary in understanding the behaviour of surfaces. Thus, an electron microscopic examination is often the first step in the study of surface properties of a solid [7].

SEM allows a clear view of the overall structure of a membrane; the top surface, the cross-section and the bottom surface can all be observed very nicely [8].

For dense membranes SEM can study a change in the morphology after exposure to aggressive conditions. The technique will not give any information about the presence of specific groups or change in separation properties, without connecting an analysis spectroscopy, example an X-ray Photoelectron Spectroscopy, to the scanning electron microscope.

All samples were cooled in liquefied nitrogen and cracked. This was done for analysis of the cross-sections of the membranes. The samples were mounted on a sample holder with carbon tape and then coated with gold. The magnifications used on the samples were between x200 to x2000. Norsk Hydro performed the SEM analyses.

5.3.4   The Differential Scanning Calorimetry (DSC)

The Differential Scanning Calorimetry (DSC) is a technique to measure transition or chemical reactions in a polymer sample. DSC determines the energy necessary to counteract any temperature difference (ΔT) between the sample and the reference upon heating and cooling. A DSC curve (Figure 5.10) allows the glass transition temperature and the degree of crystallinity to be obtained. First-order transitions such as crystallisation and melting give narrow peaks, the peak area being proportional to the enthalpy change in the polymer and the enthalpy change being related to the amount of crystalline material present, i.e. allowing estimation of the degree of crystallinity. The glass transition temperature corresponds to the second-order transition. The second-order transitions are characterised by a shift in the base line resulting from a change in heat capacity [8].

The sample is placed in an aluminium pan and sealed with a lid. It is important that the sample does not degas, because this can blow up the pan. To achieve a spectrum with clear peaks, it is necessary to use at least 15 mg of the sample in the pan.

Instrument: Perkin-Elmer Pyris 1 DSC with ice water for cooling.

All spectrum calculations are performed with the software of the instrument.
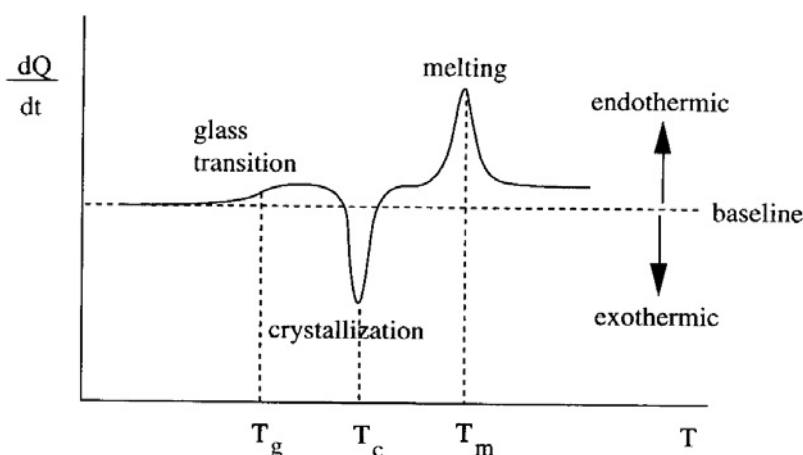
Figure 5.10: Schematic DSC-curve for a semicrystalline polymer [8].

References to chapter 5

1.   M. A. Brook, S. Balduzzi, M. Mohamed and R. Stan; Report to Norsk Hydro-Tel-Tek, Acid Lability of Silicone Membranes (confidential), Chemistry Department McMaster University, Canada 1998.
2.   M. A. Brook, M-B. Hägg, S. Balduzzi, M. Mohamed and R. Stan; Minutes of meeting Norsk Hydros Chlorine Project (confidential), McMaster University, Hamilton, Ontario, Canada, April 15th 1999.
3.   M. A. Brook; Silicone in Organic Organometallic and Polymer Chemistry, (Chapter 9), John Wiley & Sons Inc., USA 1999.
4.   M. A. Brook, S. Balduzzi, M. Mohamed and R. Stan; Report 2 to Norsk Hydro-Tel-Tek, Acid Lability of Silicone Membranes (confidential), Chemistry Department McMaster University, Canada 1998.

5.   Skoog and Leary; Principles of Instrumental analysis, (Chapter 12), 4th Ed., Saunders College Publishing, USA 1992.
6.   F. W. Billmeyer; Textbook of Polymer Science, p. 233-237, John Wiley & Sons Inc., USA1984.
7.   Skoog and Leary; Principles of Instrumental analysis, (Chapter 16), 4th Ed., Saunders College Publishing, USA 1992.
8.   M. Mulder; Basic Principles of Membrane Technology, 2nd Ed., Kluwer Academic Publishers, The Netherlands 1996.

Chapter 6: Experimental Results and Discussion

Summary

This chapter presents the results of the different membranes studied during the project. The materials are presented in separate sections with results from experiments and methods of analysis. The sections are ended with an interim conclusion of the membrane durability when exposed to chlorine gas. The materials that have been analysed are poly(dimethylsiloxane) (PDMS), Fluorel, blends of PDMS and Fluorel, and Fluorosilicone.

The PDMS was chosen due to previously documented [1] favourable permeability flux for Cl_2 and high selectivity for Cl_2/O_2. A better understanding of changes causing decreased permeability flux and degradation over time was searched for. The fluoropolymers were chosen due to well-documented chemical resistance to Cl_2 exposure.

All experiments were performed at Telemark University College, with the exception of the swelling tests for the PDMS, which were performed by McMaster University in Canada, and the NMR analyses performed by GKSS in Germany.

6.1 Poly(dimethylsiloxane), PDMS

PDMS was synthesised and cured in different ways (summarised in section 5.1) and prepared with three different degrees of crosslinking characterised as low, medium and high. All the different PDMS samples were casted as membranes.

Only the hydrosilylation cured PDMS membranes without diphenyl groups were found to be of suitable quality for permeability tests. In the beginning of the experiments many samples showed initially good selectivities. However it can be said that all samples, with the exception of the one with high crosslinking were ruined already at 30°C when exposed to chlorine gas. Higher degree of crosslinking gave in general a higher selectivity. Further discussions in section 6.1 will concern only PDMS with the highest degree of crosslinking.

6.1.1 Permeability measurements of N_2, O_2, and Cl_2

The permeability of two similar membrane samples (A and B) was measured. The samples only differed in thickness of the selective layer. Sample A was exposed to chlorine gas at 30°C for a period of 6 weeks. Sample B was first exposed to chlorine gas at 30°C for a period of 6 weeks, then at different temperatures (60°C, 80°C and 100°C) for one week at each temperature. The latter membrane was exposed to Cl_2 for 9 weeks in total. The permeability measurements were performed with a pressure on the feed side of 2 bara, while the pressure at the permeate side was about 0.6 mbar for both samples. The thickness of the selective top layer was estimated from SEM analysis. Membrane A had a thickness of 7 μm (Figure 6.1). The thickness of the top layer of membrane B was estimated from the SEM analysis to be less than 1 μm. However, the measured permeability flux of membrane B was much lower than expected. An elementary mapping analysis was therefore performed (Figure 6.3). From this it was seen that the silicone was not only in the top layer, but had flown into the substructure, making it difficult to estimate the effective thickness of the selective layer. The separation properties was however good, but the exact permeability (P) could not be found. Only the permeability flux (P/l) could be measured, and selectivity determined (Figure 6.7).

The membrane cell had a diameter of 1.9 cm giving a permeation area of 2.8 cm^2, hence the permeability [m^3(STP) m/(m^2 h bar)] could be calculated from the measured flux [bar/h] at the operating pressure.

Figure 6.1: SEM picture of PDMS for determination of the thickness of the selective layer of membrane A. Thickness: 7μm. Magnification: 1000 x.

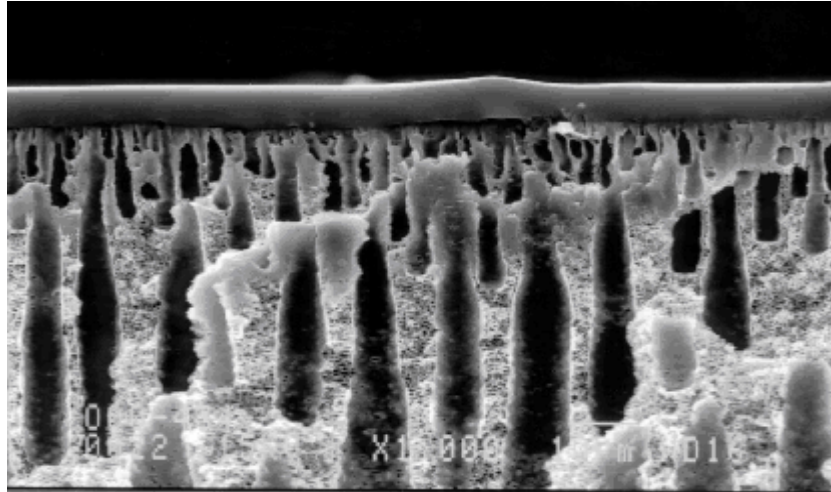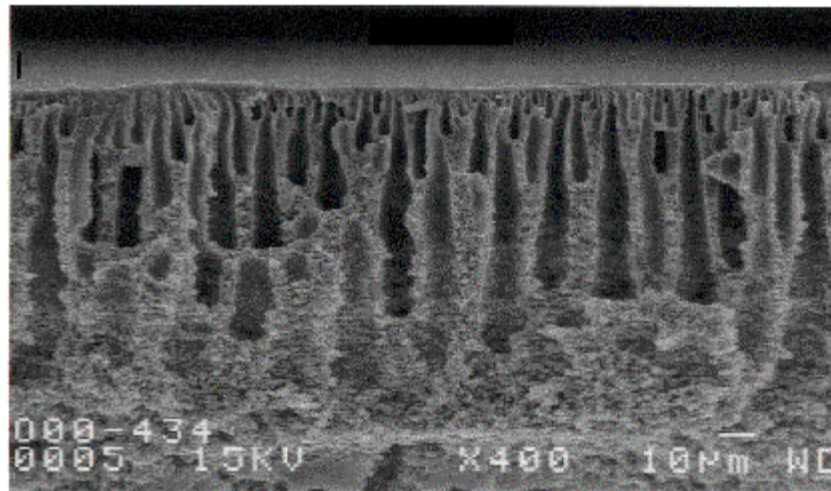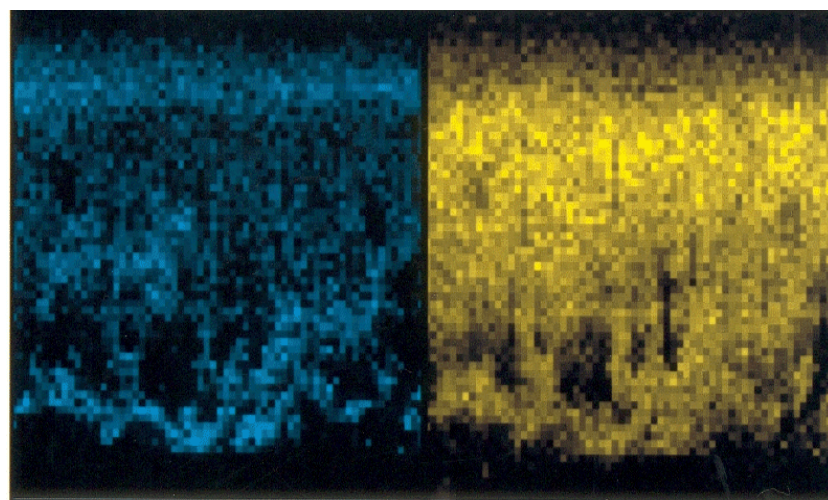*Figure 6.2: SEM picture of PDMS for determination of the thickness of the selective layer of membrane B. Magnification: 400 x.*

Fluorine   Silicon

Figure 6.3: SEM elementary mapping of PDMS membrane B. The colours indicate the distribution of the specific element in the membrane matrix of the membrane given in Figure 6.2.

Changes in permeability over time at 30°C:

Figure 6.4 to Figure 6.6 illustrate the changes in permeability and selectivity of membrane A as a function of time for N_2, O_2 and Cl_2. Figure 6.7 illustrates the selectivity of membrane B (see appendix B, Table B.1.1 and B.1.2, for measured data). The temperature of all permeability measurements was 30°C.

As can be seen from Figure 6.4 and Figure 6.5, the permeability decreased significantly for all three gases during the first week of chlorine exposure. Changes in the membrane properties are obvious. Over the next weeks the permeability was still decreasing, but to a lesser extent.

The selectivity (Figure 6.6) for O_2/N_2 was relatively constant during the exposure time of 6 weeks. The selectivity for Cl_2/O_2 increased during the first week of exposure and was mainly decreasing thereafter. This is all discussed in paragraph 6.1.2.
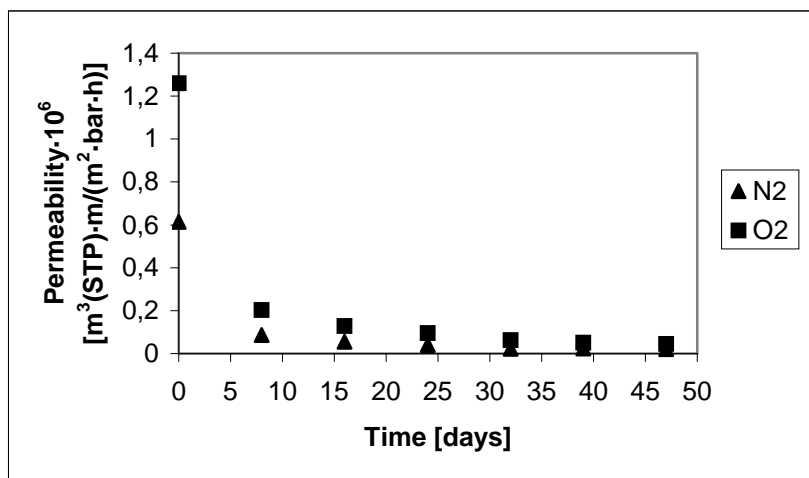
Figure 6.4: Permeability $\cdot10^6$ [m^3 (STP) m/(m^2 bar h)] as a function of time for N_2 and O_2 in PDMS (membrane A) at 30°C. Thickness: 7 μm.
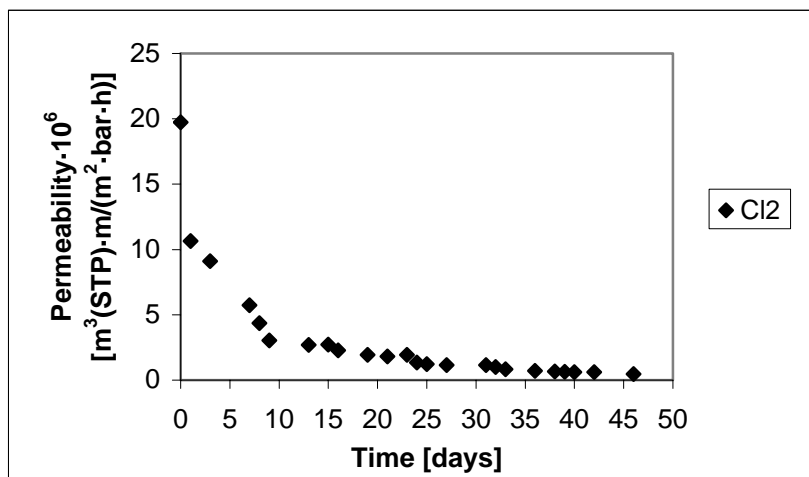
Figure 6.5: Permeability $\cdot10^6$ [m^3 (STP) m/(m^2 bar h)] as a function of time for Cl_2 in PDMS (membrane A) at 30°C. Thickness: 7 μm.
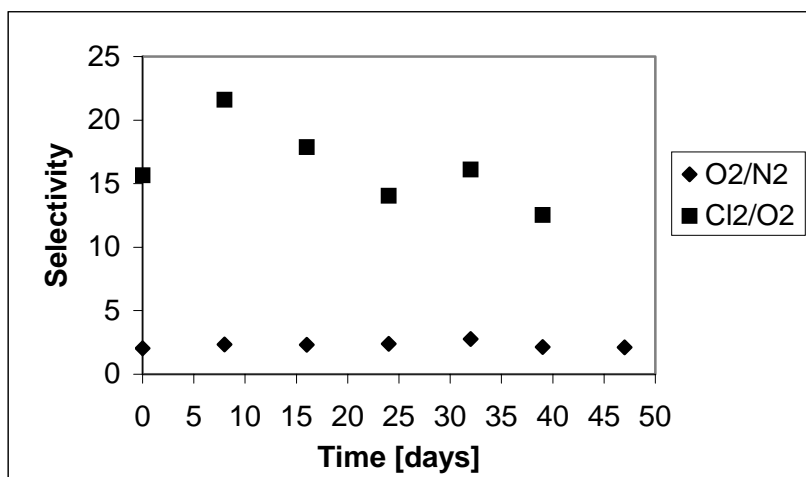
Figure 6.6: Selectivity of O_2/N_2 and Cl_2/O_2 in PDMS (membrane A) as a function of time after exposure to Cl_2 gas at 30°C. Thickness: 7 μm.
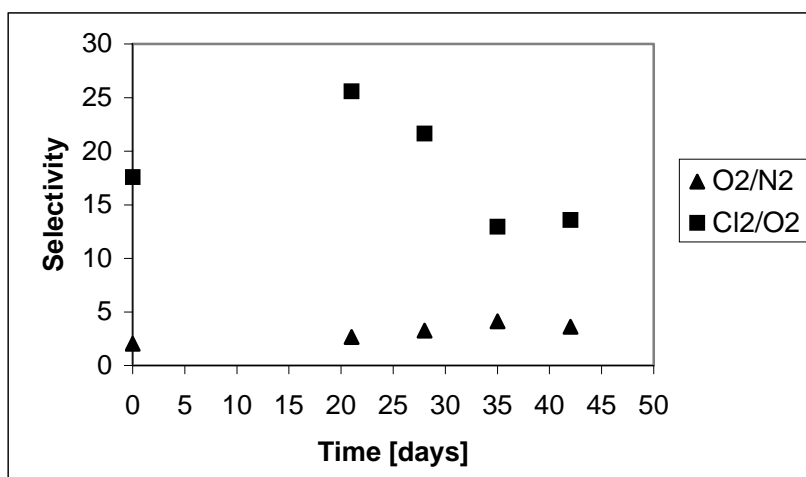
Figure 6.7: Selectivity of O_2/N_2 and Cl_2/O_2 in PDMS (membrane B) as a function of time after exposure to Cl_2 gas at 30°C.

Changes in permeability over time in temperature range 30-100°C:

Figure 6.8 a-d shows the permeability flux changes over time upon exposure to Cl_2 within the temperature range 30-100°C. The membrane was exposed to chlorine gas all the time; expect during O_2 and N_2 measurements. The experiments were performed on membrane B (with unknown thickness), thus only the permeability flux is reported. The chlorine exposure time at 30°C was 6 weeks. The selectivities are given in Figure 6.7. The fluxes were measured regularly for all three gases (N_2, O_2 and Cl_2) at this temperature. The temperature was increased to 60 °C for 1 week. The permeability fluxes of N_2 and O_2 were measured at the end of this temperature experiment, giving an O_2/N_2 selectivity of 2.6. The temperature was then raised to 80°C for 1 week and then to 100°C for an additional week. At the two highest temperatures only the flux of Cl_2 was measured.

The Cl_2/O_2 selectivity of membrane B was 18at the start of the experiment and decreased to 14 during the 6 weeks of chlorine exposure at 30°C. After 1 week of exposure to chlorine gas at 60°C the Cl_2/O_2 selectivity had decreased to 5.0. The selectivity of O_2/N_2 was 2.0 before chlorine exposure. After 6 weeks of chlorine exposure at 30°C the O_2/N_2 selectivity increased to 3.6, but decreased to 2.6 after exposure to chlorine gas at 60°C for 1 week.

An increase in temperature clearly speeds up the reactions that are causing changes in the material. These changes give a decreased permeability flux for the chlorine gas. The sudden increase in permeability flux at 100°C (Figure 6.8d) is a clear indication of a ruined membrane. This could be caused by chain scissoring of the polymer chains or pinholes created in the selective layer. When the membrane cell was opened it was confirmed that the selective layer had become somewhat brittle and that pinholes had formed.

Part of the selective layer was sticking to the Teflon poly(tetrafluoroethylene) filter and was torn off when the filter was carefully removed. The sample was only slightly discoloured although a pale yellow colour was visible in the microscope. A layer of rusty particles covered the filter, which proved that a filter indeed was necessary to protect the membrane.
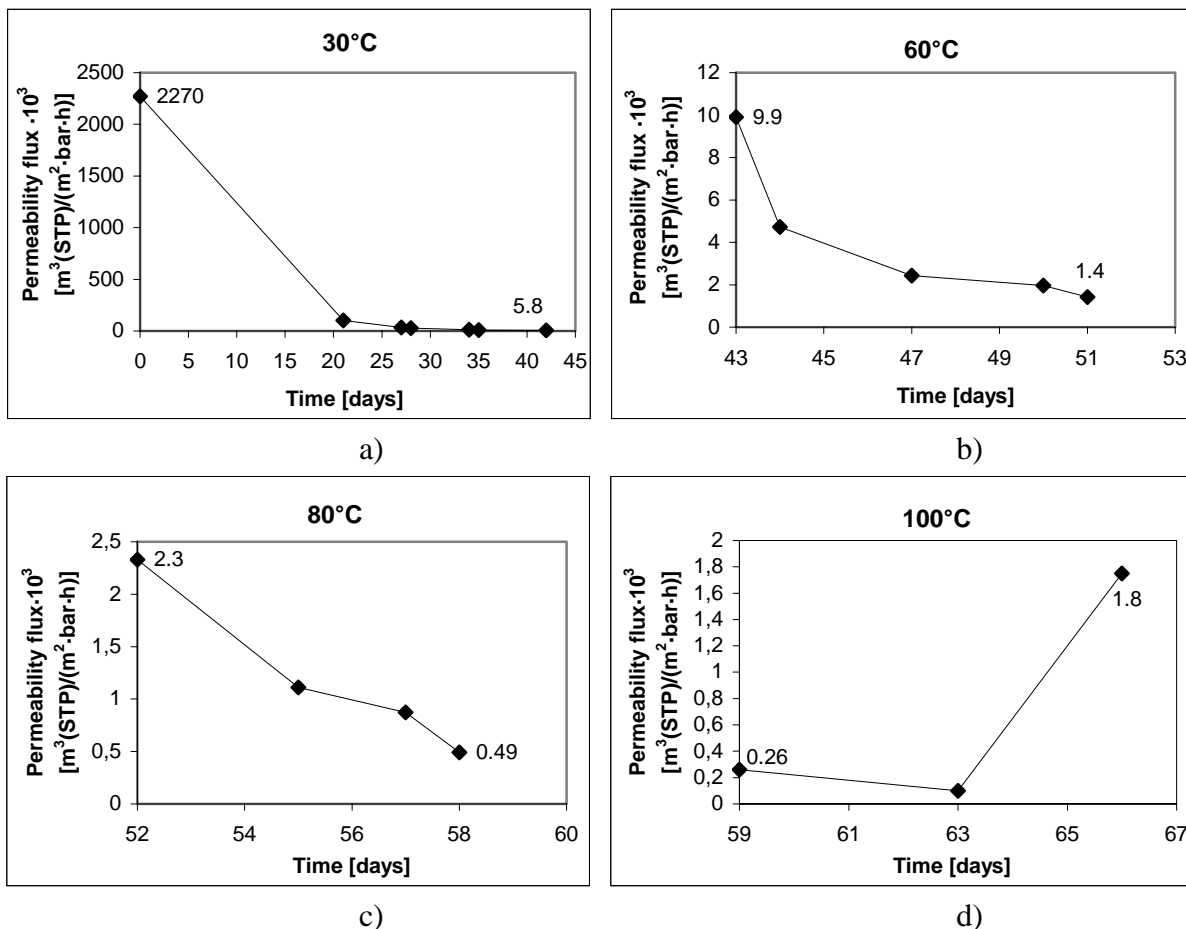
Figure 6.8: Permeability flux $\cdot 10^3$ [$m^3(STP)/(m^2$ bar h)] of Cl_2 in PDMS (membrane B) as a function of time at increasing temperatures a) 30°C, b) 60°C, c) 80°C and d) 100°C.

6.1.2 Durability discussed in view of permeability results

The general tendency was that permeability decreased over time when the membrane was exposed to Cl_2. The permeability would be expected to increase if the membrane degraded, i.e. longer polymeric chains had decomposed (see figure 4.10 and 4.17). However, if exposure to chlorine or elevated temperatures over time promoted further crosslinking (see figure 4.18 and 4.19), then a decrease in permeability could be explained. This would also explain the relative reduction in selectivity for the gas pair chlorine and oxygen. Strong interchain-interactions give a denser and more restricted polymer network. Both the diffusion and the sorption transport of gases would then be reduced and thus also the permeability.

The decreasing permeability may also be a result of a chlorination substitution reaction as a result of the exposure. By substitution, chlorine may replace hydrogen atoms in the methyl group attached to the silicon atom:

$$[Si\,(CH_3)_2O]_n + Cl_2 \rightarrow [Si(CH_3)(CH_2Cl)O]_n + HCl \qquad\qquad (\,6.1\,)$$
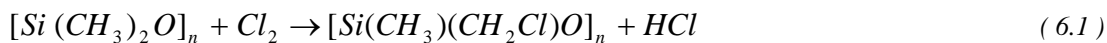
It has been reported [2] that the mean permeability ($\bar{P}$) decreases markedly as bulkier functional groups are substituted in the polymer side chains or backbone chain. The decrease in $\bar{P}$ is due to a decrease in penetrant diffusivity, which is caused by increasing rigidity of the polymer backbone and decreasing free volume available for the diffusion penetrant molecules. It should be noted that substitution of bulkier functional groups raises the glass transition temperature of the polymer. The solubility of the penetrant gases is also reduced by substitutions, but this effect is not so big as the corresponding decrease in penetrant diffusion.

The substitution of chlorine will give a bulkier side-group, due to the larger chlorine atom (compared to hydrogen). Chlorine exerts a stronger charge distribution than hydrogen. This creates permanent dipole moments in the polymer chain. Dipoles exert a strong attraction to other dipoles and the dipole-dipole interactions between the polymer chains give a denser structure in the polymer network. This polarity increases the interchain interaction. This gives a lower flexibility of the rotation around the main chain, which causes an increase in the glass transition temperature T_g (the T_g has not been measured after the exposure). This gives a decreased permeability due to the denser polymer structure.

The Cl_2/O_2 selectivity of membrane A was increasing during the first week of Cl_2 exposure, and decreased mainly thereafter. Looking carefully through the measured permeability values given in table B.1.1, in appendix B, it can be observed an 80% decrease in the permeability for both chlorine and oxygen during the first week of exposure. During the second week of exposure there was app. 40% decrease in permeability for both chlorine and oxygen. A "new" membrane material is formed due to chlorination and possible chain scissoring. The changes in the material will change the diffusion and solution parameters and this contribute to changes in selectivity.

The O_2/N_2 selectivity is relatively constant throughout the experiments. Both gases can be considered as ideal gases with small differences in size (Lennard-Jones diameter O_2 = 3.46 Å and N_2 =3.80 Å) (see Appendix D), and the solubility is low and not very different for the two gases. These factors will give a relatively constant O_2/N_2 selectivity.

In pure PDMS the permeability of Cl_2, a large molecule and easily condensable non-ideal gas, will decrease with increasing temperature. This is according to theory and clearly documented by Hägg [1]. Figure 6.8 illustrates the influence of temperature and Cl_2 exposure on PDMS (membrane B) exposed to Cl_2 for almost 10 weeks. This documentation shows that the Cl_2-permeability flux of a chlorinated PDMS increases when the temperature is raised. This is the opposite of what was found for a non-chlorinated PDMS [1]. A chlorinated PDMS will obviously have properties very different from a regular PDMS. However, the permeability flux decreases over the 60 days of chlorine exposure, indicating that the material properties are continuously changing due to chlorination.

The theoretical review in section 2.2 explains the complications with non-ideal gases like Cl_2: Diffusion and solubility have for these gases opposing effects when it comes to temperature dependency. The permeability coefficient is depending both on diffusion and sorption (P =

D·S, eq. 2.5). Material changes will also be affecting these two parameters in addition to the general temperature effect.

The permeation experiments show that a PDMS membrane with high crosslinking, can withstand Cl_2 exposure at elevated temperatures for at least 60 days even though the permeability becomes too low to be of industrial interest.

6.1.3 Durability discussed in view of permeability measurements with process gas

A few experiments were performed where the highly crosslinked PDMS was exposed to process gas from the electrolysis process at the Mg-plant at Norsk Hydro. The process gas from the electrolysis contains 90-95 vol% chlorine and the rest is mainly air. The temperature of the gas from electrolysis is app. 150°C, but had been cooled to about 80°C when it reached the membrane unit. At this temperature the toxic impurities like chlorinated hydrocarbons (CHC) in the gas stream are still in gas phase; they will precipitate at about 60°C. This was the main reason why the separation temperature initially was preferred kept at 65°C or higher. Gaseous CHCs should preferably be kept in gas phase and removed further down the line. An alternative process for removal of impurities made it feasible to cool the gas to 25°C, although a higher temperature still was preferred due to operational reasons in the industrial process. This has set the temperature range for the membrane separation tests (30-100°C) [3].

The permeability of N_2, O_2 and pure Cl_2 gas was measured before the membrane cell was evacuated to 1 mbar and filled with gas from the electrolysis process. The cell was kept at 30°C for 1 week. The membrane cell was then evacuated, and the permeability measurements of N_2, O_2 and pure Cl_2 gas were repeated. The whole procedure was repeated for another week with the same membrane. The results are presented in Table 6.1.

Table 6.1: Results from permeability measurements of PDMS exposed to process gas at 30°C. Thickness: 7μm.

Time [days]	Permeability $\cdot 10^6$ [m³(STP) m/(m² bar h)]			Selectivity	
	N_2	O_2	Cl_2	O_2/N_2	Cl_2/O_2
0	0.62	1.3	20.0	2.1	16
7	0.40	0.54	7.9	1.4	15
14	3.8	3.6	5.7	0.9	1.6

The permeability decreased for all three gases during the first week. The decrease in permeability during the first week of exposure was comparable to the results obtained with pure gas exposure. The polymer structure is becoming denser due to the chlorine exposure, reducing the gas transport through the membrane. The selectivity for Cl_2/O_2 is still high after one week of exposure to the process gas, but after an additional week of exposure the selectivity had decreased significantly. The increased permeability for nitrogen and oxygen with a decreased selectivity for both O_2/N_2 and Cl_2/O_2 indicate pinholes in the membrane.

The analysis performed in laboratory has been focused on dry pure gases. However, in the process the gases are mixed and they may interact with each other and with the polymer in more complicated ways. The combination of high temperature, and process gas containing chlorine and oxygen as well as multiple impurities may initiate more complicated degradation mechanisms than those of the pure dry chlorine gas. Moisture in the process gas will give HCl vapour, which deteriorate the membrane.

Degradation may also be initiated by the presence of impurities like CHC, particle formation and ferric ions (act as catalysts for degradation). A filter of poly(tetrafluoroethylene) (Teflon) was used to avoid direct contact between the particular impurities and the membrane. Also direct contact with steel in cell housing etc. may catalyse a degradation reaction of the polymer when it is exposed to chlorine gas.

6.1.4 Permeability measurements of HCl gas

In a parallel project [4,5] permeabilities of hydrogen and hydrochloric acid were measured. This separation is very challenging due to the aggressive nature of HCl, which is strongly corrosive in presence of humidity.

The separation of H_2 and HCl may be compared to the separation of Cl_2 and O_2 in certain aspects, but is also very different in some ways: H_2 is an ideal non-polar gas with very small molecular diameter, and is one of the most permeable gases in membrane separation. HCl is a non-ideal polar gas and a larger molecule than H_2 (see table D.1 in appendix D), and the critical temperatures of the two gases differ significantly ($T_{crit}(H_2)$= 33.5 K, $T_{crit}(HCl)$=324.8 K). These facts should in principle indicate a fairly easy separation for the gas pair. The H_2 will generally have a high permeation rate both in glassy and rubbery polymers. One would expect from the high critical temperature of HCl that the solubility factor would have a significant effect on transport of HCl through a rubbery membrane, indicating a fairly high permeability also for HCl. However, due to the chemical nature of HCl many materials will degrade in contact with the gas. It is documented in the project that perfluorinated materials will be chemically resistant to degradation upon exposure to this gas [6].

The permeability measurements referred to [4,5] (appendix B Table B.1.6) showed a permeation for HCl at 25°C and 6 bar of $25 \cdot 10^{-6}$ m³(STP) m/(m² bar h). After only 1 hour of exposure the permeability had increased to $79 \cdot 10^{-6}$ m³(STP) m/(m² bar h) indicating a ruined membrane. After opening the cell it was clear that the membrane had degraded totally, which explains the high measured permeation [4]. The value for H_2 at 25°C and 6 bar was measured to $1.6 \cdot 10^{-6}$ m³(STP) m/(m² bar h) resulting in an initial selectivity HCl/H_2 $\approx$ 16.

These measurements illustrate how efficiently HCl catalyse degradation of the PDMS. HCl can be formed as a degradation product when the PDMS membrane is exposed to chlorine gas.

6.1.5 Absorption measurements

The sorption measurements were performed on a PDMS, prepared from a two-component system of 30% silicone-product (Dehesive® 942) in petrolether. The crosslinking of the standard PDMS was done by addition of R_3-Si-H (R = alkyl) groups using platinum-catalyst. Remaining catalyst may result in reactions with free Cl_2 as well as with HCl. Further crosslinking at higher temperatures may as well take place. During membrane preparation crosslinking was done at 30°C. After a given time (when the solvent had evaporated) the films were heated to 80°C for one or two hours to terminate the crosslinking. The membrane was prepared without support. Calculation procedures for the sorption are given in appendix A.2.

Measured solubility coefficients are presented in Table 6.2 and compared to values found in literature (Table 6.3) [7].

The compressibility factor, z, for Cl_2 was calculated and used to correct for non-ideal behaviour when calculating volume of gas absorbed in the polymer [8]. The heat of solution, (ΔH_s) is found from an Arrhenius plot of the solubility coefficient, following equation 6.2.

$$S = S_0 \exp\left(-\Delta H_s / RT\right)$$

<div align="right">(6.2)</div>

The heat of solution which contains both a heat of mixing term and a heat of condensation can be either positive (endothermic) or negative (exothermic) For small gases such as H_2, He and N_2, ΔH_s is often slightly positive which indicates that the solubility increases with increasing temperature. The experimental data are plotted according to eq. 6.2 in Figure 6.9. Calculated values for ΔH_s are given in Table 6.4.

Gas solubility as a function of temperature, 30-80°C:

With increasing temperature, a slight increase in the sorption was observed for N_2, O_2 and H_2 while the sorption for chlorine was decreasing. The high sorption value measured for Cl_2 at 1 bar and 80°C (see Table 6.2) is a combination of sorption and chemical reaction between the polymer and chlorine during the time of the experiment. This value (Cl_2 at 1 bar and 80°C) is therefore not included in Figure 6.9. For the 3 bara exposure, the time of absorption was shorter since absorption equilibrium was reached more rapidly at higher pressures.

Table 6.2: Solubility coefficients in standard PDMS [1].

Temp. [°C]	Solubility coefficient, S, $[cm^3(STP)/(cm^3\,bar)]$				
	H_2 at 2 bar	N_2 at 2 bar	O_2 at 2 bar	Cl2*at 1 bar	Cl_2* at 3 bar
25	0.191	0.220	0.314	10.22	13.3
35	0.193	0.222	0.316	8.22	11.1
50	0.197	0.225	0.320	7.60	8.97
65	0.195	0.230	0.325	6.63	7.29
80		-	-	10.14	5.00

The measured data have been corrected according to compressibility (factor z)

Table 6.3: Measured solubility coefficients in standard PDMS compared with literature data [7].

	Solubility coefficients [g /100 g]	
	measured at 35°C	Blume at 40°C
N_2	0.025	0.011
O_2	0.044	0.026
H_2	0.0014	
Cl_2	2.1	
ethanol		6.5*

* For comparison with Cl_2
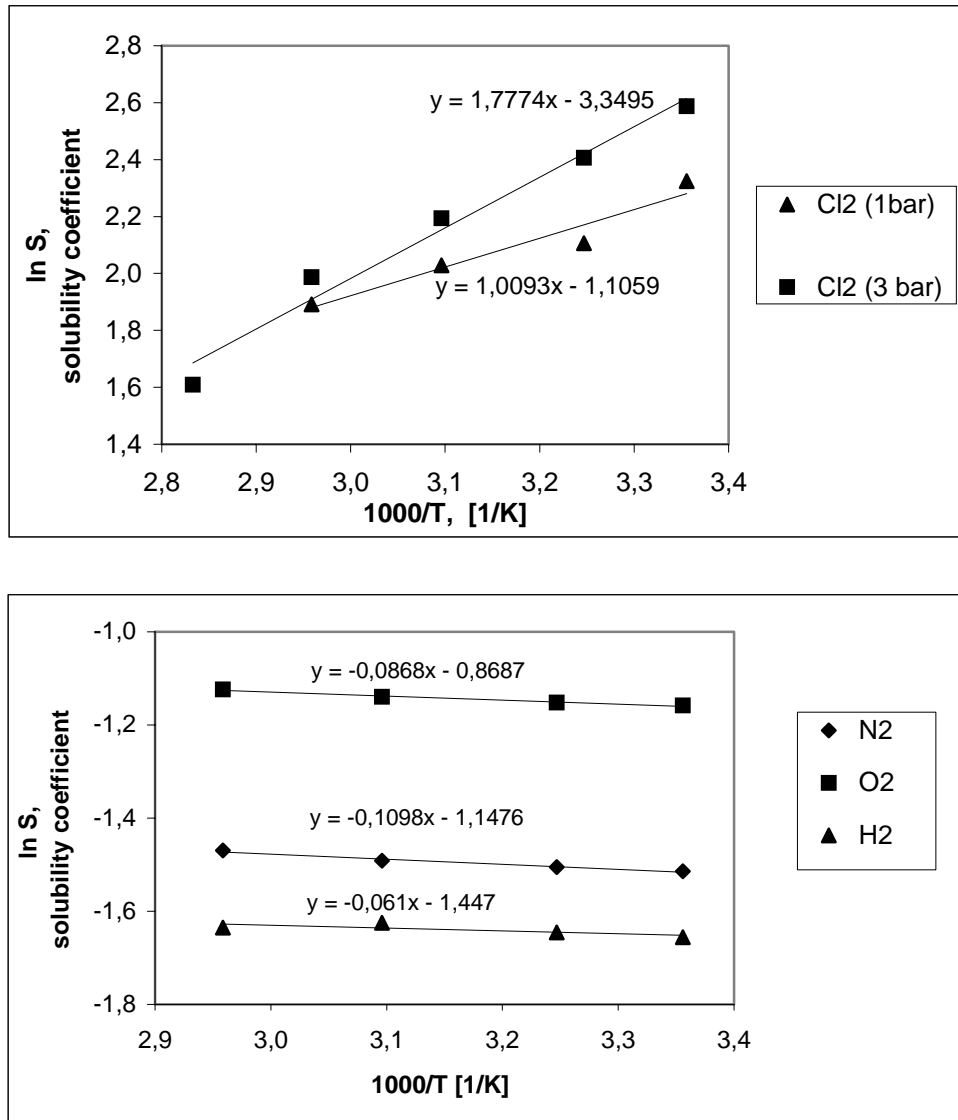
Figure 6.9: Arrhenius plots of solubility coefficients S; [cm³(STP) /(cm³·bar)] in standard PDMS as a function of reciprocal temperature , Cl₂ shown for both 1 and 3 bar (upper figure). H₂, N₂ and O₂ for 2 bar (lower figure).

Table 6.4: Heat of solution in PDMS calculated from eq. 6.2 and illustrated in Figure 6.9.

Gases	S_0	ΔH_s [kJ/mole]	Regression R^2
H_2	0.24	0.56	0.63
N_2	0.32	0.91	0.97
O_2	0.42	0.72	0.98
Cl_2 (1 bar)	0.33	-8.9	0.94
Cl_2 (3 bar)	0.035	-12.4	0.98

Density measurements

Density of the PDMS was measured after each absorption measurement. The results are given in Table 6.5. The density before exposure to chlorine gas was approximately 1.08 g/cm³. The density increased with the exposure temperature until 65°C. At 80°C the density had decreased relative to 65°C. The increase in density is most likely due to further crosslinking and increased rigidity in the polymer chains caused by chlorination. The decrease at 80°C

may be due to chlorination reactions and degradation of the polymer. Reduction of the crosslinking sites and chain scission of the polymer would give shorter polymer chains and a less dense structure and thus lower density.

Table 6.5: Density of PDMS after exposure to Cl_2 at different temperatures. Density before exposure: 1.08 g/cm^3.

Exposure temp. [°C]	Density measured at 20°C [g /cm³]
30	1.14
35	1.18
50	1.22
65	1.23
80	1.16

6.1.6   Evaluation of durability based on absorption results

There is a slight increase in the sorption of H_2, N_2 and O_2 with increasing temperature, as shown in Table 6.2. The sorption of chlorine decreases with increasing temperature. The sorption value at 80°C and 1 bar, was however much larger than expected. This can be due to an increased reaction rate between the chlorine gas and the polymer, which again indicates degradation.

A sample curve for sorption of Cl_2 in PDMS is shown in Figure 6.10. If absorption only is taking place, the sorption curve should stabilise and reach equilibrium at a constant pressure ($dp/dt = 0$). However, the observed absorption of Cl_2 in PDMS shows a pressure decay caused both by sorption and a chemical reaction. At the beginning of the experiment both processes are taking place, but after some time the membrane has reached sorption equilibrium for chlorine. Still the pressure of chlorine gas is decreasing in the cell due to the ongoing chlorination reaction. This part of the curve is used to estimate the contribution from the chlorination reaction (by assuming that chlorine sorption has ceased). Assuming that the reaction rate is constant during the time of the experiment, the real sorption of chlorine can be extracted by subtraction of the contribution of the chemical reaction from the observed absorption. As indicated in Figure 6.10, this assumption seems to hold within the time used for these experiment; the calculated sorption seems to reach equilibrium after ca. 5000 seconds. Since we (at least initially) have a rubbery membrane (non-chlorinated PDMS) it is plausible that the polymer will reach sorption equilibrium within a relatively short time. It is assumed that the chlorination reaction will not change the sorption characterisation of the material significantly during the time of the experiment. Higher temperatures will speed up the reaction rate.

Linearisation of the absorption curve was made after a given time (6000-8000 sec in Figure 6.10). The rate of the chlorination reaction is [8]:

$$Rate\ of\ reaction = k[A]^n \qquad\qquad (6.3)$$

where the rate of reaction is given as the product of the reaction coefficient, k, and the concentration of component A (in this case Cl_2), and n gives the order of the reaction. It is not verified what is the order of the reaction, but it is plausible that it is of zero or first order.
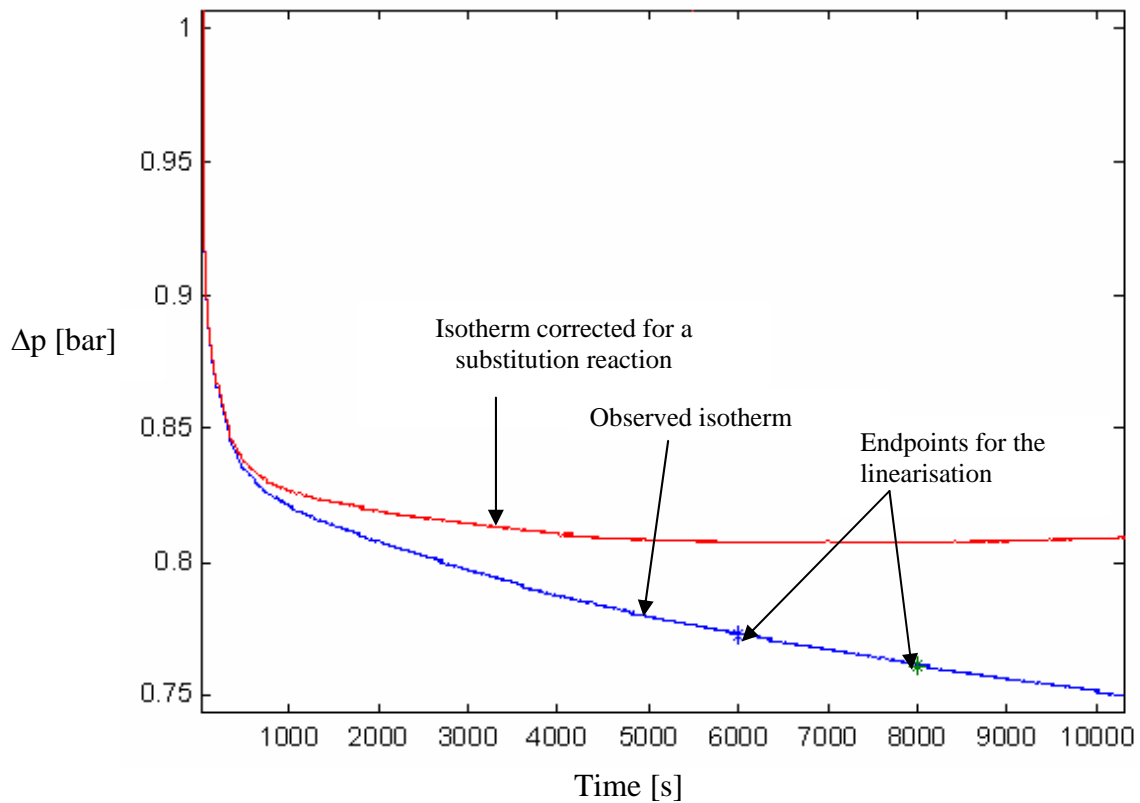
Figure 6.10: Sample curve of sorption isotherm for Cl_2 gas in PDMS at 30°C, measured as Δp (bar) as function of time
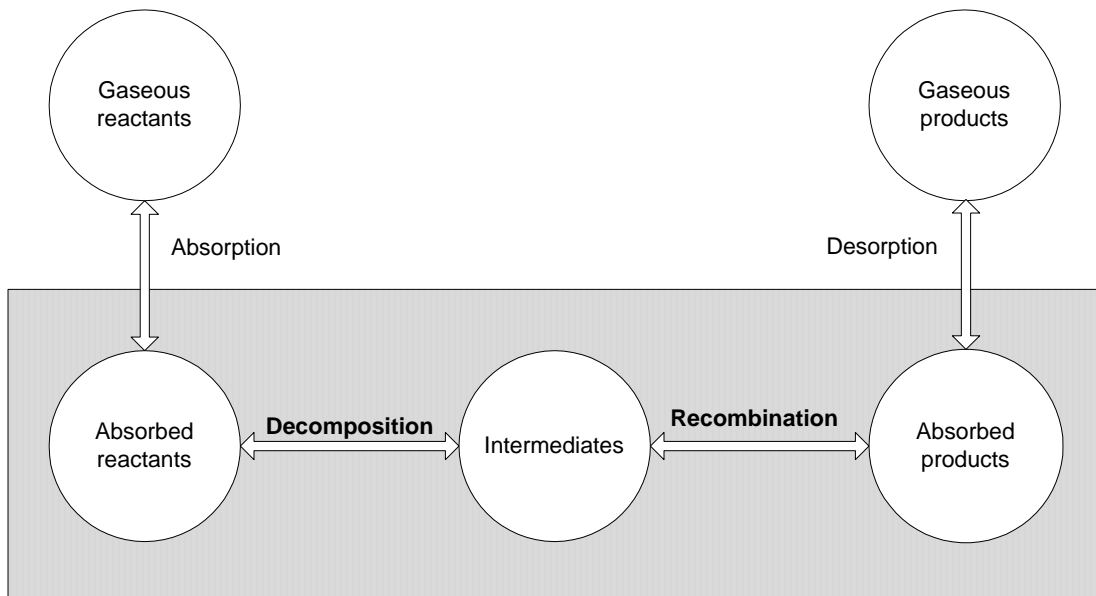
Figure 6.11: Absorption, desorption and reaction of gaseous reactants with the polymer [9].

Figure 6.11 is an illustration of a polymer absorbing gas. Relating this to absorption of Cl_2 the polymer absorbs a certain amount of gas. The gas may react with the polymer resulting in changes in the polymer structure giving reaction products (decomposition may give HCl). The

products may absorb in the polymer, or the products may be desorbed from the polymer. However the desorption may be a slow process, and can be neglected relative to the amount gas absorbed in the polymer: i.e. the products remain inside the polymer bulk. The reactants and products may also swell the polymer. These two factors might explain the decrease of the pressure in the absorption experiment for Cl_2. Since the character of the polymer is changed due to chlorine reaction this can also give other solubility properties than the original polymer. The solubility coefficient for Cl_2 is found from the corrected isotherm shown in Figure 6.10.
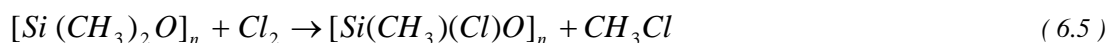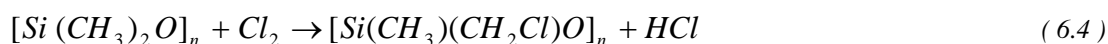
Factors that may cause a continuous decrease in the pressure due to chlorine exposure of PDMS are discussed next:

1. *Chlorine substitution* of the hydrogen atom or the methyl group in PDMS. Cl_2 may react and produce products like HCl or CH_3Cl.

$$[Si\,(CH_3)_2O]_n + Cl_2 \rightarrow [Si(CH_3)(CH_2Cl)O]_n + HCl \qquad (6.4)$$

$$[Si\,(CH_3)_2O]_n + Cl_2 \rightarrow [Si(CH_3)(Cl)O]_n + CH_3Cl \qquad (6.5)$$

   One mole Cl_2 gas is used in the reaction and one mole HCl or CH_3Cl is produced meaning that the pressure is constant. However the desorption process of the products may be a slow process. When a substitution is taking place, the properties of the polymer are also changed. The chlorine atom has a larger atomic diameter than hydrogen making the polymer less flexible due to larger sidegroups. The T_g value would increase. The chlorine atom contributes to a charge distribution in the polymer due to high electro negativity. Dipole-dipole moments induce high interchain interactions between the polymer chains. A chlorinated side groups will thus give higher interchain interactions than hydrogen and methyl. This will give a denser polymer structure. The reaction products inside the polymer bulk might be trapped and do not desorb to the surroundings.

2. *Crosslinking* of the polymer chains gives a denser structure and reduces the free volume for transport. Increasing temperature can catalyse the crosslinking due to Cl_2 exposure time. However, depending on the product formed from the crosslinking, the pressure ought to be relatively constant and the curve should reach equilibrium.

3. *Degradation* of the PDMS, due to bond scission and ring formation will cause weight loss and increased pressure in the absorption cell if the new products are volatile (or easily desorbed).

6.1.7   Evaluation of durability based on instrumental analysis

The PDMS with high crosslinking was exposed to Cl_2 in a glass chamber (see figure 5.8) for 4 weeks at both 30 and 60°C. The sample exposed to chlorine gas at 60°C had become brittle and cracked easily. The surface had clearly changed during exposure, seen by the change from glossy to dull surface. The chlorine exposed samples were analysed by FT-IR, ^{1}H-NMR, DSC and SEM.

FT-IR

Figure 6.12 shows the FT-IR spectra of the unexposed and the exposed membrane samples. The analysis was performed with HATR with a ZnSe crystal, which has a transmission range between 17000-650 cm^{-1}. Absorption bands at lower wavenumbers than 650 cm^{-1} will not be discussed here.

Typically for the PDMS is a strong peak at 2961 cm^{-1} indicating the CH$_3$ stretching vibration. The Si-CH$_3$ is characterised by a very strong sharp band at 1280-1255 cm^{-1} due to CH$_3$ symmetric deformation. The absorption at 860-760 cm^{-1} is due to methyl rocking and Si-C stretching. One methyl on a silicone usually absorbs near 765 cm^{-1}, two methyls near 855 and 800 cm^{-1} and three methyls near 840 and 765 cm^{-1}. The asymmetric CH$_3$ deformation absorbs weakly near 1410 cm^{-1}. Siloxanes are characterised by at least one strong band at 1100-1000 cm^{-1} related to asymmetric Si-O-Si stretching. In infinite siloxane chains, absorption maxima occur near 1085 and 1010 cm^{-1}. Cyclotrisiloxane rings absorb near 1020 cm^{-1}. Cyclic tetramers and pentamers have absorption near 1090 cm^{-1}. The Si-H gives rise to absorption at 2250-2100 cm^{-1}. Si-H bending frequencies absorb in the region 850-800 cm^{-1}. Si-H$_3$ group has two bands in the 950-900 cm^{-1} region due to asymmetric and symmetric deformation, and the deformation of the Si-H$_2$ group has one band in same region. The Si-H$_2$ wag vibration absorbs at 900-845 cm^{-1}, and the Si-H wag vibration absorbs at 845-800 cm^{-1}. The Si-Cl group absorbs at 625-420 cm^{-1}. The Si-Cl$_3$ group absorbs at 620-570 cm^{-1} and 535-450 cm^{-1}. The Si-Cl$_2$ group absorbs at 600-535 cm^{-1} and 540-460 cm^{-1}, and the Si-Cl vibration absorbs at 550-470 cm^{-1} [10].

A band at 2961cm^{-1}, indicating the CH$_3$ stretching vibration, is observed in the spectrum of the unexposed sample, but this disappeared in the spectra of exposed samples. Poly(hydrogenmethylsiloxane) was used for crosslinking of the membrane. The band at 2360 cm^{-1} may be due to Si-H bond, but this is a higher wave number than expected. The band around 1400 cm^{-1} is a result of the asymmetric CH$_3$ deformation. Si-CH$_3$ is characterised by a very strong sharp band at 1258 cm^{-1} in the samples due to CH$_3$ symmetric deformation. The two methyls in PDMS have bands at 840-795 cm^{-1}. PDMS was trimethyl terminated and the absorption band at 840 cm^{-1} may indicate these bonds. The length of the siloxane polymer may however dilute the effect of this bond in the spectra. The bond at 880 cm^{-1} may be due to either Si-H or to Si-OH stretching vibration. The band at 1178 cm^{-1} could be due to some C-F bond related to the support structure of poly(vinylidenefluoride) (PVDF).

Comparing spectra for the unexposed sample and the exposed sample at 30°C, the main difference is the strong reduction of the band at 795 cm^{-1}. The dimethyl groups have been changed.

The band at 731 cm^{-1} may be due to C-Cl bond after chlorination of the methyl group connected to the silicon atom. After exposure to chlorine the Si-O-Si band also changed its character in the spectra. Since cyclic tetramers and pentamers have absorption near 1090 cm^{-1}, it may indicate a depolymerisation of the main chain and formation of cyclic siloxane compounds. It is also possible that the structure of further crosslinking is seen.

The Si-Cl group absorbs at 625-420 cm^{-1} and the formation of this bond is not seen from FT-IR analysis, since this is out of the range of the crystal.
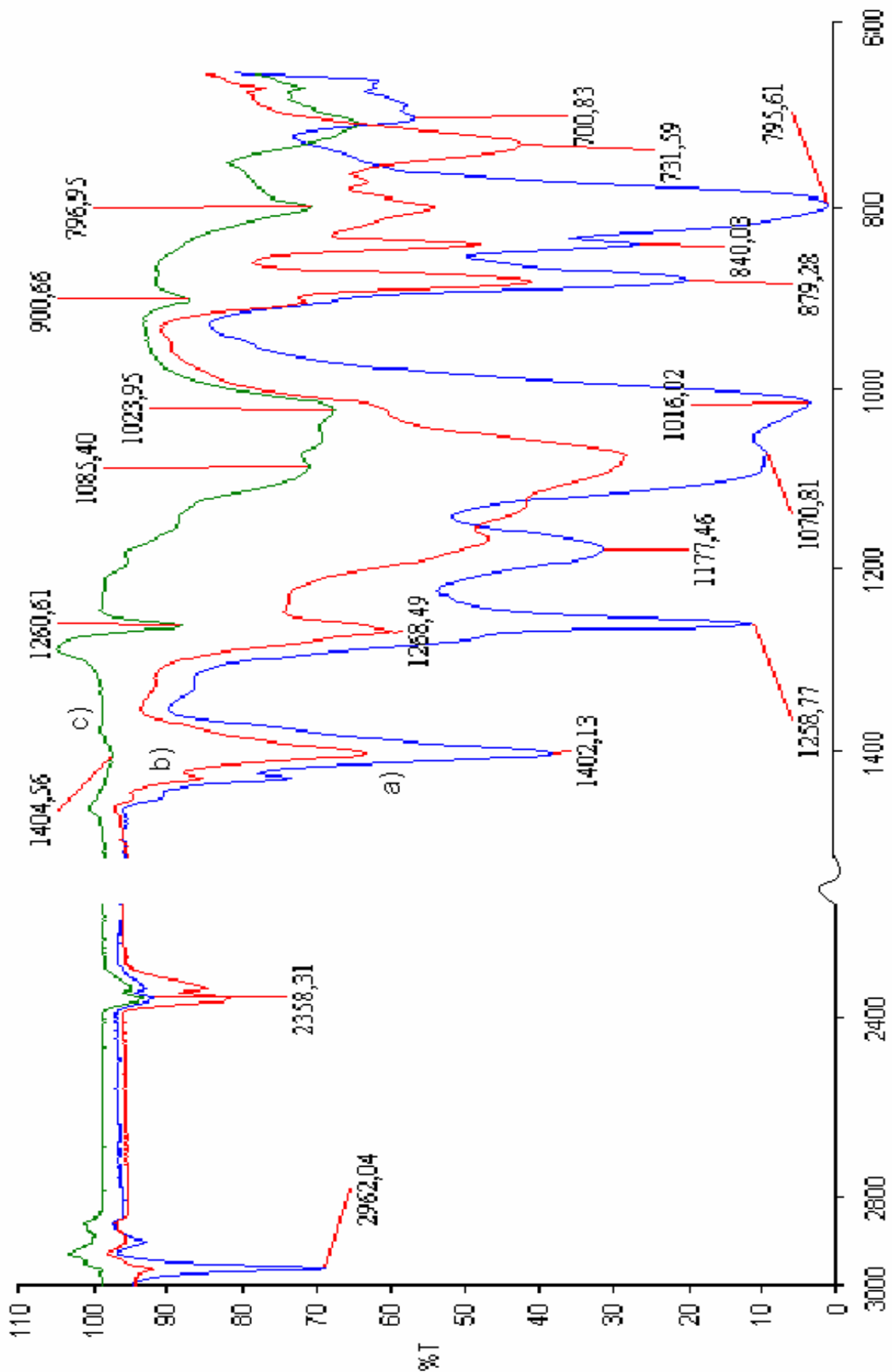
Figure 6.12: FT-IR spectra of highly crosslinked PDMS a) unexposed sample (blue line), b) sample exposed to Cl₂ at 30°C (red line) and c) sample exposed to Cl₂ at 60°C (green line).

The sample exposed to Cl_2 at 60°C had become brittle. The FT-IR spectra did not show the same intensity of the peaks as was seen from the other two samples. This might be due to changes in the surface of the sample or that the sample may not have covered the same area of the crystal.

^{1}H-NMR

NMR analyses were made of the samples, exposed to Cl_2 during the absorption measurements. The polymer was a Deh 942, a system of silicone in petrolether. Platinum was used as catalyst. The chlorine exposure time for the samples were between 3.5 - 4.5 hours. The NMR spectra reported here are only ^{1}H (proton) spectra.

Figure 6.13 shows the chemical shifts expected for hexamethylsilicone and chlorinated hexamethylsilicone respectively [11]. The spectra for an unexposed sample given in Figure 6.14, shows shifts in the range 0.06 to 0.14, which is due to $Si-CH_3$ bonds. When the PDMS is exposed to Cl_2 shifts occur at 0.25 and 2.7 (Figure 6.15) in addition to the shift for the $Si-CH_3$ bond. The shifts at 0.25 are due to $Si-CH_3$ bond as neighbour to $Si-CH_2Cl$ bond and the shift at 2.7 is due to $Si-CH_2Cl$. The polymers in these analyses were exposed to chlorine for just a few hours. This makes the concentration of the CH_2-Cl bond low, and the intensity was thus small. Long time exposure is needed before any conclusion can be draw upon degradation. These shifts indicate that the hydrogen in the methyl group is substituted by chlorine, as observed also in the FT-IR spectra.

The shifts at 1.2 to 1.5 may be due to traces of solvent used in the preparation of the membrane film. The shift at 7.3 was due to $CDCl_3$, which was used as solvent for PDMS in the preparation for the NMR analysis.

The proton spectra alone are not enough to identify all the possible reactions within the polymer upon Cl_2 exposure. Methods with ^{13}C and ^{29}Si NMR will together with the proton spectra give additional information of the chemical changes due to chlorine exposure. It is preferable to analyse samples that have been exposed to chlorine gas over an extended period of time (at least 1 week) to increase the concentrations of C-Cl bonds and eventually Si-Cl bonds.
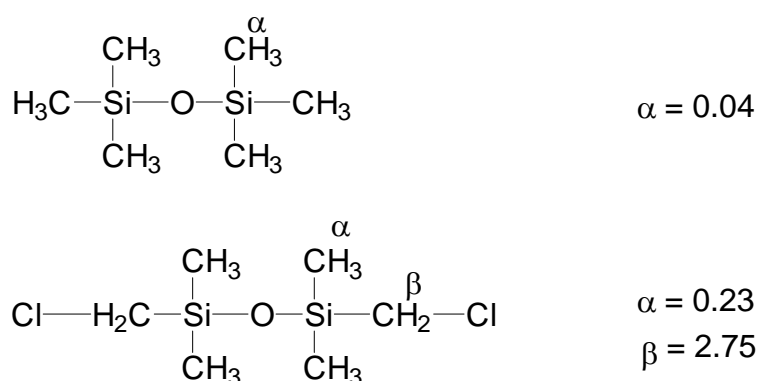

Figure 6.13: Chemical shifts in methyl siloxane and chlorinated methylsiloxane [11].
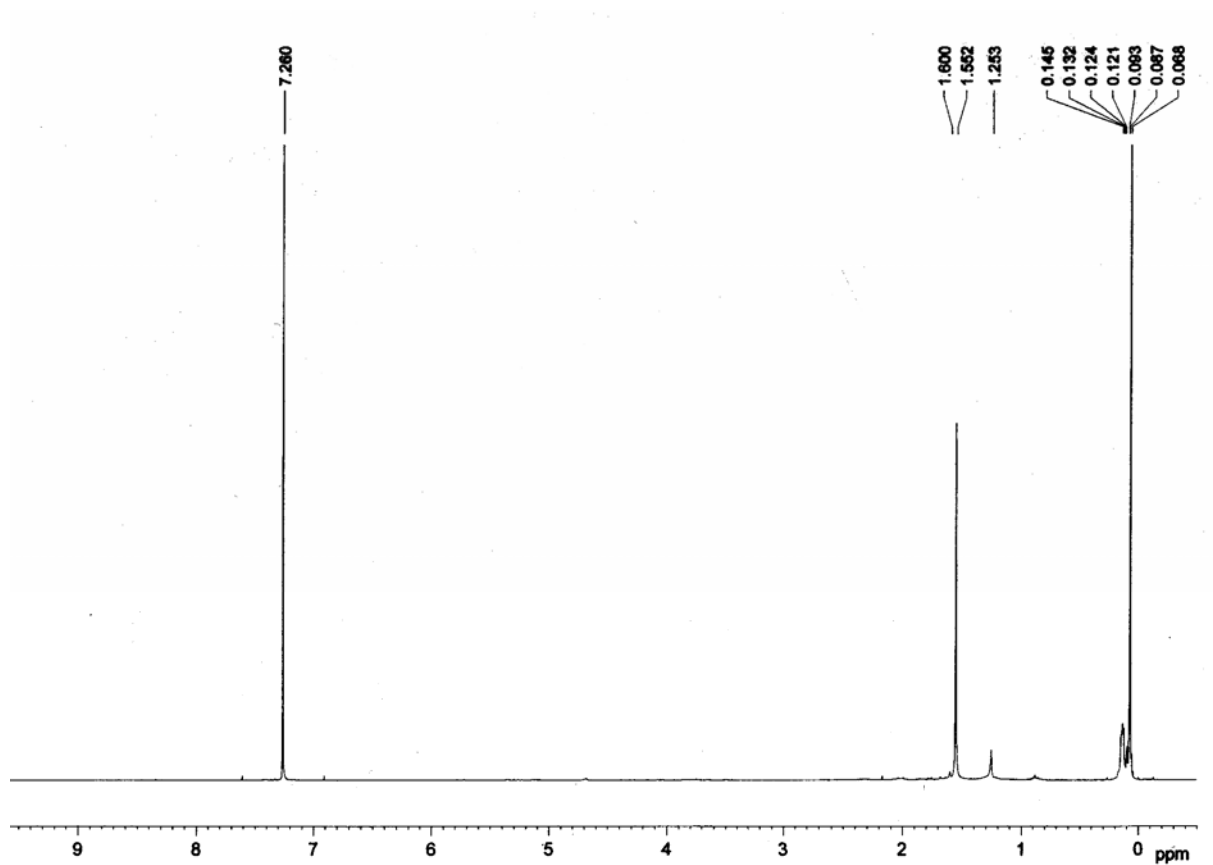
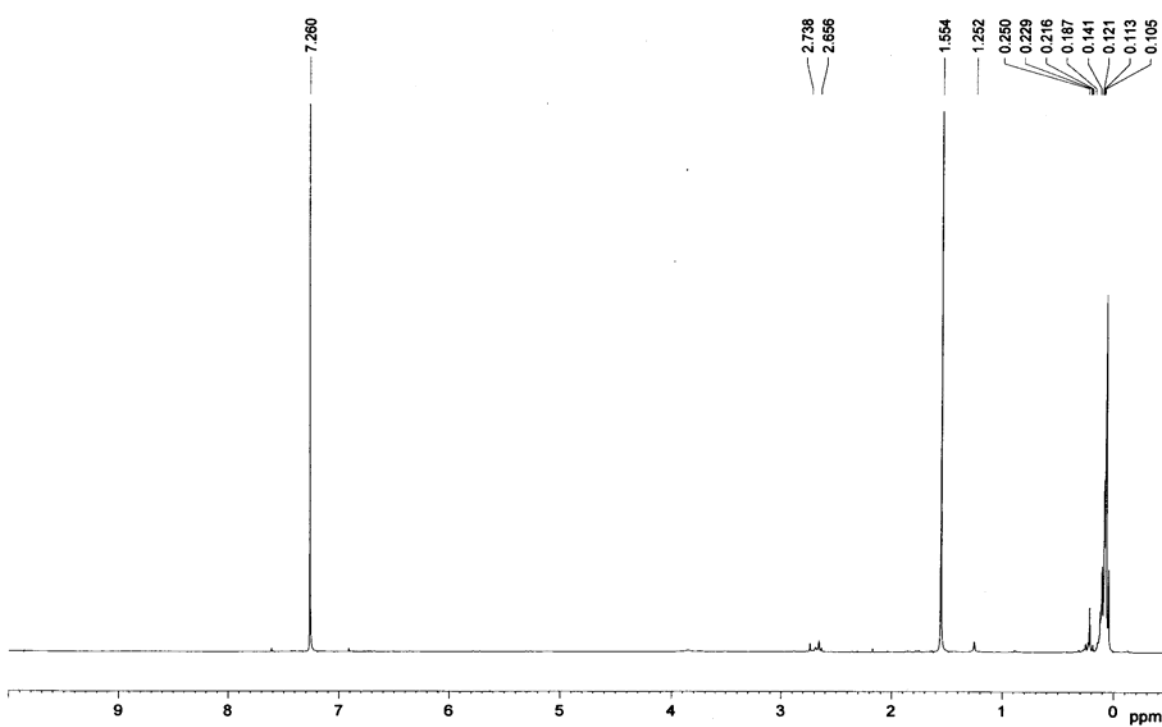*Figure 6.14: ^1H NMR spectra for unexposed PDMS. The shift at 7.26 is due to the solvent $CDCl_3$.*

Figure 6.15: ^1H NMR spectra for PDMS exposed to Cl_2 for 4.5 hours at 80°C. The shift at 7.26 is due to the solvent $CDCl_3$.

DSC

A DSC spectrum of standard PDMS Deh® 942 is given in Figure 6.17. PDMS has a melting temperature about -40°C [12], and this is not observed in this DSC spectrum since the cooling medium used is ice water. The system was run with nitrogen as purge gas. The DSC spectrum shows exothermic changes in the baseline at about 250°C and at about 380°C.

Results obtained from Clarson and Semlyen [21] shows that trimethylsilyl terminated PDMS in an inert atmosphere (nitrogen) do not thermally depolymerise under 350°C. However above 350°C references states that an endothermic process was detected. This corresponds to weight loss (depolymerisation). Clarson and Semlyen found however that the effect of oxygen on the high temperature thermal stability on PDMS resulted in thermograms with the onset of an exothermal process at approximately 250°C, which attains a maximum at about 325. This is believed to be associated with the oxidative crosslinking via methyl substituent groups.

From this information the obtained DSC spectrum of PDMS given in Figure 6.17 seem to detect that oxygen has been present in the system causing the exothermic changes.

SEM

Figure 6.16 shows SEM pictures of the composite membrane before and after exposure to air at 150°C. It can be seen that the PDMS tends to "flow" down into the support structure when the temperature is too high (viscosity decreases) [1]. Thermal oxidative degradation of the PDMS can take place under these conditions as described in section 4.3.2.

a)   b)
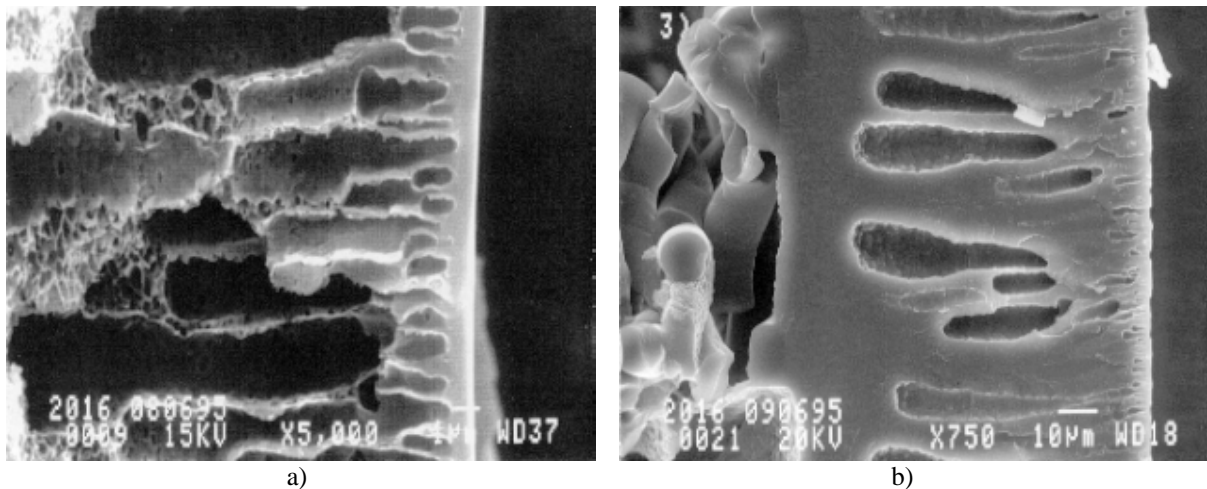
Figure 6.16: a) PDMS not exposed, b) PDMS exposed to air at 150°C for 4 days [1].
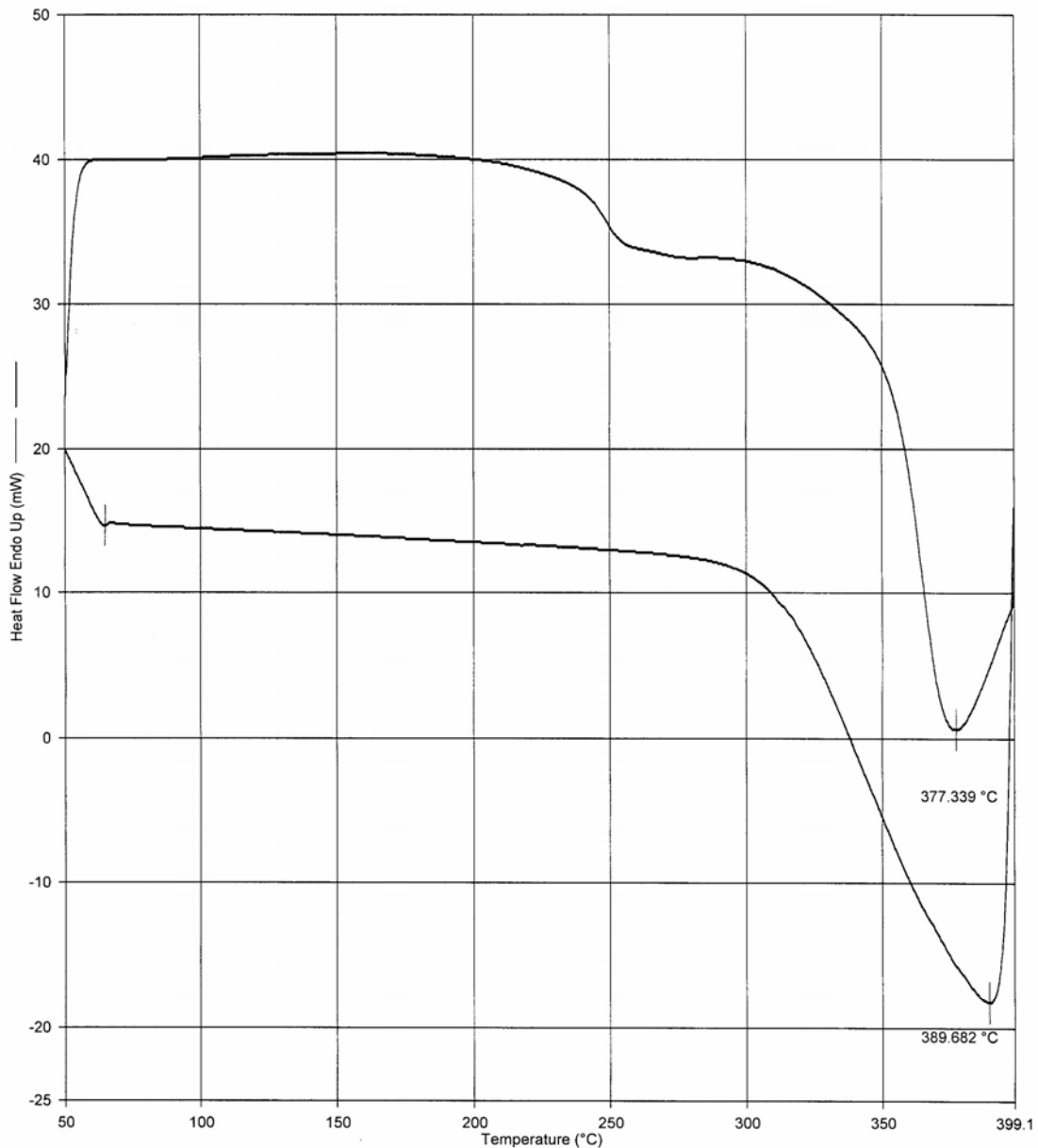
Figure 6.17:DSC thermograhm of PDMS Deh®942 in the temperature range 50-400°C. The upper line is the heating curve, while the lower line is the cooling curve.

6.1.8 Swelling of PDMS

Swelling is typically unfavourable in polymers used for separation applications because selectivity is reduced as the diffusivity of the slower penetrant is increased. By crosslinking a rubbery polymer, the swelling will be restricted and segmental motion of the polymer chains will be restrained. The selectivity may then be maintained, but the permeability will decrease [13, 14].

PDMS membranes synthesised by McMaster University were exposed to chlorine gas in our laboratory, before the samples were sent back for examination of dry weight loss and swelling%. The first parameter provides an assessment of the degree of degradation to smaller silicones, the latter of changes in crosslink density [15]. The swell % is determined from

equation 6.6 and the relative weight loss was determined from equation 6.7. The values are given in appendix B, Table B.1.7.

$$Swell\% = \frac{Swollen\ weight}{dry\ weight\ after\ heating} \cdot 100 \tag{6.6}$$

$$Rel.\ weight\ loss = \frac{weight\ before\ extraction - weight\ after\ extraction}{inital\ weight\ before\ extraction} \cdot 100 \tag{6.7}$$

The extent to which the polymer is swelled by a liquid depends on the density of crosslinking: the more crosslinks present the smaller is the amount of swelling. If the degree of crosslinking is high enough, the polymer may be a rigid solid with high melting temperature and unable to swell. Light crosslinking of chains favours the formation of rubbery elastomeric properties [14]. Thus further crosslinking upon chlorination can lead to a more glassy polymer.

Figure 6.18 shows the hydrosilylation PDMS membranes with different degrees of crosslinking and their behaviour in the swelling tests. The samples were reported to have high (H), medium (M) and low (L) crosslinking. After the Cl_2 exposure, the crosslinking had increased for all samples (lower swell %). However, from the swelling tests with cyclohexane sample (M) had a lower degree of crosslinking (higher swell %) and was much broader than sample (H) and (L) for reasons that remain unclear.
Focusing on (H) and (L) there was an increase in the swelling ability for (L) compared to (H) (ignoring (M)) as expected from the preparation of the samples (lower possible crosslink density for L).
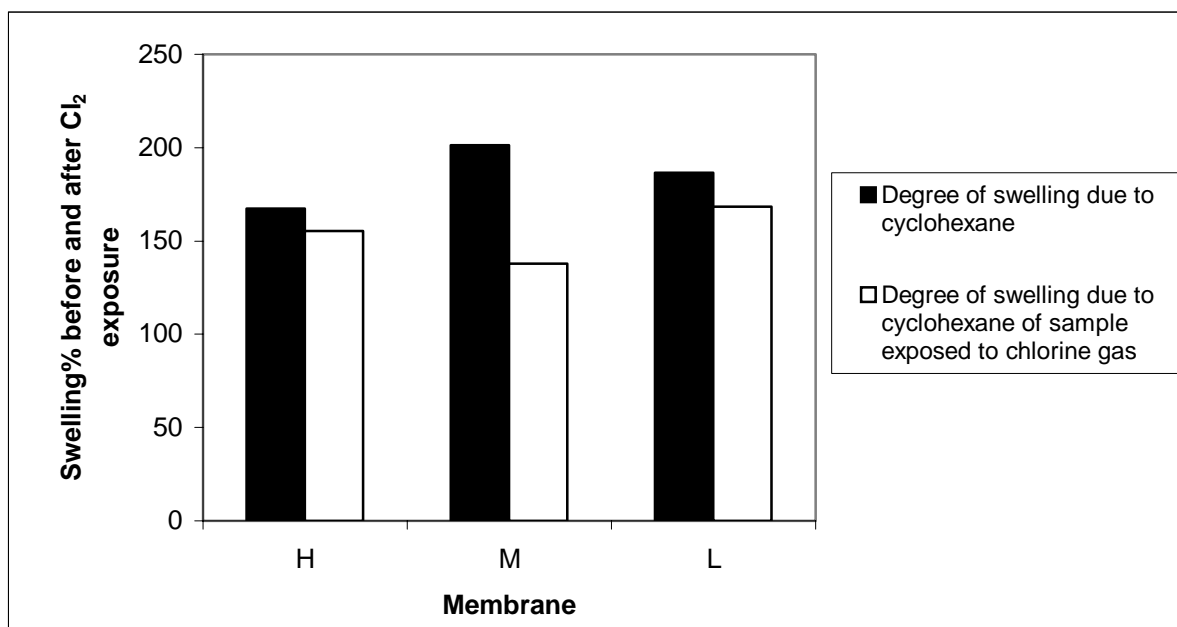

Figure 6.18: Degree of swelling (compared to dry weight) before (black bars) and after (white bars) Cl_2 treatment; high (H) medium (M) and low (L) crosslinking.
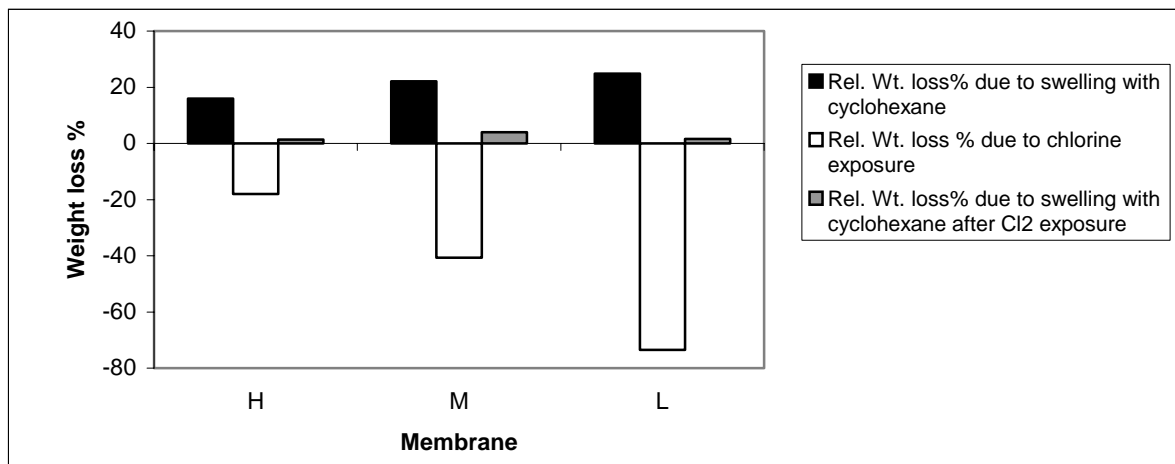
Figure 6.19: Relative dry weight loss before and after Cl₂ treatment; high (H) medium (M) and low (L) crosslinking.

Figure 6.19 gives the relative weight loss upon swelling and is an assessment of the degree of degradation. The black bars in Figure 6.19 gives the weight loss after swelling a pure sample with cyclohexane. The white bars show a weight gain (positive sign means a weight loss, negative sign means a weight gain) after chlorine exposure, while the grey bars give the weight loss after swelling the chlorine-exposed samples with cyclohexane. It seems from this figure that the weight loss due to swelling of cyclohexane decreases after the exposure to the chlorine gas. This may be due to further crosslinking when the polymer is exposed to chlorine. It could also be a result of chlorination, which increases the interchain interactions between the polymer chains. The chlorination changes the structure of the polymer and thus also the swelling abilities.

From Figure 6.19 it is seen that the relative weight loss due to Cl₂ is in agreement with what would be expected for (H), (M) and (L). Considering the weight loss; the conclusion will be that the chlorination process is grafting unbound silicone to crosslinked silicone. The action of the chlorine is, to increase crosslinking of the silicone as can be judged by the absence of weight loss after chlorination, related to the relatively high weight loss of the "before" sample. These results suggest that chlorine is reacting with silicone in some way and graft unbound silicone to crosslinked silicone [15]. The swelling tests in Figure 6.18 showed that the degree of crosslinking increases for all samples after chlorine exposure and therefore this conclusion can be made: The PDMS is further crosslinked upon exposure to chlorine gas.

The results indicate the following possibilities:
  i.   Chlorine reacts primarily with the silicone. Reaction could be through the SiH groups or through carbon or via residual vinyl groups, in which case the weight may or may not increase, (more experiments would be necessary to establish which of these are relevant).
 ii.   The reaction conditions lead to binding of "free" silicone to the crosslinked material and inevitably, further crosslinking
iii.   If chlorination occurs in the silicone the crosslinking will cease once the Si-H is consumed; or more likely, crosslinking will continue via no chlorination process, with the inevitable outcome of increased brittleness and poorer membrane selectivity.
iv.   After exposure to chlorine for several weeks, there is almost no weight loss (taking into account the weight gain during chlorination), suggesting that the problems of HCl

degradation that were earlier proposed are not very important over the time frame examined.
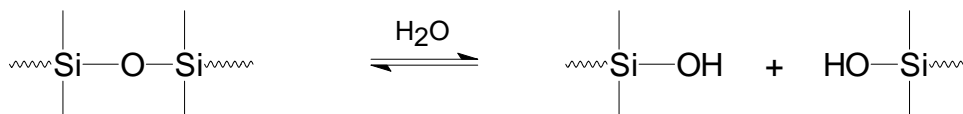
These results are quite positive from material perspective. Cl_2 exposure to the silicone appears to initially stabilise the film and, over time, is likely to lead to brittleness since the chlorination gives a less flexible structure. The weight loss of silicone after chlorination was almost negligible; weight gain suggests some chlorination of the silicone material. The presence of (presumably covalently bound) chlorine will likely affect membrane performance (selectivity/permeability flux) and, to a lesser extent, mechanical properties of the silicone.

6.1.9   Problems with impurities

The material degraded very quickly when placed directly on a metallic sinter in the membrane cell. The cell metal (Fe) reacted with the chlorine gas to give iron halide. This product is a Lewis acid and is known to catalyse a degradation reaction of the polymer by depolymerisation. This reaction product could further catalyse oxidative modification of the methyl groups and enhance degradation of the membrane material. Thus, care must be taken to avoid direct contact between the membrane material and the steel in the membrane cell used. Teflon sinters and Teflon filters were used, therefore, to protect the membrane material from contact with steel. In the absorption cell, a small glass cylinder was used for the protection of the polymer material. Similarly, the long-term exposure chamber was made out of glass to obviate membrane/steel contact.

Rinsing the composite membrane in water was part of the production process. It is very important to ensure that no particles are trapped in the membrane during this operation: These spots may later be propagation sites for degradation in presence of chlorine gas. From observations under microscope, chemical erosion of this type seemed to be particularly problematic at the junction between the support material PVDF and the PDMS. Deionised, ultra pure water should be used in the future.

Silicone chains also undergo hydrolytic scission in contact with water producing lower molecular weight silanol terminated polymers

$$\text{\textasciitilde\textasciitilde Si-O-Si\textasciitilde\textasciitilde} \quad \overset{H_2O}{\rightleftharpoons} \quad \text{\textasciitilde\textasciitilde Si-OH} \;+\; \text{HO-Si\textasciitilde\textasciitilde}$$

Traces of water in PDMS would react with Cl_2 to produce HCl. It has been shown that HCl is deteriorating to PDMS and water must be removed from the polymer before use.

Problems with degradation may occur if the silicone is not cured properly. Residual functional groups (Si-H) can react with chlorine. Small amounts of water will react with the new Si-Cl groups to give HCl, which may be deleterious to the silicone [15].

Cautions must also be taken in the preparation of the polymer avoiding hydroxyl terminated polymer chains. These may very easily react with the chlorine gas and give free radicals. The polymer chain will thus be degraded by chain cleavage.

With the Pt-complex as a catalyst one might expect residual catalyst in the material, which promotes silicone depolymerisation [16].

6.1.10 Interim conclusion for PDMS

A main conclusion may be drawn with respect to how the PDMS membrane changes upon chlorine exposure: there is not a decomposition taking place if the membrane is fully protected against impurities but rather a chlorination and additional crosslinking. Permeation in silicone membranes will be dramatically affected by chemistry taking place in the active layer. However, the actual effect of chlorination on selectivity and permeability flux will depend on the exact chemical processes. First descriptions of the major chemical processes that can occur in these systems are given. The obtained results for PDMS membrane are summarised as follows:

Chlorination of the methyl groups on silicones, a free-radical substitution process, changes both the character of the silicone and produces important catalyst by-products. As shown in Figure 6.20A, B the process leads sequentially to bulkier side-groups with the result of less flexibility of rotation around the main chain. Such changes are expected, based on the properties of other silicones with non-methyl side chains, to have higher values of T_g (the T_g was, however, not measured after the exposure to chlorine). An increase in T_g is also expected to result from the greater polarity of these chlorine-modified silicones.

Crosslinking in these polymers can occur by a variety of processes. The chlorination noted above, in the presence of oxygen, can generate carbon radicals. These, as in high temperature vulcanisation, can lead to crosslinks via two carbon bridges (Figure 6.20C,D). Further oxidation of these activated carbons generates trifunctional silane units (Figure 6.20E). Alternatively, such groups may be obtained from residual Si-H groups on the polymer chain either by reaction with Cl_2 or HCl (Figure 6.20F) [17]. Moisture will lead to silicone crosslinking of such polymers irrespective of their source (Figure 6.20G).

Depolymerisation of the silicone is catalysed by HCl and by Lewis acids, such as the metal halides, including $FeCl_3$, produced by the chlorination of steel. These depolymerisation processes are accompanied by the formation of silicone cyclics which may be lost by evaporation or swell the polymer. It is necessary to emphasise that the membrane must be totally protected from contact with humidity, particles and steel since all these factors catalyse degradation. Caution must also be taken when preparing the polymer to avoid hydroxyl terminated polymer chains. Hydroxyl reacts very quickly with the HCl to give depolymerisation as noted above.

Chlorination and crosslinking of the silicone membrane are expected to have a profound effect on the behaviour of the membrane. As the silicone becomes more rigid via both these mechanisms, the permeability flux of the membrane should decrease. This is due to a denser polymer structure and reduction of the free volume. The solubility will also decrease when the polymer becomes denser.

Chain cleavage of the polymer chain, initiated by acid, should lead to higher permeability fluxes and higher sorption coefficients, because of shorter polymer chains. These reactions can also be accompanied by loss of crosslinking, which results in increased swelling and weight loss due to evaporation of cyclic silicone by-products.
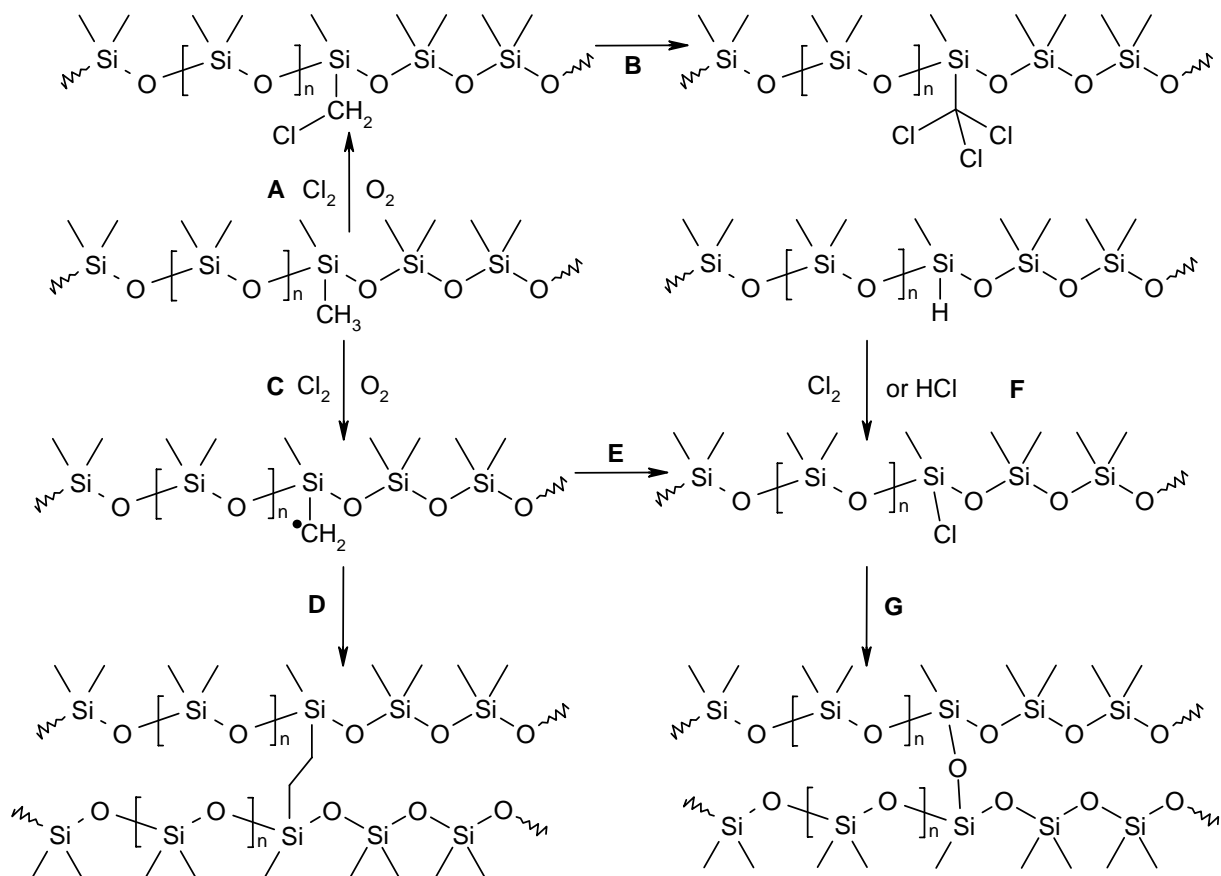
Figure 6.20: Chlorination reactions and crosslinking mechanisms in PDMS.

The permeation experiments shows that a PDMS membrane with high crosslinking, can withstand Cl_2 exposure at elevated temperatures for at least 60 days even though the permeability became too low to be of industrial interest.

The permeability decreased during the 6 weeks of exposure to Cl_2 at 30°C. Increasing the temperature also gave a further decrease in the permeability flux. The permeability is expected to increase if the membrane degrades via depolymerisation, which is causing pinholes. However, if exposure to chlorine over time promotes further crosslinking, then the decrease in permeability for the gas pair Cl_2 and O_2 can easily be explained: Further crosslinking of the polymer chains gives a denser structure, the polymer chains become more restricted to motion, and the free volume for transport will decrease within the polymer, resulting in a reduced permeability.

With Cl_2 being a non-ideal easily condensable gas, and O_2 the opposite, the decrease in permeability for both will follow different mechanisms depending on time and temperature, and may therefore result in even an increased selectivity, as a function of crosslink density, at certain intervals. The general tendency was, however, a slightly reduced selectivity over time for Cl_2/O_2 (documented in Figure 6.6).

The decreasing permeability may also be a result of chlorination substitution reactions as a result of the chlorine exposure, explained as follows: Chlorine may replace, by substitution, hydrogen atoms in the methyl group attached to the silicon atom given in Figure 6.20 A.

Figure 6.8 illustrates the temperature dependency of the Cl_2 permeability flux in a PDMS membrane over almost 10 weeks. This documentation shows that the Cl_2-permeability flux of a chlorinated PDMS increases when the temperature is raised. Referring to Equation 2.5, the permeability (P) is the product of the diffusivity coefficient (D) and the solubility coefficient (S). If there were no changes in the material structure (like crosslinking or chlorination) there would still be a temperature effect on the permeability coefficient (see Equations 2.16 and 2.20). The permeabilities for O_2, N_2, H_2 will increase and the permeability for Cl_2 will decrease. This is well documented by Hägg [3] for experiments of short duration. A chlorinated PDMS will obviously have properties very different from a regular PDMS. However, the permeability flux decreases over the 60 days of chlorine exposure, indicating that the material properties are continuously changing due to chlorination.

The general tendency is that permeability decreases over time for all gases examined once the PDMS membrane has been exposed to Cl_2. This observation is consistent with the increased chain rigidity and interactions due to side-chain chlorination and to increased density due to crosslinking. The decrease in permeability for the gas pair Cl_2 and O_2 in these membranes can easily be explained: Further crosslinking of the polymer chains gives a more dense structure, the polymer chains become more restricted to motion, and the free volume for transport will decrease within the polymer, resulting in a reduced permeability.

The results from the sorption measurements are given in Table 6.2. The solubility for H_2, N_2 and O_2 slightly increased with increased temperature, and the values are comparable with what has been reported in the literature [7]. The Cl_2 solubility coefficient was decreasing with increasing temperature. The sorption curve for Cl_2 in PDMS documented that chlorine will enter the membrane after sorption equilibrium has been reached; being consumed in a chlorination reaction (illustrated in the schematic curve Figure 6.10). The sorption measured at 80°C and 1 bar, was much higher than expected (Table 6.2). The sorption performed under these conditions occurred over long time chlorine exposures, meaning that degradation reactions may have begun. As a result of the higher pressure at the 3 bara exposure, the absorption time was shortend and the absorption equilibrium was reached more rapidly. Higher temperatures speed up the chlorination reaction. The sorption increases with higher critical temperature of the molecules:

$$(T_{crit.Cl_2} > T_{crit.O_2} > T_{crit.N_2} > T_{crit.H_2}).$$

The non-ideal nature of Cl_2 is confirmed by the negative value for ΔH_s found from the Arrhenius plot (Table 6.4). The decreasing Cl_2-permeability flux with increasing temperature documented in the current work may thus be understood both as a function of the physical properties of Cl_2 and changes in the material, which depends on how long the material has been exposed to Cl_2.

Density increased upon chlorine exposure at elevated temperatures. For the increased Cl_2 solubility coefficient at 80°C a decrease in density was observed. At this point degradation seems to take place.

The FT-IR analysis (Figure 6.12) confirms that the material is chlorinated with substitution of hydrogen atoms in the methyl group. The formation of Si-Cl bonds is however not confirmed by FT-IR because the wavenumber is out of range for the ZnSe crystal used. The IR-spectra also gave an indication of formation of cyclic compounds or crosslinks.

Crosslinking leads to denser polymer structures resulting in a decreased permeability flux. Chlorinated polymer chains have dipole-dipole moments, which give stronger interchain interactions, resulting in a denser polymer structure. The flexible rotation of the polymer chains would be reduced and thus the glass transition temperature T_g may increase.

^{1}H-NMR analyses of the PDMS showed that the polymer becomes chlorinated. A substitution reaction has taken place and the C-Cl bond is confirmed. The samples used in these analyses have however only been exposed to chlorine for a few hours, giving a rather low concentration of the C-Cl bond. NMR analysis of the PDMS should be performed with ^{13}C and ^{29}Si for a better understanding of the chemical changes upon chlorination in the polymer.

The DSC spectra showed for a pure PDMS (Deh ® 942) that the thermal degradation of the crosslinked polymer starts at about 250°C.

SEM pictures of a PDMS (Deh ® 942) showed that in air at 150°C (not Cl_2 exposed) the PDMS had become viscous and run down into the support material.

The relative weight loss due to Cl_2 is in agreement with what would be expected for the samples with different degrees of crosslinking (H, M and L). Considering the weight loss; the conclusion would be that the chlorination process is grafting unbound silicone to crosslinked silicone. The action of the chlorine is, to increase crosslinking of the silicone as can be judged by the absence of weight loss after chlorination, related to the relatively high weight loss of the "before" sample. These results suggest that chlorine is reacting with silicone in some way and graft unbound silicone to crosslinked silicone [15]. The swelling tests show that the degree of crosslinking increases for all samples when exposed to chlorine.

The conclusion is that PDMS is both chlorinated and further crosslinked upon exposure to chlorine gas.

6.2 Fluorel

Fluorel is a copolymer that consists of poly(vinylidenefluoride) (PVDF) ($-CF_2CH_2-)_n$ and hexafluoropropylene (HFP) ($-CF_2CFCF_3-$), the chemical structure is given in Figure 6.21. The Fluorel used in these tests have fluorine content of 66%, which corresponds to a ratio between ($-CF_2CH_2-$) and ($-CF_2CFCF_3-$) of about 3.5:1.

$$\sim\sim\sim (CF_2CH_2)_n (CF_2CF)_m \sim\sim\sim$$
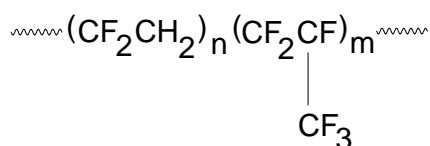$$|$$
$$CF_3$$

Figure 6.21: Chemical structure of Fluorel.

Fluorel is known to be thermal stable and durable at conditions found in many chemical aggressive processes. A study of the Fluorel polymer is performed for evaluation of the separation properties and the durability of the polymer.

6.2.1 Permeability measurements of N$_2$, O$_2$ and Cl$_2$

The permeabilities and selectivities for N$_2$, O$_2$ and Cl$_2$ in Fluorel are given in Figure 6.22 and Figure 6.23 respectively and measured values are also given in table B.2.1 in appendix B. The measurements were performed for 7 weeks at 30°C. The feed pressure was 2 bara and the permeate pressure was 0.6 mbar. The testing started with evacuation over night, and then permeability was measured in sequences of N$_2$, O$_2$ and Cl$_2$. The membrane had an average thickness of 43 µm, measured by a digital micrometer. The membrane cell had a diameter of 1.9 cm giving a permeation area of 2.8 cm^2.

Changes in permeability over time at 30$^\bullet$C:
The permeability of Cl$_2$ in the Fluorel was very low compared to the initial permeability in PDMS (P$_{Cl2}$(Fluorel) = 0.154·10^{-6} m^3(STP)m/(m^2 h bar), P$_{Cl2}$(PDMS) = 19.7·10^{-6} m^3(STP)m/(m^2 h bar). The permeability measurements show a slight decrease for N$_2$ and O$_2$ during the first 12 days of exposure (Figure 6.22), and thereafter it is relatively constant, before the permeability starts to increase at day 47. The increased permeability is a result of the starting degradation of the membrane. The exposure to chlorine is done for a total of 57 days. The permeability increased significantly (P$_{Cl2}$(Fluorel) = 17.3·10^{-6} m^3(STP)m/(m^2 h bar)) in the last measurement due to formation of holes in the membrane. This point is therefore not included in Figure 6.22 (see also table B.2.1 in appendix B).

The initial O$_2$ /N$_2$ selectivity was very low ($\alpha_{O2\ /N2}$ =1.03). After chlorine exposure of the Fluorel membrane at 30°C, an increased selectivity with time was observed during the first two weeks. The selectivity was then decreasing slightly during the next 5 weeks. This may indicate the early formation of a hole in the selective membrane. The increased selectivity at day 49 was not logical and difficult to explain, but most likely degradation had started. The Cl$_2$/O$_2$ selectivity was also very low compared to the selectivities in PDMS ($\alpha_{Cl2/O2}$(Fluorel) = 1.2, $\alpha_{Cl2/O2}$(PDMS) = 15.7).
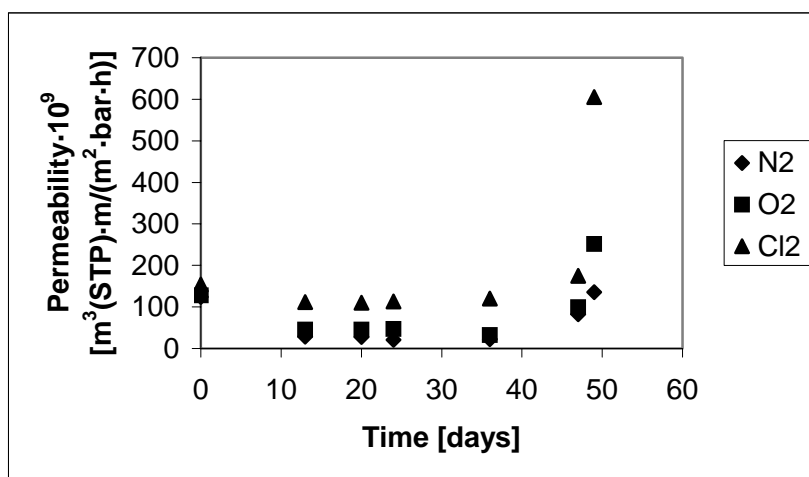

Figure 6.22: Permeability ·10^9 [m^3(STP)m/(m^2 h bar)] of N$_2$, O$_2$ and Cl$_2$ through Fluorel as function of time after exposure to Cl$_2$ gas at 30°C. Thickness: 43µm.
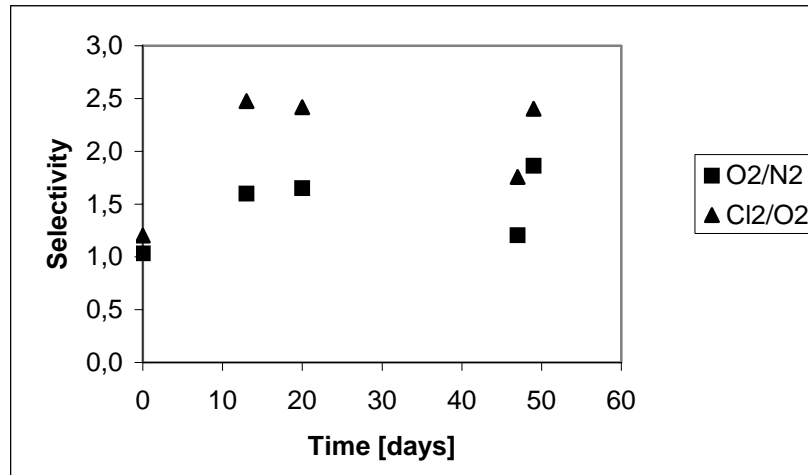
Figure 6.23: Selectivity of O_2/N_2 and Cl_2/O_2 through Fluorel as function of time after exposure to Cl_2 gas at 30°C. Thickness: 43μm.

Changes in permeability over time in the temperature range 30-60°C:

The permeability of Cl_2 was measured as a function of temperature. The results are given in Table 6.6. The permeability was measured at the start of each temperature interval, and then again after exposing the membrane for chlorine gas for 1 week, before increasing the temperature. Problems with the temperature regulator occurred during the week of 60°C exposure, where an uncontrolled temperature increase inside the cabinet ruined the equipment and the membrane. Only a single measurement was therefore reported at 60°C (Table 6.6).

From the results given in Table 6.6 it could be observed a decrease in the chlorine permeability during the chlorine exposure. However increased temperature caused an increase in the permeability. The selectivity increased as the temperature increased.

Table 6.6: Permeability and selectivity of N_2, O_2 and Cl_2 with increasing temperature. Thickness: 130μm.

Temp. [°C]	Time [days]	Permeability $\cdot 10^9$ [m^3(STP)m/($m^2 \cdot h \cdot bar$)]			Selectivity	
		N_2	O_2	Cl_2	O_2/N_2	Cl_2/O_2
30	0	20.7	26.8	46.0	1.29	1.72
30	6	22.9	28.0	44.2	1.23	1.58
50	8	54.7	75.1	136	1.37	1.80
50	15	30.9	57.1	107	1.85	1.87
60	16	45.9	86.4	197	1.88	2.28

6.2.2 Permeability measurements of HCl

Permeability measurements with HCl were performed, the results are presented in Figure 6.24 and in Table B.2.2 in appendix B. This is of interest since HCl is a possible degradation product for Fluorel when exposed to Cl_2. The HCl exposure was done at 30°C, for a period of 12 days. The permeability measurements were done using a feed pressure at 2 bara and vacuum at the permeate sides (0.6 mbar). The membrane cell (diameter of 1.9 cm) was evacuated over night before the measurements started. The N_2 and O_2 permeability was measured every second day, and the HCl permeability the day in between, with evacuation every night.

Changes in HCl permeability over time at 30°C:

Figure 6.24 gives the permeability of N_2, O_2 and HCl, and Figure 6.25 gives the selectivity of the gas pair O_2/N_2 and O_2/HCl.

The permeability of N_2 and O_2 was decreasing slightly during the measurement time, while the permeability of HCl was increasing significantly upon exposure. After 4 to 6 days the permeability and the selectivity seemed to stabilise. The permeability of the HCl was unexpectedly low (P_{HCl} (Fluorel) = $0.45 \cdot 10^{-9}$ m^3(STP)m/(m^2 h bar)). HCl is a polar molecule with a smaller kinetic diameter than both oxygen and nitrogen, (table D.1 in Appendix D), which will give a higher diffusivity due to size. HCl has a higher critical temperature than both oxygen and nitrogen, which should give a higher sorption in the polymer. Additionally, since Fluorel is a material with $T_g \approx -20°C$ (see table 3.2) the membrane is in its rubbery state which should support the theory of fast permeation for HCl. However if the polymer structure is highly crystalline the transport properties may be quite complicated. This is discussed in section 6.2.3. Another issue is that the polar HCl molecule may interact with the C-F bonding to form hydrogen bonds, and thus the transport is reduced. Chemical and/or physical changes occur in the polymer during the first few days of HCl exposure, before the permeability stabilises and becomes relatively constant thereafter.
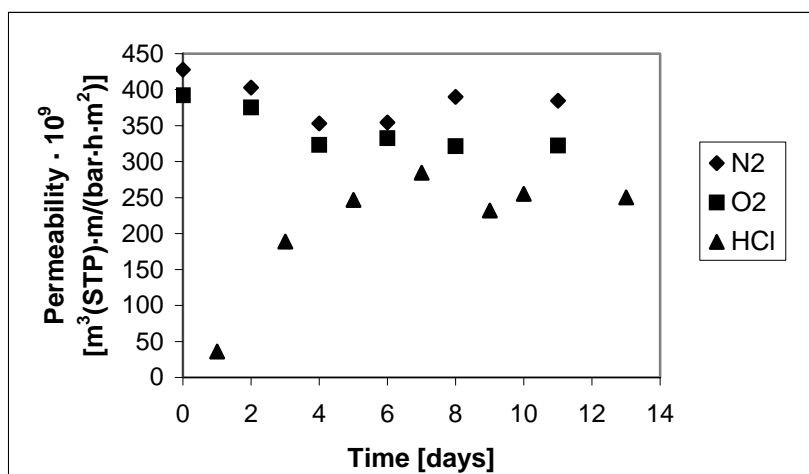
Figure 6.24: Permeability $\cdot 10^9$ [m^3(STP) m/($m^{2\cdot}$h bar)] of N_2, O_2 and HCl through Fluorel as a function of time after exposure to HCl gas at 30°C. Thickness: 80 μm.

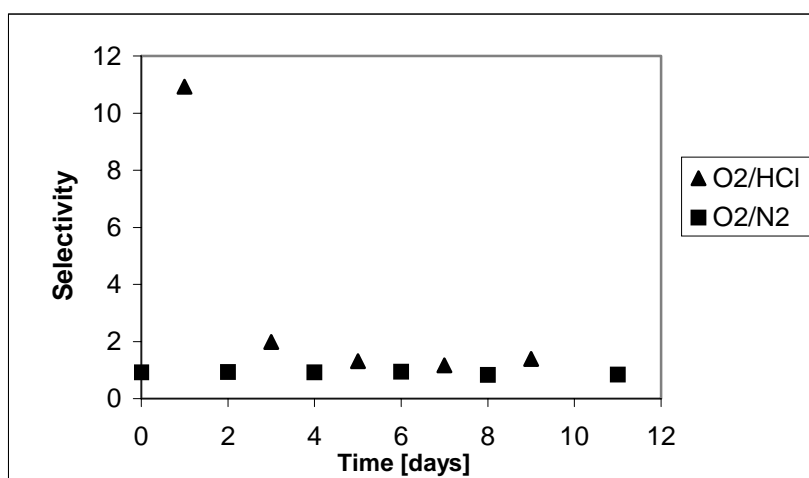*Figure 6.25: Selectivity of O_2/N_2 and O_2/HCl through Fluorel as a function of time after exposure to HCl gas at 30°C. Thickness: 80 μm.*

6.2.3 Durability discussed in view of permeability results

The permeability in Fluorel was very low for all gases measured (N_2, O_2, Cl_2 and HCl). A relatively constant permeability could be observed upon exposure to Cl_2. For HCl exposure the HCl permeability increased the first few days before it became relatively constant. The permeability of nitrogen and oxygen decreased slightly under the exposure to both Cl_2 and HCl.

These low permeabilities and selectivities exclude the Fluorel as a suitable membrane material for the separations in question, even though it showed exceptionally good durability when exposed to the aggressive gases Cl_2 and HCl.

The HCl gas was obviously interacting to a larger degree than Cl_2 with the polymer, but when the reaction has reached equilibrium after few days the separation properties remained constant, and the polymer seems stable against HCl.

If a polymer is highly crystalline, the permeation through the polymer will depend on the thermal history and annealing. The crystalline structure will often vary considerably whether the material is being annealed (slowly cooled) or quenched (quickly cooled) in the production process [18]. The crystallinity will increase upon annealing usually with the result of reduced diffusivity. It may however, be observed in some cases that the diffusivity increases. This is explained by the fact that increased crystallinity may cause a decrease in tortuosity of the diffusion path by crystals become more isometric. Formation of crystalline defects large enough to allow passage of the diffusing molecule may also increase the diffusivity. Studies of gas sorption and transport properties through crystalline domains strongly support the notation of the impermeability of even tiny gas molecules. The solubility coefficient ($S_i = c_i/p_i$) is essentially proportional to the volume fraction of the amorphous material, i.e., the solubility increases with the volume fraction of amorphous material [13].

The annealing process is continuously ongoing when the material is being repeatedly heated and cooled over a wide temperature range. The permeation through semi-crystalline polymers is difficult to comment on unless one has detailed information about the crystallinity and related factors.

Easily condensable gases like HCl and Cl_2 will show low permeabilities in crystalline materials. The permeability data obtained for Fluorel can be compared with the data reported by Hägg [6] for perfluorinated membranes (see Table 6.7). Poly(tetrafluoroethylene) (PTFE) is highly crystalline and this explains the low permeability. PTFE-X is a copolymer of PTFE and an unknown cyclic perfluorinated monomer. PTFE-X is also crystalline but exhibits a larger free volume available for transport due to its structure. Fluorel is not a fully fluorinated material but contains also carbon-hydrogen bonds. During the preparation of the Fluorel membrane the solvent was evaporated at 80°C, and then the membrane was cooled slowly to room temperature. The polymer may have become crystalline during annealing; this explains the low permeability of the Fluorel. The membranes used in the two different separations, Cl_2 and HCl respectively, were made in two different batches. The membrane used for the HCl separation had most likely become more crystalline in the preparation due to annealing.

Table 6.7: Comparison of the permeability of N_2, O_2 , Cl_2 and HCl at 30°C in Fluorel, PTFE and PTFE-X [6].

Polymer	Permeability $\cdot 10^9$ $[m^3(STP)m/(m^2 h\ bar)]$			
	N_2	O_2	Cl_2	HCl
Fluorel	124	128	154	36
PTFE	8	18	13	9
PTFE-X	55	83	86	72

Increased permeability is observed with increasing temperature when the polymer is exposed to chlorine gas. Chlorine substitution will change the characteristics of the polymer, which again influence the separation properties. An increase in temperature will enhance further chlorination. The increased temperature may also reduce the crystallinity, due to larger freedom of motion between the polymer chains. Reduced crystallinity will increase the permeation due to increased volumes of amorphous phases.

6.2.4   Absorption measurements

Fluorel dissolved in 90:10 vol% ethylmethylketone:MeOH respectively, was preformed as a thin membrane on a glass petridish. The solvent was evaporated at 80°C over night and slowly cooled to room temperature. The Fluorel was released from the petridish with water at room temperature and then dried overnight to remove water. The absorption cell with the polymer was evacuated over night before absorption measurements started. The sorption curves of chlorine gas in Fluorel had the same profile as was discussed for PDMS exposed to chlorine gas (Figure 6.10) (see also Figure B.2.1 in appendix B); the absorption curve was not reaching equilibrium. The sorption data for chlorine gas was determined by extracting the contribution of chlorination reaction. This was done by the linearisation of the absorption curve after 5 hours. The total time of the measurements was app. 10 hours.

The absorption was measured with new samples at each temperature, and in sequences of N_2, O_2 and Cl_2.

Gas solubility as a function of temperature, 30-80•C:
The results of the absorption measurements for Fluorel are given in Table 6.8. The solubility coefficients for nitrogen and oxygen in Fluorel were decreasing from 30°C to 65°C. At 80°C the solubility increased significantly for these two gases. This might be due to the thermal influence of the crystalline domains in the Fluorel. The sorption of oxygen was higher than the sorption of nitrogen, but the sorption selectivity was just slightly above unity $(S_{O2}/S_{N2}(30°) =1.11)$.

The sorption for chlorine gas was increasing in the temperature interval from 30°C to 65°C; with a deviation at 35°C for reasons that remain unclear. At 80°C the sorption value decreased. The sorption selectivity of Cl_2/O_2 is 13.6 at 30°C, which is significantly higher than the permselectivity.

Some of the absorption measurements for Fluorel were run for parallel testing (Table B.2.3 in appendix B) with large variation in the results. The values in the table should thus not be taken as absolute but just an indication of the size of the solubility coefficients in Fluorel. The variation could be due to differences in the batches where the heating and cooling rate may

give different degrees of crystallinity. As discussed in section 2.1.4 and in 6.2.3, crystallinity will influence the transport properties.

Table 6.8: Solubility coefficients in Fluorel. Pressure 1 bara.

Exposure Temp. [°C]	Solubility coefficient, S [cm³(STP) /(cm³·bar)]		
	N_2	O_2	Cl_2
30	0.27	0.30	2.2
35	0.26	0.30	0.90
50	0.24	0.31	4.3
65	0.21	0.25	5.3
80	0.44	0.51	3.7

Density measurements

The sample was weighted before and after the absorption measurements. The density was measured with a pycnometer after the Cl_2 exposure (Table 6.9). The density of Fluorel was about 1.73 -1.79 g/cm³. The density given in the "before" column in Table 6.9 were all measured before exposure and at room temperature. They have not been heated to the exposure temperature of the absorption experiment. The tendency was that the density decreased after the exposure to chlorine gas. The density increases with increasing temperature of the chlorine exposure experiment.

Table 6.9: Density of Fluorel before and after exposure to Cl_2 in absorption cell at different temperatures

Exposure Temp [°C]	Density measured at 20°C [g/cm³]	
	before	after
30	1.73	1.66
35	1.79	1.69
50	1.73	1.75
65	1.73	1.75
80	1.75	1.83

Weight changes after absorption measurements

The chemical reaction that may occur between Fluorel and chlorine gas, is a substitution of a hydrogen atom by a chlorine atom. This will increase the polymer weight due to a higher molecular weight of the chlorine atom. After the absorption test the absorption chamber was evacuated. Components, which may have absorbed, chemically or physically, in the polymer may then desorb. The chemical (irreversible) bonded chlorine in the polymer after the absorption test may be registered by weighing the sample. Table 6.10 gives the weight before the measurement and the percent increase during the absorption, negative sign indicates a weight loss. As seen from Table 6.10 the weight increases after the absorption. At temperatures at 65°C and above it was observed a weight loss. This can be due to degradation or crosslinking. Degradation might give low molecular weight compounds that are desorbed and removed during evacuation. Crosslinking may cause formation of hydrofluoric acid; HF (Figure 6.29).

Table 6.10: Weight before and after the absorption measurements.

Temp [°C]	Weight before absorption [g]	Weight increased after absorption measurements [%]
32	2.00	0.25
35	2.81	0.20
50	2.63	0.24
65	2.86	-0.95
80	1.32	-0.25

6.2.5   Evaluation of durability based on absorption results

Large variations in the absorption values were observed at parallel analyses. This might be due to different degrees of crystallinity in the different polymer batches made for the analyses. The rate of diffusion will depend on crystalline domains, tourtorsity and formation of crystalline defects. The solubility coefficients for N_2 and O_2 decreases with temperature, while the solubility coefficients of Cl_2 increase with temperature in the temperature range 30-65°C. At 80°C the trend is changing: The solubility coefficients for N_2 and O_2 increase, while the solubility coefficients of Cl_2 decrease. The latter may be due to changes in the degree of crystallinity, since the polymers were prepared at 80°C, cooled and next heated again.

The density decreased after the polymer was exposed to chlorine, but increased with temperature. The polymer gained weight at the lowest temperature, but at 65-80°C the weight decreased. Chlorine is a larger atom than hydrogen and substitution of this will increase the polymer weight. The highly electronegative chlorine and fluorine will resist interactions, thus giving a lower density. At the highest temperatures crosslinking may have taken place. Crosslinking causes a weight loss due to extraction of HF (Figure 6.29). The polymer structure becomes denser.

The absorption curve for chlorine gas had the same profile as for PDMS (Figure 6.10). The absorption did not reach equilibrium during the time of exposure. This may be due to low diffusivity into the polymer bulk, which may be rate determining for the absorption process. A stable sorption value could thus not be expected during the time (10 hours) of the absorption measurement.

6.2.6   Evaluation of durability based on instrumental analysis

The Fluorel membrane was exposed to chlorine in the glass chamber for 4 weeks at 30°C and 60°C. No colour or elasticity changes have been observed after the exposure.

FT-IR
The samples have been analysed by FT-IR and the spectra is presented in Figure 6.27. The groups CF_3 and CF_2 are difficult to differentiate in the infrared region. The CF_3 group absorbs strongly at 1350-1120 cm^{-1} and CF_2 at 1280-1120 cm^{-1}. Four- or five member cyclic CF_2 compounds absorb at 1350-1140 cm^{-1}. Another band involving the CF_3 group occurs 780-680 cm^{-1}. The narrower region of 745-730 cm^{-1} is characteristic for the group CF-CF$_3$. The group CF=CF$_2$ absorbs strongly at 1340-1300 cm^{-1} [10].

Figure 6.27 shows no significant changes in the chemical structure of the polymer in the measured area. Only a small shift in the wave number and a variation in intensity due to reflectance could be observed. The variation in intensity may be due to change of gloss of the surface, the pressure of the clamp at the ATR assocery, or that the samples have not covered the same area of the crystal.

The CF_3 group is identified at 1350-1120 cm^{-1} and CF_2 compounds at 1280-1120 cm^{-1}. The band at 780-680 cm^{-1} show the CF_3 group. The band at 1430-1395 cm^{-1} identifies deformation vibrations of CH_2 compound, and the band at 880-820 cm^{-1} is due to CH wag.

No evidence of the C-Cl (830-560 cm^{-1}) bond is seen in the spectra for the exposed samples. This bond can however be hidden by the absorption band of the C-F bond.

Thermal Analysis
A thermogravimetric analysis of Fluorel is shown in Figure 6.26. The Fluorel exhibit a high stability at high temperatures, the weight loss is only 0.26% at 350°C.
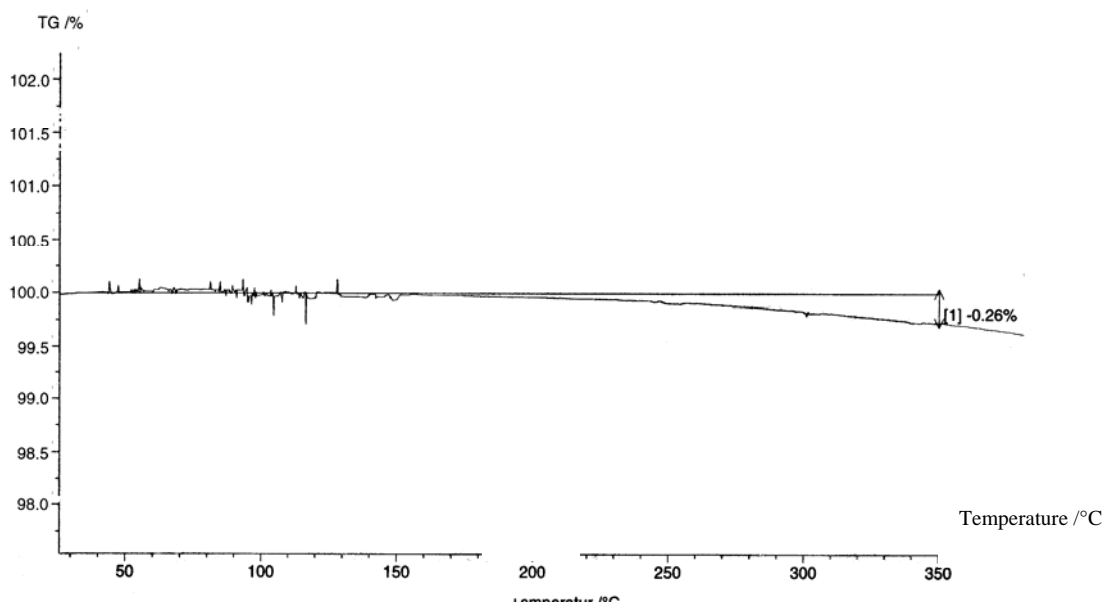

Figure 6.26: TGA analysis of Fluorel

DSC spectra of chlorine exposed Fluorel samples (from the absorption measurements at different temperatures) show no big changes in the temperature range 50-400°C. No conclusions can be made about degradation.
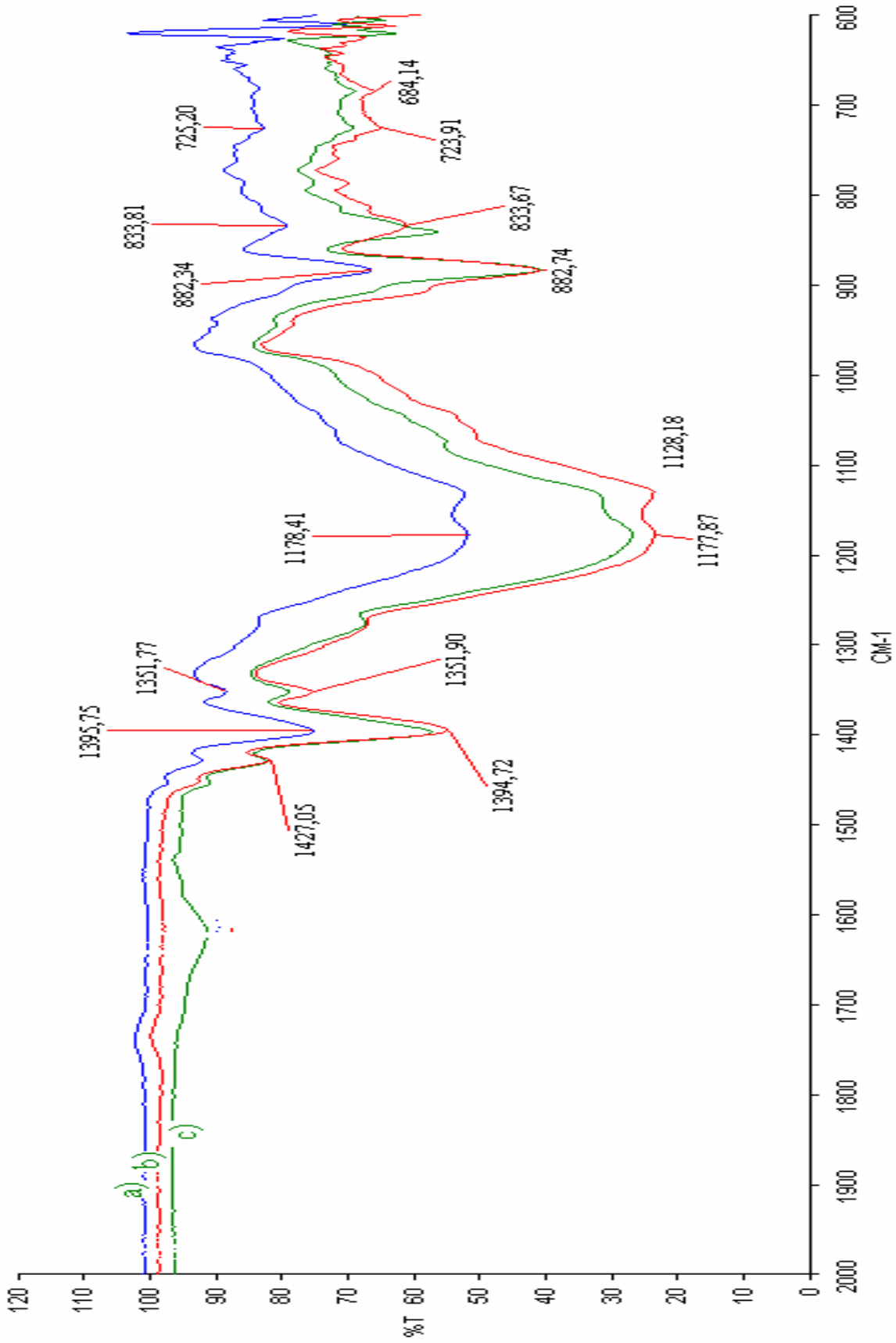
Figure 6.27: The FT-IR analysis of Fluorel a) unexposed sample (blue line), b) sample exposed to Cl_2 for 4 weeks at 30°C (red line), c) sample exposed to Cl_2 for 4 weeks at 60°C (green line).

6.2.7 Interim conclusion for Fluorel

The polymer chains may be crosslinked as a result of the chlorine or hydrochloric acid exposure. The hydrogen atoms in Fluorel may also be substituted with chlorine atoms, causing the structure of the polymer to change and thus also the separation properties. The degree of crystallinity will also influence on the gas transport through the membrane.

Chlorination of the polymer chain (Figure 6.28) will give an increase in polymer weight. Since the chlorine atom is larger than the hydrogen atom the structure will change, and may increase its glass transition temperature T_g, and reduce the chain flexibility. This will decrease the permeability.
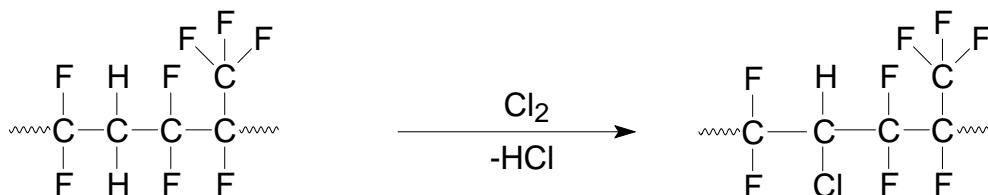

Figure 6.28: Substitution of Cl_2 in Fluorel.

Crosslinking in Fluorel may take place between hydrogen and fluorine atoms. This would give hydrofluoric acid, HF. These crosslinking mechanisms of Fluorel may be activated by heat or ionising radiation, (Figure 6.29) [19]. Crosslinking will give a denser polymer structure.
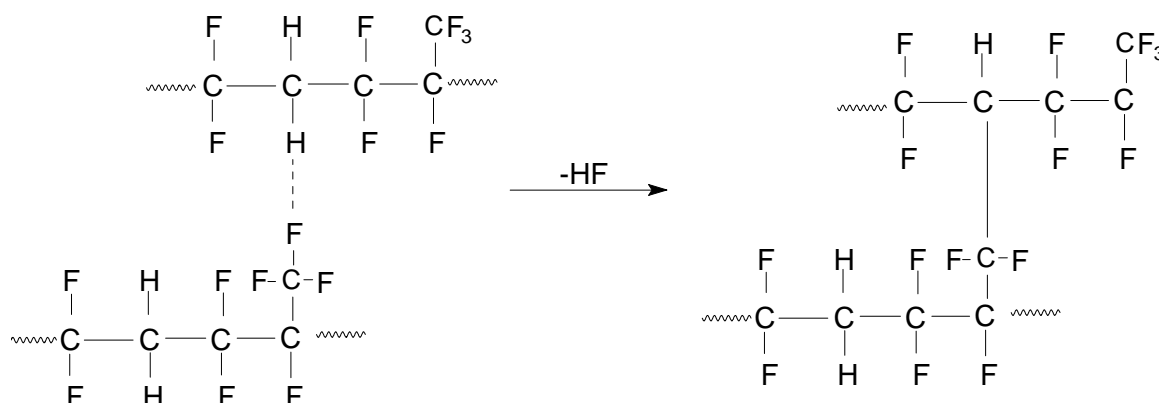

Figure 6.29: Crosslinking mechanisms of Fluorel, which can be activated by heat or ionising radiation [19].

An alternative reaction schema is given in Figure 6.30. Here the trifluoromethyl group is extracted from the polymer chain, and a free radical is formed. Chlorine may react with the radical, or the radical may induce further crosslinking.
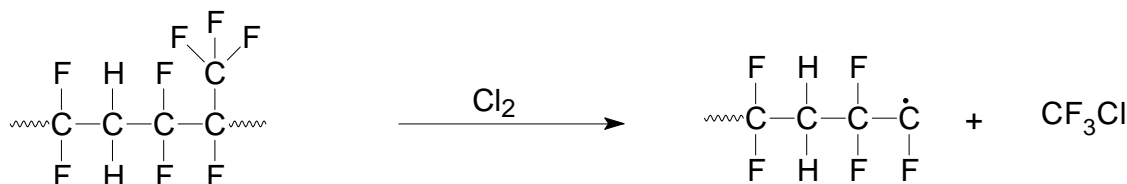

Figure 6.30: Depolymerisation of Fluorel, inducing chlorination or further crosslinking.

Crystalline domains in the polymer may give very small permeability fluxes. The crystallinity will increase upon annealing usually with the result of reduced diffusivity. The permeation through semi-crystalline polymers is difficult to comment on unless one has detailed information about the crystallinity and related factors. Easily condensable gases like HCl and Cl_2 will show low permeabilities in crystalline materials.

During the preparation of the Fluorel membrane the solvent was evaporated at 80°C, and then the membrane was cooled slowly to room temperature. The polymer may have become crystalline during annealing; this explains the low permeability of the Fluorel. The membranes used in the two different separations (Cl_2/O_2 and HCl/H_2 respectively) were made in two different batches. The membrane used for the HCl separation had most likely become more crystalline in the preparation due to annealing.

The permeability and selectivity of Fluorel are both too low to be considered in an industrial process. It was however interesting to verify that the permeability was slightly decreasing during exposure to chlorine gas, resulting in increased selectivity. Increased temperature may reduce the crystallinity, due to larger freedom of motion between the polymer chains, and the permeability will increase through the enlarged volume of amorphous phases.

The sorption measurements showed a decrease in sorption of nitrogen and oxygen from 30°C to 65°C. At 80°C the sorption increased. The sorption of chlorine is increasing from 30°C to 65°C. At 80°C the solubility coefficient decreased. The changes in the solubility coefficient at the highest temperature may be due to thermal influence on the crystallinity. The polymers were prepared at 80°C and the reheating of the polymer to this temperature again will change the degree of crystallinity. The absorption curve for chlorine gas in Fluorel had the same profile as for PDMS (Figure 6.10). The absorption was not reaching equilibrium. This may be due to low diffusivity of the polymer bulk, which can make this a rate-determining step for the absorption measurements.

The tendency was that the density decreased after the exposure to chlorine gas. When the temperature was increased the density increased. The weight increased after chlorine absorption. At temperatures above 65°C it was observed a weight loss.

The FT-IR spectra in Figure 6.27 showed no significant changes in the chemical structure of the polymer.

The TGA analysis showed that Fluorel exhibit a high stability at high temperatures, the weight loss was only 0.26% at 350°C.

Conclusion; Fluorel has good stability when exposed to chlorine gas in the temperature range tested. The permeabilities and selectivities are too low to be of industrial interest. Domains of crystallinity in the polymer are likely to cause the low permeabilities and selectivities of the membrane.

6.3   Blend of PDMS and Fluorel

PDMS showed a decrease in the permeability by exposure to chlorine. The industrial interest of PDMS in a membrane application, would require a relatively high permeability and that the membrane should be chemical resistant. It was made an attempt to blend Fluorel and PDMS to see if this could inhibit degradation of PDMS while maintaining a high permeability.

Different ratios of PDMS and Fluorel have been tested. Blends with 2 or 2.5 parts of PDMS and 1 part Fluorel gave the best selectivities for nitrogen and oxygen ($\alpha_{O2/N2} \approx 2.1$). The PDMS used in the blends was Deh ® 942.

6.3.1   Permeability measurements of N_2, O_2 and Cl_2

These experiments were performed with a membrane cell with a diameter of 5 cm, giving a permeation area of 20 cm^2. The temperature was kept at 30°C. Pressure on the feed side was 2 bara and the pressure at the permeate side was app. 0.6 bar. The thickness of the 2:1 sample of PDMS and Fluorel respectively had a thickness of 7 μm, while the 2.5:1 sample of PDMS and Fluorel respectively had a thickness of 23 μm, measured by a digital micrometer.

Changes in permeability over time at 30°C:
Table 6.11 gives the permeability and selectivity of the two samples. The initial permeability is significantly higher for the blend than the pure PDMS and pure Fluorel (refer to Figure 6.4, Figure 6.5 and Figure 6.22.) Higher concentrations of PDMS gave increased permeability. The permeability and selectivity are quite good at the start. The permeability for the chlorine gas decreased significantly during the first 7 days. After 11 days the permeability of all gases have decreased. This indicates crosslinking or chlorination. Simultaneously the selectivities also decrease and degradation of the membrane is likely.

Table 6.11: Results from permeability measurements for PDMS/Fluorel at 30°C.

Polymer	Time [days]	Permeability · 10^6 [m^3(STP) m/(bar h m^2)]			Selectivity	
		N_2	O_2	Cl_2	O_2/N_2	Cl_2/O_2
2 PDMS : 1 Fluorel	0	2.4	4.9	87.	2.1	17.7
	7			1.8		
	11	0.26	0.31	1.5	1.1	4.8
2.5 PDMS : 1 Fluorel	0	4.3	8.9	200	2.1	22.6
	7			5.5		
	11	1.8	1.8	5.9	1.0	3.2

6.3.2   Durability discussed in view of permeability results

The permeability of all gases is higher in the blended samples compared to the pure materials. These are positive indications on that the resulting membrane might show acceptable performance. However the permeability decrease significantly upon chlorine exposure, and the decreased selectivity indicates a degraded membrane.

The preparation of the polymer blend might have been insufficient, giving an inhomogeneous polymer matrix. A closer study of blends and their properties is needed for a deeper

understanding of the transport mechanisms. Mixtures need to be homogenous to exhibit enhanced polymer properties. Curing and crosslinking of the materials might be necessary to achieve a resistant polymer structure due to the exposure conditions. The preparation of the blends is important to optimise the membrane properties.

In section 3.3 blends of silicone rubber and fluoroelastomers were discussed. It was stated from Langstein [20] that the two polymers were immiscible. Processes to cure these two polymers have been discussed in several patents. Studying the preparation methods of the membranes can give an understanding of what have taken place. The polymer blends have likely been inhomogeneous and not properly cured. Because of the low surface tension of PDMS this will probably lie on the top of the membrane and the Fluorel will lie between the PDMS and the support. However the permeability was initially higher than that of both PDMS and Fluorel, but decreased significantly after chlorine exposure. The reasons for the decreased permeability in the blend can be the same as discussed for pure PDMS in section 6.1.10: Chlorination and crosslinking. Both factors lead to a denser polymer structure, and thus a reduced permeability. A better understanding of the curing process is thus necessary to obtain a "perfect" blend.

6.3.3   Evaluation of durability based on instrumental analysis

The membrane blend of PDMS and Fluorel was exposed to chlorine gas at 30°C and 60°C for 4 weeks each in a glass chamber.

FT-IR
It was difficult to study the FT-IR spectra, because of the composition of the polymer. The selective layer consists of poly(dimethylsiloxane) ($SiO(CH_3)_2$) and the copolymer Fluorel; which is composed of vinylidenefluoride ($C_2H_2F_2)_n$ and hexafluoropropylene ($C_3F_6)_n$. Difficulties lay in the fact that the siloxane and fluoro components have, in some cases, the same band range.

The FT-IR spectra for exposed and unexposed samples of the membrane with the blend 2:1 PDMS and Fluorel respectively are shown in Figure 6.31. The membrane with the blend 2.5:1 PDMS and Fluorel respectively, was similar and the discussion here will also apply to this membrane.

The spectrum of the unexposed "blended " membrane is quite similar with the spectrum of pure unexposed PDMS (Figure 6.12.). This may indicate that the polymer mixture has separated into two phases and that the PDMS will be covering the surface of the selective membrane layer. Also the lack of any bonds around 1350 cm^{-1}, which would be C-F bonds in Fluorel, indicates phase separation.

The peak at 2961cm^{-1} is assigned to the methyl group and occurs in the unexposed sample but has disappeared completely after the chlorine exposure at both temperatures. During the exposure experiment it seems like the Si-CH$_3$ bond (wavenumber 2961, 1402 and 1258 cm^{-1}) has degraded.

The strong double peak at about 1086 cm^{-1} and 1015 cm^{-1} (Si-O-Si bond) have decreased in intensity after exposure to chlorine gas, and is reduced to a broad single peak at about 1067 cm^{-1}. This might be due to formation of cyclic compounds or crosslinking. The occurrence of the band at 902 cm^{-1} may be due to formation of Si-OH, which absorbs at 915-830 cm^{-1}. The

disappearing of the band at 795 cm^{-1}, which is due to CH$_3$, and the occurrence of the band at 727 cm^{-1}, which is due to C-Cl bond indicate clearly a chlorination of the polymer blend. The peaks in the range from 790-880 cm^{-1} have also decreased in intensity after exposure to chlorine gas. It is likely that the membrane has changed its chemical character and degraded after exposure to chlorine gas. The FT-IR band for the two exposed samples is similar. The temperature seems not to have any strong influence.

DSC

The DSC was used to see if the melting properties of the material changes after exposure to the chlorine gas. The DSC analysis were performed on the composite membrane samples, where the blend constitute the selective layer, while the support is poly(vinylidenefluoride) and poly(tetrafluoroethylene) (Figure 6.32). Vinylidenefluoride has a melting temperature of about 170°C. The melting temperature for PTFE is 327°C [12]. The DSC analysis in the temperature range 50-400°C gives one peak at 165°C and one at 270°C (Table 6.12). This is most likely due to PVDF and PTFE respectively. The PDMS has a low melting temperature (-40°) [12] and will not show in this spectrum. The Fluorel has been shown not to have any melting peaks in the actual temperature range, thus the support material presumably causes the obtained values.

The melting temperature is relatively constant after the material has been exposed to chlorine gas. This applies both to the 2 PDMS: 1 Fluorel and for the 2.5 PDMS: 1 Fluorel. From Table 6.12 it seems like the enthalpy is decreasing after exposure to chlorine gas. This could be due to weaker bonds, or degradation of bonds within the polymer. However, this does not apply to ΔH$_1$ for 2.5 PDMS: 1 Fluorel, so no clear conclusion about degradation can be made.

Table 6.12: Melting and solidification temperature, and enthalpy.

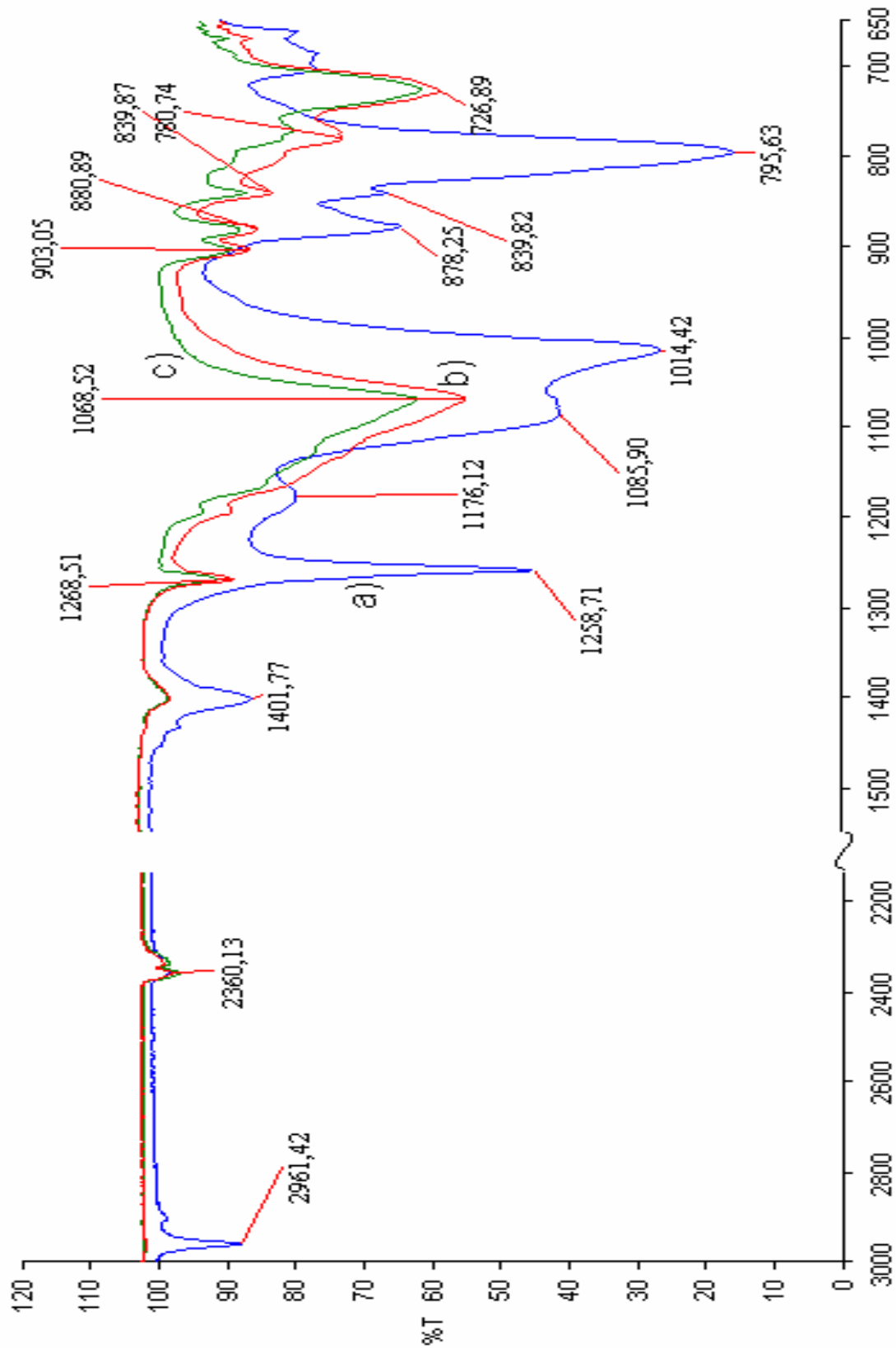| Polymer	T$_m$ [°C]	T$_m$ [°C]	ΔH$_1$ [J/g]	ΔH$_2$ [J/g]
2 PDMS : 1 Fluorel				
Unexposed material	164.2	270.4	11.10	35.96
Material exposed for chlorine gas at 30°C	166.5	272.0	10.21	29.56
2.5 PDMS: 1 Fluorel				
Unexposed material	165.5	272.0	10.75	36.36
Material exposed for chlorine gas at 30°C	166.1	271.0	12.69	28.93

Figure 6.31: FT-IR spectra of 2 PDMS: 1 Fluorel a) unexposed sample (blue line), b) sample exposed to chlorine gas at 30°C for 4 weeks (red line), and c) sample exposed to chlorine gas at 60°C for 4 weeks (green line).
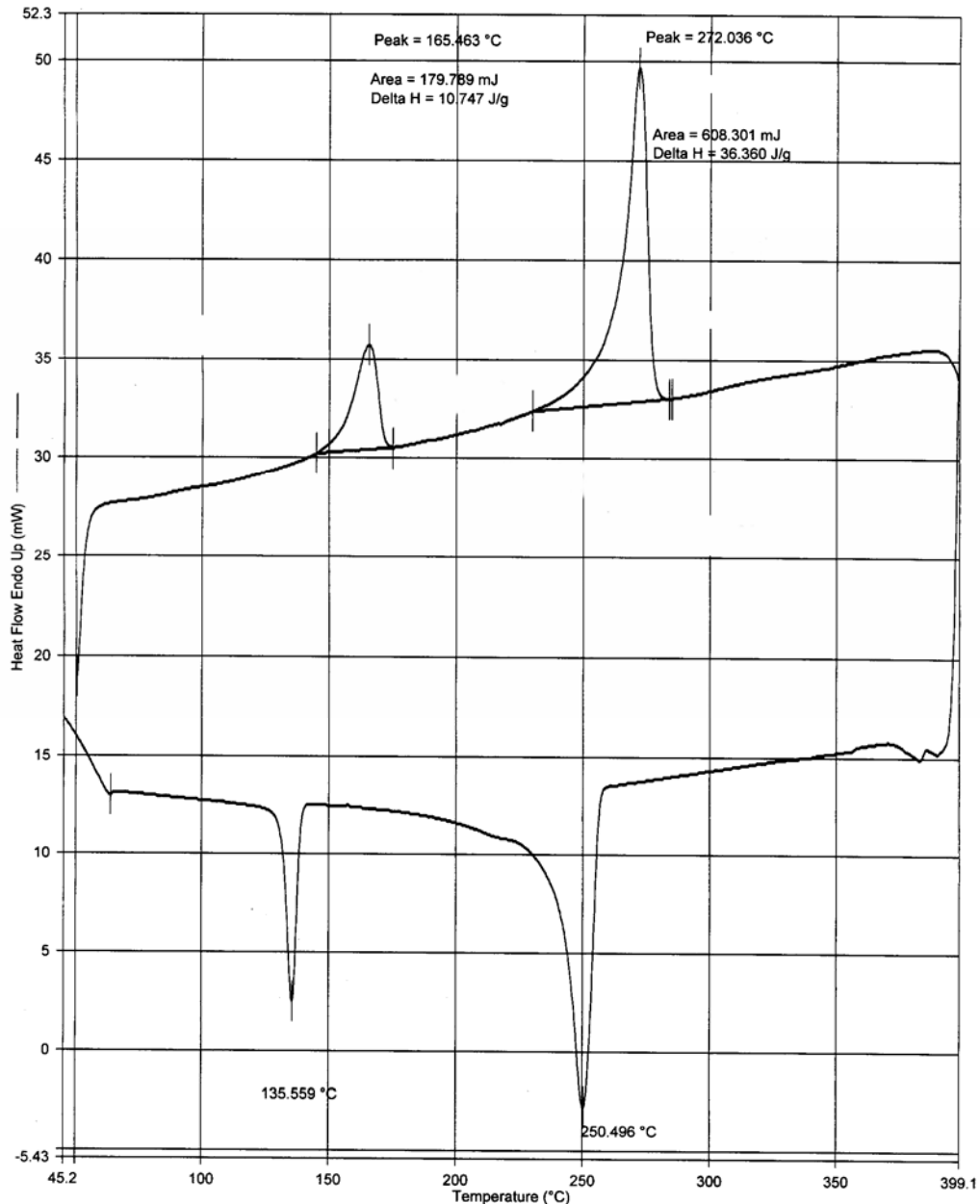
Figure 6.32: DSC spectra of unexposed 2.5 parts PDMS and 1 part Fluorel. The upper line is the heating curve; the lower line is the cooling curve.

6.3.4 Interim conclusion for PDMS/Fluorel blend

Two samples with different PDMS concentration were examined before and after exposure of chlorine gas at 30°C. The blend ratios were 2 parts PDMS: 1 part Fluorel and 2.5 parts PDMS: 1 part Fluorel both on PVDF and Teflon support.

The permeability measurements showed initially good permeability and selectivity (Table 6.11). However, the permebility were significantly reduced after exposure to chlorine gas, and the selectivities also decreased.

The membranes made from the blend show higher permeabilities than the pure PDMS material. This indicates that the structure of the membrane is more open and the permebility is

increased. The PDMS used in the blend (Deh 942) has however not the same degree of crosslinking as the one referred to in section 6.1, and will thus degrade more readily than the highly crosslinked PDMS.

Crosslinking may take place between the PDMS and the Fluorel during blending these two very different polymers, curing at 90°C, (Figure 6.33). However, fluorinated carbon groups directly attached to silicone atoms or with one spacer of CH$_2$ are insufficiently hydrolytically and thermally stable [19]. This can be a problem with respect to the degradation of the blended material.
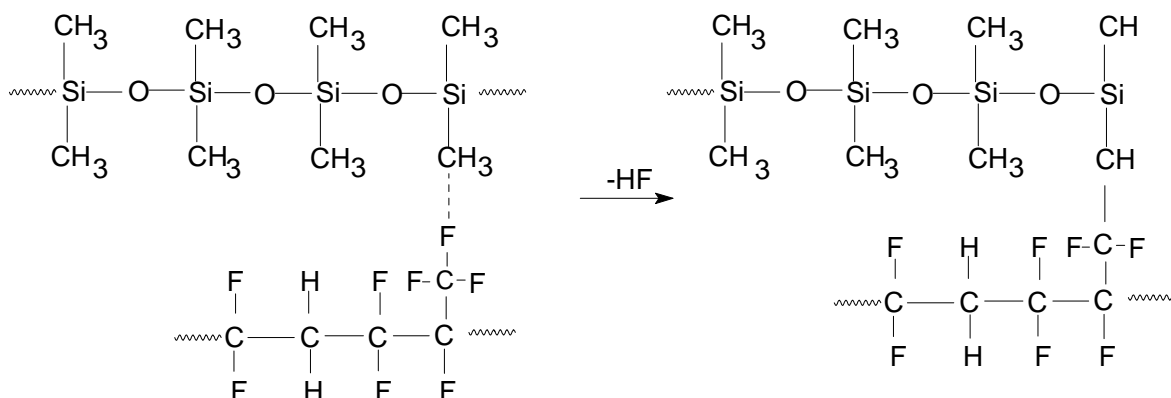

Figure 6.33: Crosslinking between PDMS and Fluorel.

The FT-IR spectra of the unexposed "blended" membrane (Figure 6.31) were quite similar to the spectrum of pure unexposed PDMS (Figure 6.12). This may indicate that the polymer mixture has separated into two phases and that the PDMS is covering the surface of the selective membrane layer. Also the lack of any bonds around 1350 cm^{-1} (C-F bonds) indicates phase separation. FT-IR analysis clearly indicated that the selective layer of the composite membranes has changed its chemical character, and degradation is indicated. Some of the changes observed for the blend are the same as for the pure PDMS: chlorination of the methyl group, (C-Cl bond) and formation of cyclic compounds or crosslinking.

DSC shows small changes in melting and solidification temperature, and in enthalpy. These changes are due to the support material and not to the selective layer. The DSC did not give enough information to conclude whether there is any degradation or not.

Looking at the obtained results, the present membranes made from the blend of PDMS and Fluorel are not suited for the chlorine separation. A deeper understanding of the behaviour of blends and different crosslinking/curing systems ought to be considered.

6.4   Fluorosilicone

Three types of Fluorosilicone membranes have been tested. Two membranes were prepared at the McMaster University in Canada. The membranes were coated on poly(vinylidenefluoride) support, and had a black surface. The first, A, was directly applied on the support and dried for 3 hours at room temperature and for 5 min. at 120°C. The other, B, was cured with THF (tetrahydrofuran) and also dried for 3 hours at room temperature and for 15 min. at 120°C. The third membrane, C, was a transparent homogenous membrane delivered from Specialty Silicone Fabricators, USA. The chemical structures are shown in Figure 6.34.
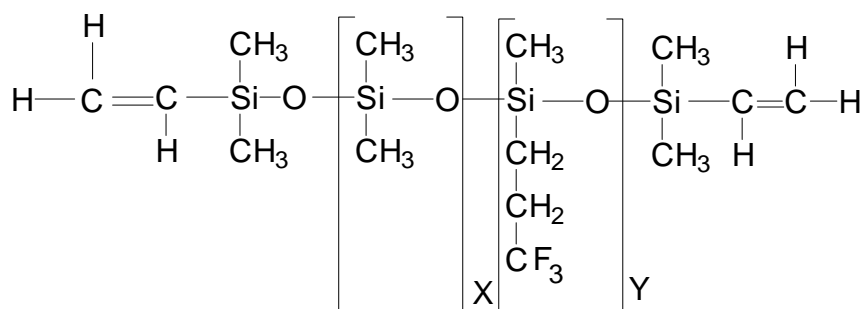
Figure 6.34: The chemical structures of the Fluorosilicone(C).

6.4.1   Permeability measurements of N_2, O_2 and Cl_2

For the membranes delivered from McMaster University, only Fluorosilicone A was suitable for permeability measurements. The one prepared with THF, Fluorosilicone B, had pinholes and could not be used. The permeability results for the Fluorosilicone A are given in Figure 6.35 and in Table B.4.1. The thickness of the selective layer was approximately 59 μm with a very uneven surface. Fluorosilicone C had a thickness of 115 μm and the permeability results are given in Table 6.13. However, when prepared as an industrial membrane the thickness of the selective layer must be reduced to 1-3 μm in order to obtain a high permeability flux. A membrane cell with diameter of 1.9 cm (giving a permeation area of 2.8 cm^2) was used for the permeability measurements. The feed pressure was 2 bara and the permeate pressure was 0.6 mbar.

Changes in permeability of Fluorosilicone A:
The permeabilities and selectivities of Fluorosilicone A are shown in Figure 6.35 and Figure 6.36 respectively. The chlorine permeability decreased during the first 11 days of exposure. At this point there was a pinhole in the membrane and the permeability increased. Opening the membrane cell after the exposure, the membrane was very brittle and easily cracked. The material was not suitable for chlorine separation.

Changes in permeability of Fluorosilicone C:
Permeability and selectivity results of the Fluorosilicone C membrane are given in Table 6.13. The permeability is slightly decreasing during the first week of chlorine exposure at 30°C. After another week the permeability increased significantly indicating holes and degradation of the membrane. Opening the membrane cell, it was seen that the membrane had become very brittle and had cracked. The membrane is not suited for chlorine separation, even though the initially selectivity of $\alpha_{Cl2/O2} = 12.8$ was very good. The permeabilities are comparable with those of PDMS, but the selectivity is poorer for the Fluorosilicone.
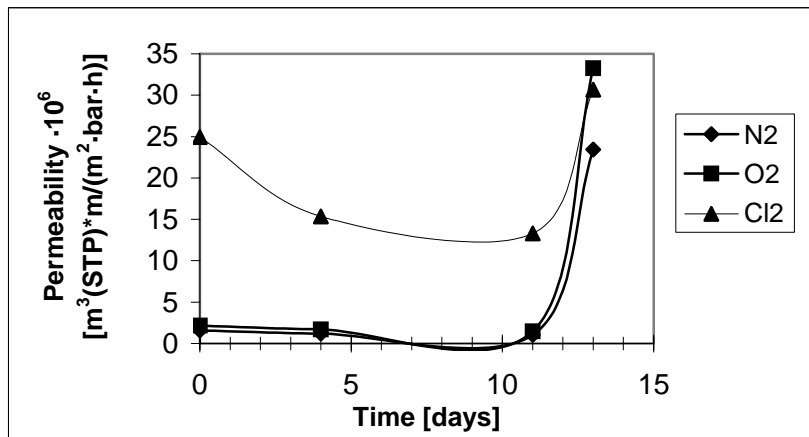
Figure 6.35: Permeability · 10^6 [m^3(STP) m/(m^2 bar h)] of N_2, O_2 and Cl_2 at 30°C in Fluorosilicone A. Thickness: 59 μm.
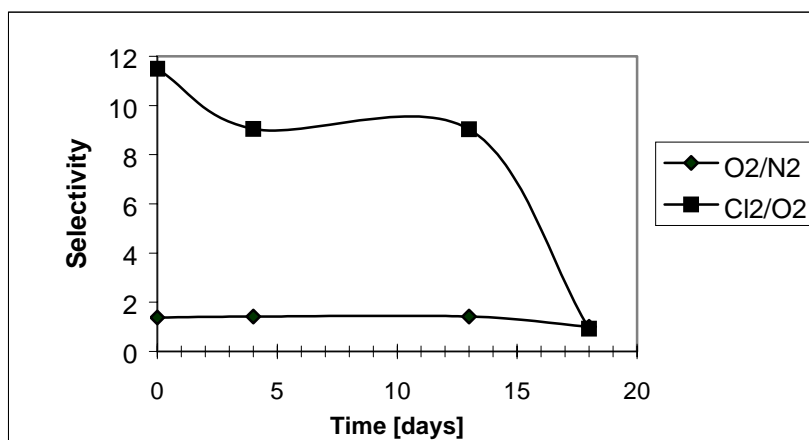

Figure 6.36: Selectivity of O_2/N_2 and Cl_2/O_2 at 30°C in Fluorosilicone A. Thickness: 59 μm.

Table 6.13: Permeability and selectivity of N_2, O_2 and Cl_2 in Fluorosilicone C at 30°C. Thickness: 115 μm.

Time [days]	Permeability·10^6 [m^3(STP)m/(m^2 h bar)]			Selectivity	
	N_2	O_2	Cl_2	O_2/N_2	Cl_2/O_2
0	1.03	1.58	20.2	1.53	12. 8
7	0.986	1.49	17.7	1.51	11.9
13	9170	8910	-	-	-

6.4.2 Permeability measurements of HCl

Some measurements were performed with gaseous hydrochloric acid on the two types of Fluorosilicone membranes described in the previous section.

Changes in permeability of Fluorosilicone A:
The permeability in Fluorosilicone A is increasing after just a few days of HCl exposure. The membrane is ruined after the HCl exposure. The membrane became brittle, and it easily cracked after the exposure.

Table 6.14: Permeability and selectivity of HCl in Fluorosilicone A at 30 °C. Thickness: 59μm.

Time [days]	Permeability $\cdot 10^6$ $[m^3(STP)\ m/(m^2\ bar\ h)]$			Selectivity	
	N_2	O_2	HCl	O_2/N_2	HCl/O_2
0	1.59	2.53	19.3	1.6	7.6
4	25.0	25.5	52.7	1.0	2.0
7	974	1340			

Changes in permeability of Fluorosilicone C:

Similar results can be seen for the Fluorosilicone C. The results are given in Table 6.15 and show that this fluorosilicone cannot stand any exposure of HCl. Even at the first measurement the permeability increased significantly during the experiment. The value given in Table 6.15 was taken in the very beginning of the measurement. At the end of the experiment (after 40 min.) the permeability was 4 times higher than reported in the table. The membrane had become brittle and very easily cracked.

Table 6.15: Permeability and selectivity of HCl in Fluorosilicone C at 30°C. Thickness: 115μm.

Time [days]	Permeability $\cdot 10^6$ $[m^3(STP)\ m/m^2\ bar\ h]$			Selectivity	
	N_2	O_2	HCl	O_2/N_2	HCl/O_2
0	0.83	1.31	10.4	1.6	8.0
3	25.0	29.0	52.7	1.2	1.8
7	1840	1615	-	-	-

6.4.3 Durability discussed in view of permeability results

The results from the permeation experiments with both Cl_2 and HCl show a severe degradation. The membrane samples become very brittle after the exposure. The supplier of the Fluorosilicone C could inform that the polymer is vinyl terminated, with double bonds as indicated in the structural formula in Figure 6.34. The double bonds in the polymer chains can be chlorinated by addition reactions. However unknown factors in the polymerisation and preparation processes may lead to depolymerisation and shorter polymer chains, with a resulting increased permeability.

6.4.4 Absorption measurements

Only the Fluorosilicone C was used in the absorption measurements. The measurements were performed over the temperature interval 25-80°C for the gases N_2, O_2 and Cl_2. The absorption was measured in the sequence N_2, O_2 and Cl_2. A new sample was used at each temperature.

The sorption curves of chlorine gas in Fluorosilicone had the same profile as was discussed for PDMS exposed to chlorine gas (Figure 6.10) (see also Figure B.3.1 in appendix B); the absorption curve was not reaching equilibrium. The sorption data for chlorine gas was determined by extracting the contribution of chlorination reaction. This was done by the linearisation of the absorption curve after 5 hours.

Gas solubility as a function of temperature, 25-80°C:

The results of the absorption measurements of Fluorosilicone C are presented in Table 6.16. The results show small variations in the sorption value for nitrogen and oxygen from 25°C to

50°C. Increasing the temperature further increases the sorption values. This can be due to thermal influence of the material, causing the polymer to increase its free volume and thus absorb more gas. Alternatively, higher temperatures could initiate thermal degradation of the vinyl group, resulting in decomposition of the polymer. For the chlorine gas the sorption was generally decreasing from 30°C to 80°C. At 35°C the value is lower than the general trend of reasons that remain unclear.

Table 6.16: Solubility coefficients in Fluorosilicone. Pressure 1 bara.

Temperature [°C]	Solubility coefficient, S [cm^3(STP) /(cm^3 bar)]		
	N_2	O_2	Cl_2
23	0.386	0.454	11.8
30	0.377	0.441	12. 8
35	0.364	0.468	5.16
50	0.365	0.460	9.19
65	0.448	0.545	7.34
80	0.529	0.600	4.02

Density measurements
The density was measured after the absorption measurements, and the results are presented in Table 6.17. The density before exposure was 1.28 g/cm^3. It can bee seen that the density generally increases after the absorption. The density decreases however with temperature, but increases again at 80°C.

Table 6.17: Density of Fluorosilicone C after exposure to Cl_2 at different temperatures

Exposure Temp [°C]	Density measured at 20°C [g /cm^3]
25	1.40
30	1.31
35	1.34
50	1.28
65	1.23
80	1.44

Weight changes
Table 6.18 gives the weight before the measurement and the percent increase after the absorption, (negative sign indicates a weight loss). As seen from Table 6.18 the weight increases after the absorption at 24°C. At temperature over 30°C it was observed a weight loss, which can be due to degradation.

Table 6.18: Weight before and after the absorption measurements

Temp [°C]	Weight before absorption	Weight increase after absorption measurements [%]
24	0.94	0.52
30	1.26	-0.58
35	1.19	-1.68
50	1.29	-1.01
65	1.08	-2.02
80	0.835	-2.44

6.4.5   Evaluation of durability based on absorption results

The sorption of N_2 and O_2 is not changing much at lower temperatures (25-50°C). At higher temperatures (65-80°C) the solubility coefficient increases with increasing temperature. This can be due to thermal degradation of the vinyl group in the Fluorosilicone C, initiating free radical reactions that can form low molecular weight products or new sites for crosslinking. The formation of free radicals may also consume gas and hence the observed sorption can increase.

The sorption of chlorine is generally decreasing with temperature. This can be due to reaction and degradation between the chlorine and the polymer. This degradation may also explain why density and weight decreases.

Chemical reactions in Fluorosilicone as a result of chlorine gas exposure can occur. Chlorine substitution may take place on hydrogen atoms in the methyl group. The trifluorpropylene group has fluorine groups out in space, and will inhibit chlorine substitution of hydrogen atoms in the vinyl group. Vinyl terminated polymer chains may be saturated by chlorine addition and should be stabilised. However unknown factors in the polymerisation and preparation processes may lead to depolymerisation which can influence on the degradation process. Impurities, residual functional groups and water are all factors that may lead to degradation.

6.4.6   Evaluation of durability based on instrumental analysis

The Fluorosilicone C membranes were exposed to chlorine gas at 30°C for 4 weeks in the glass chamber.

FT-IR
The spectra of Fluorosilicone will in general attribute the same bands as for PDMS, due to similar chemical structures. In addition the characteristics of the C-F bond will occur in these spectra.

A peak at 2963 cm^{-1}, which occurred in the unexposed sample due to CH_3 stretching vibration, had disappeared in the exposed sample. The band at 1446 cm^{-1} was a result of CH_2 scissors deformation and the CH_3 asymmetric deformation [10]. The band at 1261 cm^{-1} is due to CH_3 symmetric deformation. The bond at 800 cm^{-1} is due to the two methyl groups attached to the silicon atom. One methyl on silicon usually absorbs near 765 cm^{-1}. The band at

900 cm^{-1} indicates the alkyl group -CH$_2$CH$_2$CF$_3$. The Si-O-Si has a broad strong band at 1100-1000 cm^{-1}. The CF$_3$ group absorbes strongly in the region at 1350-1120 cm^{-1} and CF$_2$ at 1280-1120 cm^{-1}. Another band involving the CF$_3$ group should occur at 780-680 cm^{-1}.

Comparing the spectra of exposed samples and unexposed samples it is difficult to find evidence of any chemical changes. It seems that methyl groups attached to silicon to some degree have changed character due to chlorination. This is confirmed by the disappearance of the bond at 2961 cm^{-1}. The bond for Si-O-Si is more narrow in the exposed sample than in the unexposed sample and it can be related to depolymerisation and ring formation. Cyclotrisiloxane rings absorb near 1020 cm^{-1}. Otherwise the spectra are relatively similar.

DSC of Fluorosilicone C
DSC analyses of Fluorosilicone after the absorption measurements show the same spectra, without any peaks, for all temperatures. No conclusions can be drawn from the DSC analyses.

6.4.7   Interim conclusion for Fluorosilicone

The main conclusion is that the present Fluorosilicone cannot be used in an industrial membrane application for Cl$_2$-O$_2$ separation. The durability of the material is insufficient for long time exposure. The visual changes in the material are the brittleness after the chlorine exposure.

The permeabilities and selectivities in the membrane are initially good, but the increased permeability and loss of selectivity after Cl$_2$ exposure ruled out this material.

The solubility coefficients of N$_2$ and O$_2$ have small variations up to 50°C, but increased significantly at higher temperatures (65°C-80°C). The solubility coefficient for Cl$_2$ decreases with increasing temperature. The density increases after chlorine exposure, but decreases with increasing temperature. A weight loss is observed after exposure to Cl$_2$.

The FT-IR spectra show a narrower peak for the Si-O-Si bond indicating formation of cyclic compounds or crosslinks.

Vinylterminated fluorosilicone may be chlorinated by addition reaction (Figure 6.38). The reaction should then be terminated after chlorine addition, and thus be stabilised. However the polymer have been totally degraded upon the chlorine exposure. This may be due to factors in the production line of the membrane, factors that are unclear. Polymerisation may have given hydroxyl-terminated polymer chains, which in contact with chlorine may give HCl. Acids, may initiate chain scission and depolymerisation reactions. Impurities from the production, water and solvents in the polymer may all influence on the degradation of the fluorosilicone polymer. Thus more information is needed to draw a conclusion about the degradation of the polymer.
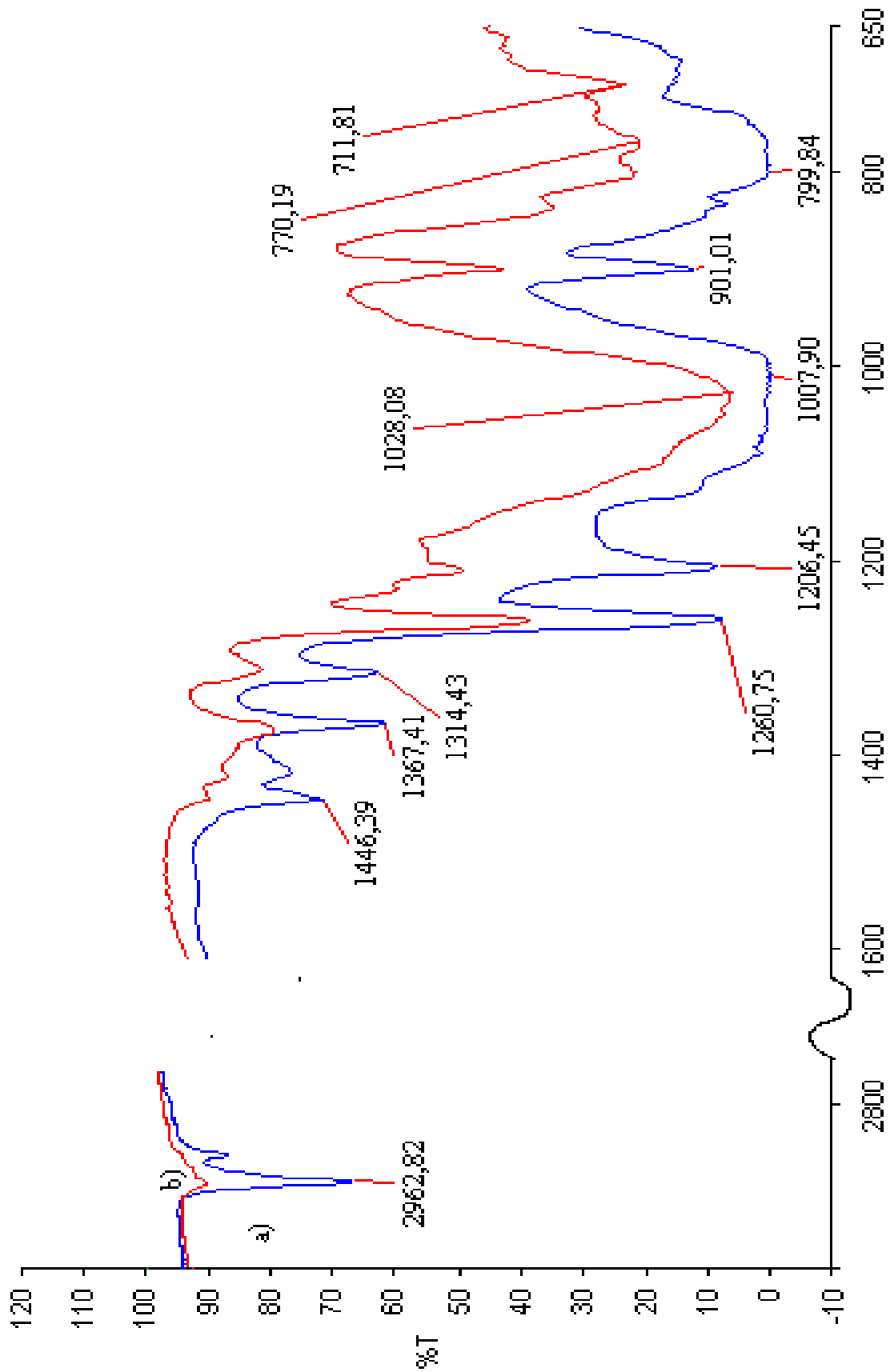
Figure 6.37: The FT-IR analysis of Fluorosilicone (C) a) unexposed sample (blue line), b) sample exposed to chlorine gas for 4 weeks at 30°C (red line).
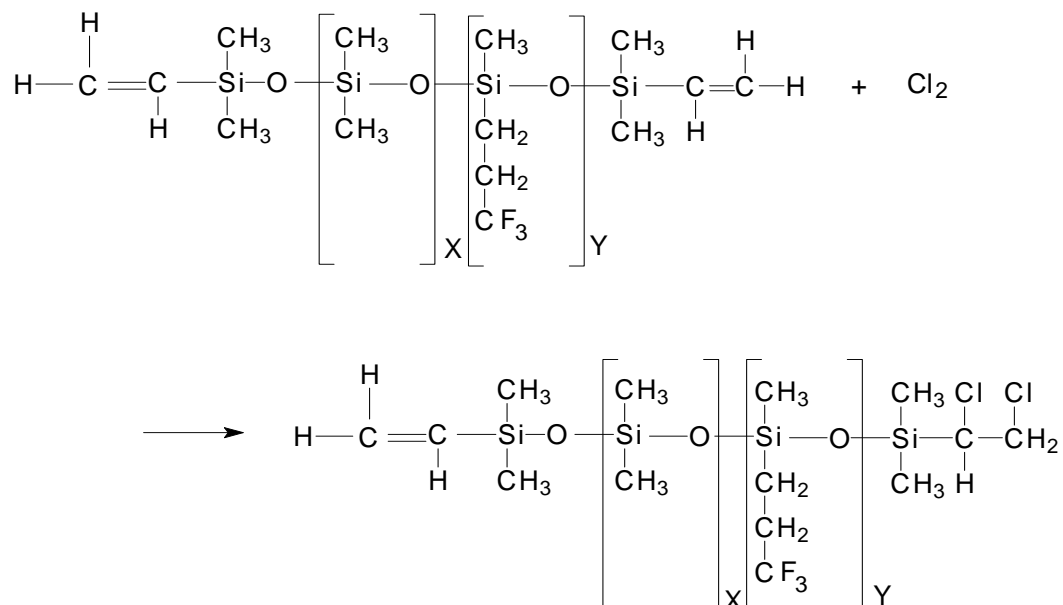
Figure 6.38: Cl$_2$ addition of vinyl terminated Fluorosilicone.

6.5   Support material

The support material consists of poly(vinylidenefluoride) (PVDF) substrate on poly(tetrafluoroethylene) (PTFE) support. The permeability flux for the support material is found to be ca. 500 times larger than for PDMS and will thus not restrict the gas transport through the membrane.

6.5.1   Evaluation of durability based on instrumental analysis

The support material was exposed to Cl$_2$ gas at 60°C for 4 weeks in the glass chamber.

FT-IR
Analysing the support material with FT-IR the exposed and unexposed samples showed similar spectra (Figure 6.39).

The CF$_3$ group absorbs strongly at 1350-1120 cm^{-1} and CF$_2$ at 1280-1120 cm^{-1}. Four- or five member cyclic CF$_2$ compounds absorb at 1350-1140 cm^{-1}. Another band involving the CF$_3$ group occurs at 780-680 cm^{-1}. The band at 1430-1400 cm^{-1} is due to deformation vibrations of CH$_2$ compound, and the band at 880-820 cm^{-1} is due to CH wag.

No bands indicate the C-Cl bond (830-560 cm^{-1}) in the spectra for the exposed samples. This band can however be hidden in the band of the C-F bond.

DSC

The DSC spectra discussed in section 6.3.2 will apply here. From the conclusion in this section there is no evidence of degradation of the support material.

6.5.2 Interim conclusion for the support material

The support material is satisfying the requirement of being chemical and thermal stable under the exposure of Cl_2 at 60°C over a period of 4 weeks. The support material did not restrict the permeability flux.

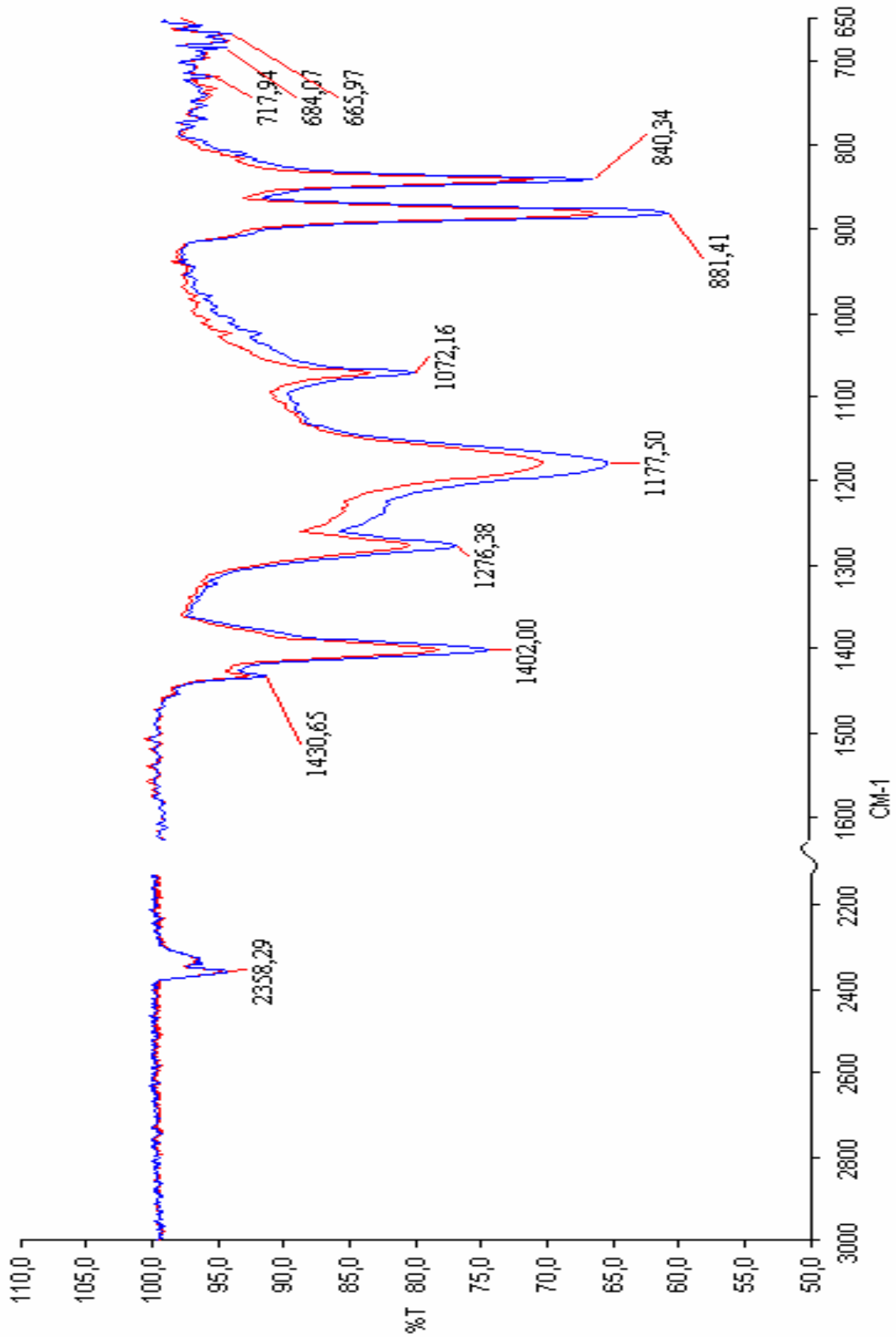The support material of PVDF and PTFE was found to be suitable for the membranes used for the separation of Cl_2 gas.

Figure 6.39: FT-IR spectra of the support material a) unexposed sample (blue line), b) sample exposed to Cl$_2$ at 60°C for 4 weeks.

Reference for Chapter 6

1. M-B Hägg; Membrane Purification of Cl_2 gas I: Permeabilities as a function of temperature for Cl_2, O_2, N_2 H_2 in two types PDMS membranes, J. Membr. Sci., vol 170, p.173-190, 2000.
2. S.A. Stern, V. M. Shah and B. J. Hardy; Structure-permeability Relationships in Silicone Polymers, J. Polymer Phys., vol. 25, p. 1263-1298, 1987.
3. M-B Hägg; Membrane purification of chlorine gas: Contributions towards an integrated process solution in Magnesium production, Dissertation Dr.Tech, The Norwegian University of Science and Technology, Trondheim, Norway 2000.
4. M-B. Hägg et. al.; Separation of H_2 and HCl with membranes (I) Tel-Tek report no. 23008-1 (confidential), Research Centre Norsk Hydro, Porsgrunn, Norway 1997.
5. M-B. Hägg et. al.; Separation of H_2 and HCl with membranes (II) Tel-Tek report no. 23008-2 (confidential), Research Centre Norsk Hydro, Porsgrunn, Norway 1997.
6. M-B Hägg; Membrane Purification of Cl_2 gas II: Permeabilities as a function of temperature for Cl_2, O_2, N_2, HCl in perfluorinated, glass and carbon membranes, J. Membr. Sci., vol. 177, p.109-128, 2000.
7. I. Blume, P. J. F. Schwering, M. H. V. Mulder and C. A. Smolders; Vapour sorption and permeation properties of poly(dimethylsiloxane) films, J. Membr. Sci., vol. 61. p. 85-97, 1991.
8. J. M. Smith, H. C. Van Ness, Introduction to chemical engineering thermodynamics, 4th Ed., McGraw Hill International Editions, Singapore 1987.
9. A. W. Adamson; Physical Chemistry on Surfaces, 3rd Ed., John Wiley & Sons Inc., USA 1976.
10. N. B. Colthup, L. H. Daly, S.E Wiberley; Introduction to IR and Raman spectroscopy, 2nd Ed., Academic Press, USA 1975.
11. W. W. Simons (Editor); The Sadtler Hanbook of Proton NMR Spectra, p. 698-699, Sadtler -Heyden, USA 1978.
12. J. M. Charrier; Polymeric Materials and Processing, Hanser Publisher, Germany 1991.
13. Mark, Bikales, Overberger and Menges; Transport Properties, in Encyclopaedia of Polymer Science and Engineering, Suppl. vol., 2nd Ed., John Wiley & Sons Inc., p. 724 - 799, USA 1989.
14. H. R. Allock, F. W. Lampe; Contempary Polymer Chemistry, Prentice Hall Inc., USA 1981.
15. M. A. Brook, S. Balduzzi, M. Mohamed and R. Stan; Report 3 To Norsk Hydro, Acid Lability of Silicone Membranes (confidential), Chemistry Department McMaster University, Canada June 1999.
16. M.B. Hägg et al; Purification of Chlorine Gas by Membranes Tel-Tek report no. 23003-6 (confidential), Research Centre Norsk Hydro, Porsgrunn, Norway 1997.
17. M. A. Brook, S. Balduzzi, M. Mohamed and R. Stan; Report 2 To Norsk Hydro, Acid Lability of Silicone Membranes (confidential), Chemistry Department McMaster University, Canada February 1999.
18. W. R. Vieth; Diffusion In and Through Polymers- Principles and Applications, Hanser Publishers, Munich Germany 1991.
19. J. Scheirs (editor), M.T. Maxson, A.W. Norris, M. J. Owen; Modern Fluoropolymers: high performance polymer for diverse applications, Chapter 20, John Wiley & Sons Inc., Great Britain 1997.
20. G. Langstein, R. Krüger, H. Alberts, H. H. Moretto; EP 0 582 841 B1, BAYER AG, Leverkusen, Germany 1994.

21. S. J. Clarson, J. A. Semlyen; Siloxane Polymers, Ellis Horwood - PTR Prentice Hall, USA 1993.

Chapter 7: Conclusion and Recommendations

Summary

This thesis have been focusing on the durability of selected membrane materials over time when exposed to chlorine gas in the temperature range 30-100°C. Studies of changes of the membrane separation properties and the mechanisms promoting these changes attributed to the exposure conditions have been in focus.

The selected membrane materials were poly(dimethylsiloxane) (PDMS), Fluorel®[6], Fluorosilicone, and blends of PDMS and Fluorel.

---

[6] Fluorel is the trademark of 3M for the copolymer of vinylidenefluoride and hexafluoropropylene, and is similar to Viton the trademark of DuPont

7.1 Objectives for the work

The objectives for the present work have been:

Objective 1: *Document the durability of selected membrane materials over time when exposed to pure chlorine gas at temperatures from 30°C to 100°C.*

Objective 2: *Study the mechanisms that promote changes in the materials when exposed to chlorine gas.*

Objective 3: *Study changes in the separation properties of the membrane.*

For each of the polymeric materials investigated, comments to the above defined objectives will be given in the following section.

7.2 Goals achieved in view of objectives

7.2.1 PDMS

The PDMS was chosen because of its initial high permeabilities for chlorine gas, and high Cl_2/O_2 selectivities.

Objective 1:
A main conclusion may be drawn with respect to how the PDMS membrane changes upon chlorine exposure: the membrane did not decompose when it was fully protected, but rather chlorinated and further crosslinked. After chlorination and crosslinking the permeabilities of the gases became too low for the material to be of industrial interest.

Objective 2:
Crosslinking of the polymer chains gives a more dense structure, the polymer chains become more restricted to motion, and the free volume for transport will decrease within the polymer, resulting in a reduced permeability. *Chlorination* substitution reaction is a result of the chlorine exposure. Chlorination of the methyl groups in silicones, a free-radical substitution process, changes both the character of the silicone and produces by-products. These changes result in less flexibility of rotation and again reduced permeability.

Objective 3:
The general tendency was that the permeability decreased over time for all gases examined when the PDMS membrane had been exposed to Cl_2 This observation was consistent with the increased chain rigidity and interactions due to side-chain chlorination and increased density due to crosslinking. With Cl_2 being a non-ideal easily condensable gas, and O_2 the opposite, the decrease in permeability for both will follow different mechanisms depending on time and temperature, and may therefore result in even an increased selectivity, as a function of crosslink density, at certain intervals. The general tendency was, however, a slightly reduced selectivity over time for Cl_2/O_2. This is because the chlorination of PDMS makes a new polymer with higher glass transition temperatures, lower solubility coefficients etc. The sorption curve for Cl_2 in PDMS documented that additional chlorine would go into the membrane after sorption equilibrium had been reached; and that the chlorination reaction was taking place. Both *FT-IR analysis* and the *^{1}H-NMR* analysis confirmed that the material was

chlorinated with substitution of hydrogen atoms in the methyl group. The IR-spectra also gave indication of formation of cyclic compounds or crosslinks. *The relative weight loss* due to Cl_2 was in agreement with what would be expected for the samples with different degree of crosslinking. Considered the weight loss; the conclusion would be that the chlorination process was grafting unbound silicone to crosslinked silicone.

7.2.2   Fluorel

Fluorel is a copolymer of vinylidenefluoride (VDF) and hexafluoropropylene (HFP), and have been studied for the purpose to blend it with PDMS to achieve a better stability of the membrane and increase the permeability of the chlorine gas.

Objective 1:
Fluorel showed good stability when exposed to chlorine gas in the temperature range tested. Changes in separation properties could be observed after HCl exposure and in minor degree for Cl_2 exposure. The permeabilities and selectivities for the material were too low to be of industrial interest.

Objective 2:
The polymer chains may be crosslinked as a result of the chlorine or hydrochloric acid exposure. The hydrogen atoms in Fluorel may also be substituted with chlorine atoms, such as the structure of the polymer was changed and thus also the separation properties. These two factors would give a denser polymer structure and a decrease in the permeability. Due to the preparation of the material the Fluorel may be crystalline, and the degree of crystallinity may vary in the different samples used. This will also determine the transport properties of the gases through the membrane.

Objective 3:
The gas permeabilities and selectivities in Fluorel are too low to be considered in an industrial process. It was however found that the permeability was decreased during chlorine exposure with the result of increased selectivity. This may be a result of chlorination or crosslinking. Increased temperatures gave increased permeability, which may be due to changes in the degree of crystallinity. The sorption curve for Cl_2 in Fluorel documented that additional chlorine would go into the membrane after sorption equilibrium had been reached; and that the chlorination reactions was taking place. From FT-IR analysis no significant changes was shown in the polymer structure.

7.2.3   PDMS/Fluorel blend

Two samples with different PDMS concentration were examined before and after exposure of chlorine gas at 30°C. The blend ratios were 2 parts PDMS: 1 part Fluorel and 2.5 parts PDMS: 1 part Fluorel both coated on PVDF and Teflon support.

Objective 1:
The membrane made of the blend shows higher permeabilities than the pure PDMS material. This indicates that the structure of the membrane is more open and the permeability flux is increased. Looking at the obtained results the membranes made from the blend of PDMS and Fluorel were not suited for the chlorine separation at this point of the study, this because of increased permeability after few days of Cl_2 exposure. A deeper understanding of the

behaviour of blends and different crosslinking/curing systems ought to be considered to obtain better separation properties and durability.

Objective 2:
During blending these two different polymers and curing at temperatures at 90°C a crosslinking may take place between the PDMS and the Fluorel. However fluorinated carbon groups directly attached to silicone atoms or with one spacer of CH_2 are insufficiently hydrolytically and thermally stable. This can be a problem due to degradation for the blended material. Crosslinking occurs also between the PDMS polymer chains, and the PDMS may also be chlorinated as discussed for the pure PDMS. These factors lead to a denser polymer structure and a decreased permeability.

Objective 3:
The permeability measurements showed initially good permeability and selectivity. However, the permeability were significantly reduced after exposure to chlorine gas, and the selectivities also decreased. The FT-IR spectra of the unexposed "blended" membrane were quite similar with the spectrum of pure unexposed PDMS. This could indicate that the polymer mixture was separated in to two phases and that the PDMS would be covering the surface of the selective membrane layer. FT-IR analysis clearly indicated that the selective layer of the composite membranes had been changed in the chemical character, and degradation was indicated. Some of the same changes were observed from the blend as for the pure PDMS, chlorination of the methyl group, (C-Cl bond), and formation of cyclic compounds or crosslinking.

7.2.4   Fluorosilicone

Fluorosilicone has been studied as an alternative membrane material. Like PDMS, fluorosilicone exhibits high permeabilities for chlorine gas, and high Cl_2/O_2 selectivities. The polymer structure is more open and should maintain a high permeability upon chlorine exposure.

Objective 1:
The main conclusion was that Fluorosilicone could not be used in an industrial membrane application for Cl_2 -O_2 separation. The durability of the material was insufficient for long time exposure. The observable change in the material was brittleness after chlorine exposure.

Objective 2:
Vinylterminated fluorosilicone may be chlorinated by addition reaction. The reaction should be terminated after chlorine addition, and thus be stabilised. However the polymer have been totally degraded upon the chlorine exposure. This may be due to factors in the production line of the membrane that was unclear. The polymerisation process may have given hydroxyl-terminated polymer chains, which in contact with chlorine would give HCl. Impurities from the production, water and solvents in the polymer may all influence on the degradation of the fluorosilicone polymer. Thus more information is needed to draw a conclusion about the degradation of the polymer.

Objective 3:
The permeabilities and selectivities in the membrane were initially good, but the increase in permeability and loss of selectivity ruled out this material. Also for Fluorosilicone the sorption curve for Cl_2 documented that additional chlorine would go into the membrane after sorption equilibrium had been reached; and that the chlorination reactions were taking place. The FT-IR spectra show a narrower peak for the Si-O-Si bond indicating formation of cyclic compounds or crosslinks.

7.2.5 Support material

Poly(vinylidenefluoride) (PVDF) and poly(tetrafluoroethylene)(PTFE) exhibit both chemical and thermal stability upon the process conditions, and are therefore used as support layer for the membrane.

Objective 1:
The support material fulfilled the requirement of being chemical and thermal stable under the exposure of Cl_2 at 60°C over a period of 4 weeks. The support material did not reduce the permeability flux of the composite membrane. The support material of PVDF and PTFE was found to be suited for the composite membranes used in the exposure of Cl_2.

7.3 General conclusion

None of the tested materials will be suitable for the separation in question (Cl_2-O_2) judged from the permeation properties.

The initially most promising material, highly crosslinked PDMS membrane could withstand Cl_2 exposure at elevated temperatures for at least 60 days even though the permeability became too low to be of industrial interest. The permeability was decreasing too much as a result of changes in the material due to chlorination and crosslinking.

The permeability and selectivity in Fluorel are both too low to be considered in an industrial process, but the material showed good durability in chlorine environment.

The blend of PDMS and Fluorel was not suited for the chlorine separation at this point of the study due to degradation. A deeper understanding of the behaviour of blends and different crosslinking/curing systems ought to be considered to obtain better separation properties and durability.

The studied Fluorosilicone could not be used in an industrial membrane application for Cl_2 - O_2 separation. The durability of the material was insufficient for long time exposure to chlorine gas.

Support material of PVDF and PTFE was found to be suitable for the composite membranes used in the exposure of Cl_2.

7.4   Recommendations

Some recommendations are given for further studies of the selected membrane materials:

Poly(dimethylsiloxane) is now documented to become dense upon chlorine exposure and thus the permeability becomes too low to be of industrial interest. However the polymer may be modified to achieve a more open structure. An attempt of this was made blending PDMS and Fluorel. This was not successfully achieved in this work. However studying blends and their behaviour it might be possible to achieve a membrane material with a more open structure and also a stable membrane for the chlorine exposure.

Fluorosilicone exhibits high permeability for chlorine gas, and high Cl_2/O_2 selectivities. The polymer structure is more open than PDMS and should maintain a high permeability upon chlorine exposure. The chemical structure of fluorosilicone is indicating that the material should be stable to chlorine exposure. Although the current work showed degradation, further studies may give a deeper understanding of the degradation mechanisms and actions could be taken to prevent degradation. This could make fluorosilicone attractive for separation of chlorine - oxygen.

Appendix A: Calculation Procedures and Accuracy of Experimental Measurements

A.1 Permeability

A.1.1 Experimental

Figure A.1 shows the flow sheet of the system used for permeability measurements. This system was fully automated with valve actuators and pressure controllers, and the process was operated from a computer. The system was mounted in a temperature controlled insulated cabinet. There was a high-pressure tank on the feed side, and a low-pressure tank on the permeate side; each tank had a volume of 1 dm^3. MKS Instrument pressure transducers were connected to each tank. The membrane cell can easily be disconnected from the apparatus for cleaning or change of membrane.
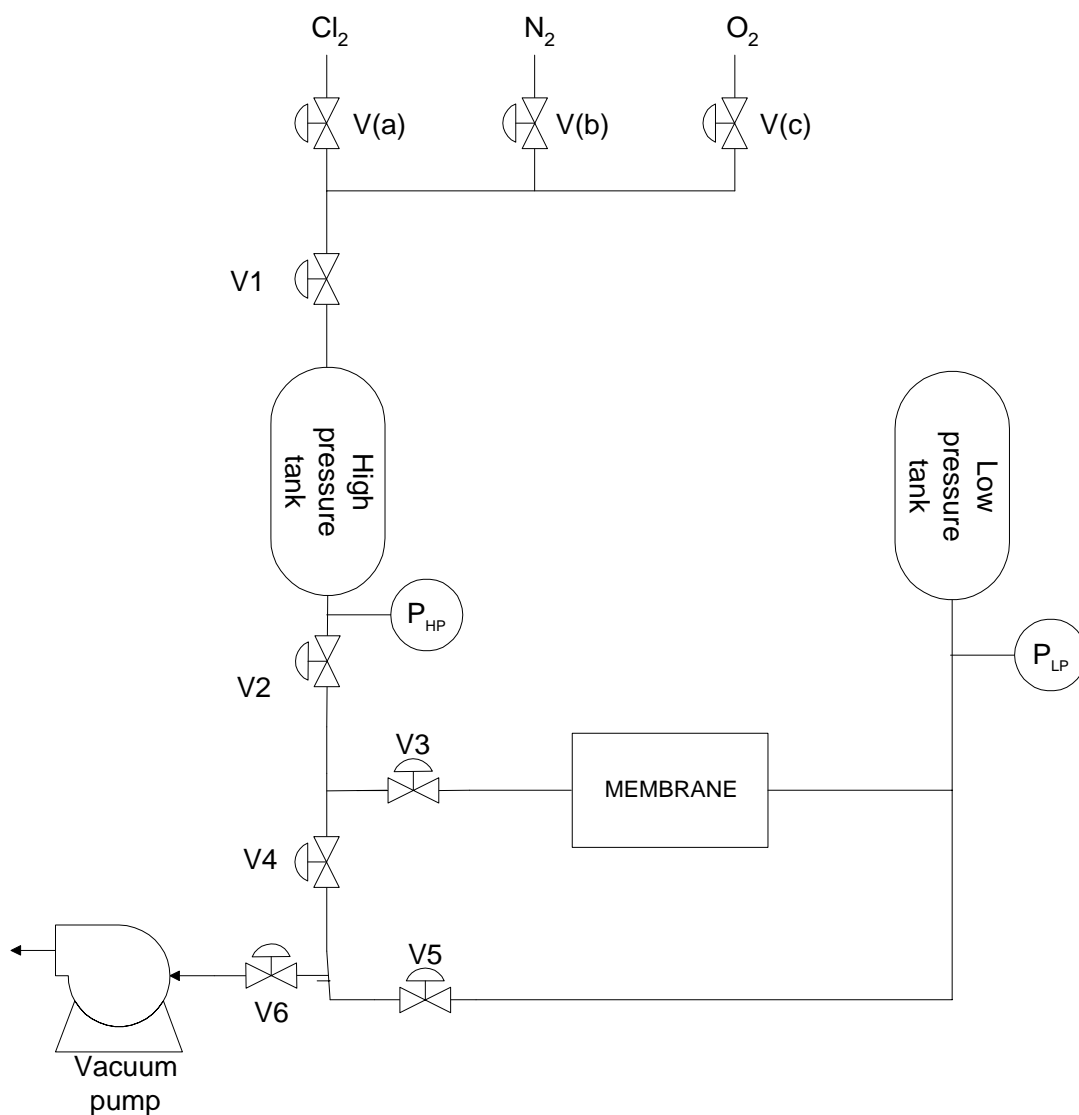
Figure A.1: Flow sheet of the set-up for permeability measurement.

When the measurement is started a pressure difference exists over the membrane, and the increase in pressure at the low-pressure side is measured as a function of time (dp/dt). The permeability coefficient (P/l in $(m^3 (STP)/m^2$ bar h) is then calculated in a MatLab program with given temperature and membrane area. Example plot of a logging is as given in Figure A.2.

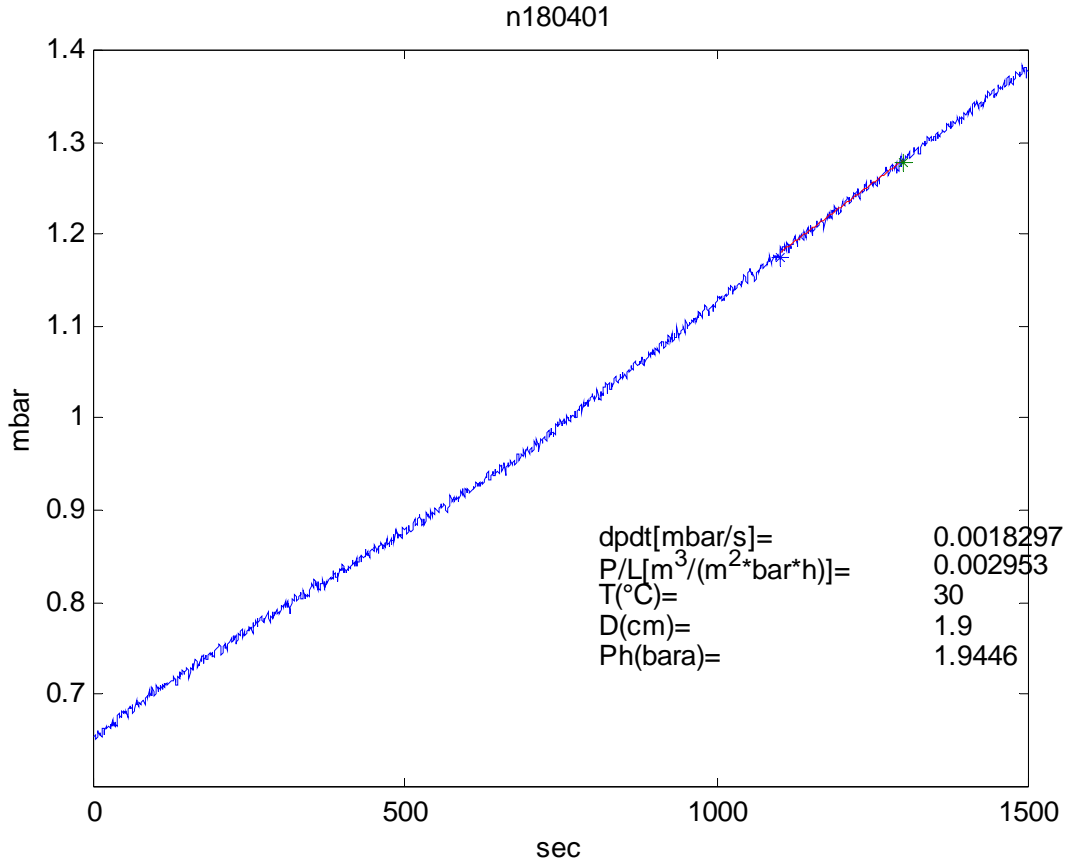*Figure A.2:Example of permeability measurement plotted as permeate pressure vs. time and calculated P/l by MatLab.*

A.1.2 Calculation of the permeability flux (P/l) from dp/dt [bar/h]

The high-pressure tank on the feed side and the low-pressure tank on the permeate side, have both a volume of 1 dm^3. The volume of the tubes between pressure tanks and the volume of the membrane cell is neglected related to the pressure tanks itself. It is assumed that steady state permeation is achieved if constant gas pressure p_h (the high pressure side) and p_l (the low pressure side) are maintained at the membrane interface, and the driving force for the transport $\Delta p = p_h - p_l$ through the membrane is constant, (i.e. p_h=2 bara, p_l=0.8·10^{-3} bara (vacuum) give $\Delta p \approx 2$ bara). The temperature is constant inside the cabinet and measured by a temperature transducer. The temperature can be read on a panel outside the cabinet. Figure A.3 gives a sketch of the permeability experiment.
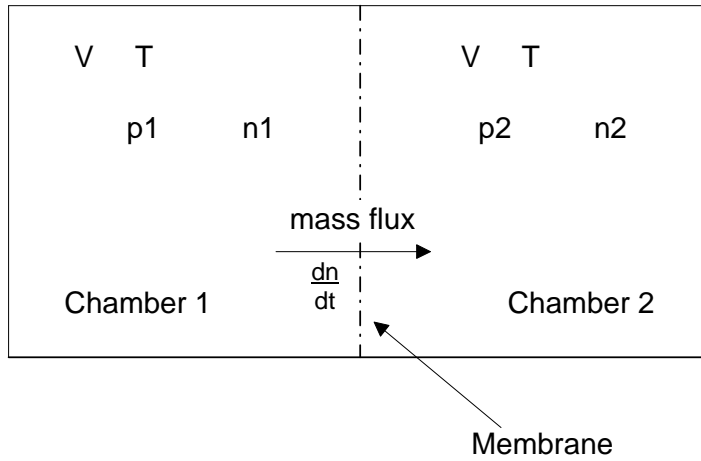
Figure A.3: Principal sketch of a membrane cell

Both chamber 1 (high pressure side) and chamber 2 (low pressure side) have a relatively low pressure ($p_1 > p_2$), and only simple diatomic non-polar gases are used, so the ideal gas law is a good description of the system.

$$pV = nRT \qquad (A.1.1)$$

where:

p = pressure [Pa]
V = volume [m^3]
n = mol [mole]
R = gas constant [J /(K mole)]
T = temperature [K]

When ideal gas law is used for chamber 2, with constant T and V, the mole change in chamber 2 is given as:

$$\frac{dn_2}{dt} = \frac{V}{RT}\frac{dp_2}{dt} \qquad (A.1.2)$$

In permeability measurements it is common to convert the mole change to a gas volume at standard pressure and temperature;

where :
p_0= 1.01325 bar is standard pressure
T_0 =273.15 K is standard temperature.

Ideal gas law is used to give this relation;

$$\frac{dV_{0,2}(n_2)}{dt} = \frac{T_0 R}{p_0}\frac{dn_2}{dt} \qquad (A.1.3)$$

where the subscript 0 indicates standard pressure and temperature conditions.

The flux describes a mass flow through a given permeation area A:

$$J = \frac{dV_{0,2}(n)}{dt}\frac{1}{A} \qquad (A.1.4)$$

where:

$$A = \frac{\pi\, D^2}{4 \cdot 10^{-4}}, \quad D = \text{diameter of the membrane} \tag{A.1.5}$$

Since the flux is generally given by:

$$J_i = \frac{P_i\,(p_h - p_l)}{l} = \frac{P_i}{l}\Delta p \tag{A.1.6}$$

The relationship between the flux J, and the permeability coefficient P_i/l is given by:

$$\frac{P_i}{l} = \frac{J}{p_1 - p_2} \tag{A.1.7}$$

Combining equation A.1.2, A.1.3, A.1.4, and A.1.7 gives the relation between the pressure change dp/dt and the permeability coefficient P/l [m^3(STP)/(m^2 Pa h)]:

$$\frac{P}{l} = \frac{1}{A}\frac{VT_0}{Tp_0(p_1 - p_2)}\frac{dp_2}{dt} \tag{A.1.8}$$

A.1.3 Accuracy of measurements

For the permeability measurements two pressure transducers (MKS Instrument type 626A) were used at low-pressure side; one from 0-10 mbar and one from 10-100 mbar. The error of both transducers is 0.25 % (of the measured value). At the high-pressure side a MKS Instrument pressure transducer (range 5000 mbar) with error of 0.5 % was used. Any effect of variations in temperature is estimated to be only 0.3 % based on given accuracy for the temperature controller.

The main error in calculated permeabilities is thus caused by variations in the thickness of the selective membrane layer and not by the system or permeation procedures. The numbers used in the permeation calculations presented in chapter 6 and appendix B is based on average thickness found by a digital micrometer or by Scanning Electron Microscope images. The thickness estimated has a relative uncertainty of ±5%.

When the permeation flux in a membrane is very low due to the thickness of the membrane, it was observed a change in the slope (figure A.2). The permeate side was generally evacuated to 0.5-0.7 mbar. When running the experiment the increase in pressure at the permeate side was recorded. At approximately 0.9 -1 mbar the value of dp/dt changed increased a bit. The reason for this change in slope is most likely due to the pressure transducer and not the polymer All the results referred in table B.2.1 are taken from the upper slope, but the number indicated with an * in the tables in appendix B is from the lower slope and thus too low to compare to the other results. This observation was observed for all gases in Fluorel. These values are therefore left out in the figures.

A.2 Absorption

A.2.1 Experimental

A weighted sample of polymer was placed in the sample cell. The sample cell was mounted in an insulated temperature controlled cabinet equipped with MKS Instruments pressure transducer, Figure A.4. The volume of the sample cell and connected tubing had been carefully calibrated. The exact weight and density of the polymer sample were measured before it was placed into the sorption chamber. The system was evacuated before the absorption measurements started. The time of the evacuation may differ from polymer to polymer, depending on whether it is in its glassy or rubbery state and the production method of the membrane (solvent left in the polymer matrix). The evacuation time was recommend to be at least two times the sorption time (and minimum 12 hours).

After evacuation valve V5 was closed. The system was filled with gas and all valves were closed. The pressure in the reference volume (volume between V4 and V5) had to be high enough to obtain wanted pressure in the sample cell when opening V5 (e.g. 1.66 bar in the reference volume will give 1 bar in the absorption cell when opening V5). LabView logged the pressure before and after V5 was opened. The measurement was running until the pressure gradient in the sorption cell was zero ($dp/dt = 0$). Absorption equilibrium is reached for gas saturation in the polymer sample. The sorbed volume of gas in the polymer sample is calculated from the reduction in pressure (mbar), and given either as solubility coefficient, S [cm^3(STP)/(cm^3 bar)], or as sorption level, C [(g gas)/(100 g sample)]. The analysis of the data (logged by LabView) was done with a MatLab program. The pressure at the start and the end of each measurement were recorded and the sorption was calculated.

A.2.2 Calculation of the solubility coefficient, S, from dp/dt [bar/h]

The start pressure is calculated from the initial pressure in the system using the ideal gas law, where temperature and mole gas gas is constant.

$$P_1V_1 = P_2V_2 \qquad (A.2.1)$$

Consider the volume between valve V4 and V5 as volume V_1, and the total volume when V5 is opened as V_2. The pressure P_1 is related to V_1, which is calculated to achieve a wanted pressure in the total volume (usually $P_1 \approx 1.7$ bar to achieve $P_2 \approx 1$ bar in the absorption cell for PDMS, this may vary with the polymer mass and density). Opening V5 give will cause the mass in V_1 to be distributed into V_2. The volume of the polymer is determined from the weight and density of the polymer. So the starting pressure in the absorption cell will be:

$$P_{start} = \frac{P_1\,V_1}{total\ volume - volume\ polymer} \qquad (A.2.2)$$
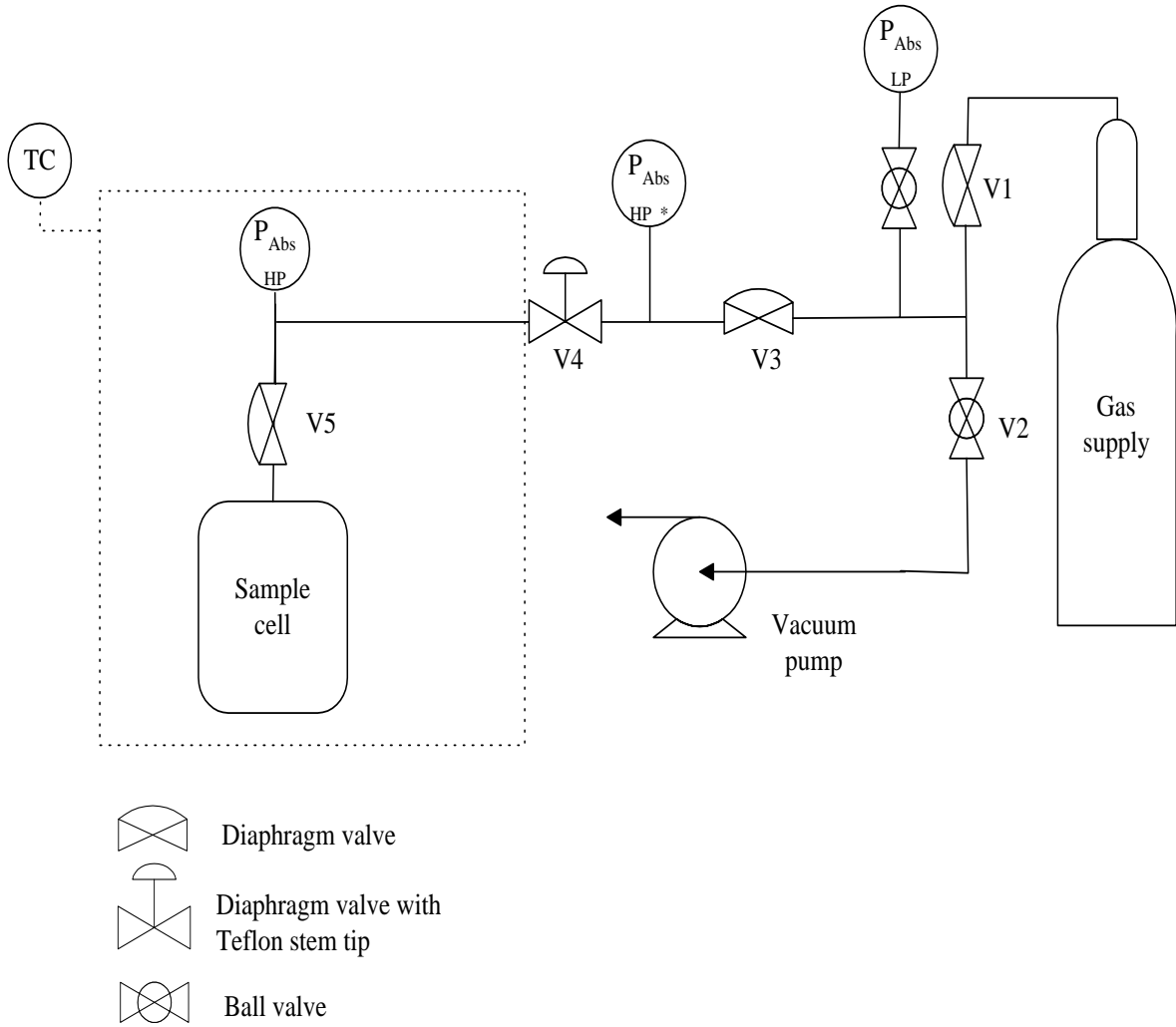
Figure A.4: : The flow sheet of the absorption system. The dotted line indicates the temperature-regulated closet.

The sorption (S) is calculated from equation A.2.3 with the unit [cm^3(STP)/ (cm^3(polymer) bar)]

$$S = \frac{(P_{start} - P_{end})\ total\ volume\ T_o}{volume\ polymer\ T\ P_{end}\ P_o}$$

(A.2.3)

where:

P_{end} is found from the sorption curve (figure A.5)

T is the temperature in Kelvin

and P_o and T_o is standard pressure and temperature respectively

Calculating the sorption to g (gas)/100 g polymer

$$S* = S\ \frac{\rho_{gas} T_{ref}\ 0.1\ P_{end}}{\rho_{polymer}\ T_o}$$

(A.2.4)

where:

ρ_{gas} is the density of the gas in [g/cm^3]

$\rho_{polymer}$ is the density of the polymers in [g/cm^3]

T_{ref} is the temperature for the given gas density

S^* is the sorption in g (gas)/100g (polymer)

The volume of the gas must be corrected by the compressibility factor, Z, for gases like Cl_2 and HCl. In this work only the first viral coefficient is used

$$Z^0 = 1 + B^0 \frac{P_r}{T_r} \tag{A.2.5}$$

where

$$B^0 = 0.083 - \frac{0.422}{T_r^{1.6}} \tag{A.2.6}$$

$$P_r = \frac{P}{P_{crit}} \tag{A.2.7}$$

$$T_r = \frac{T}{T_{crit}} \tag{A.2.8}$$

A.2.3 Accuracy of measurements

The absorption equipment used a MKS pressure transducer (range 5000 mbar) with accuracy of 0.5 % (relative to the measured value). The temperature regulator have a stability of $\pm 1°C$. The weight has a precision of ± 0.00005 g and is negligible related to other measurement errors. The density measurement with a pycnometer was done until two or three successive measurements gave an error of 0.2% or less.

For absorption measurements errors in the registered data will mainly be caused by: possible inaccuracy in volume estimation for tubes and sorption chambers in the experimental set-up (estimated to $\pm 2\%$). The system is very sensible even to small temperature changes.

Appendix B: Results presented in Table Form

This appendix gives a summery in table form of the results presented in chapter 6 as curves. In addition illustrations of the sorption curves for Cl_2 in Fluorel and Fluorosilicone are also given.

B.1 Poly(dimethylsiloxane) (PDMS)

B.1.1 Permeability and selectivity of N_2, O_2 and Cl_2 in PDMS

Table B.1.1: Permeability and selectivity of N_2, O_2 and Cl_2 in highly crosslinked PDMS (membrane A) at 30°C. Thickness: 7μm. Upstream pressure 2 bara, downstream pressure 0.6 mbar.

Time [days]	Permeability $\cdot 10^6$ [m^3(STP)m/($m^2 \cdot h \cdot bar$)]			Selectivity	
	N_2	O_2	Cl_2	O_2/N_2	Cl_2/O_2
0	0.615	1.26	19.7	2.05	15. 7
1			10.6		
3			9.10		
7			5.73		
8	0.0868	0.202	4.37	2.33	21.6
9			3.04		
13			2.70		
15			2.72		
16	0.0551	0.128	2.29	2.330	17.9
19			1.95		
21			1.81		
23			1.94		
24	0.0397	0.0952	1.34	2.40	14.0
25			1.23		
27			1.16		
31			1.15		
32	0.0227	0.0630	1.02	2.78	16.11
33			0.840		
36			0.721		
38			0.672		
39	0.0235	0.0501	0.628	2.14	12.5
40			0.611		
42			0.614		
46			0.466		
47	0.0211	0.0443		2.10	

Table B.1.2: Permeability flux and selectivity of N_2, O_2 and Cl_2 in highly crosslinked PDMS (membrane B) at 30°C. Thickness <1μm. Temperature 30°C. Upstream pressure 2 bara, downstream pressure 0.6 mbar.

Time [days]	Temp. [°C]	Permeability flux $\cdot 10^3$ [m^3(STP) /(m^2 h bar)]			Selectivity	
		N_2	O_2	Cl_2	O_2/N_2	Cl_2/O_2
0	30	63.5	129	2270	2.03	17.6
21	30	1.49	3.95	101	2.65	25.6
27	30			33.3		
28	30	0.407	1.33	28.8	3.27	21.7
34	30			13.4		
35	30	0.201	0.826	10.7	4.11	13.0
41	30			5.81		
42	30	0.118	0.428		3.61	

Table B.1.3: Permebility flux and selectivity of N_2, O_2 and Cl_2 in highly crosslinked PDMS (membrane B) at 60°C. Thickness <1μm. Temperature 30°C. Upstream pressure 2 bara, downstream pressure 0.6 mbar.

Time [days]	Temp. [°C]	Permeability flux $\cdot 10^3$ [m^3(STP) /(m^2 h bar)]			Selectivity	
		N_2	O_2	Cl_2	O_2/N_2	Cl_2/O_2
43	60			9.90		
44	60			4.73		
47	60			2.43		
50	60			1.96		
51	30			1.42		
51	30	0.103	0.270		2.62	

Table B.1.4: Permeability flux and selectivity of N_2, O_2 and Cl_2 in highly crosslinked PDMS (membrane B) at 80°C. Thickness <1μm. Temperature 30°C. Upstream pressure 2 bara, downstream pressure 0.6 mbar.

Time [days]	Temp. [°C]	Permeability flux $\cdot 10^3$ [m^3(STP) /(m^2 h bar)]			Selectivity	
		N_2	O_2	Cl_2	O_2/N_2	Cl_2/O_2
52	80			2.33		
55	80			1.11		
57	80			0.874		
58	80			0.492		

Table B.1.5: Permeability flux and selectivity of N_2, O_2 and Cl_2 in highly crosslinked PDMS (membrane B) at 100°C. Thickness <1μm. Temperature 30°C. Upstream pressure 2 bara, downstream pressure 0.6 mbar.

Time [days]	Temp. [°C]	Permeability flux $\cdot 10^3$ [m^3(STP) /(m^2 h bar)]			Selectivity	
		N_2	O_2	Cl_2	O_2/N_2	Cl_2/O_2
59	100			0.258		
66	100			0.0999		
63	100			1.75		

B.1.2 Permeability and selectivity of N_2 O_2 and HCl in PDMS

Table B.1.6: Permeability of HCl in PDMS as function of pressure. Temperature=25°C. Thickness: 2μm.

Pressure [bar]	Permeability $\cdot 10^5$ [m^3(STP)m/(m^2 h bar)]
	HCl
6	2.53
1	5.03
2	5.26
3	5.10
4	4.74
5	4.74
6	7.89

B.1.3 Swelling

The following protocol was thus adapted for swelling tests [4]:
1. Weigh the membrane (initial dry weight on manufacture)
2. Swell the membrane (subjected to soxhlet extraction using cyclohexane for 12 hours, weigh swollen)(on manufacture)
3. Dry the membrane at 70°C for 12 hours (weigh dry, difference in weight 1-3 reflects loss of starting materials)
4. Weigh the membrane (initial dry weight during chlorination)
5. Expose the sample to chlorine gas
6. Dry the membrane at 70°C for 12 hours (weigh dry, difference in weight 4-5 reflects loss of starting materials)
7. Weigh the membrane (initial dry weight after chlorination)
8. Swell the membrane (subjected to soxhlet extraction using cyclohexane for 12 hours, weigh swollen)(after chlorination)
9. Dry the membrane at 70°C for 12 hours (weigh dry, difference in weight 7-9 reflects loss of starting materials)

Table B.1.7: Absolute and relative weights of the membranes. Swelling performed with cyclohexane.

Sample id.	Initial dry mass [g]	Swollen mass [g]	Dry mass after heating [g]	wt loss [g]
On manufacture				
High crosslinking (H)	1.1433	1.6093	0.9609	0.1824
Medium crosslinking (M)	1.2502	1.9621	0.9739	0.2736
Low crosslinking (L)	1.1815	1.6543	0.8875	0.294
During chlorination				
High crosslinking (H)	1.0458		1.2340	-0.1882
Medium crosslinking (M)	1.0399		1.4625	-0.4226
Low crosslinking (L)	1.0463		1.1851	-0.1388
Swelling tests after chlorination				
High crosslinking (H)	1.2404	1.8990	1.2236	0.0168
Medium crosslinking (M)	1.4680	1.9419	1.4089	0.0591
Low crosslinking (L)	1.1884	1.9691	1.1692	0.0192

Table B.1.8: Degree of swelling due to cyclohexane before and after chlorine exposure in PDMS membrane.

	Swell % before Cl_2 exposure	Swell % after Cl_2 exposure
High crosslinking (H)	167.5	155.2
Medium crosslinking (M)	201.5	137.8
Low crosslinking (L)	186.4	168.4

Table B.1.9: Relative dry weight loss before and after Cl_2 exposure.

	Rel. wt. loss % due to swelling of cyclohexane before Cl_2 exposure	Rel. wt. loss % Cl_2 exposure	Rel. wt. loss % due to swelling of cyclohexane after Cl_2 exposure
High crosslinking (H)	15.95	-18.00	1.354
Medium crosslinking (M)	22.10	-40.64	4.026
Low crosslinking (L)	24.88	-73.48	1.616

B.2 Fluorel

B.2.1 Permeability and selectivity of N₂, O₂ and Cl₂ in Fluorel

Table B.2.1: Permeability and selectivity of N₂, O₂ and Cl₂ in Fluorel at 30°C. Thickness: 43 μm. Upstream pressure 2 bara, downstream pressure 0.6 mbar.

Time [days]	Permeability $\cdot 10^9$ $[m^3(STP)m/(m^2 h \, bar)]$			Selectivity	
	N_2	O_2	Cl_2	O_2/N_2	Cl_2/O_2
0	124	128	154	1.03	1.20
13	28.2	45.2	112	1.60	2.48
20	27.5	45.5	110	1.65	2.42
24	21.1[*]	47.2	114	2.23	2.41
36	22.3	32.2[*]	120	1.44	3.74
47	82.5	99.4	175	1.20	1.76
49	135.	252	605	1.86	2.40
57	7920	16920	17250	2.14	1.02

[*] These values are to low as a result of the permeability measurement time was too short to receive the change in the slope. See comment in the appendix A.1.1

B.2.2 Permeability and selectivity of N₂, O₂ and HCl in Fluorel

Table B.2.2: Permeability and selectivity of N₂, O₂ and HCl in Fluorel at 30°C. Thickness: 80 μm. Upstream pressure 2 bara, downstream pressure 0.6 mbar.

Time [days]	Permeability $\cdot 10^9$ $[m^3(STP)m/(m^2 h \, bar)]$			Selectivity	
	N_2	O_2	HCl	O_2/N_2	O_2/HCl
0	427.7	392.4		0.92	
1			35.90		11
2	402.9	375.3		0.93	
3			189.2		2.0
4	353.2	323.4		0.92	
5			246.8		1.3
6	354.3	332.5		0.94	
7			284.5		1.2
8	389.8	321.6		0.82	
9		232.1			1.4
10			255.4		
11	384.8	322.4		0.84	
12			250.4		1.3

Table B.2.3: Solubility coefficients in Fluorel. Pressure 1 bara.

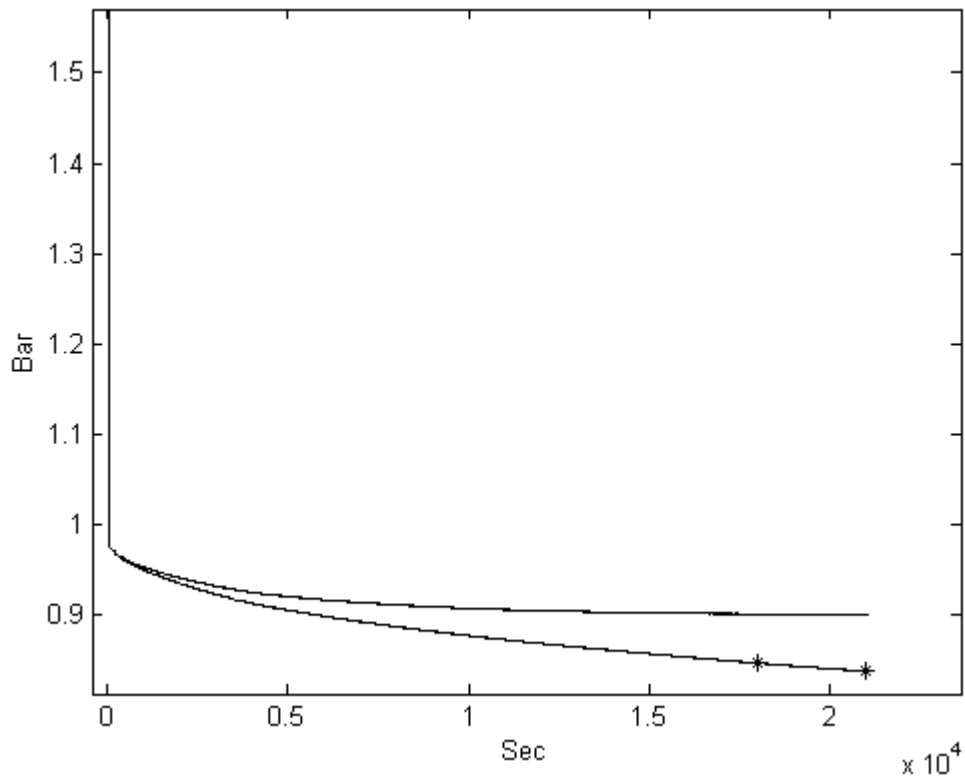| Exposure Temp. [°C]	Solubility coefficient, S [cm^3(STP) /(cm^3·bar)]		
	N$_2$	O$_2$	Cl$_2$
30	0.27	0.30	2.2
35	0.26	0.30	0.90
35	0.31	0.34	6.2
50	0.24	0.31	4.3
65	0.21	0.25	5.3
65	0.39	0.45	3.5
80	0.44	0.51	3.7

Figure B.2.1: Sample curve: sorption isotherm for Cl$_2$ gas in Fluorel at 30°C, measured as Δp (bar) as function of time. Linearisation between 18000-21000 sec

B.3 Fluorosilicone

B.3.1 Permeability and selectivity of N_2, O_2 and Cl_2 in Fluorosilicone

Table B.3.1: Permeability and selectivity of N_2, O_2 and Cl_2 in Fluorosilicone at 30°C. Thickness: 59 μm. Upstream pressure 2 bara, downstream pressure 0.6 mbar.

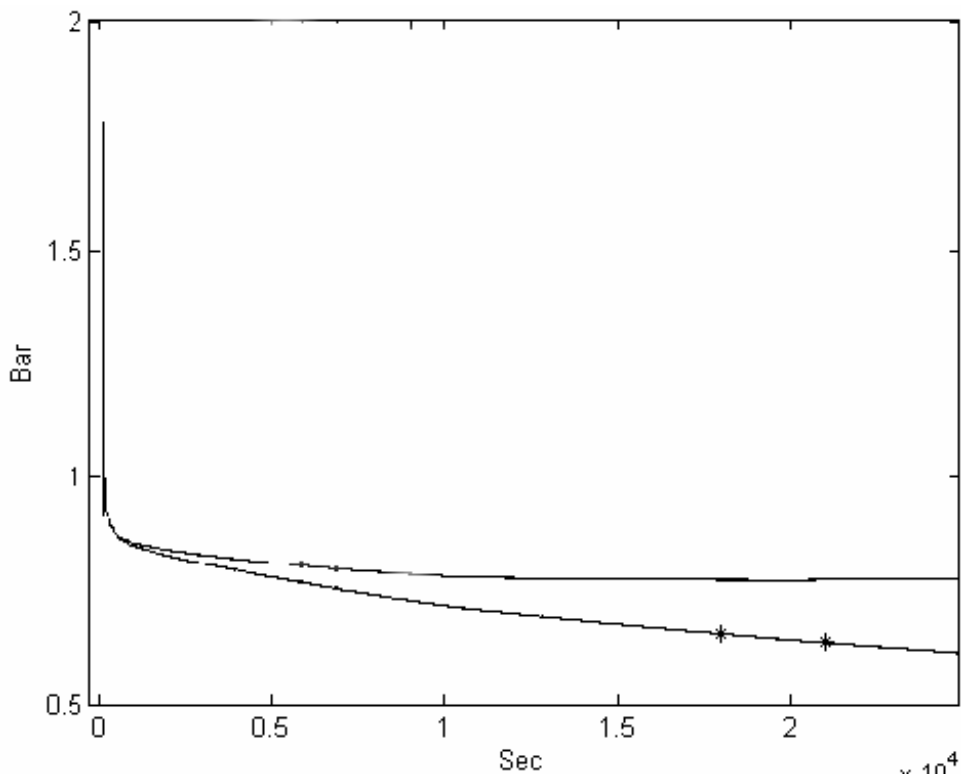| Time [days]	Permeability $\cdot 10^6$ $[m^3(STP)m/(m^2\,h\,bar)]$			Selectivity	
	N_2	O_2	Cl_2	O_2/N_2	Cl_2/O_2
0	1.58	2.17	24.9	1.37	11.5
4	1.19	1.70	15.4	1.42	9.05
11	1.04	1.48	13.3	1.42	9.03
13	23.4	33.3	30.7	1.42	0.920
18	1333	1335	-	1.00	

Figure B.3.1: Sample curve: sorption isotherm for Cl_2 gas in Fluorosilicone C at 30°C, measured as Δp (bar) as function of time. Linearisation between 18000-21000 sec

Appendix C: Analytical Methods

Summery

This appendix will give a brief discussion about the analytical methods used in the thesis. The methods will be presented in alphabetic order starting with Fourier Transform Infrared spectroscopy, going through theories about the Nuclear Magnetic Resonance, the density measurements by the Pycnometer, and surface analysis with Scanning Electron Microscopy. Thermal behaviour is described in the last chapter called thermal analysis. The section will give a short introduction to the principles about each analysis method. For a complementary study of each instrumental technique the interested reader is recommend going in the comprehensive literature in this field.

C.1 Infrared Spectroscopy

C.1.1 Introduction

The infrared region of the spectrum encompasses radiation with wavenumbers ranging from 12800 to 10 cm^{-1}. The infrared spectrum is conveniently divided into near-, mid-, and far-infrared radiation, with rough limits of each are shown in table C.1.1 [1].

Table C.1.1: Infrared Spectral Regions [1].

Region	Wavelenght (λ) Range, μm	Wavenumber ($\bar{v}$) Range, cm^{-1}	Frequency (v) Range, Hz
Near	0.78 to 2.5	12800 to 4000	$3.8 \cdot 10^{14}$ to $1.2 \cdot 10^{14}$
Middle	2.5 to 50	4000 to 200	$1.2 \cdot 10^{14}$ to $6.0 \cdot 10^{12}$
Far	50 to 1000	200 to 10	$6.0 \cdot 10^{12}$ to $3.0 \cdot 10^{11}$
Most used	2.5 to 15	4000 to 670	$1.2 \cdot 10^{14}$ to $2.0 \cdot 10^{13}$

Infrared spectroscopy finds widespread application in quantitative and qualitative analyses. Its most important use has been for identification of organic compounds whose mid infrared spectra are generally complex and provide numerous maxima and minima that are useful for comparison purpose. The mid-infrared spectrum of an organic compound provides a unique fingerprint, which is readily distinguished from the absorption patterns of all compounds. Infrared spectroscopy is probably the method most extensively used for the investigation of polymer structure and the analysis of functional groups [1].

C.1.2 Theory

When infrared light is absorbed through a sample some of the frequencies are absorbed while other frequencies are transmitted. The transitions involved in infrared absorption are associated to molecular species for which small energy differences exist between various vibrational and rotational states. In order to absorb infrared radiation a molecule must undergo a net change in dipole moment as a consequence of its vibrational and rotational motion. Only under these circumstances can the altering electrical field of the radiation interact with the molecule and cause changes in the amplitude of one of its motions [1].

Different bonds present in the compound have different vibrational frequencies. The presence of these bonds in compounds can be detected by identifying characteristic frequencies as absorption bands in the infrared spectrum.

There are two general types of molecular vibration [2]:
- Stretching vibration is a rhythmical movement along the bond axis such as the interatomic distances increases or decreases.
- Bending vibration may consist of (a) a change in the bond angles between bonds with a common atom, or (b) movement of a group of atoms with respect to the reminder of the molecule without movement of the atoms in the group with respect to one another.

A molecule of n atoms has 3n vibrational degrees of freedom: three of the degrees of freedom describe rotation and three describe translation; the remaining 3n-6 degrees of freedom are vibrational degrees of freedom of fundamental vibrations [2]. The 3n-6 rule does not apply for linear molecules, because by definition, all of the atoms lie on a single, straight line. Rotation about the bond axis is not possible, and two degrees of freedom suffice to describe rotational motion. Thus the number of vibrations for linear molecule is given by 3n-5 [1].

C.1.3 Instrument

Fourier Transform (FT) infrared spectroscopy is a technique, which uses an interferometer (instead of a monochromator) e.g. a Michelson interferometer (figure C.1.1). The interferometer consists of two plane mirrors at a right angle to each other and a beam splitter at an angle of 45° to the mirrors. One mirror is fixed in a stationary position and the other can be moved in a direction perpendicular to its front surface at a constant velocity [2].

The beam splitter divides the incoming light from the source: 50 % is transmitted to the moving mirror which reflects the beam back to the beam splitter which then reflects part of this beam through a sample to a detector. The other half of the beam from the source is reflected from the beam splitter to a fixed mirror, which reflects the beam through the beam to the detector via the sample [3]. A compensator is placed in one arm of the interferometer to equalise the optical path lengths in both arms [2].
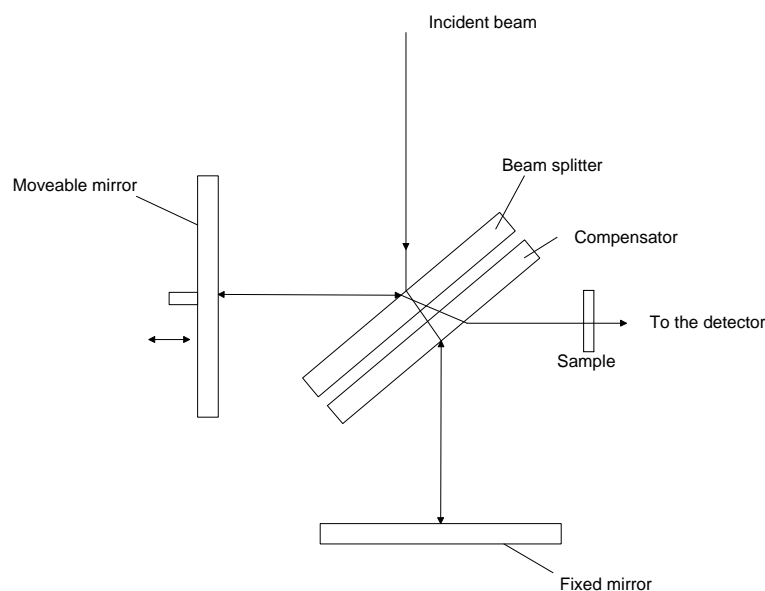

Figure C.1.1: Diagram of the Michelson Interferometer [2].

When the position of the moving mirror produces two beams travelling equal distances and falling on the detector, the detector should obtain a strong signal. When the moving mirror is scanned through a distance each side of the central position corresponding to zero path distance the detector registers an interference pattern. Michelson realised that this interference pattern contained spectral information.

The development of the technique for recording an interference pattern by scanning the moving mirror through a distance of x/2 produces a total path difference of x. The resultant interference is shown in figure C.1.2, for (a) a source of monochromatic radiation and for (b) a source of polychromatic radiation. The former is a simple cosine function but the latter is of more complicated form because it contains all the spectral information of the radiation falling on the detector [3].
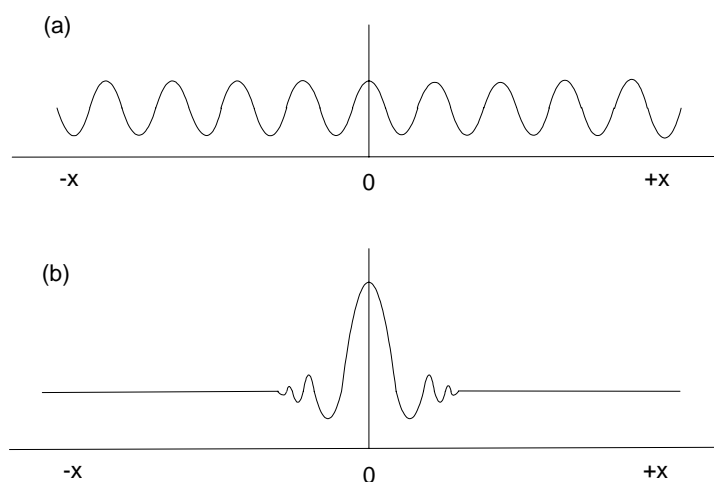
Figure C.1.2: Output of the Michelson interferometer as a function of mirror displacement (x) for: (a) a monochromatic source; (b) a broadband source. Zero refers to the mirror position for equal optical length in both arms of the interferometer [2].

The interferogram also contains information on the intensity of each frequency in the spectrum. The output information from the detector is digitalised in a computer and transformed to the frequency domain-each individual frequency is filtered out from the complex interferogram (Fourier transforms). Then the signals are converted into a conventional infrared spectrum. A block diagram of the FT-IR spectrometer is shown in figure C.1.3 [2].

An entire spectrum can be reordered, computerised, and transformed in a few seconds. (In normal infrared measurements, spectra require several minutes to be recorded).
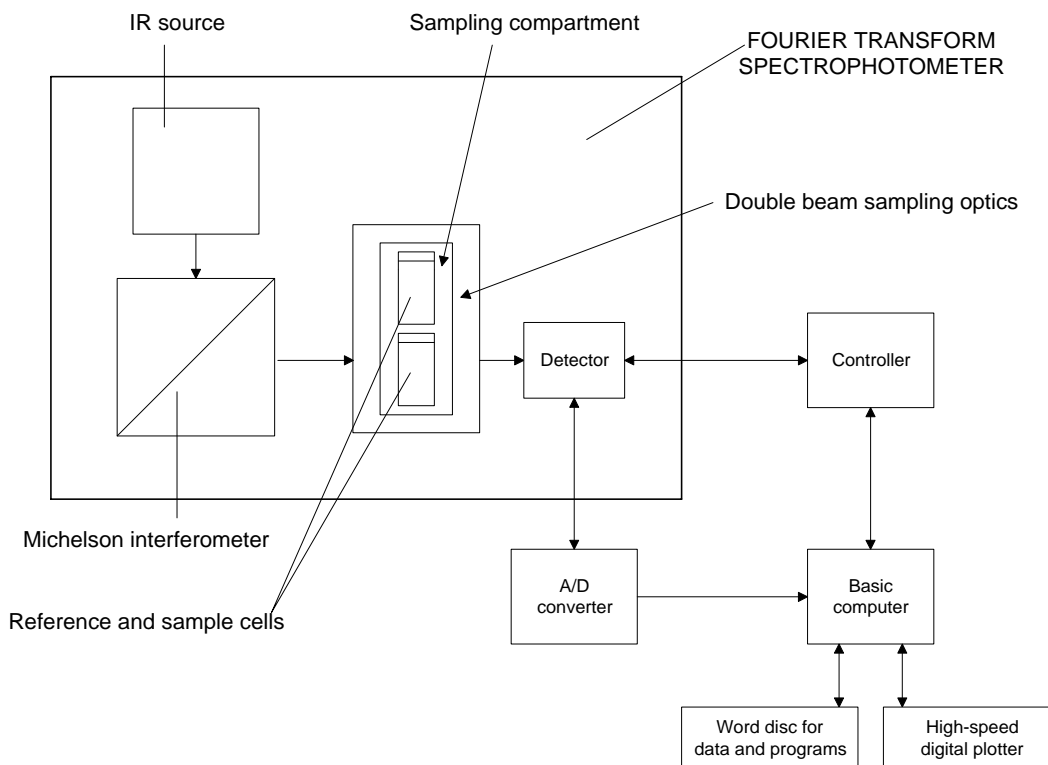
Figure C.1.3: Block diagram of the basic components of a FT infrared spectrometer [2].

C.1.4 Attenuated total reflectance

Internal reflection spectroscopy is a technique for obtaining infrared spectra of samples that are difficult to deal with, such as solids of limited solubility, films, threads, pastes adhesives and powders. When a beam of radiation passes from a denser to a less dense medium, reflection occurs. The fraction of the incident beam that is reflected increases as the angle of incidence becomes larger; beyond a certain critical angle, reflection is complete. It has been shown both theoretically and experimentally that during the reflection process the beam acts as if it penetrates a small distance into a less dense medium before reflection occurs. The depth of penetration, which varies from a fraction of a wavelength up to several wavelengths, depends upon the wavelength, the index of refraction of the two materials, and the angle of the beam with respect to the interface. The penetrating radiation is called the evanescent wave. If the less dense medium absorbs the evanescent radiation, attenuation of the beam occurs at wavelengths of absorption bands. This phenomenon is known as attenuated total reflectance (ATR) [1].

In attenuated total reflectance, an infrared beam enters a crystal made from a material that transmits infrared and that also has a high refractive index. Internal reflection of the beam within the material creates an evanescent wave. At each reflection, the wave continues beyond the crystal surface and into a sample that is held in close contact. The penetration depth of the beam is typically of the order of few microns, which means that materials that are to thick for transmittance measurements can be sampled with little preparation [4].

Figure C.1.4 shows a simplified optical diagram of horizontal ATR (HATR). In the diagram, the sampling surface is the top surface of the crystal. Infrared radiation from the sampling surface is the top surface of the crystal. Infrared radiation from the spectrometer is directed in

a beam to the beveled, input face of the ATR crystal. The beam then reflects through the crystal and, with each reflection along the top surface, passes a finite amount of radiation into the sample. At the output end of the crystal, the beam is directed down to a mirror and back into the usual beam path of the spectrometer.

By varying the angle of the bevels and the refractive index of the crystal material, you can change the total number of reflections through the crystal, the depth of penetration at each reflection, and the effective path length of the HATR. The most useful crystal for most applications is the 45° Zinc Selenide (ZnSe) crystal. There are 12 reflections at the crystal angle of 45° [4].
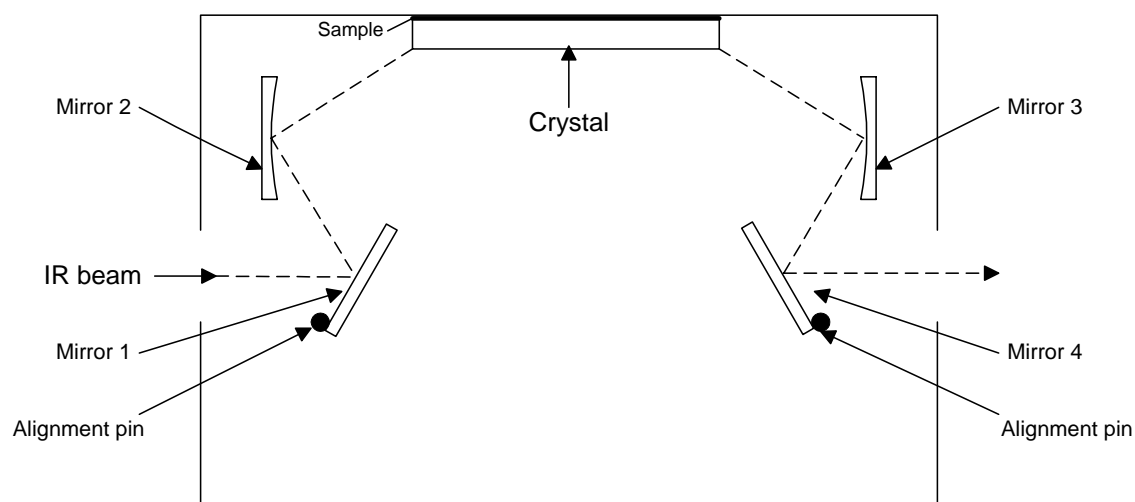

Figure C.1.4: The optical path of the HATR [4].

References

1. D. A. Skoog, J. J. Leary; Principles of Instrumental Analysis, 4th Ed., International Edition, Saunders College Publishing, USA 1992.
2. J. F. Rabek; Experimental Methods in Polymer Chemistry, (Chapter 15), John Wiley & Sons, Sweden 1980.
3. B. George, P. McIntyre; Infrared Spectroscopy, Analytical Chemistry by Open Learning, John Wiley & Sons, Great Britain 1987.
4. FT-IR spectroscopy, Horizontal ATR Accessory, user manual, Perkin Elmer, United Kingdom.

C.2 Nuclear Magnetic Resonance (NMR)

C.2.1 Introduction

Nuclear Magnetic Resonance (NMR) spectroscopy is a powerful method for elucidating chemical structures. The result is often delineation of complete sequences of groups of arrangements of atoms in the molecule. The sample is not destroyed in the process. NMR can also be used for a particular facet of a structure, such as chain length, and in the study of polymer motion by relaxation measurements. Kinetic studies of reactions at high temperatures in the range from -150 to 200°C are another application.

Integration of areas under the absorption peaks and the peak of the internal standard enables quantitative analysis to be performed [1].

NMR is a technique which records transition between the energy levels of magnetic nuclei in an external magnetic field. NMR spectroscopy involves absorption of the energy of electromagnetic radiation in the radio frequency region by a sample placed in an external magnetic field. Absorption is a function of the magnetic properties of some atomic nuclei in the molecule. A plot of the absorption of radio-frequency energy versus the external magnetic field gives a NMR spectrum [2].

C.2.2 Theory

Certain nuclei behave though they are spinning. Because nuclei are charged and a spinning charge creates a magnetic field, these spinning nuclei behave like tiny magnets. The most important nuclei of organic structure determination are ^{1}H (ordinary hydrogen) and ^{13}C a stable non-radioactive isotope of ordinary carbon. Although ^{12}C and ^{16}O are present in most organic compounds, they do not possess a spin and do not give NMR spectra. When nuclei with spin are placed between the poles of a powerful magnet, they align themselves with or against the field of the magnet. Nuclei aligned with the field have a slightly lower energy than those aligned against the field. By applying energy in radio frequency range, it is possible to excite nuclei in the lower energy state to the higher energy spin state. Figure C.2.1 [3].

The circulation of nuclear charge generates a magnetic dipole along the axis. The intrinsic magnitude of the generated dipole is expressed in terms of the nuclear magnetic moment (μ). The angular momentum of the spinning charge can be described in terms of the spin quantum numbers, I, with values 0, ½, 1, $^3/_2$, 2 etc.(I=0 denotes a nucleus with no spin).

Each proton and neutrons has a spin. I is the resultant of these spins. If both of the protons and neurones are even, I is zero and there is no NMR signal. Those nuclei having a nuclear spin of ½ have a uniform spherical charge distribution. Nuclei having nuclear spins greater than ½ have a non-spherical distribution that gives rise to nuclear quadrupole moment. Only nuclei with I = ½ will be considered here.

no applied field
(random orienation)

applied
field

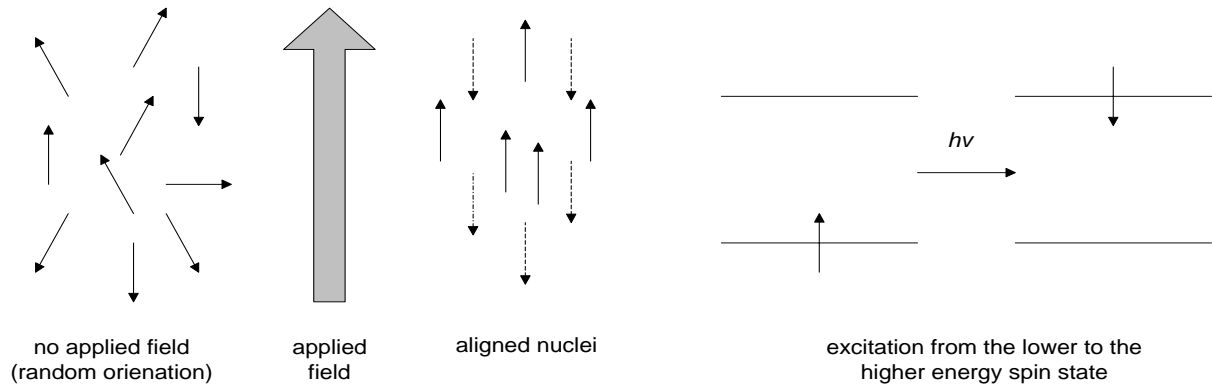aligned nuclei

excitation from the lower to the
higher energy spin state

Figure C.2.1: Orientation of nuclei in an applied field and excitation of nuclei from the lower to the higher energy spin state [3].
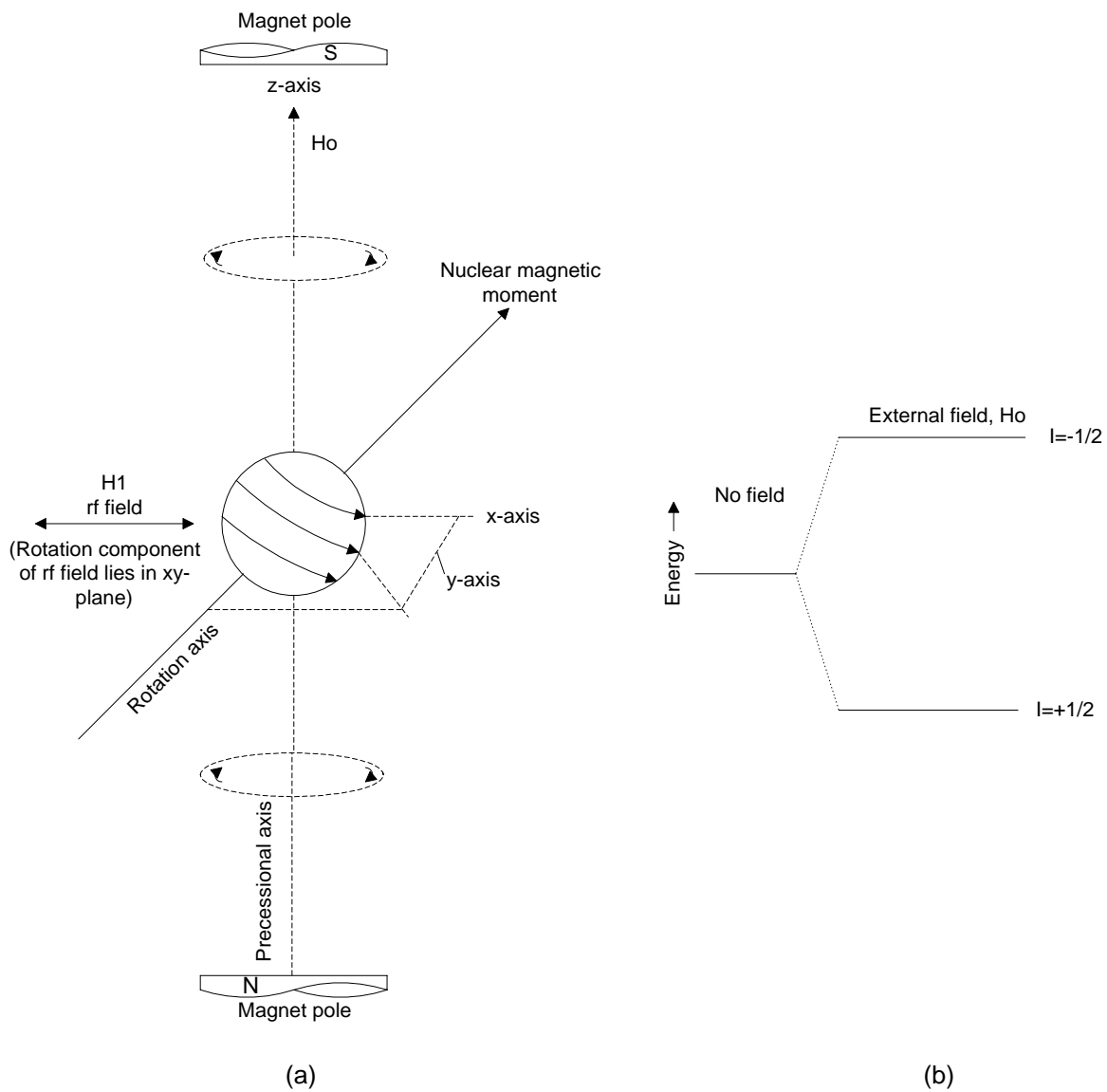

(a)

(b)

Figure C.2.2: (a) spinning nucleus in a magnetic field. (b) Energy-level diagram for a nucleus with a spin of 1/2 [1].

The spin quantum number I determine the number of orientation a nucleus may assume in an external uniform magnetic field in accordance with the formula 2I +1. For a spin I = ½ nuclei, there are two orientations in an applied uniform magnetic field: parallel with the aligned field (aligned with the field) or antiparallel (aligned against the field). The former is the lower energy state whereas the latter is the high-energy state (see figure C.2.2). Energy levels are a function of the magnitude of the nuclear magnetic moment, μ, and the strength of the applied external field; H_0. The energy difference between the upper and the lower energy state is in the radio frequency range. The transition between energy states of the nuclear spin is showed in figure C.2.2. Each magnetic nucleus will absorb a specific radio frequency and "flip" from the lower energy state to the upper energy state. After absorption of energy by the nuclei, they must have a mechanism whereby they can dissipate the energy and return to the lower energy state. There are two primary processes for relaxation to the lower energy state: (a) spin-lattice relaxation and (b) spin-spin or transverse relaxation. Spin-lattice relaxation, T_1, involves the transfer of energy from the nuclei to the environment of the molecular lattice. Spin-spin relaxation, T_2, arises from direct interactions between spins of different nuclei that can cause transverse relaxation without any energy transfer to the lattice. Its electron cloud shields the nucleus. Technique aspect of NMR is that the nuclei in different parts of the molecule will have different electronic environments depending on the nature of the bonding and other surrounding groups, which leads to differences in the in the field required to realign or "flip" the spin of the nuclei an consequently to different absorption frequencies. This is referred to as a chemical shift from a standard reference. Reference materials are materials that are chemically inert, magnetically isotropic, and dissolve in the same solvent as the compound to be analysed [4].
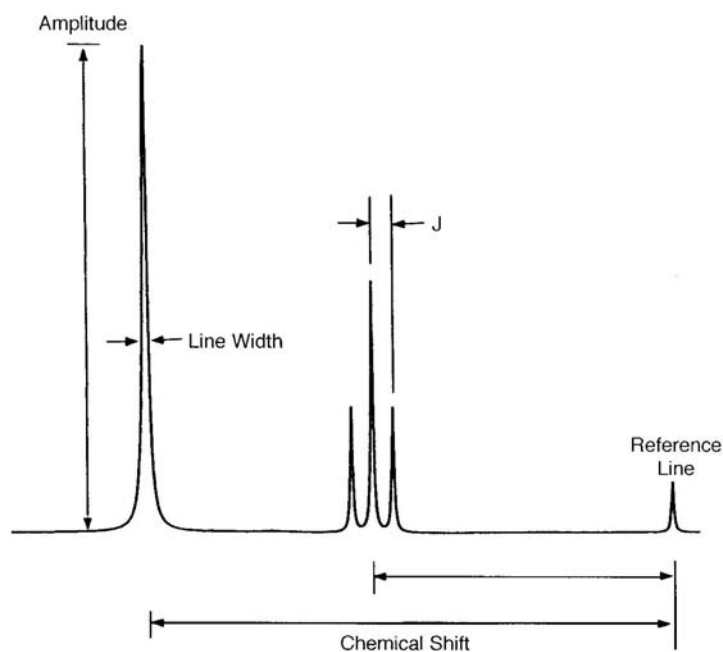

Figure C.2.3: representative NMR spectrum [4].

The NMR spectrum provides detailed information for polymer characterisation. Some significant parameters are frequency or chemical shift, intensity (or peak area) line width, J-coupling constants and relaxation rates (T_1 and T_2). The NMR spectrum is a series of absorption peaks representing nuclei in different chemical/electronic environments (figure C.2.3). Each absorption area is proportional to the number of nuclei it represents, which

provides considerable information about the molecule. However, there is another complication or refinement to structure determination that involves spin-spin coupling an indirect coupling of the nuclei spins through the intervening bonding electrons. Briefly, it occurs because there is some tendency for bonding electron to pair its spin with the spin of the nearest spin ½ nuclei: the spin of a bonding electron, having been thus influenced, the electron will affect the spin of the other bonding electron and so on through the next spin ½ nuclei. Coupling for protons is ordinarily not important beyond three bonds unless there is a bond delocalisation as in unsaturated or aromatic systems or ring strain as in small rings or bridged systems [4].

Instrumentation for NMR spectroscopy
NMR instrumentation involves these basic units [1]:

- A magnet to separate the nuclear spins energy states.
- (a) One radio frequency channel for field or frequency stabilisation, which produces stability for long-term operation.
- (b) One radio frequency channel to furnish irradiating energy to sample.
- (c) A third channel that may be added for decoupling nuclei.
- A sample probe that houses the sample and also coils for coupling the sample with the radio frequency transmitter and the phase sensitive detector. It is inserted between the pole faces of the magnet.
- A detector to collect and process the NMR signals.
- A sweep generator for sweeping the radio frequency field through the resonance frequencies of the sample. Alternatively, the magnetic field may be swept and the radio frequency field held constant.
- A recorder to display the spectrum.

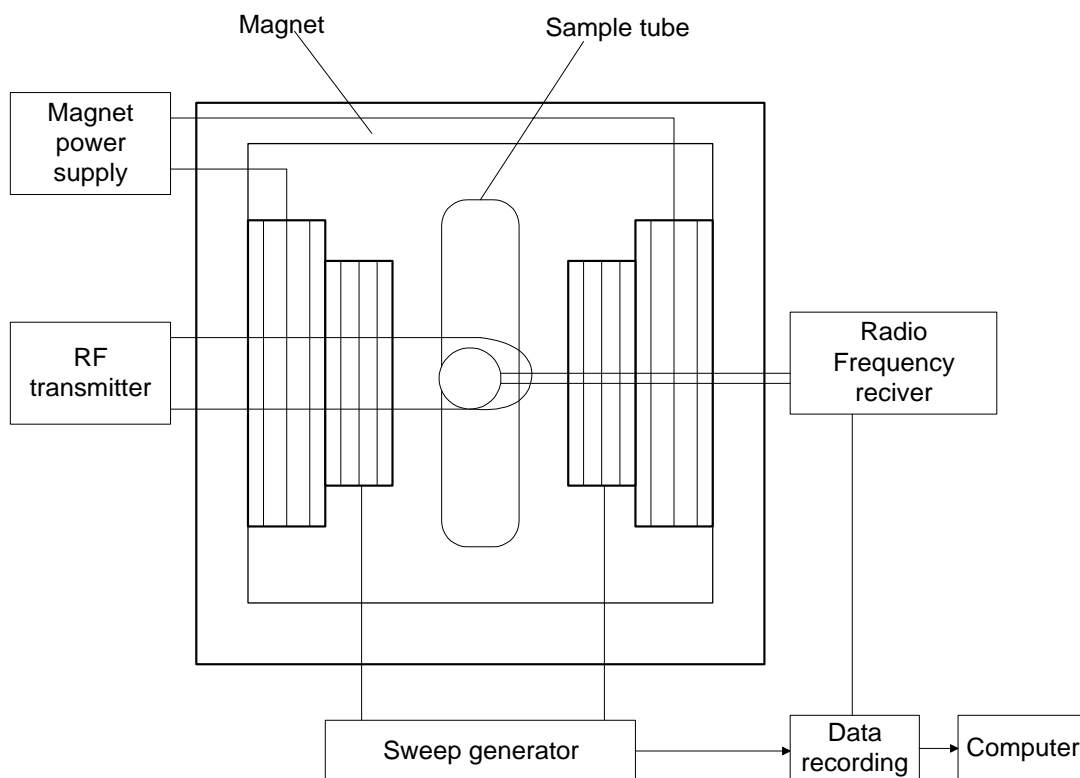Figure C.2.4 gives a schematic representation of a NMR spectrometer.

Figure C.2.4: A schematic diagram of a NMR spectrometer [1].

References

1. J. A. Dean; Analytic Chemistry Handbook, (Section 12), University of Tennessee, Knoxville, McGraw-Hill Inc., 1995.
2. J. F. Rabek; Experimental Methods in Polymer Chemistry, (Chapter 20), John Wiley & Sons, Sweden 1980.
3. H. Hart; Organic Chemistry; a short course, 8th Ed., Houghton Mifflin Company, USA 1991.
4. S. R Sandler, W. Karo, J-A. Bonesteel, E. M Pearce; Polymer Synthesis and Characterization, A laboratory Manual, Academic Press, USA 1988.

C.3 Pycnometer - Density Measurements

C.3.1 Introduction

The "Absolute Density" (ρ) is defined as:

$$\rho = m\,/V \qquad [kg/m^3] \tag{C.3.1}$$

where m is the mass of the sample [kg] and V is the unit volume of the sample [m^3].

The volume depends upon temperature and pressure and for that reason the temperature at which the density is measured is indicated in tables of physical data - usually in degrees Celsius [1].

C.3.2 Theory

The pycnometer is an instrument specifically designed to measure the true volume of various quantities of solid materials. The technique employs Archimedes principle of fluid displacement to determine the volume. The displaced fluid is gas, which can penetrate the finest pores to assure maximum accuracy. For this reason helium is recommended since it is small atomic dimensions assures penetration into crevices and pores approaching an Angstrom (10^{-10} m). Its behaviour as an ideal gas is also desirable. Other gases such as nitrogen can be used, often with no measurable difference. Figure C.3.1 is a flow diagram of the Pycknometer
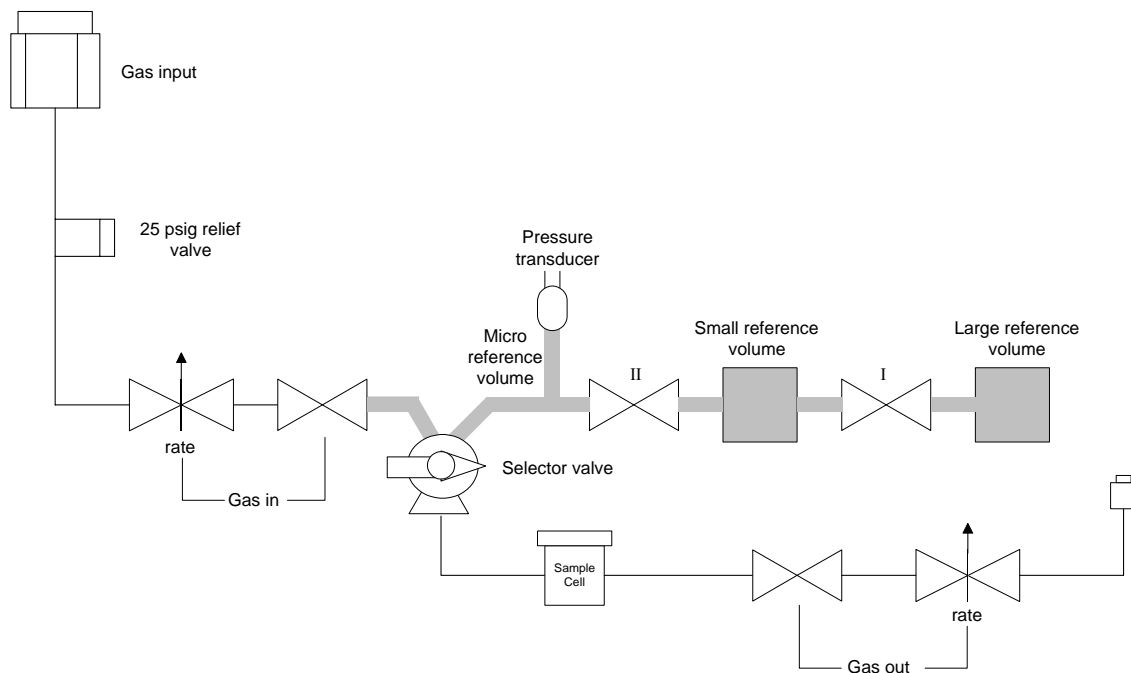

Figure C.3.1: Schematic diagram of the Pycnometer [2].

The pycnometer determines the true density of solid or powder samples by measuring the pressure difference when a known quantity of helium under pressure is allowed to flow from a precisely known reference volume (V_R) into a sample cell containing the solid or powered material.

The shaded area in figure C.3.1 represents the known reference volume V_R. After the system is purged with helium the selector valve is turned to in such a way that the system is open, the "GAS OUT" valve is opened and the "GAS IN" valve is closed. The system is now at ambient pressure P_a and the state of the sample cell with sample is defined by:

$$P_a \left(V_C - V_P \right) = n_a\, RT_a \qquad\qquad\qquad (C.3.2)$$

where n_a is the number of gas occupying the cell volume (V_a) including the powder volume (V_P), R is the gas constant and T_a is ambient temperature.

When the reference volume is pressurised (selector valve is closed) to approximately 17 psi (=1.17 bar) above ambient. The state of the reference volume (V_R) can be expressed as:

$$P_1 V_R = n_1\, RT_a \qquad\qquad\qquad (C.3.3)$$

where P_1 represents a pressure above ambient and n_1 is the total number of moles of gas in the reference volume (V_R).

When the selector valve is turned to connect the sample cell, the pressure will fall to a lower pressure P_2, given by:

$$P_2 \left(V_C - V_P + V_R \right) = n_a\, RT_a + n_1\, RT_a \qquad\qquad\qquad (C.3.4)$$

Substituting into equation C.3.4 $P_a(V_C-V_P)$ and $P_1 V_R$ for $n_a RT_a$ and $n_1 RT_1$, respectively, gives:

$$P_2 \left(V_C - V_P + V_R \right) = P_a \left(V_C - V_P \right) + P_1\, V_R \qquad\qquad\qquad (C.3.5)$$

or

$$(P_2 - P_a)(V_C - V_P) = (P_1 - P_2)\, V_R \qquad\qquad\qquad (C.3.6)$$

Then

$$(V_C - V_P) = \frac{(P_1 - P_2)}{(P_2 - P_a)} V_R \qquad\qquad\qquad (C.3.7)$$

Since P_a is made to read zero on the digital meter, that is, all pressure measurements are relative to P_a, equation C.3.7 becomes:

$$(V_C - V_P) = \frac{(P_1 - P_2)}{(P_2)} V_R \qquad\qquad\qquad (C.3.8)$$

or

$$V_P = V_C - V_R \left[\frac{P_1}{P_2} - 1 \right]$$

<div align="right">*(C.3.9)*</div>

Equation C.3.9 is the working equation employed in the pycnometer [2].

C.3.3 Errors

Source of errors include non-ideal gas behaviour. Equation C.3.9 was derived using the equation of state for and ideal gas, therefore; dry helium is recommended for use in the pycnometer. However, dry nitrogen can also be used at room temperature. If air or other gases, which contain absorbable impurities, are used the pressure readings will be affected due to absorption on the powder surface. The extent of the resulting error depends upon the amount and nature of the impurities as well as the solid's area.

Many samples contain impurities on their surface and within pores. The presence of these impurities can affect the results in several ways:

1. The actual weight of the sample is less than the weight indicated when weighed
2. Contaminants fill pores causing a large sample volume to be observed.
3. Volatile impurities will cause erroneous readings.

Successive volume determinations yielding results trending in one direction are usually an indication that contaminations are being removed after each depressurisation. Measurements should be continued until two or three successive determinations are obtained to within 0.2%. Another indication of the presence of volatile contaminates is gradual pressure increase when sample is included in the flow path after purging with dry helium. This occurs at the contaminants leave the surface and establishes an equilibrium partial pressure.

An additional source of error caused by high surface area powders is the annulus volume created between the powder surface and the centre of mass of the gas phase molecules at the interface. Assuming that the closest approach of the centre of mass of the gas molecules to the powder surface is 0.5 Å ($5 \cdot 10^{-11}$ meter) and that the powder surface is in the order of 1000 square meters per gram, there will exist an annulus volume of $5 \cdot 10^{-8}$ m^3 ($5 \cdot 10^{-2}$ cm^3) per gram of powder. Thus, with samples of about 1 gram of high specific surface area, volume errors of 0.05 cm^3 can occur. Corrections for this error can be made with knowledge of the effective diameter (i.e., Van der Waals diameter) of the gas molecules and the powder's specific surface area. [2]

References

1. J F. Rabek; Experimental Methods in Polymer Chemistry, (Chapter 31), John Wiley & Sons Inc., Sweden 1980.
2. R. A. Mariani; The Leader in Powder Technology, User Reference Manual for Pycnometer Model MVP-3, Quantachrome Corporation, USA 1997.

C.4 Scanning Electron Microscope

C.4.1 Introduction

Scanning Electron Microscope (SEM) provides morphologic and topographic information about the surfaces of solids that is usually necessary in understanding the behaviour of surfaces. Thus, an electron microscopic examination is often the first step in the study of the surface properties of a solid [1].

The Scanning Electron Microscope offers a fairly high resolution and since it is possible to use bulk specimens (specimen thickness being of no consequence), specimen preparation is easy. In addition to which, the depth of focus is large, thereby enabling 3-dimensional observation [2]. Magnification is achievable to a range from about 10X to 100000X [1].

C.4.2 Theory

The operational principle of the scanning electron microscope is illustrated in figure C.4.1. In obtaining an electron microscope image the surface of a solid sample is swept in a raster pattern with a finely focused beam of electrons. A raster is a scanning pattern similar to that used in cathode-ray tube (CRT), in which an electron beam is (1) swept across the surface in a straight line, (2) returned to its starting point, and (3) shifted downward by a standard increment. This process is repeated until a desired area of the surface has been scanned.
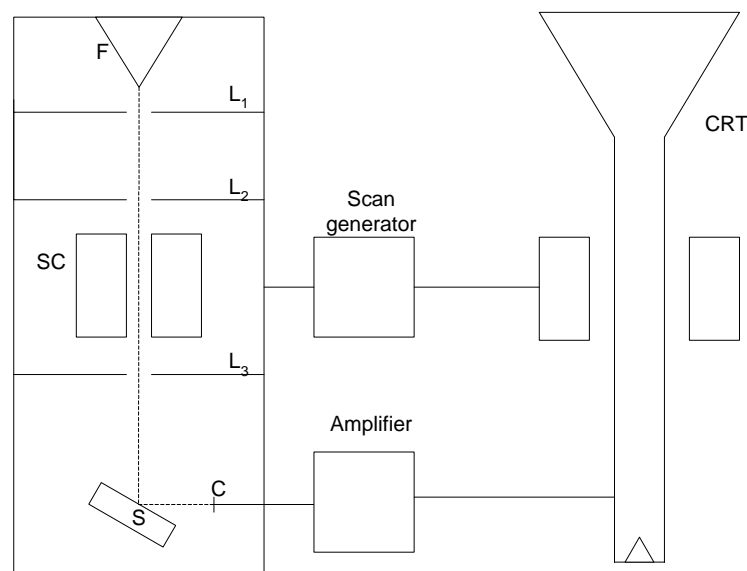

Figure C.4.1: Schematic representation of Scanning Electron Microscope [3].

Electrons from the filament (F) are accelerated through a potential field, which can be varied between 1-30 kV. The electrons are sent through a column of three magnetic lenses. L_1 and L_2 are condenser lenses, while L_3 is an objective lens. The lenses will focus the electron beam to the surface of the sample (S). The scanning coil (SC) is often placed between lens 2 and 3 and is providing the electron beam to sweep over a raster of the surface. The signals are then detected and fed to a synchronously scanned CRT as an intensity-modulating signal, thus

displaying a specimen image on the CRT screen. The CRT raster width divided by electron probe scanning width gives the image magnification [3].

Several types of signals are produced from a surface when it is scanned with an energetic beam of electrons (Figure C.4.2). These signals have been used for surface studies, but the two most common are secondary and backscattered electrons [1]. Each signal has detector their own. The signals have to go in to the detector with enough energy and high enough speed.
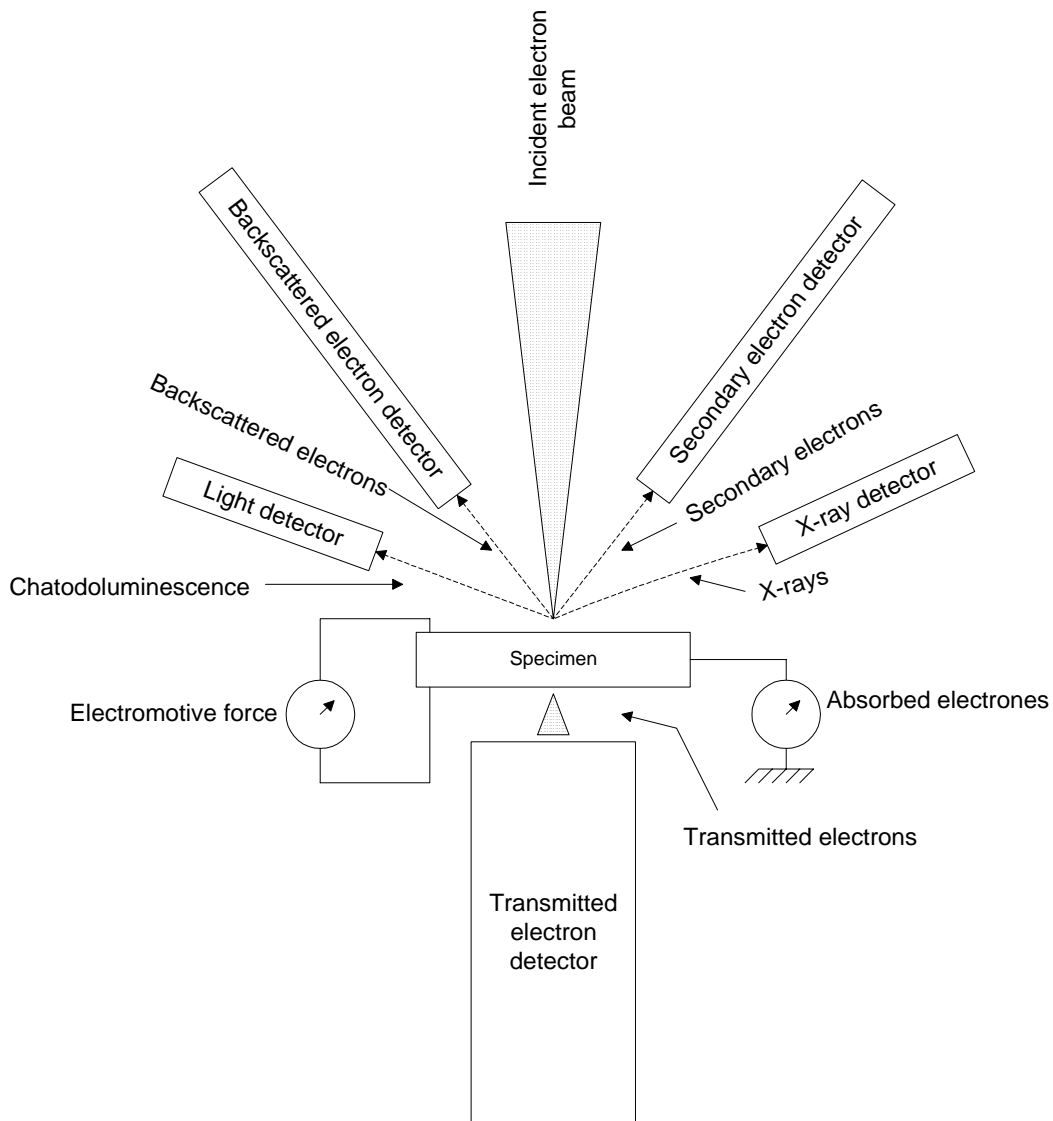

Figure C.4.2: Signals emitted by specimens [2].

Sample chambers are designed for rapid changing of samples. Large-capacity vacuum pumps are used to hasten the switch from ambient pressure to 10^{-6} bar or less. Samples that conduct electricity are easiest to study, because the unimpeded flow of electrons to ground minimises artefacts associated with the build-up of charge. In addition, samples that are good conductors of electricity are usually also good conductors of heat, which minimises the likelihood of their thermal degradation. Unfortunately polymers, among many other materials are not conducting. A variety of techniques have been developed for obtaining SEM images of non-conducting samples, but the most common approaches involve coating the surface of the sample with a thin metallic film produced by sputtering or by vacuum evaporation.

Regardless of the method of producing a conductive coating, a delicate balance must be stuck between the thinnest uniform coating achievable and an excessively thick coating that obscures surface details [1].

References

1.   D. A. Skoog, J. J. Leary; Principles of instrumental analysis, 4th Ed., International Edition, USA 1992.
2.   JEOL, Instructions JSM-T300 Scanning 'Microscope, JEOL Ltd./ JEOL Technics Ltd., Japan
3.   J. Hjelen; Scanning electron mikroskopi (in Norwegian), SINTEF, Department for Metallurgy, Metallurgical institute NTH, Norway 1989.

C.5 Thermal Analysis

C.5.1 Introduction

Thermal analysis is a term to cover a group of techniques in which a physical property of a substance and/or its reaction product(s) is measured as a function of temperature.

Well over a dozen thermal methods, which differ in the properties measured and the temperature programs, can be recognised. This discussion shall confine two methods, which provide primarily chemical rather than physical information about the samples of matter. These methods are Thermogravimetric Analysis (TGA) and Differential Scanning Calorimetry (DSC).

C.5.2 Thermogravimetric Analysis (TGA)

Introduction
Thermogravimetric analysis uses heat to drive reactions and physical changes in the material. TGA provides quantitative measurements of any mass change in the polymer or material associated with a transition or thermal degradation. TGA can directly record the change in mass due to dehydration, decomposition, or oxidation of a polymer with time and temperature. Thermogravimetric curves are characteristic for a given polymer or compound because of the unique sequence of the physiochemical reaction that occurs over specific temperature ranges and heating rates and are function of the molecular structure. The changes in mass are a result of the rupture and/or formation of various chemical and physical bonds at elevated temperatures that lead to the evaluation of volatile products or the formation of heavier reaction products. From TGA curves, data concerning the thermodynamics and kinetics of the various chemical reactions, reaction mechanisms and the intermediate and final reaction products are obtained [1].

Theory
By definition, thermogravimetric analysis is a technique in which the mass of a substance is measured as a function of time or temperature while the substance is subjected to a controlled temperature program. Because mass is a fundamental attribute of material, any mass change is more likely to be associated with a chemical change, which may, in turn, reflect a compositional change. The sample is placed in a furnace while being suspended from one arm of a precision balance (figure C.5.1) [1].

The change in sample weight is recorded while the sample is either maintained isothermally at a temperature of interest or subjected to a programmed heating. The TGA curve may be plotted in either (a) the weight loss of the sample or (b) in differential from (the change of sample weight with time) as a function of temperature (figure C.5.2) [1].
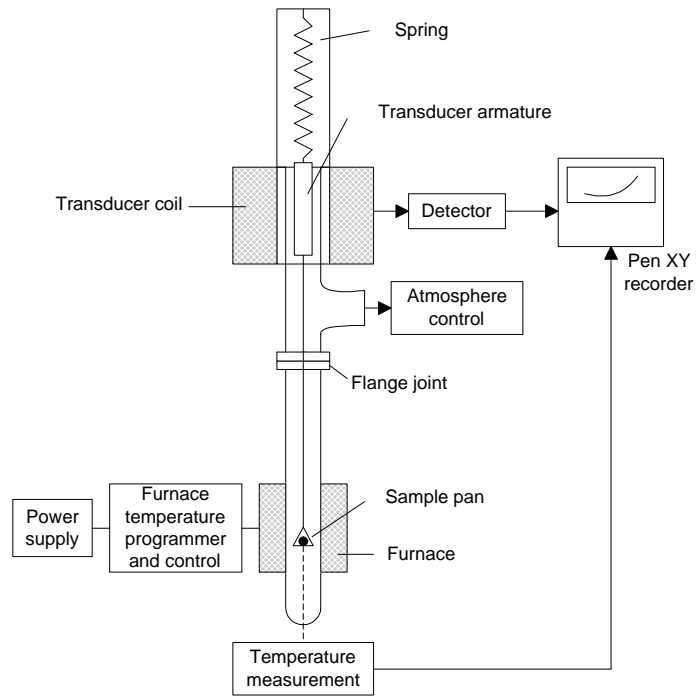
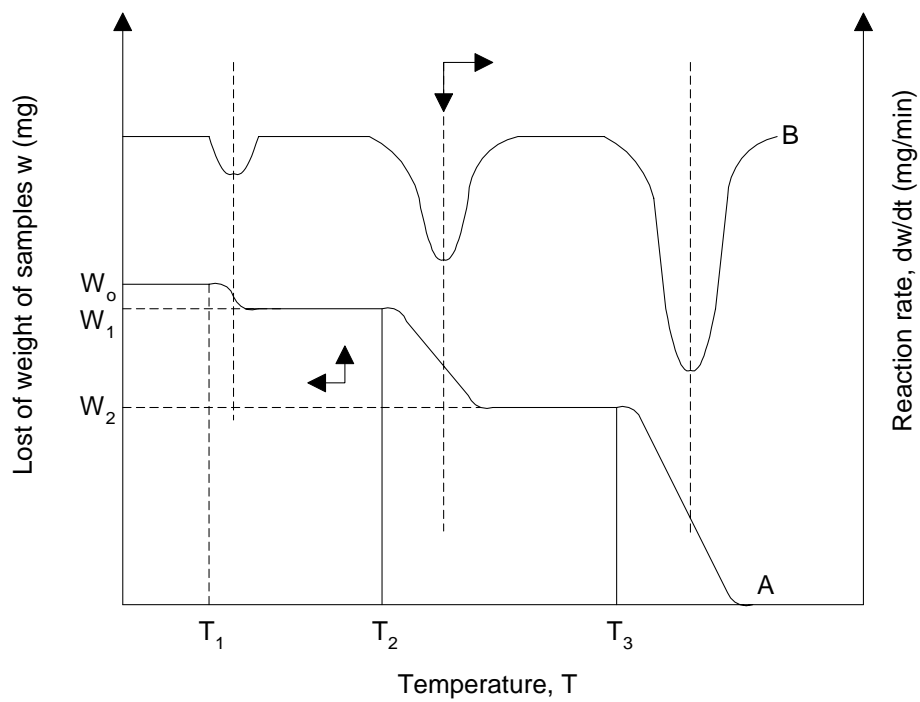*Figure C.5.1: Schematic representation of a vertical balance [2].*

Figure C.5.2: Typical thermograms: curve A, a thermogravimetric (TG) curve; curve B, a derivate thermodynamic (DTG) curve [2].

The mass loss can be calculated after equation C.5.1:

$$Percent\ mass\ loss = 100 \cdot \frac{(W_0 - W_f)}{W_i}$$
(C.5.1)

where W_0 and W_f refer to the initial and final mass, respectively.

$$\frac{dw}{dt} = kw^n$$
(C.5.2)

which represents the rate of mass loss, where n represents the order of the reaction, and k is the rate constant and given by

$$k = A \exp\left(-\Delta E / RT\right)$$
(C.5.3)

where A is the pre-exponential factor, E is the Arrhenius activation energy, R is the gas constant (8.134 J/mole K) , and T is the temperature in Kelvin [1].

Applicability
The TGA can be applied to most materials that degrade due to instability brought on by increased temperature. However, there are limitations to applying this technique to unknown materials. Because recorded value is mass loss, this is not exactly a unique attribute. However, some interesting developments in combining TGA with other techniques, such as, mass spectrometry, Fourier transform infrared, or titrators have expanded the utility of this technique to the identification of unknown materials [1].

Accuracy and precision
Accuracy and precision vary with instrument model and total, initial, sample size, and sample preparation. 0.05% accuracy and a precision of 0.1 μg can be achieved with a electro balance. Reproducibility between runs, expect in relative pure materials, is usually significant poorer. Absolute accuracy has no real meaning in this experiment; critical information consists of significant changes in mass loss or temperature of mass loss between samples. Inhomogeneity of samples, sample geometry, and sample size differences can have adverse effects on the reproducibility of data [1].

C.5.3 Differential Scanning Calorimetry (DSC)

Introduction
DSC measures the heat required to maintain the same temperature in the sample versus an appropriate reference material in a furnace. Enthalpy changes due to a change in state of the sample are determined. DSC may measure a number of important physical changes in a polymer. These include the glass transition temperature (T_g), the crystallisation (T_c), the melt temperature (T_m), and the degradation or decomposition temperature (T_D). Chemical changes due to polymerisation reactions, degradation reactions, and other reactions affecting the sample can thus be determined [1].

Theory

There are two types Differential Scanning Calorimeters. (a) Power compensated DSC (ΔP) and (b) Heat flux DSC (ΔT). Subsequent section of this experiment will not distinguish between the two types. In either type of calorimetric, the measurement is compared to that for a reference material having a known specific heat.

In DSC sample and reference are provided with individual heaters, and energy is supplied to keep the sample and reference temperatures constant. In this case the electrical power difference between sample and reference (dΔQ/dt) is recorded. Schematic representation of DSC is given in figure C.5.3. Data are plotted as dΔQ/dt on the ordinate against temperature on the abscissa. Such plots are called thermograms. The major advantages of DSC is the peak areas of thermograms are related directly to enthalpy changes in the sample, hence may be used for measurements of heat capacities, heats of fusion, enthalpies of reactions, and the like [3].
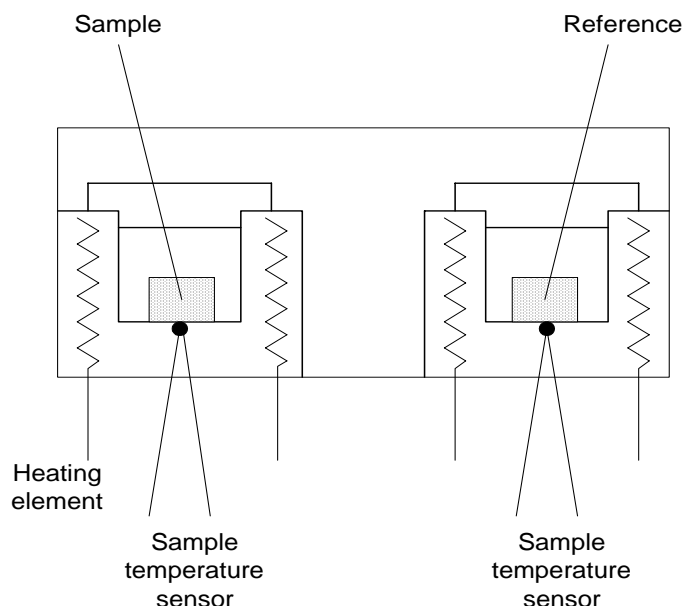

Figure C.5.3: Schematic representation of Differential Scanning Calorimetry [3].

An idealised DSC thermogram for a hypothetical crystallisable polymer is depicted in figure C.5.4, which illustrates the types of transitions of interest to polymer chemists.

The glass transition causes an endothermic shift in the initial baseline because of the sample's increased heat capacity. In reporting transition temperatures, it is important to indicate whether one is referring to onset of the transition or to the inflection point or peak maximum.
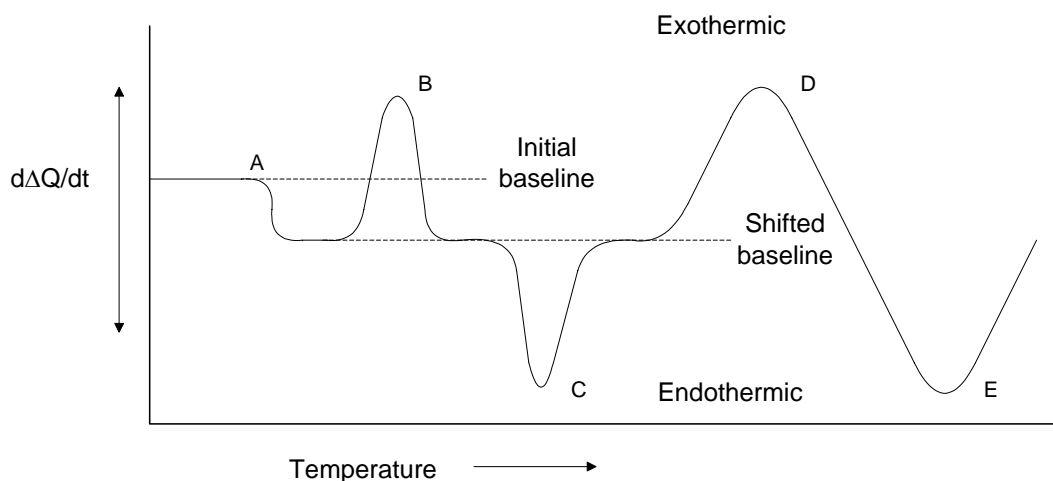
Figure C.5.4: Idealised differential scanning calorimetry (DSC) thermogram: (A) temperature of glass transition, T_g; (B) crystallisation; (C) crystalline melting point, T_m; (D) crosslinking; and (E) vaporisation. $d\Delta Q/dt$ = electrical power difference between sample and reference [3].

Applications

Differential Scanning Calorimetry is applicable to the measurements of transition temperatures, specific heats, and heats of transition or reaction for all non-volatile materials that do not evolve significant amounts of volatiles by reaction. The usual temperature range is covered is -150 to 725°C [1].

Accuracy and precision

It is essential that the sample be homogenous and representative as milligram quantities of the sample are used. Heats of transition and specific heats can be determined with a precision of about ±5%, with careful calibration and accurate weighing [1].

References

1. S. R Sandler, W. Karo, J-A. Bonesteel, E. M. Pearce; Polymer Synthesis and Characterization, A laboratory Manual, Academic Press, USA 1988.
2. J. F. Rabek; Experimental Methods in Polymer Chemistry, (Chapter 32), John Wiley & Sons, Sweden 1980.
3. M. P. Stevens; Polymer Chemistry; an introduction, 3rd Ed, Oxford University Press, USA 1999.

Appendix D: Properties of the gases measured

D.1 Properties of gases

The components Cl_2, O_2 and N_2 are present in the electrolysis gas in addition to minor impurities (Chapter 1). The physical properties of the gases will strongly influence on membrane separation. N_2 and O_2 are more ideal gases, while Cl_2 is non-ideal and the physical properties are of great importance for the separation process. Cl_2 is a non-polar gas, and is also very reactive and corrosive in the slightest presence of water vapour. This put critical demands on material durability, both for module equipment as well as the membranes. Table D.1 are presenting molecular sizes and physical properties for gases in question. Additional information of the gases may be found in handbooks [1-3].

Table D.1: Physical properties of some gases at 101 kPa [1].

	H_2	N_2	O_2	Cl_2	HCl
Molecular weight [g/mol]	2.01	28.01	32.00	70.91	36.46
Melting point [^{o}C]	-259.14	-209.86	-218.78	-100.98	-114.8
Boiling point [^{o}C]	-252.87	-195.8	-182.96	-34.6	-84.9
Density [g/l] at 15°C	0.085	1.185	1.354	3.042	1.552
Critical temperature [K]	33.19	126.0	154.6	417.0	324.65
Critical pressure [MPa]	1.32	3.29	5.043	7.79	8.36
Critical density [g/L]	0.0314	0.519	0.436	0.573	0.450
Kinetic diameter L-J [Å]	2.89	3.80	3.46	4.22	3.34

D.1.1 Chlorine

Chlorine, element number 17, is a member of the halogen family with an atomic weight of 35.453 g/mole. At normal pressures and temperatures chlorine exists as a diatomic gas (Cl_2) with a yellowish-green colour and a characteristic pungent odour. Its density is approximately two and one half times that of air. Chlorine, gas or liquid, is neither explosive nor flammable; however, like oxygen it is capable of supporting combustion. It reacts with most elements under specific conditions, often with extreme rapidity. Chlorine reacts with sulphur, phosphorus, iodine, bromine and fluorine. It also reacts with nearly all metals, under suitable conditions, to form soluble metal chlorides [3]. A summary of the properties of chlorine is given in table 5.1.

The density of chlorine gas at 101.3 kPa is a function of temperature illustrated in table 5.2:

Table D.2: Density of chlorine as a function of temperature [3].

T [°C]	0	50	100	150
ρ [kg/m^3]	3.213	2.700	2.330	2.051

The density up to 300°C is higher than that of an ideal gas because of more complex molecules like Cl_4. In the range 400-1450°C the density approximates that of an ideal gas, and above 1450°C thermal dissociation takes place reaching 50% at 2250°C [3].

At certain temperatures chlorine reacts spontaneously with hydrogen to produce hydrogen chloride. This occurs slowly in the dark, but explosively in sunlight at temperatures above 250°C. Obviously hydrogen in chlorine during chlorine purification is of great concern.
Chlorine does not react directly with nitrogen or oxygen. Although the oxides and nitrogen compounds are well known, they must be prepared by indirect methods [3].

Chlorine is very slightly soluble in water. When dissolved (maximum solubility is about 1% at 9.6^{0}C), it reacts reversibly to form hypochlorous and hydrochloric acids:

$$Cl_2 + H_2O \leftrightarrow HClO + HCl \qquad\qquad\qquad\qquad (D.1)$$

The solubility of chlorine in water decreases with rising temperature. The formation of hypochlorous and hypochloric acids causes corrosion of metals that are ordinarily unaffected by dry chlorine [3].

D.2 Cl_2 safety considerations

The chlorine gas is a respiratory irritant. The gas irritates the mucous membranes and the liquid burns the skin. As little as 3.5 ppm can be detected as an odour, and 100 ppm is likely to fatal after a few deep breaths. Exposure to chlorine should not exceed 1 ppm (8-hr time weighted average 40 hr week).

Experiments with chlorine gas demands special focus on equipment and safety. Material quality of the experimental set-up must be carefully considered; stainless steel or Inconel are being used, linings and gaskets are Viton or Teflon, instruments must be guaranteed for chlorine exposure. Safety precautions related to the chlorine gas demand that the Cl_2 gas permeates are sent to a liquid trap with caustic solution, thus reducing Cl_2 to Cl^- and ClO^-, which can easily be disposed of. The whole system is thoroughly purged with N_2 after each experiment with Cl_2 since the slightest presence of humidity (for instance from humid air leaking in on vacuum side) would easily cause corrosion in combination with Cl_2 [4].

References to Appendix D

1.   R. C. Reid, J.M Prausnitz, T.K. Sherwood; The properties of Gases and Liquides, 3rd Ed., McGraw-Hill, NY.
2.   W. Gerhartz (Editor), Chlor-Alkaline, in Ullmann's Encyclopaedia of Industrial Chemistry, 5th Ed., vol. A6, VCH, Weinheim 1986.
3.   M.Grayson (Editor.), Kirk Othmer, Encyclopaedia of Chemical Technology, Alkali and Chlorine Products, vol. 1, p. 799-865, 3rd Ed., USA 1978.
4.   M-B. Hägg, Membrane Purification of chlorine gas-contributions towards an integrated process solution in magnesium production, Dissertation Dr.tech, Norwegian University of Science and Technology, Trondheim, Norway 2000.